A METHODOLOGY FOR STRUCTURAL TECHNOLOGY PERFORMANCE CHARACTERIZATION TO ENABLE REDUCTION OF STRUCTURAL UNCERTAINTY

A Thesis
Presented to
The Academic Faculty

by

Jason A. Corman

In Partial Fulfillment
of the Requirements for the Degree
Doctor of Philosophy in the
School of Aerospace Engineering

Georgia Institute of Technology
May 2017

A METHODOLOGY FOR STRUCTURAL TECHNOLOGY PERFORMANCE CHARACTERIZATION TO ENABLE REDUCTION OF STRUCTURAL UNCERTAINTY

Approved by:

Professor Dimitri N. Mavris,
Committee Chair
School of Aerospace Engineering
Georgia Institute of Technology

Professor Daniel Schrage
School of Aerospace Engineering
Georgia Institute of Technology

Professor Graeme Kennedy
School of Aerospace Engineering
Georgia Institute of Technology

Dr. Neil Weston
School of Aerospace Engineering
Georgia Institute of Technology

Dr. Vivek Mukhopadhyay
NASA Langley Research Center
Georgia Institute of Technology

Date Approved: April 6, 2017

To my parents

ACKNOWLEDGEMENTS

My time at Georgia Tech has been an extremely fulfilling experience. I have had the opportunity to work with organizations and in fields that I could have only dreamed about when I was younger, and going through this process makes me realize how little I actually knew before I started. The development of this research would not have been possible without an abundance of support I have had available to me.

First, I owe a sincere debt of gratitude to my advisor, Prof. Dimitri Mavris. I would not be in the position I am today without his guidance, compassion, and his willingness to see potential. Dr. Mavris has the innate ability to garner the most out of the people around him and facilitate a more complete understanding of how the world works, albeit mostly through Greek mythology analogies. He has made this Ph.D. journey an extremely gratifying one, and it has been an honor to be under his tutelage.

My thesis committee was an absolute wealth of knowledge and experience, and the research presented in this thesis is undoubtedly more complete and well thought out as a result of discussions with them. I am immensely grateful to Prof. Graeme Kennedy, Dr. Vivek Mukhopadhyay, Prof. Daniel Schrage, and Dr. Neil Weston for helping me see this problem in a different light; their feedback was instrumental in guiding the process. Additionally, the research teams at NASA Langley Research Center, Boeing Research and Technology, and the Aerospace Systems Design Lab helped provide a much more exhaustive understanding of the motivation for this problem and I am thankful for their continued advice, especially Ms. Dawn Jegley, Dr. Jimmy Tai, and Mr. Trevor Laughlin.

I would also like to thank my friends for making my time in Atlanta exceedingly

enjoyable. Your support in the last few months while finishing this degree is greatly appreciated, in particular my girlfriend, Erin. This document would not have gotten finished if it were not for your patience, love, and willingness to take care of literally everything else in my life.

Finally, I would like to thank my family for their continued and unwavering love and support. My brother, Kevin, has been a constant role model throughout my life and helped me strive to be the best I can. Most importantly, my parents have helped put everything into perspective time and again, and they taught me the value of hard work, dedication, and perseverance. It is truly humbling to see the example they lead every day, and I cannot even begin to explain how much better my life has gotten since my dad got a cell phone and learned how to text. I owe everything to you both.

TABLE OF CONTENTS

LIST OF TABLES

LIST OF FIGURES

SUMMARY

The role of structural technology performance characterization is important because it acts as a means of communication between low level technology development and higher level technology selection and implementation in conceptual design. Technology development programs, such as NASA's Environmentally Responsible Aviation (ERA), are in search of potential solutions to meet ambitious aircraft performance goals of the next generation air transport system. It is the responsibility of decision makers at this level to decide which aircraft concepts and technologies are best suited to meet requirements and ensure design feasibility of future aircraft. On the other end, it is the responsibility of the technology development team to provide estimated technology impacts at the conceptual design level, and ensure confidence in those estimates, so that these decisions can be made. For structural technologies, structural weight reduction is the identified metric that will allow the technology to "buy" its way onto an aircraft.

Many challenges exist in creating the ability to characterize weight reduction performance of structural technologies. One technology in particular is identified in this research because of its potential to enable hybrid wing body (HWB) design and therefore potentially feasible environmental performance within established goals of fuel burn, emissions, and noise. The Pultruded Rod Stitched Efficient Unitized Structure (PRSEUS) technology is a stitched, resin-infused (S/RI) composite configuration that possesses favorable characteristics for the structural challenges associated with a pressurized HWB centerbody passenger cabin. The complex design characteristics and structural behavior of the PRSEUS technology require higher fidelity structural models for accurate performance estimation. A benchmark process is established

in this scenario to estimate potential weight reduction of the structural technology. However, it is hypothesized that an incomplete characterization of structural technology performance introduces risk in conceptual design implementation and technology experiment design.

This hypothesis stems from the notion that aircraft structural weight is dependent on conceptual design parameters, i.e. aircraft outer model line (OML), and is empirically modeled in this manner in traditional conceptual design tools. Unless this relationship is exactly the same for a structural technology of interest and the state of the art baseline structure to which it is compared, then it stands to reason that technology weight reduction performance would be dependent on the OML as well. The objective of this research is to be able to systematically characterize this relationship and assess its significance to ensure resources are only expended for added value in the performance characterization.

The approach developed in this research, Structural Technology Evaluation for Experimental Design (STEED), operates within a framework synthesized to overcome gaps in the benchmark performance estimation process. Steps of this approach are performed at three levels of design spaces in a generalized physics-based structural weight estimation process, and at each level, the potential influence of the outer mold line on structural weight reduction is evaluated. It is shown that for the PRSEUS technology, structural weight reduction performance does in fact have a significant functional relationship with OML. Studies in treatment of the structural layout for each OML design point showed that surrogate-enabled topology optimization can take place for each structural configuration without substantially influencing computational expense. Results show that in this formulation, compared to a benchmark definition of performance in which structural layout was held constant for both baseline and technology configurations during the estimation process, PRSEUS enables more weight efficient structural layouts than the baseline structure, which accounts

for a component of its performance.

The functional relationship between structural technology performance the aircraft OML is also shown to be a significant source of potential error or uncertainty when implemented in conceptual design. Variability in PRSEUS performance as a result of this relationship rivals uncertainty due to technology immaturity, indicated by the technology's readiness level (TRL). Therefore, neglecting functional performance presents a significant risk in conceptual design technology selection and implementation. Additionally, the number of potential objectives that can be examined in the technology experiment design process increases combinatorially with each additional metric at each design space level considered beyond the benchmark approach.

CHAPTER I

INTRODUCTION

1.1 Motivation and Background

There has been a significant effort in the aircraft design community over the last decade to increase efficiency of air travel. While the air transportation system plays an important role in the economy, a projected steady increase in commercial passenger air traffic [3, 4] has government entities and regulating agencies in the United States investigating means to mitigate the effect that growth will have on the environment. The Federal Aviation Administration's (FAA) Continuous Low Energy, Emissions, and Noise (CLEEN [77]) and the National Aeronautics and Space Administration's (NASA) Environmentally Responsible Aviation (ERA [12]) programs have been catalysts for this movement. For instance, the ERA program provided vital support for goals established by NASA Aeronautics Research Mission Directorate (ARMD) to reduce noise margin, NO_x emissions, and fuel consumption by the 2020 N+2 time frame, shown in Fig. 1. Moreover, these goals are to be achieved simultaneously. Outcomes of these programs have the potential to influence consumer air travel for upcoming generations.

1.1.1 Conceptual Design for Environmental Concerns

The ability to meet these demanding goals is a burden first experienced by the conceptual aircraft design process. The role of conceptual design is to investigate a large number of design alternatives, analyze trades in performance and cost, identify the general shape and configuration of the aircraft, and determine whether requirements can result in a feasible, viable design. Traditionally, the conceptual phase is a serial process that begins with derivative investigation of conventional configurations. This

	TECHNOLOGY GENERATIONS (Technology Readiness Level = 4-6)		
TECHNOLOGY BENEFITS*	N+1 (2015)	N+2 (2020**)	N+3 (2025)
Noise (cum below Stage 4)	- 32 dB	- 42 dB	- 71 dB
LTO NOx Emissions (below CAEP 6)	-60%	-75%	-80%
Cruise NOx Emissions (rel. to 2005 best in class)	-55%	-70%	-80%
Aircraft Fuel/Energy Consumption‡ (rel. to 2005 best in class)	-33%	-50%	-60%

* Projected benefits once technologies are matured and implemented by industry. Benefits vary by vehicle size and mission; N+1 and N+3 values are referenced to a 737-800 with CFM56-7B engines, N+2 values are referenced to a 777-200 with GE90 engines

** ERA's time phased approach includes advancing "long-pole" technologies to TRL 6 by 2015

‡ CO_2 emission benefits dependent on life-cycle CO_{2e} per MJ for fuel and/or energy source used

Figure 1: Representative 2020 N+2 goals for NASA ARMD

iterative approach relies on traditional empirical design models which are statistically regressed from historical data of production aircraft. These models typically focus on the aerodynamics, propulsion, and weights [101] disciplines. To better account for current state of the art (SoA) aircraft technologies, impact factor terms are included in historical weight regressions. These factors can also enable implementation of future technologies and the ability to forecast technology performance requirements.

If design feasibility cannot be achieved with a conventional configuration and state of the art technologies, options still exist for the program in its search for a design to meet requirements, which include:

1. expanding the current design space of the conventional configuration,
2. applying new or alternative technologies with predicted future performance,
3. investigating advanced unconventional aircraft concepts,
4. determining if any of the requirements can be relaxed, or
5. any combination of these options. [51]

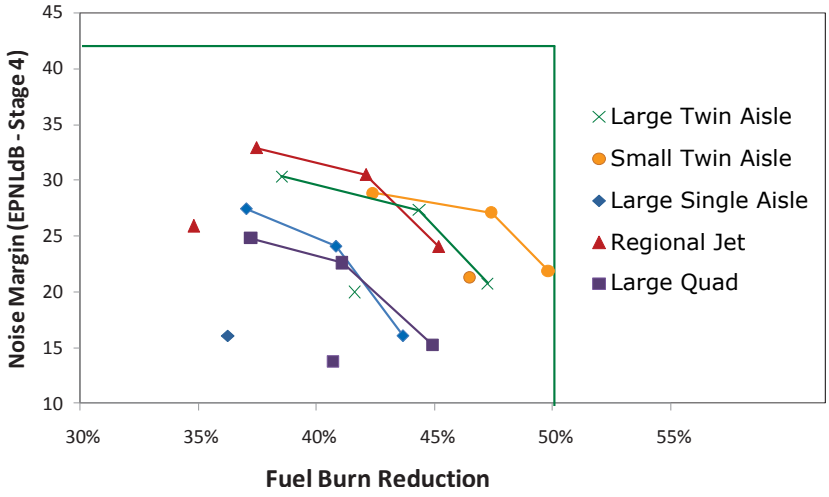

Figure 2: Conventional tube-and-wing configuration design infeasibility investigated during the NASA ERA program [94]

In the case of the NASA ERA program, a sufficient conventional design space had been considered. Additionally, changing requirements is one of the final alternatives of an early-phase design program. Therefore, developing technologies and advanced concepts were investigated. To obtain a sense of what types of technologies should be considered in the program, a process called technology impact forecasting (TIF) can be used which performs trade studies on the technology impact factors included in traditional conceptual design models. This process helps determine the level of improvement required from a technology portfolio to meet objectives, and then specific technologies can be subsequently considered. Research supporting the ERA program examined a portfolio of potential technologies, with a possible $1,800$ technology combinations for five different scales of conventional test vehicles: Large Twin Aisle (LTA), Small Twin Aisle (STA), Large Single Aisle (LSA), Regional Jet (RJ), and Large Quad Engine (LQ) [94]. Pareto frontiers of performance for each conventional configuration are shown in Fig. 2. This plot shows that all configurations have failed to reach a feasible design region outside the bounds defined by the environmental requirements.

With infeasibility still an issue, the next step in the design process was to push the envelope and investigate unconventional aircraft concepts. The ERA program considered multiple advanced concepts and supporting research found that, under the assumptions made, the hybrid wing body (HWB) aircraft configuration had the greatest potential of meeting environmental goals, as shown in Fig. 3 [94]. The same general design process was used for unconventional configurations with one caveat. These concepts are outside the realm of traditional design models, so design data must be augmented by other means. Infusing immature technologies to these configurations presents another challenge. The design process becomes an exercise in the ability to forecast performance. In this process, unconventional concepts and new technologies, which are in the early stages of development, tend to show pure benefit in their assumptions. While it is infeasible to perform full-scale testing and certification for a development program like ERA, it is beneficial to somehow anchor these predictions in reality. Therefore, certain technologies were chosen for further development and demonstration for ERA. This leads to an important motivating question: *How is the decision made to determine which technologies are to be selected for further development in a technology demonstration program*? Before this question can be fully addressed, the hybrid wing body aircraft configuration warrants further examination to help understand criteria by which potential technologies are compared.

1.1.2 Hybrid Wing Body as a Potential Solution

The HWB concept, also referred to as the blended wing body (BWB), was the result of a push to identify a renaissance for long-haul transports [58]. An example HWB, the NASA/Boeing N2A is shown in Fig. 4 with each vehicle section defined. The HWB configuration was recognized for its potential increase in aerodynamic efficiency over conventional tube-and-wing (T&W) transports, and one of the configuration features

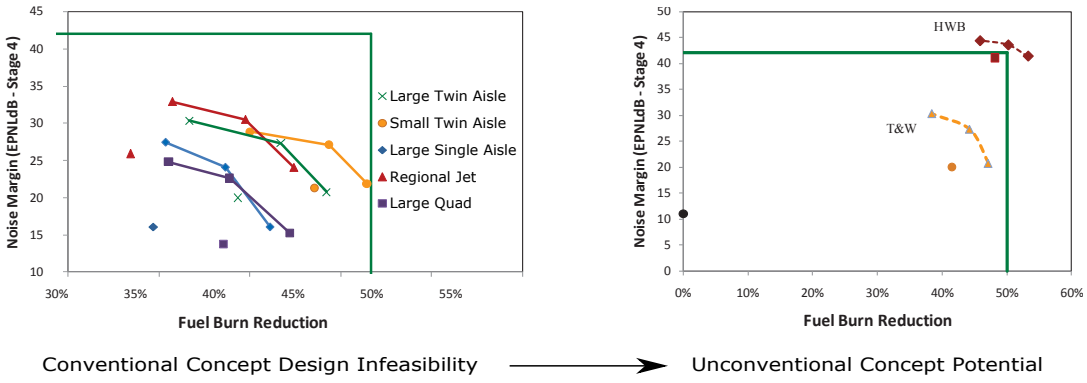

Figure 3: Potential design feasibility through investigation of HWB vehicle configuration [94]

that enable this efficiency is a multi-faceted center section. This section of the commercial transport was unique in the sense that it needed to: 1) contain pressurization loads from the passenger cabin, 2) accept bending loads from the outboard and trapezoidal wing sections, and 3) contribute a major portion of aircraft lift. A significant challenge for the HWB was the ability to design a weight-efficient solution for the centerbody section under this combined loading condition.

The evolution of a circular- or elliptical- cross section for conventional fuselages has been a result of material and structural configuration developments since the dawn of aviation. The ability to create a metallic thin-shelled structure resulted in an efficient mechanism to withstand the required pressure differential for commercial transport passenger cabins. Using simplified theory presented in Reference [71], the membrane, or hoop stress, in the skin of a circular cross-section fuselage is defined on the order of:

$$\sigma_{membrane} = O\left(pR/t\right) \tag{1}$$

where p is the pressure differential due to cabin pressurization, R is the radius of the fuselage, and t is the thickness of the fuselage skin. In comparison, bending stresses would be introduced into the skin of a cuboid-shaped centerbody section for the HWB

on the order of:

$$\sigma_{bending} = O\left(p\left(R/t\right)^2\right) \tag{2}$$

from the pressure differential alone on the flat skin panels. A relationship between the stress in the fuselage skin of a cuboid and cylindrical configuration results in:

$$\sigma_{bending} = \sigma^2_{membrane} \tag{3}$$

The cyclic nature of cabin pressurization means that fatigue is a critical concern for a non-circular centerbody section, especially if metallic materials were considered.

The HWB centerbody section, however, is not subjected to pressure alone; it is under combined loading conditions for most certification load cases defined by airworthiness standards in FAA Federal Aviation Regulations, Chapter 1, Subchapter C, Part 25 (FAR-25) [2]. Lift and moment distributions generated by the outboard

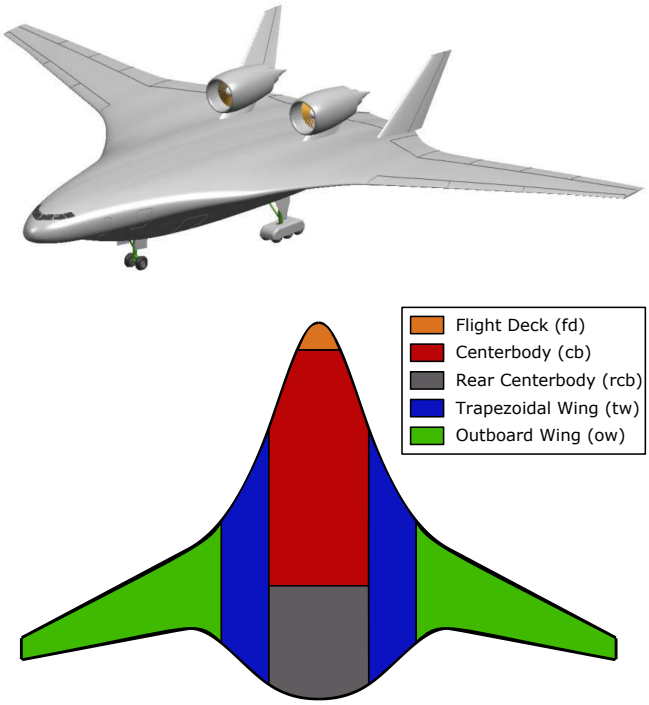

Figure 4: A 3-D view of the NASA/Boeing N2A[111] and the vehicle sections defined on the planform[53]

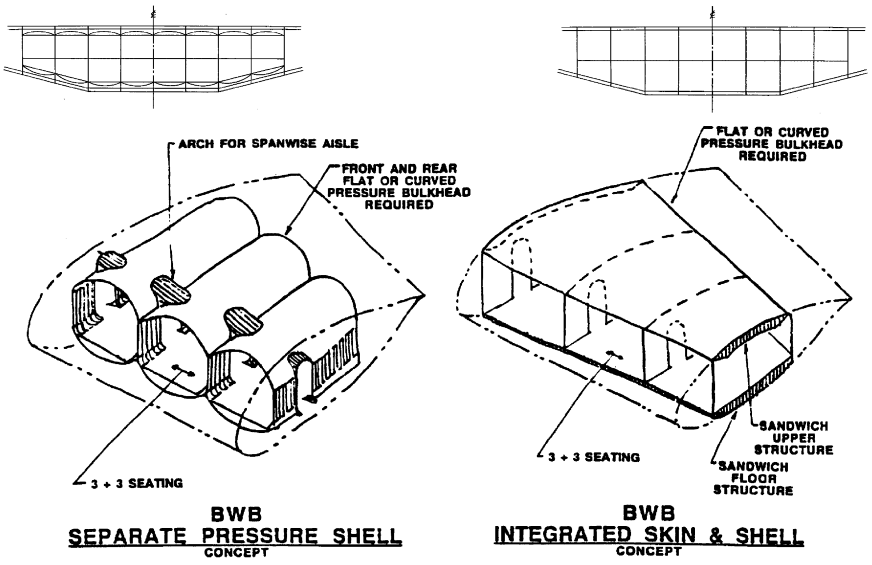

Figure 5: HWB centerbody concepts for structural layout [58]

wing section are transferred to the centerbody section, exacerbating structural challenges for this configuration. For example, in a 2.5G positive maneuver load case, the upper skin receives compressive load from the outboard wing. Concurrently, this surface is under cabin pressurization, creating a positive deflection in the skin. Under these conditions, buckling of the structure becomes a major concern and is potentially critical for its design. Two main configuration layouts were examined in an attempt to withstand combined loading conditions in the HWB centerbody, separate pressure shells and an integrated skin and shell, shown in Fig. 5 [58, 72]. Although the separate pressure shells could carry internal pressure loads in an efficient manner with hoop stress, the redundant structure added a weight penalty. The integrated skin and shell concept had the potential to save weight under the assumption that a structure with sufficient strength and stiffness properties could be found.

The assumption of efficient structural weight is embedded in the superior predicted aerodynamic efficiency, (L/D), of the HWB configuration. Validity of this assumption was called to question until a suitable structural technology is found that enables an integrated skin and shell structural layout. There have been multiple

structural concepts considered, and NASA ERA was interested in pursuing one of these technologies for further development and demonstration during Phase II of the program. This refocuses the motivating question presented in the previous section for a research effort in the structures discipline.

Motivating Question 1: How is the decision made to determine which structural technologies are to be selected for further development in a technology development and demonstration program?

As shown in Fig. 3, the inability to meet environmental goals without the infusion of technologies requires a down-selection from a portfolio. It has been shown that aircraft structures play a significant role in the feasibility of the HWB design and the challenges it presents. How are structural technologies compared to each other and what factors are considered for the selection process? One of the structural technologies that was considered in the ERA program is described in the following subsection, and this question will be revisited once further clarity has been provided.

1.1.3 Stitched, Resin-Infused Composite Technologies

The Pultruded Rod Stitched Efficient Unitized Structure (PRSEUS) technology is a specific configuration of stitched, resin-infused composites (S/RI), and is shown in Fig. 6. These composite technologies are an evolution from the NASA Advanced Composite Technologies (ACT) program and a significant achievement in both performance and manufacturing [19]. One of the major benefits of current state of the art composites for airframe manufacturing is the ability to co-cure stiffened, thin shelled structural configurations. Co-curing alleviates the need for rivets and other fasteners, which can significantly reduce structural weight. The drawback to this configuration, however, is its inability to arrest damage propagation, effectively removing the tear strap typically implemented between the thin wall and stiffeners

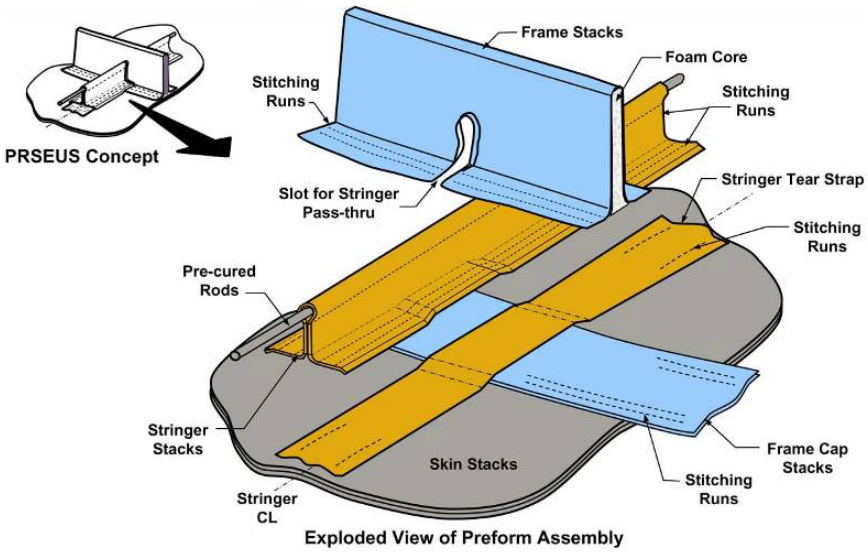

Figure 6: PRSEUS attributes [105]

in metallic constructed aircraft. Therefore, delamination as a result of out-of-plane loads is a critical failure mode of SoA aircraft composites. S/RI composites, however, use stitching as a mechanism of damage arrestment and can therefore use a damage tolerant design philosophy rather than the safe-life philosophy required of SoA composites [13]. The stitching also helps increase out-of-plane strength without compromising in-plane properties. In addition, the pultruded rod stringer and foam core frames of PRSEUS provided comparable stiffness properties in both panel directions. This helped make the technology configuration a potentially suitable solution for the specific structural challenges of combined loading conditions of the HWB centerbody. Beyond the HWB centerbody, PRSEUS was an attractive alternative to SoA composites for all aircraft configurations because of its damage arresting properties. While more details of the design characteristics of these technologies are provided in Sec. 2.3.2, this brief introduction to the technology serves as a foundation for discussion of structural technology selection.

Why are new structural technologies developed for aircraft? What are some characteristics of these technologies and how do they affect the design of aircraft? Table 1

lists examples within various categories of structural technologies. Each of these technologies has a specific characteristic at the detailed technology design level that gives it an advantage over current state of the art airframe structure, e.g. increased strength, superior stiffness characteristics, resistance to creep and damage propagation, reduction of fabrication and assembly costs, etc. The decision of whether or not to implement the technology in an aircraft program, however, is made at a higher level where early-phase aircraft design occurs. The technology must be able to "buy" its way onto the aircraft, which generally refers to its ability to enable superior aircraft performance, a reduction in cost, or increased safety. There are instances in which aircraft structures act as enabling technologies, which allow advantageous designs or performance attributes in disciplines other than structures, e.g. aerodynamics. However, the weights discipline in conceptual design is generally where structural technologies manifest the most significant performance impact. While weight, cost, and safety are all important in the aircraft design process, the context of this research is in the ability to satisfy environmental goals, which are performance-driven rather than cost-driven or safety-driven. Therefore, the decision-making level comparative metric for structural technologies is their ability to **reduce structural weight**.

If technologies are compared at the conceptual design level by structural weight reduction, then local technology performance metrics, such as strains, deflections, and local loads, need to be propagated to the structural weight level. Therefore, a modeling platform must be created that connects conceptual design with detailed structural models in order to generate the required structural weight performance metrics and compare and select technologies. Traditional empirical design models for weight require the output of such a modeling platform to implement the technology in conceptual design and cannot, therefore, be used for this task. Additionally, these historical models do not exist for unconventional configurations. As a result, the move to a physics-based modeling approach was made, and the approach taken for

Table 1: Potential Characteristics of Structural Technologies

Technology	Description
Material	New materials are developed with advantageous properties (Ex: alloys, composites, polymers)
Configuration	Structures are attached, assembled, shaped, or arranged in a new beneficial manner (Ex: stiffener shaping, sandwich composites, stitched composites, tow-steered composites, bio-inspired structures)
Manufacturing	New fabrication processes enable structures otherwise impossible (Ex: CAPRI for composites, additive manufacturing)
Repairs	Structures designed for repairing damage rather than replacement of failed parts when applicable (Ex: bolt-on stiffener repairs)
Structural Health Monitoring	Sensors infused directly into structures enable the constant monitoring for signs of cracks, fatigue, delamination, and other damage (Ex: fiber optics, lamb-wave sensors)

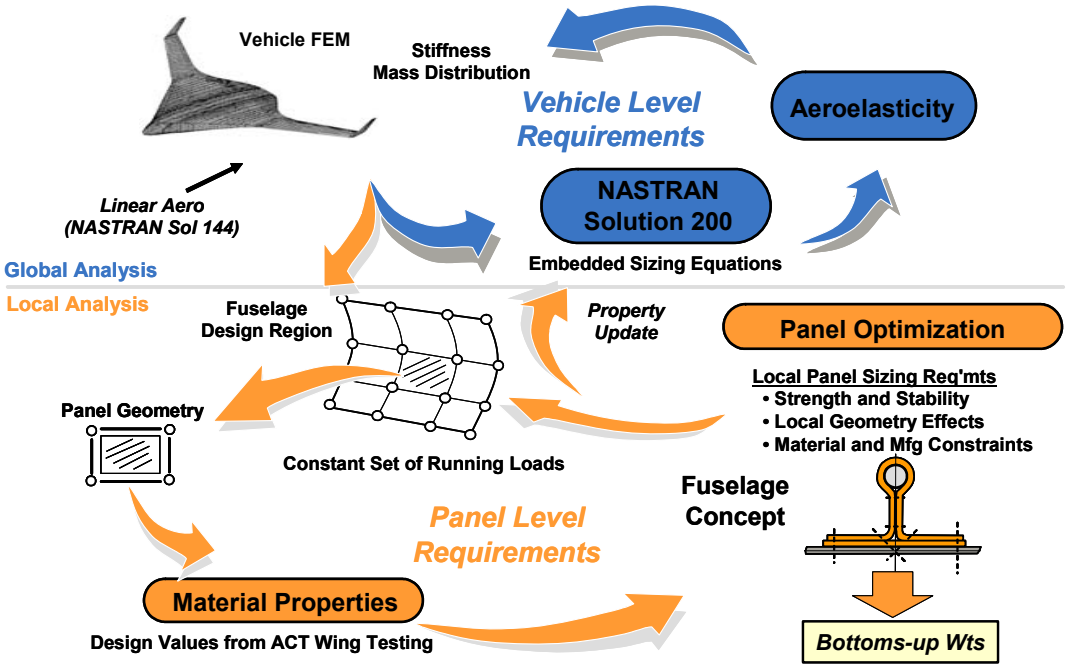

Figure 7: Approach for structural sizing to determine PRSEUS weight reduction performance [105]

PRSEUS is outlined in Fig. 7. It shows a global-local structural sizing process in which a full vehicle finite element model (FEM) is created to establish global loads and deflections which in turn, are used for local component sizing with detailed technology characteristics. Significant challenges exist in the ability to generate structural weight in this scenario, and assumptions must be made to do so.

First, generating a full aircraft finite element model is no menial task. An experienced user can take on the order of weeks to months to pre-process one shell-based FEM that represents the entire primary, load-bearing structure of an aircraft. Pre-processing is further complicated by the local sizing process, in which the FEM must communicate with third party software. In practice, the result of tedious model development is an inability to analyze more than a single aircraft configuration. Technology performance estimation for a single configuration aligns with a benchmark technology selection approach that is presented in Sec. 2.2.1. Figure 8 shows an overview

of the steps of the process described in that section. Steps 1 through 5 represent the conceptual design space exploration approach that has thus been described in the context of a technology development program. Beyond Step 5, however, a single baseline aircraft design is carried through to assess technology alternatives. The chosen baseline aircraft in these steps is the one that is closest to meeting design feasibility, and presumably, this would be the baseline chosen for the performance estimation process in Fig. 7. Although a single weight reduction estimate is sufficient for the benchmark technology selection approach, how is technology performance implemented in conceptual design for trade studies? If the conceptual designer wishes to assess trades for other configurations in the conceptual design space, is this scalar performance value accurate throughout the entire design space?

Calibration and validation of physics-based structural weight estimation, in particular for the HWB, also suffer from the lack of production weight data and limited access to industry estimates. While small-scale prototypes like the NASA X-48B have been built [89], structural weight data from this configuration is not directly applicable to a commercial-scale HWB, because it was not designed to withstand the same loading conditions. For instance, there was no need for a pressurized passenger cabin in this small-scale HWB, and therefore structure of the centerbody section of the X-48B was not representative of a HWB commercial transport. An additional consequence of a lack of historical weight data is the ability to estimate global vehicle weights, which are required for load case analyses. For instance, gross weight of the aircraft is needed in order to define required lift and generate aerodynamic loads for specific load cases in the mission analysis. In lieu of historical weight data, assumptions are made on these parameters. Lastly, depending on the stage of technology development, material and sectional properties, which are required by the structural weight estimation environment, may be purely physics-based or may not even exist at all. Given these challenges, enumerating the assumptions and constraints applied to

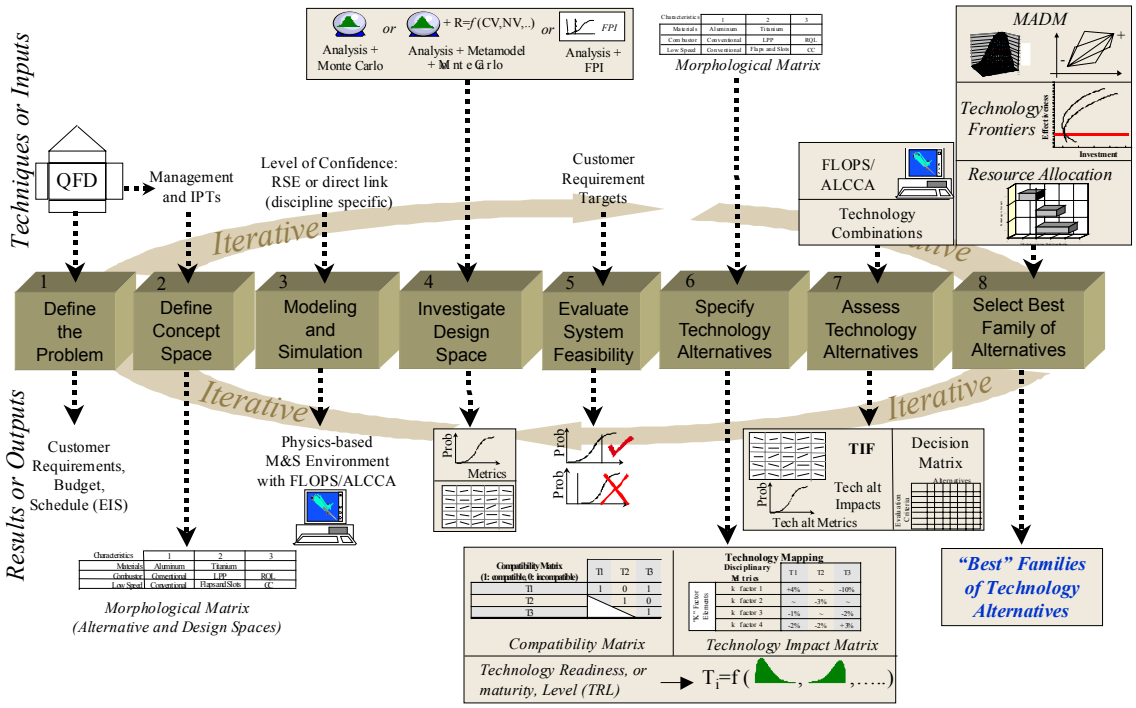

Figure 8: Technology Identification, Evaluation, and Selection method [51]

the process is of significant importance. It also brings to question: can the estimated values for structural weight reduction of a technology actually be achieved in reality and how can increased confidence in those projections be achieved?

1.1.4 Development and Demonstration of New Structural Technologies

Building confidence in structural weight estimation models for a specific technology begins with the structural technology development team. As mentioned, this team operates at a different level than the decision-makers for aircraft design and technology selection programs, and the performance modeling platform described in the previous subsection is what bridges these two levels together. The differences between each of these levels is highlighted by example design variables, metrics, and models listed in Table 2. It is the responsibility of the development team to advance the technology and ensure greater confidence in the property estimates that are used as inputs for technology performance estimation. Those estimates are further used in

the systems models for conceptual design and technology selection to assess the technology's suitability for implementation to meet systems level requirements. How can the technology team instill confidence in the parameters it provides to performance estimation models?

Designers often use the Technology Readiness Level (TRL) scale to assess the maturity of a technology and the perceived "believability" of its performance [64]. This scale relies on a tiered schedule of demonstrations that increases directly with the reality of the technology's operating conditions in those demonstrations. Advancement of structural technologies, then, is dependent on experimentation and demonstration. In this context, there are many forms of experimentation for structural technologies, including computational experiments, physical performance experiments, and experiments in fabrication or assembly. Each of these experiment types can have a number of potential objectives as well, which are discussed further in Sec. 2.4.1. It is safe to assume that a technology development and demonstration program has finite resources at its disposal to perform experiments. Therefore, it is important to ensure that the investment by the program is worth the return, leading to the second motivating question for this research:

Motivating Question 2: Which experiments should be performed in a structural technology development program to most significantly advance the technology?

The ability to answer Motivating Question 2 is dependent on multiple conditions that the decision-maker needs to consider: 1) the current maturity level and predicted performance of the technology, 2) the objective of the technology development program, 3) the resources available for a particular experiment, and 4) the current state of assumptions made regarding technology modeling and operating conditions. In a sense, the decision-maker is responsible for determining how advancement of

Table 2: Examples of systems level (decision-making) and technology development level characteristics

Characteristic	Systems	Performance	Technology
Design Variables	– # of Passengers – Wing Area – Engine Thrust	– Aggregate Section Properties – Load Cases – Non-Optimum Factors	– Skin Thickness – Stiffener Height – Material
Metrics	– Fuel Burn – Emissions – Noise	– Structural Weight – Weight per Load Case – Critical Failure Modes – Internal Forces	– Local Failure Load – Strains – Deflections
Operating Conditions	– Local Failure Load – Strains – Deflections	– Mission Analysis (Load Cases) – Constraint Analysis – Regulations	– Global Load Cases – Local Forces – Local Moments – Pressure – Boundary Conditions
Models	– FLOPS [68] – EDS [50] – APD [81, 60]	– Full Aircraft Linear FEM – Hypersizer [88]	– Handbook Equations – Linear & Nonlinear FEM – Hypersizer

the technology is defined, and it coincides with the knowledge that is desired to be gained. For example, technology performance is completely dependent on the ability to fabricate a particular piece of structure. If the manufacturing process has been theorized but not tested, it is potentially a showstopper. In this case, technology development management may decide to test the fabrication process before any other computational modeling is done to ensure the structure can be built. If successful or unsuccessful, how is the effectiveness of this particular experiment measured, and how can it be compared to other potential experiments?

The previous example is also a case in which an experiment in fabrication can be easily combined with a physical test. Structural technology experiments are explained in further detail in Sec. 2.4, but a basic experiment can be defined by the following:

Test Article Whether computational simulation or physical test, the configuration of the structure needs to be defined. All detailed design parameters of the technology need to be set, such as material and skin thickness, as well as the global test article dimensions like component length. Using PRSEUS as an example, 15 parameters define the technology configuration (listed in Table 11). A simple rectangular test article would create a total of 17 design variables for the test specimen. The number of design variables is greatly increased for assembly test articles.

Loading Conditions Local loading conditions such as forces and moments, in contrast to global load cases (e.g. 2.5G maneuver, -2.0G taxi bump, etc.), are also to be defined for a structural technology experiment. Typically, more complex loading conditions will require a more sophisticated test apparatus. For a skin-stiffened panel technology like PRSEUS, either a single panel or assembly could be subjected to: axial forces, lateral forces, bending moments, normal pressure, torque, or a combined loading condition. The magnitude of the load over time must also be designed, and this increases the complexity of the experiment if

multiple load sets are to be examined serially.

Metrics/Sensors Success of the experiment also needs to be defined through technology metrics. Typical sensors for a structural technology experiment include: load cells, strain gauges, linear variable differential transformers (LVDTs), Video Image Correlation for 3-Dimensions (VIC-3D) cameras, and general visual inspection. These sensors help to determine aggregate strengths and stiffnesses by examining strains, deflections, and failure indications as a function of loads.

Auxiliary There are other extraneous conditions that could be used for a structural technology experiment. For example, since PRSEUS was proposed as a damage arresting technology, it was important to test this assumption for performance estimates. Therefore, damage was introduced in a number of ways to assess progressive failure modes, delamination, and the ability of the configuration to carry load under failure. Both barely visible impact damage (BVID) and saw cuts were introduced in the skin and stringers. These auxiliary features of an experiment are in place to test important assumptions regarding technology characteristics and performance.

Most examples mentioned for these experiment features are tailored toward physical structure experiments; however, the same basic setup is required for a computational model or hand calculation. The desired metrics must be implemented as responses in the model or equation, ensuring that a node or element (if applicable) exists in the location of interest on the test article.

With a large number of design variables existing for structural technology experimental design, how are they all determined? This is another instance in which the low level technology development must interact and share information with performance estimation. The full vehicle structural model from this task is needed to translate global load cases into local internal loads of the structure, e.g. upper wing skin compression loads that result from a 2.5G flight maneuver. This model also helps derive

design variables for the test article from results of the structural sizing algorithm. The PRSEUS experimental plan for the NASA ERA program will be used to clarify this flow of information, but it provides only limited insight into the expert-driven decision-making process for experimental design.

The goal for PRSEUS advancement during the ERA program was to demonstrate the technology in a relevant operating environment. At the outset of the program, PRSEUS was an anlytical proof of concept with limited physical testing for validation purposes, which categorized it as a TRL 3 technology. While advancing the technology in terms of maturity, there was also a desire to test PRSEUS as an enabler for the HWB centerbody configuration. If local loading conditions of the most critical load cases could be withstood without failure in an integrated skin-shell centerbody assembly, it would be seen as a validation of this centerbody configuration and assumptions made regarding the HWB itself. With sufficient resources, a "building-block" experimental approach was designed with the HWB centerbody in mind to achieve this goal. The approach, shown in Fig. 9, begins with trade studies to characterize performance against SoA composites, which was discussed in the previous subsection. From this model and the results obtained through structural sizing, internal loading conditions were decoupled and the local sizing results were tabulated for each PRSEUS component in the centerbody. From top to bottom and left to right in Fig. 9, test article configurations and loading conditions become more complex, resulting in a Multi-Bay Box (MBB) test at the bottom right. This experiment was an 80% scale mock-up of the Boeing BWB-5-200G design used in the performance trade studies.

These experiments of the benchmark approach were all derived from a single HWB outer mold line (OML) design, with a single structural layout configuration and a vehicle section of interest already in mind. The question was posed in the previous subsection regarding the accuracy of scalar performance estimates throughout the HWB conceptual design space. The relationship between structural technology

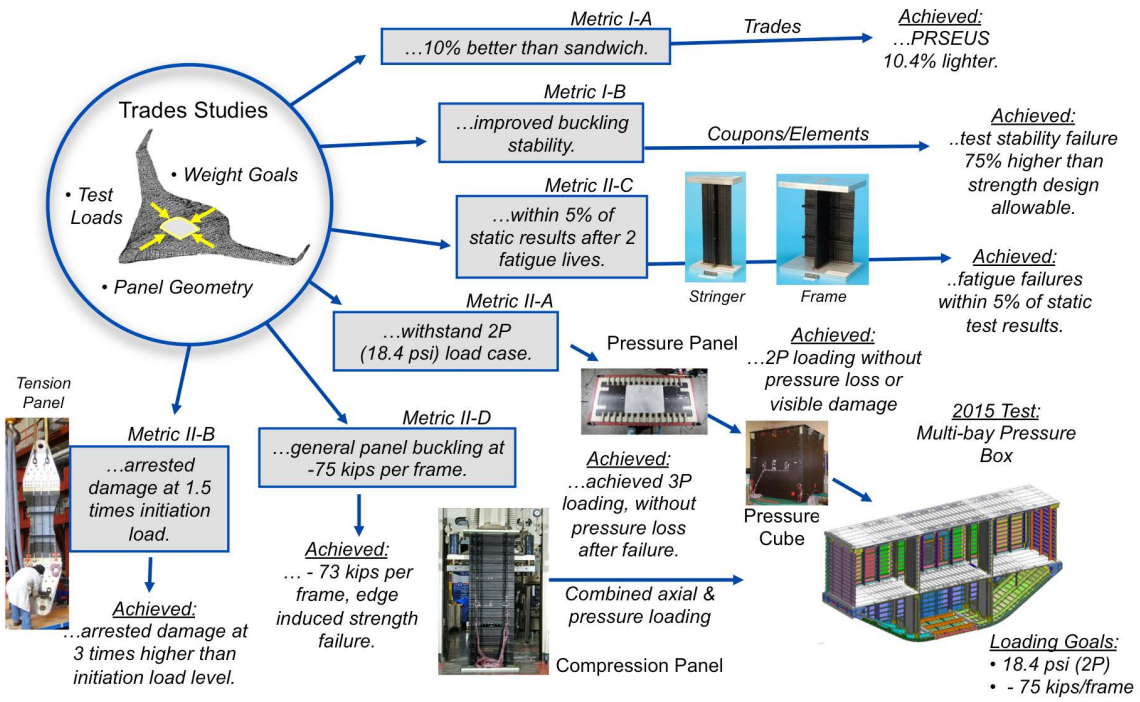

Figure 9: The "building-block" approach that was used for PRSEUS experiments during the NASA ERA program [39]

performance and the conceptual design space has implications for technology experiments as well. If experimental test articles and loading conditions were derived from a single OML design with a single structural layout, as was the case with the PRSEUS approach, are the results obtained and conclusions drawn from that experiment applicable throughout the entire conceptual design space? Additionally, does a single point design baseline need to be identified in order to derive design variables and assumptions for a technology experiment, or can this be performed as a function of a design space? Are answers to these questions dependent on the objective(s) of the experiment? The questions, challenges, and other issues examined in this motivation section are the foundation on which the research presented in this thesis is built. The following section molds these points of contention into a formal research objective, which guides the research approach presented in this thesis.

1.2 Problem Statement and Research Objective

1.2.1 Summary of Motivation

This section provides a review of the research motivation discussed in the previous section to provide context for problem identification, and an overview of the flow of information can be seen in Fig. 10. First, entities like NASA ARMD have set goals for desired performance and efficiency of consumer air travel in a forecasting exercise. Programs such as NASA ERA and FAA CLEEN are tasked with determining whether or not these goals are attainable, which relies on the conceptual phase of the aircraft design process – a phase in which configurations are relatively fluid. The environmental goals in Fig. 1 act as *Requirements* for conceptual design, and ERA provides the mission specifications in which these requirements are to be met. The *Conceptual Design* process, highlighted by light grey ovals, is a serial, iterative process that begins with conventional, state of the art concepts and technologies and moves toward more *Unconventional Concepts* and immature technologies if design feasibility cannot be achieved. Part of the design process when infeasibility occurs is technology forecasting, and it was shown in research supporting the ERA program that the hybrid wing body configuration exhibited the greatest potential in meeting the environmental goals set up by the program. Then, one of the final steps in the conceptual aircraft design process is *Technology Selection*. In the case of the HWB configuration, a structural technology is specifically desired to overcome HWB centerbody structural challenges and provide greater confidence in assumptions made regarding HWB performance.

The benchmark technology selection approach introduced in the previous section finds a baseline single point design within the conceptual design space that is closest to satisfying all of the constraints set up by environmental requirements. This approach aligns with the TIES method [49] that is presented in Sec. 2.2.1 and is representatively shown in the *Technology Selection* element in Fig. 10. However, for

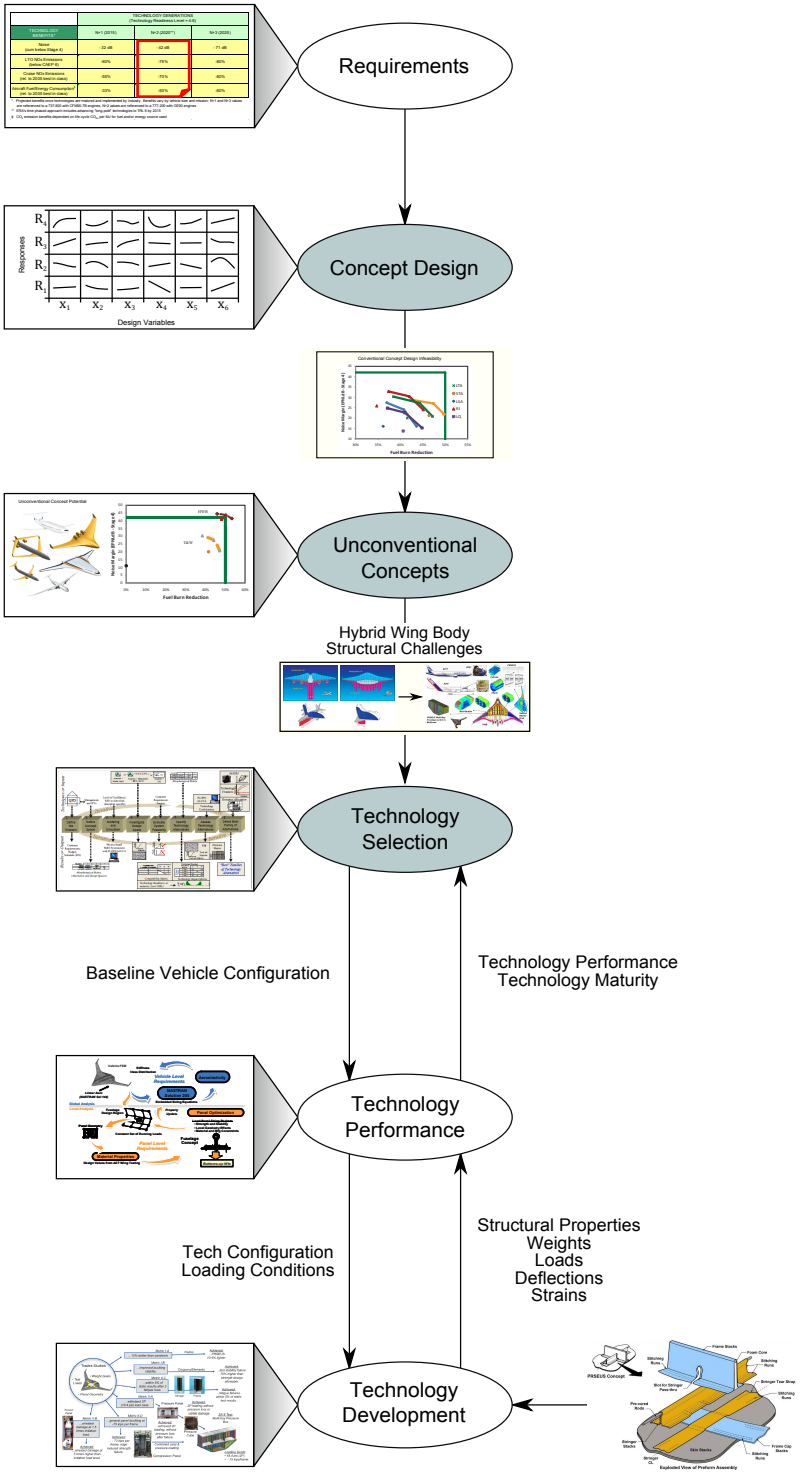

Figure 10: Summary of research motivation

the selection of structural technologies to commence, there must be some metric established with which to compare them. It was discussed that while there are many potential benefits of structural technologies, in an environmental context, the most relevant was their ability to reduce structural weight. This metric is an input to the systems level technology selection process, and it has a direct impact on fuel burn, while implicitly affecting noise and emissions. A potential metric that can capture the source of this implicit relationship with greater sensitivity is takeoff gross weight, W_{TO}. Since weight reduction is an input to traditional conceptual design models, another modeling framework must be used to generate estimates for aircraft level *Technology Performance*, i.e. structural weight reduction. The benchmark process required for technology performance estimation is at a somewhat higher fidelity compared to most full vehicle structural models, and its global-local sizing approach needs inputs from the *Technology Development* team. Since the HWB has no historical data from production aircraft to draw from and the PRSEUS technology was relatively immature, more detailed structural technology level experiments were needed in order to increase confidence in performance estimates and anchor them in reality. To help decide which experiments were to be performed, technology development in the ERA program drew on data provided by the performance estimation model. It can be observed, then, that the technology side of this motivating problem is centered around *Technology Performance Estimation*, with information flowing to and from *Technology Selection* and *Technology Development*.

1.2.2 Problem Statement

Along with Motivating Questions 1 and 2, several questions have been posed regarding the applicability of technology performance estimates and results from technology experiments that are derived from a baseline single point concept design. If the conceptual design (OML) changes, does the estimated structural weight reduction

for the technology also change? The outer mold line shape also dictates the shape of the internal structure and has a potential effect on the aerodynamic, inertial, and cabin pressure loads for a given load case. Are these effects significant enough to change the results of the structural sizing process for each structural configuration, i.e. baseline and technology, and in turn, the estimated technology performance? What consequences does a change in performance have on structural technology selection and experimental design? If a development program like NASA ERA is willing to invest millions of dollars into a technology, a more complete characterization may be desired to make decisions. Therefore, the research problem is defined as:

Problem Statement: Risk is introduced in decision-making for selection, implementation, and experimental design of a structural technology by a potentially limited characterization of its weight reduction performance.

The following subsection provides an objective for synthesizing a solution to this problem and discusses potential consequences and challenges that correspond to the development of that solution.

1.2.3 Research Objective

There are many challenges surrounding the problem of technology performance estimation and experimental design. Some have been previously mentioned, but a summary is as follows:

Multiple Levels of Design Spaces Inherently, this problem is difficult because the goal is to determine trends at a high level of conceptual design while operating at a low level detailed representation of the technology. Spanning these multiple levels requires thought and interpretation at every step.

Configuration Moving into the realm of unconventional concepts reduces the applicability of traditional design models. Even in traditional conceptual design, very little is known about the design of the structure - the knowledge from the structures discipline is embedded in the weights discipline and implicitly derived from historical data. In the case of the HWB, there are, however, sections that are similar to conventional tube-and-wing aircraft. The simple layout of the outboard wing structure makes it a close comparison to a conventional wing, while the trapezoidal wing lattice-like structure relates to a highly swept military fighter wing. These models can still be somewhat leveraged; however, the move must be made to higher order physics-based modeling with limited knowledge of the structural design. Validation of a full HWB vehicle structural model is also difficult without any historical weight data to compare. Additionally, the comparison of a structural technology to a state of the art baseline structural concept requires two function calls of the performance estimation model, since the baseline structure for comparison also lacks historical data and needs to go through the same weight estimation process.

Structural Modeling Manual generation of a single full HWB structural model is considerably time-consuming in its own right, but the investigation of a full design space for the OML is intractable without parametric automation. Investigation of the structural layout design space to make up for early design phase structural uncertainty is additionally taxing. The run-time for higher order structural sizing for an entire aircraft model is on the order of tens of minutes to hours, making sweeps of design variables that much more computationally cumbersome.

Technology Modeling Keeping in mind that data from performance estimation needs to be used for experimental design, the technology must be modeled with sufficient detail to not sever that connectivity. Maintaining detail in a

full aircraft model further intensifies the computational taxation for a single performance estimate. For example, the 15 design variables required to define the PRSEUS configuration represent degrees of freedom for every technology component in the full aircraft model.

Data Management Moving from a single point design to a design space is a combinatorial problem. For a single point design, it is necessary to collect internal loads, failure modes, technology design variables, weight, and other information from *every component* in the aircraft structure. This can be upwards of hundreds of parameters for hundreds of components that could influence structural technology experimental design. Expanding this to a design space is a challenge in data management. Translating technology performance for implementation beyond a single scalar requires planning as well.

Miscellaneous Other issues exist that can affect this problem too. For example, decisions are not necessarily made based on performance or cost - there may also be politics involved. If a decision is made based on extenuating circumstances, is there a significant impact on performance estimation and experimental design?

A solution to the problem that can address these challenges requires a systematic process, because the outcomes can be technology dependent and configuration dependent. Therefore, the objective of this research is to:

Research Objective: Develop an approach to systematically characterize structural technology performance at the aircraft level to enable implementation in conceptual design and selection of suitable experiments that add the most value to advancement of the technology.

This approach should also involve quantifying potential risks of making decisions with limited technology performance information to determine the significance of the

problem. If the approach enables decision-makers at the systems level and technology level to 1) generate new observations that they were otherwise incapable of obtaining, 2) reduce risk in implementation of structural technology performance in conceptual design, and 3) reduce risk in the design of structural technology experiments, then the research effort is considered a success. The approach is intended to avoid a costly realization of late-phase design infeasibility and redesign due to ill-informed implementation of a structural technology.

1.3 Thesis Organization

There are many concepts that were introduced in this chapter in order to facilitate a basic understanding of the problem and objective of this research. Greater detail can be found in the following chapters regarding these ideas. Benchmark processes have been introduced and eluded to for technology selection, technology performance estimation, and experimental design. These elements are organized into a problem framework in Chapter 2 and synthesized into a single instantiation of a benchmark process within that framework. Identification of gaps in the benchmark processes is discussed in Chapter 3, as well as questions and hypotheses that comprise the research formulation. This chapter also describes the framework in which the synthesized methodology, described by the research objective, operates. Implementation of the methodology is presented in Chapter 4. Experiments and results regarding structural technology performance estimation are shown in Chapter 5, and impacts of the functional relationship of performance with the aircraft OML on conceptual design are discussed in Chapter 6. Details of structural technology experiment design in terms of a functional structural technology performance are discussed in Chapter 7 and final conclusions are presented in Chapter 8.

CHAPTER II

BENCHMARK PROCESS

In Chapter 1, a problem was introduced for the selection, implementation, and experimental design of structural technologies. This chapter discusses in further detail how this problem is currently solved. Much of this benchmark approach is taken from Boeing and NASA studies from the ERA program and the development of the PRSEUS technology. In some instances, it is because of the challenges presented in Section 1.2.3 and lack of resources to address these challenges that the process exists in its current form. The approach synthesized throughout this chapter augments processes from the ERA program with methods from other areas of research that align with the objectives and level of complexity of the NASA ERA research.

First, the architecture of setting up structural technology performance estimation is presented, and each subsequent section in this chapter shows the benchmark process for each element of that architecture. Although many of the examples and characteristics of the process for each element are shown in terms of PRSEUS, the benchmark is not just applicable to this technology or S/RI composites alone. The architecture itself is not model dependent and it is anticipated that it can be used for any structural technology with the following characteristics:

- has a quantifiable impact on structural weight, either directly through technology properties or implicitly through design assumptions,
- requires higher order vehicle level structural modeling for weight predictions,
- can be modeled with simplified aggregate, or "smeared," shell properties in a structural model.

For example, a structural repair technology may not be suited for the type of architecture described in the following sections, unless its effect on design assumptions was able to be effectively characterized in terms of material and sectional properties. The ability to characterize a structural technology in a manner that can be implemented to an appropriate vehicle structural model is one of the basic assumptions for this approach, i.e. there must be a way to implement the technology in an aircraft structural weight estimation model. A full synthesized approach based on methods from the benchmark process of each element is introduced in the last section of this chapter. This process is the basis of comparison for the research formulation in this thesis.

2.1 Problem Architecture

The architecture for the benchmark process presented in this chapter is shown in Fig. 11. This is the generalized framework in which information is passed and each of the three elements – Conceptual Design, Technology Performance, and Technology Development & Demonstration – has a specific task and process that is currently used. Conceptual design in this architecture, shown on the left, represents the process of 1) performing trade studies to explore the design space and find trends, 2) determining design feasibility as a function of requirements, and 3) selecting and implementing technologies if needed. As previously described, in order to select and implement technologies, performance estimates are required in a form that is applicable to the systems level conceptual design models.

Technology development and demonstration (shown on the right), however, occurs at a lower detailed level. Performance at this level is defined by detailed technology metrics such as loads, panel weights, deflections, and strains, for example. These metrics cannot be directly applied to conceptual design to assess the technology's

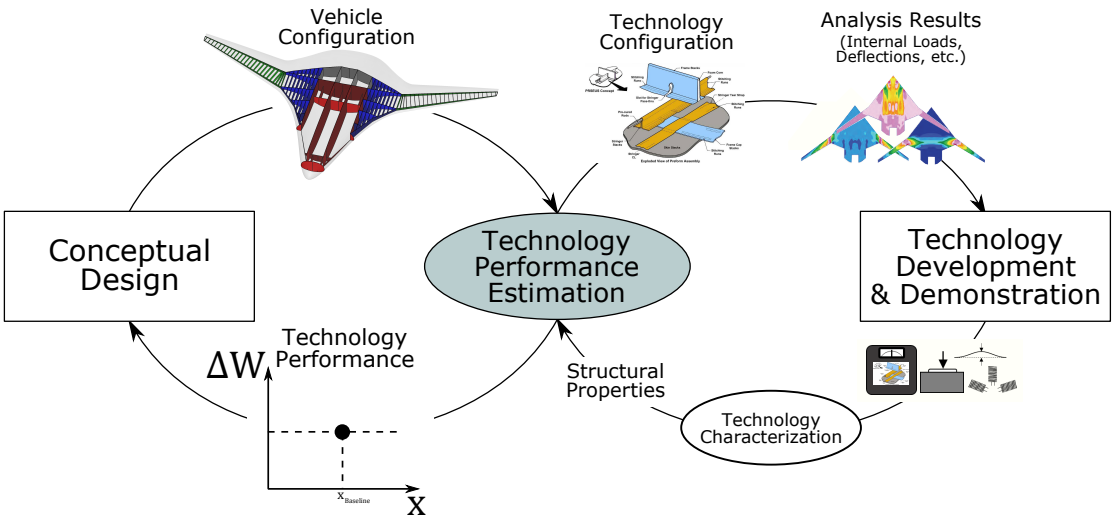

Figure 11: The connection between conceptual design and technology development is technology performance estimation.

impact on systems level metrics like fuel burn and noise. Similarly, operating conditions for detailed structural technology models and test articles in the development and demonstration process, i.e. forces, moments, and boundary conditions, cannot be derived simply from a vehicle mission analysis or global load cases defined at the systems level. Therefore, a transfer function is needed to connect the systems and the technology levels to translate the required information into useful forms. That transfer function is the *Technology Performance Estimation* element, and it represents the estimation of structural weight reduction for a technology in terms of the entire aircraft. The architecture is centered around this element and the flow of information exists as follows, beginning with its required inputs:

Conceptual Design → Performance Estimation From the systems level, the vehicle configuration, load cases, and other systems level assumptions are sent toward the technology level. This is generally the result of a technology selection process and the reason for passing the data is to establish the conditions in which the technology must operate. The vehicle configuration is generally the result of conceptual design: a baseline OML ($\mathbf{X}_{OML}$) and propulsion configuration.

Load cases are defined by the mission analysis and applicable regulations.

Technology Development → Performance The Technology Development & Demonstration element contains all the low level properties and detailed design information for the technology. When computational simulations and physical experiments are performed, technology level metrics are calculated/tabulated. This information is sent towards the systems level, along with any other published results that are applicable to the technology, to help characterize performance at that level. These metrics and parameters are not necessarily conditioned for implementation in a full vehicle structural model or conceptual design model. Therefore, it is necessary for the *Technology Characterization* step to translate this technology data into relevant structural properties that can be used in the models of the *Technology Performance Estimation* element.

The outputs of the *Technology Performance Estimation* element are driven by the inputs needed by the other elements:

Performance Estimation → Technology Development As described in Chapter 1, in order for technology level development and demonstration to take place, a technology configuration and its operating conditions are required. This information must be generated by the Technology Performance Estimation transfer function.

Performance Estimation → Conceptual Design Finally, vehicle level structural technology performance is calculated and can be sent to the Conceptual Design element to enable technology selection or for implementation in trade studies.

This architecture and flow of data was described generically for flexibility in modeling, depending on the technology, conceptual design configuration, or technology development objectives. The benchmark processes that follow are described both in generic terms and tailored to the PRSEUS test case.

2.2 Conceptual Design

The conceptual phase of aircraft design is responsible for translating customer requirements into a feasible, viable configuration. A brief description of the conceptual design process was provided in Chapter 1, and the main portion of the process relating to this research is the selection of technologies to help improve design feasibility. For a development program like NASA ERA, technical advancement of a portfolio of technologies with potential to help meet environmental goals was desired. Referring to the first motivating question, how were these technologies selected? This element of the architecture sets up the motivation for a comprehensive process for characterization of structural technology performance to enable selection and implementation of the technology. Technology selection, in and of itself, is a problem in decision making. While many decision-making frameworks exist, as it pertains to aircraft design and this research, the approach that aligns best with the benchmark process of structural technology performance estimation is the Technology Identification, Evaluation, and Selection (TIES) method [49]. An overview of the process is shown in Fig. 8, and it incorporates approaches for design space exploration (DSE), technology compatibility, and probabilistic assessments. This process is described to help better understand why certain data is passed to the *Technology Performance Estimation* element and what assumptions are embedded in that data.

2.2.1 TIES Method

The first two steps in the TIES process – 1) Define the Problem and 2) Define the Concept Space – are performed by the technology development program and were discussed in the previous chapter. A set of conceptual phase design variables is chosen for investigation and bounds are put on the space. This is done for each concept under investigation, e.g. conventional T&W, HWB, truss-braced wing (TBW), etc. The conceptual design tool that was used for research supporting ERA is called

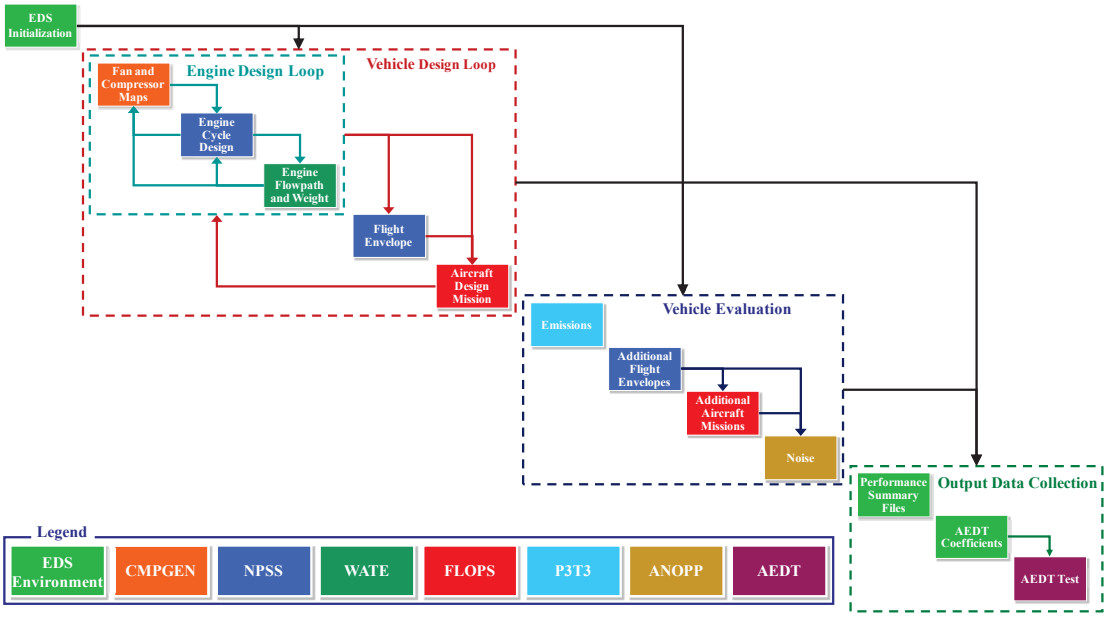

Figure 12: Environmental Design Space conceptual design framework [50]

Environmental Design Space (EDS), and it was synthesized as a comprehensive suite of design and analysis tools for assessment of aviation impacts on the environment for the FAA Office of Environment and Energy, Transport Canada, and NASA [50]. A design structure matrix of the framework is shown in Fig. 12. Many of the codes implemented in EDS enable higher fidelity propulsion assessments, but the main tool for the airframe is NASA's Flight Optimization System (FLOPS)[68]. This code contains empirical regressions for the weights discipline, which possess terms for structural weight, including primary load-bearing, secondary, and auxiliary.

The next step in the TIES method is to investigate the design space and examine trades between design variables and desired responses. The outer mold line is a subset of conceptual design variables that has the most significant impact on structural weight, so design variables relating to this shape, $\mathbf{X}_{OML}$, are of particular interest. Therefore, unless otherwise stated, $\mathbf{X}_{OML}$ and conceptual design space are herein synonymous. A notional plot of design space exploration is shown in Fig. 13, in which

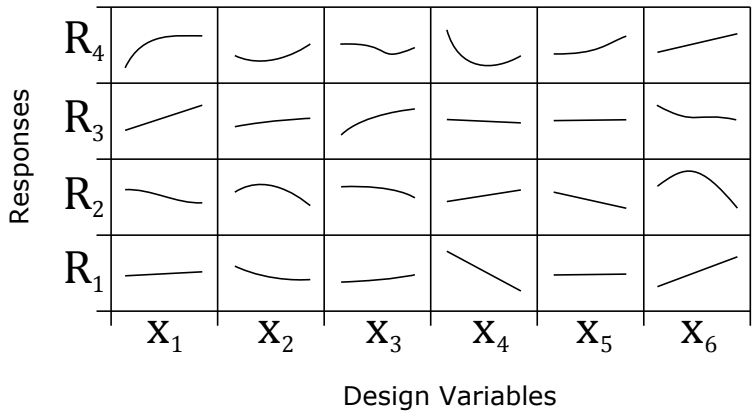

Figure 13: Notional conceptual design space exploration to determine trends in responses as a function of design variables

the x-axis represents the conceptual phase design variables ($x \equiv \mathbf{X}_{OML}$) and the y-axis represents the responses of interest R. Each of the lines represents a sensitivity of the response to the design variables at their current settings (x_i^*). Interactive exploration of this design space is enabled through statistical regression of design data. This data is generated by sampling the conceptual design environment, EDS, with an appropriate Design of Experiments (DoE) that captures the intended effects. Depending on the nature of the relationship between design variables and responses - ranges, continuous vs. discrete, linearity, potential dependent relationships, etc. - a suitable surrogate model form is chosen for the regression. A review of surrogate modeling techniques can be found in Reference [98]. There are many approaches to generating these approximation functions, depending on variability in the phenomena [26], prior knowledge [17], and each has its own hyperparamters which must be tuned to the particular problem or code [14].

Once the design space has been explored to verify trends, explore important trades, and potentially reassess design space limits, system feasibility is assessed through a

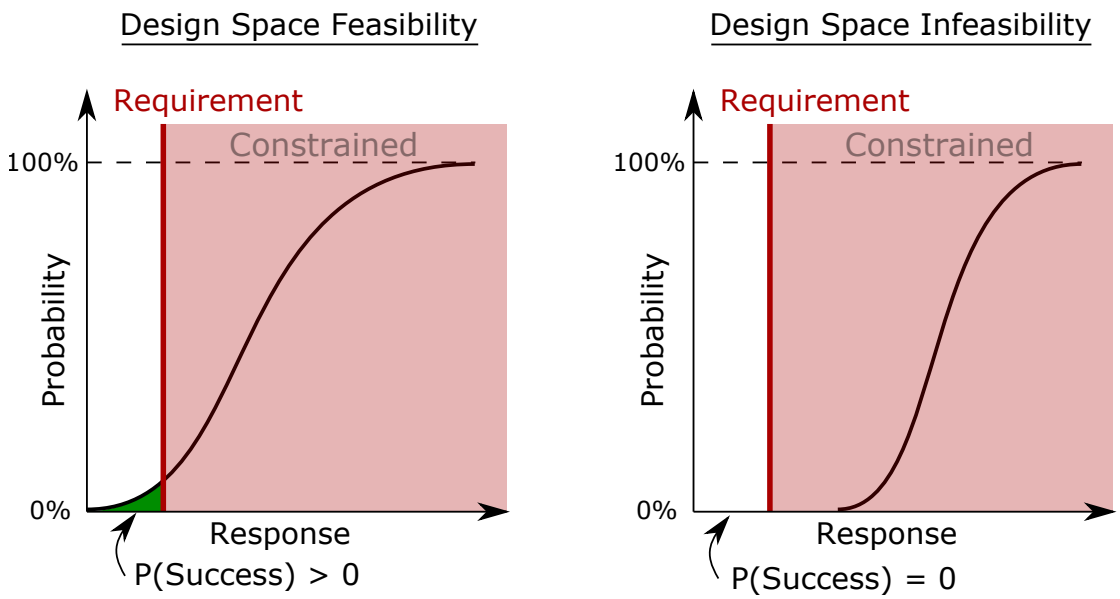

Figure 14: Notional metric CDFs for probabilistic assessments of design feasibility

probabilistic approach (Step 5). A Monte Carlo simulation is performed on the surrogate models, using uniform distributions of the design variables, to generate histograms, or discrete approximate probability density functions (PDFs), and cumulative distribution functions (CDFs) of the responses. The response (metric) CDFs represent the entire design space and are checked against the conceptual design requirements to show the probability of success that a feasible solution can be found. This is shown notionally in Fig. 14. If there is an infeasible metric, this is also a way to quantify the gap between the requirement and a desired level of confidence of design feasibility that needs to be filled by implementation of technologies. If infeasibility exists and technologies are required, a baseline conceptual design point for technology infusion is determined through optimization using a desirability function [18]. The process, up to this point, is representative of the tasks performed in the first three elements of the motivation summary in Fig. 10, i.e. *Requirements*, *Concept Design*, and *Unconventional Concepts*.

The TIES method as described thus far is an exercise of characterizing the design

problem at hand to set the motivation for selecting technologies. Technology selection is represented through Steps 6 through 8, and these elements are most applicable to this thesis research. A set of potential technologies is identified and characterized in Step 6. Down-selection of hundreds of technologies was required for the ERA program, and eight were chosen for integrated technology demonstrations (ITDs) of Phase 2. A subset of the total list of technologies can be found in categories in deterministic [94] and probabilistic [44] technology assessments for ERA. There are two main parts of the characterization for the entire technology portfolio: defining technology impacts and compatibility. Technology impacts must be characterized in terms of responses of the conceptual design tool so that they can in turn be included as terms in the surrogate models. For structural technologies affecting structural weight, these terms already exist as inputs to the FLOPS component of EDS and are easily implemented. Characterization of impacts also include degradation to other metrics, if it exists, in addition to the projected benefit. A better understanding of potential degradation in the operating environment is part of the reason for further technology development and demonstration, i.e. a more complete understanding of the technology. Compatibility is simply defined as a Boolean between technologies. Both characterizations are organized in matrices: the Technology Impact Matrix (TIM) and Technology Compatibility Matrix (TCM).

Once the technology space is defined, technology impact forecasting (TIF) can be performed [66]. This is an exercise in design space exploration for the technology impact space, and it can be performed both deterministically and probabilistically to account for distributions in technology performance representative of each technology's TRL. The last step is to select the best family of alternatives, and this is where the decision-making process is implemented. The benchmark approach is a multi-attirbute decision making technique (MADM) called the Technique for Order Preference by Similarity to Ideal Solution (TOPSIS) [102]. Similar to the desirability

function previously mentioned, TOPSIS uses an overall evaluation criterion (OEC) to translate multiple objectives to a single objective [20]. Each of the contributing objectives (metrics) are weighted in accordance to preferences of the decision maker, and an ordered list of technology portfolios is the outcome. Further information for multi-criteria decision making techniques can be found in References [103, 115], which discuss applicability for multiple types of problems.

A baseline conceptual design, $\mathbf{X}^*_{OML}$, now exists that has been infused with technologies. Before taking this configuration to preliminary design or before making the final decision on which technologies to pursue in the development program, the design space is re-investigated with one or more of the top technology portfolios. DSE at this stage with a specific technology combination captures any enabling phenomena of technologies due to vehicle resizing that would otherwise be overlooked. This has been mentioned previously as *implementation* of the technology in the conceptual design space, and the same values are used in the TIM and TCM from Step 6.

2.2.2 Summary of Observations

The TIES approach follows a generic top-down decision support process presented in Reference [65] and shown in Fig. 15. It presents a framework to generate data at the conceptual design level to help make decisions for selection of technologies. How are these technologies discovered and how are their impact factors and correlation/covariance with other technologies and with the conceptual design variables determined? If this information is gathered from literature, are enough details provided to generate a TIM and TCM or does other off-line modeling need to be done to supplement literature findings? Lack of knowledge regarding technology impacts and all the factors in the conceptual design process that affect it could present risk in the selection and implementation process. A probabilistic assessment based on technology uncertainty due to immaturity was discussed to account for this lack of knowledge, but

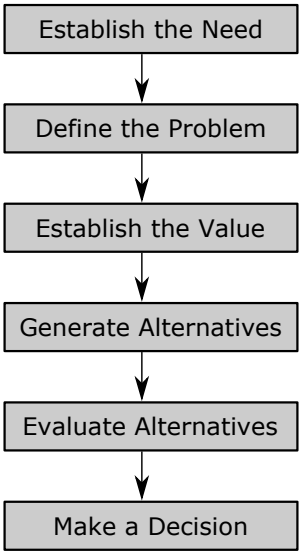

Figure 15: Top-down decision support process

how is the probability distribution for a technology generated? Formulations have been identified in References [27] and [38] that quantify uncertainty for proper implementation in conceptual design and for selecting technology development tasks. Another potential avenue that addresses uncertainty in compatibility is to investigate technologies concurrently under the same modeling and evaluation platform, similar to the integrated technology demonstrations (ITDs) of the NASA ERA program. If technologies are analyzed using those same assumptions, the interdisciplinary effects could potentially be accounted for. Furthermore, a common modeling and evaluation platform supports determining whether or not technology effects are additive or if there is any covariance between effects. These issues highlight the importance of the process by which technology performance is quantified in addition to the performance results themselves.

2.3 Technology Performance Estimation

The architecture presented in Section 2.1 shows that the *Technology Performance Estimation* element connects the systems level to the technology level. This gives

the performance estimation task the significant pivotal role of transforming the information that must go in and come out of each other other elements into usable forms. It has been mentioned that technology performance at the aircraft level is logically defined by its ability to reduce structural weight, because this is consistent with input parameters in conceptual design models. Therefore, this metric helps conceptual designers and technology development program managers help make decisions on selection and implementation of the technology. However, to assess performance, a basis of comparison is required.

The baseline for comparison is a very important definition because it also must be consistent with conceptual design models, especially empirical models built from historical data. The following convention for aircraft level structural technology performance was used in this research:

Structural Technology Performance

Reduction in structural weight $\equiv \Delta W_S$

$$\Delta W_S = W_{S,B} - W_{S,T} \tag{4}$$

---

where $W_{S,B}$ is the airframe structural weight of an aircraft implemented with baseline structure, and $W_{S,T}$ is the airframe weight of an aircraft implemented with the technology. This convention was used so that "increased performance" could be denoted as an increase to the value for ΔW_S, and therefore, positive values of performance denote a decrease in structural weight. Implementation of performance impact in conceptual design, using "k" to be consistent with the TIES method, is defined as a scale factor on weight, or:

$$k_{ST} = 1 - \frac{\Delta W_S}{W_{S,B}} = \frac{W_{S,T}}{W_{S,B}} \tag{5}$$

In the NASA conceptual design tool FLOPS, historical data points for traditional T&W aircraft regression models encompass airframes that were built with some type

of thin-shelled skin-stiffened aluminum. For implementation of composite structures, a weight reduction factor is typically applied itself. Therefore, proper definition of baselines is important to avoid potential mishaps in bookkeeping. For example, consider traditional conceptual design models that were generated with aluminum-based aircraft configurations; however, the baseline chosen for higher fidelity technology performance estimation was a composite structure. In this case, technology performance is defined as:

$$\begin{aligned} \Delta W_{S,total} &= W_{S,CD} - W_{S,T} \\ &= (W_{S,CD} - W_{S,B}) + (W_{S,B} - W_{S,T}) \\ &= \Delta W_{S,B} + \Delta W_{S,T} \end{aligned} \tag{6}$$

where $W_{S,CD}$ is the structural weight estimated by the traditional conceptual design model, and $\Delta W_{S,B}$ represents performance of the composite baseline over the aluminum "baseline" in the traditional conceptual design model. This scenario can potentially occur for the HWB, even though an "as-built" baseline does not exist. FLOPS contains regression equations for the outboard wing section based on conventional wing (aluminum construction) data. If a structural technology like PRSEUS is implemented on the HWB outboard wing but compared to a baseline composite during high fidelity structural weight estimation, then Eqn. 6 is applicable. Similarly for the HWB centerbody, Eqn. 6 must be used if the higher fidelity SWE baseline does not match the regressions that were built in FLOPS based on FEA performed by Bradley [10].

With a definition of structural technology performance in place, how does its estimation help facilitate the transfer of data that is required by problem architecture? This section introduces key attributes of the *Technology Performance Estimation* element and synthesizes them into the benchmark process. This process includes the *Technology Characterization* element shown in Fig. 11 because its implementation

is highly integrated in the performance estimation process. First, benchmark structural weight estimation is discussed for the generation of $W_{S,B}$ and $W_{S,T}$. Next, design characteristics of structural technologies are presented to better understand the applicability of performance estimation. Then, specific features of the test case structural technology (PRSEUS) are presented for provide context for characterization and implementation in the structural weight estimation process. Finally, the full benchmark process is presented and observations are made regarding benefits, drawbacks, and potential areas of improvement.

2.3.1 Aircraft Structural Weight Estimation (SWE)

Structural weight estimation modeling capabilities – in the context of technology performance – are completely dependent on input data and its assumptions. Revisiting the architecture Fig. 11, the first source of data is the *Conceptual Design* element, and it was established that the technology impact, k_{ST}, must be characterized for the entire aircraft to enable selection. Implementation in *Conceptual Design* models, however, required performance to be broken down by aircraft section. This establishes some of the necessary outputs for structural weight estimation. However, from the data passing descriptions in Section 2.1, it can be seen that the weight estimation model must be scoped to conceptual level assumptions for the full aircraft while also considering detailed structural property inputs from the technology development level. With these two requirements, this subsection investigates the potential modeling options available.

2.3.1.1 SWE in the Conceptual Design Phase

In the conceptual design phase, very little is known about the aircraft beyond requirements it must adhere to and its general configuration. The goal of the structures (weights) discipline in conceptual design is to provide reasonably accurate weight estimates in terms of empty weight, useful load, and gross weight. As the concept matures

through the design process, the role of this design group shifts to more detailed weight breakdowns, weight target management for each design group, and monitoring design changes and its effect on performance, stability, and controls. Traditional early phase weight estimates were generated without much knowledge regarding structural layout, systems configurations, etc. because of conventional statistical regression models from a historical database of production aircraft [101].

When referring to weights in the conceptual phase, takeoff gross weight (W_{TO}) typically provides a designer with a large amount of information and helps predict performance of the aircraft. Takeoff gross weight can be broken down into

$$W_{TO} = W_{crew} + W_{payload} + W_e + W_f \tag{7}$$

where W_e refers to operational empty weight and W_f refers to required fuel weight. Since crew and payload weights are dependent on requirements or design variables that will be instantiated in the design process, takeoff gross weight can be found through algebraic manipulation as

$$W_{TO} = \frac{W_{crew} + W_{payload}}{1 - (W_e/W_{TO}) - (W_f/W_{TO})} \tag{8}$$

This implementation [87] is used because statistical regressions exist for empty weight fractions, and fuel weight fraction can be determined through a breakdown of the mission analysis. Operational empty weight is the portion of aircraft weight that includes the airframe structural weight (W_S), as shown in the breakdown in Fig. 16.

Three factors need considered when estimating structural weight: 1) configuration, 2) design requirements, and 3) intended technologies. These considerations will help choose an appropriate weight estimation approach from the following methods: *Introduction to Aircraft Weight Engineering* [101] identifies four main approaches to structural weight estimation for an aircraft:

Statistical Functional relationships between weight and global vehicle design parameters are developed through statistical regression of production aircraft data,

Analytical Physics-based approaches that consider the structural layout, loads, material properties, and failure constraints with some weight calculated with empirical relationships (quasi-analytical),

Actual design A more detailed approach in which all components are the aircraft are fully designed and the weight is determined as the product of volume and density for each part,

Policy-driven A more rare approach where weights are determined based on policies.

These are similar to the three-class categorization defined by Elham [21], in which Class I represents a fully statistical approach, Class II is a semi-empirical breakdown based on statistics and first principles of structural analysis, and Class III is a full finite element physics-based approach. While conventional conceptual phase weight estimation has been largely statistical in nature with limited use of other methods, analytical models are more widely required for unconventional configurations and advanced concepts in which historical data do not exist.

It should be noted that this discussion is in the context of structural weight estimation capabilities in academia. Although the approaches and methods used by private airframe industry are similar, industry weight estimates typically have less uncertainty associated with them because more resources and proprietary data are available. To increase accuracy in academic models, they can be calibrated with industry data; however, standalone trends between results of academic institutions and industry are consistent since they are based on the same basic principles. This research operates within academic limitations.

2.3.1.2 Conventional Statistical Weight Estimation

Developing structural weight estimation regressions for conceptual design requires that a database of vehicle weights is available. While early efforts for this task focused

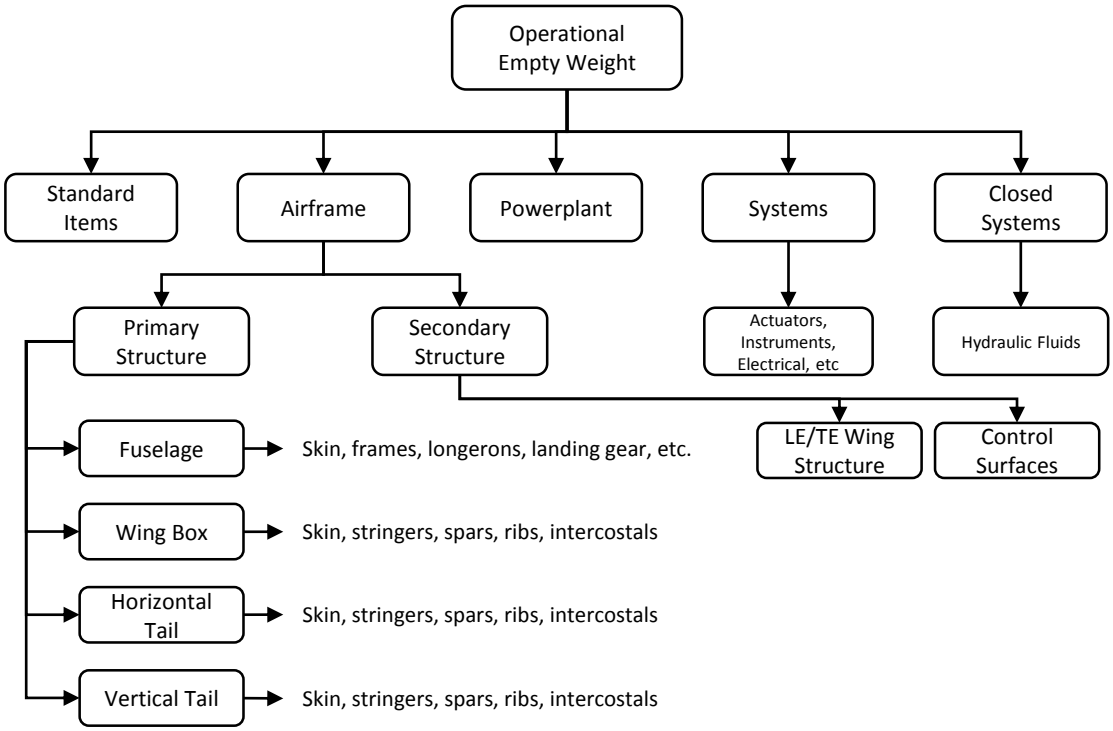

Figure 16: Breakdown of operational empty weight (W_e) for traditional T&W aircraft

on unit weight relationships, the logical progression was developing equations for each of the functional sections of the vehicle, i.e wing, fuselage, horizontal tail, vertical tail, and landing gear. These equations were built first upon an expected relationship between the weight metric and the conceptual level design variables. An example base equation was shown for wing weight (W_w) as

$$W_w = C_{sd} \left(W_{dg} N_z\right)^{n_1} S_w^{n_2} AR^{n_3} \Lambda^{n_4} \left({}^{t}/_{c}\right)_r^{n_5} \tag{9}$$

where C_{sd} is a "statistically determined constant," N_z is the load factor and W_{dg} is the design gross weight that together define required lift, S_w is the wing planform area, AR is the aspect ratio, Λ is the sweep (defined somewhere along the chord length), and $\left({}^{t}/_{c}\right)_r$ is the thickness-to-chord ratio at the wing root [101]. The parameters n_i are to be determined statistically with the historical database with least squares regression or a similar method. To examine examples of equations developed with this approach, see References [101, 87], and for an approach in which statistical parameters

are determined through principal component analysis for dimensionality reduction, see [90].

It is obvious to see that this type of a weight estimation approach belongs in the *Conceptual Design* element of the architecture. Input mechanisms for detailed structural technology properties are not available in conventional weight estimation models. The functional form of Eqn. 9, is notable, however, because it shows that structural weight is a function of the conceptual design space.

2.3.1.3 Physics-Based Approaches

The alternative to statistical weight estimation is developing analytical approaches, or Class II and Class III methods according to Elham [21]. Three fundamental features of analytical and numerical derivations of weight are defined as

Design Intent Functional requirements of the aircraft, which help define the loads,

Sizing Criteria Identification of structural properties, boundary conditions, and constraints, and

Production Design Translating calculated weight to expected production weight through calibration [101].

Using these features, Class II methods implement geometry, loading, structural analysis, and material property simplifications to come up with an analytical function that represents the structural sizing and weight estimation process. FEM-based approaches typically consider more detail in the process. To create a modeling environment capable of generating weight estimates as a function of conceptual design variables, a parametric geometry model of the vehicle shape is of paramount importance. From there, a structural geometry must be defined and loads are developed for the configuration. For the benchmark technology performance estimation approach, these features were not implemented, and this is further discussed later in the chapter. Through structural analysis, the externally applied loads are translated to internal

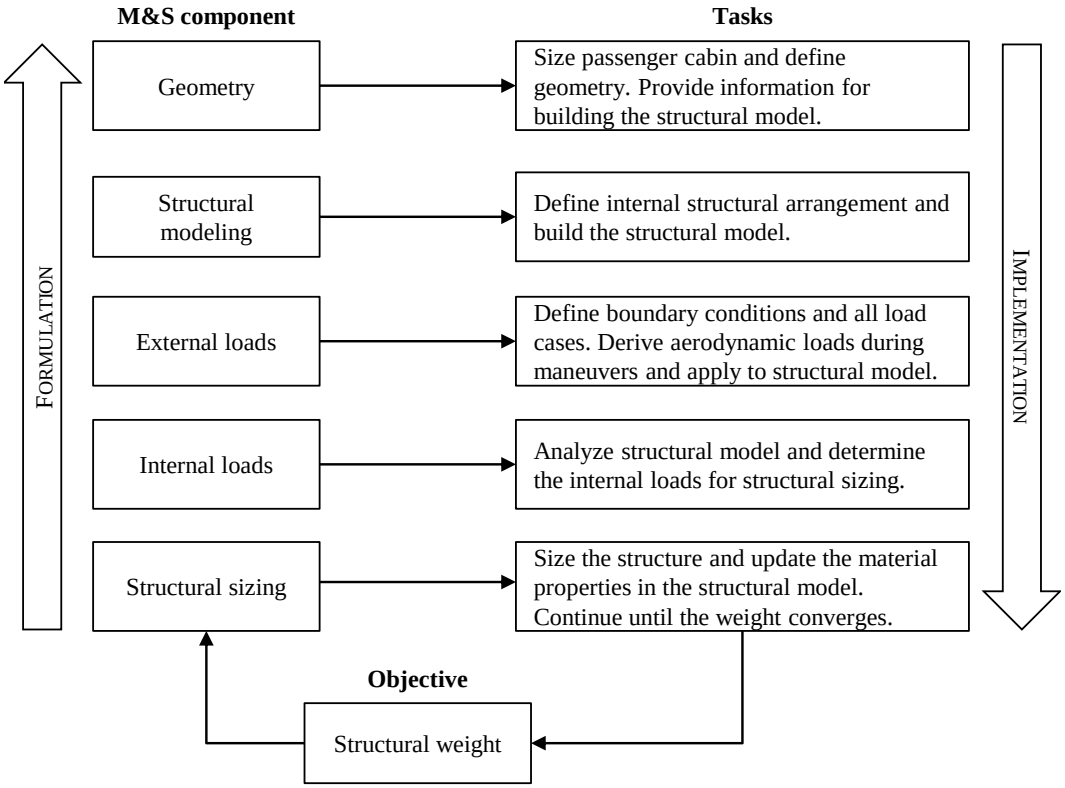

Figure 17: Formulation of generalized physics-based weight estimation [53]

loads which can then be sent to structural sizing, where detailed design variables are set to satisfy constraints. The final sized structure provides the weight through Eqn. 18. Formulation of this process by Laughlin [53] is shown in Fig. 17. The structural analysis and structural sizing tasks presented in this diagram are described in the following subsections with reviews of previous research in each of the areas.

Structural Analysis

With an OML and structural topology (layout) in place, the process shifts to structural analysis. This task requires: 1) load case development, 2) sectional and material properties, and 3) physics assumptions. Through structural analysis solutions, the externally applied loads are translated to internal loads, which are defined as forces and moments per unit surface area or thickness. If baseline values are already chosen for detailed structure variables, then stresses and strains can be examined.

In the conceptual phase, the number of load cases to be used in a structural weight

estimation approach can vary from a handful to hundreds, depending on the complexity of the geometry, the detail contained in requirements, and available computational resources. Some example types of loads include: maneuver and gust aerodynamics, inertia, pressure differential from the passenger cabin, fuel slosh and pressure, crashworthiness requirements, maintenance, actuator, landing and taxi bump, and many more. This information is derived from the conceptual phase mission analysis, regulations, and other assumptions about the configuration. The practical application of forces, moments, pressures, etc. based on these load cases is not necessarily a straight-forward process [78].

Firstly, it must be determined which loads are specifically accounted for in each case. For example, during maneuver loads, will inertial relief from the fuel tanks be modeled and what percentage of fuel is in the wing tanks? For a FEM-based approach, this is difficult to implement parametrically, depending on the geometry, mesh, and whether or not loads are generated from an outside source. For example, the translation of aerodynamic loads to the structure can be performed through multiple mechanisms:

Assumption of Lift & Moment Distributions This approach is used in most analytical approaches and some FEM methods, where based on a particular load case, lift and moment distributions are assumed which integrate to the total required lift from the wing/fuselage, HWB, etc. Then these distributions are either implemented in the analytical equations or addressed by the next approach.

Aggregation to Reference Points In a structural FEM, loads can be collapsed to points on the structure that promote easy translation for aerodynamic analyses and transfer the loads to the rest of the structure in a realistic manner. An example of this is collapsing lift and moment loads to reference locations on wing ribs that reside on a best-fit line through rib centroids. The point of

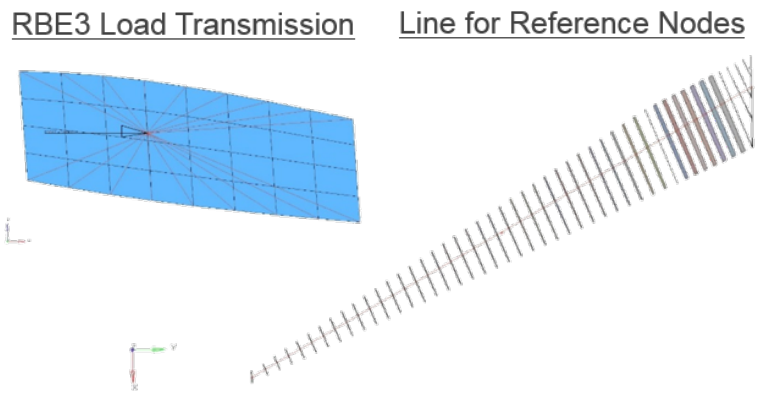

Figure 18: A reference line through the centroid of wing ribs to which aerodynamic forces are applied

this load application is then connected to the upper and lower edges of the rib through rigid body elements, as shown in Fig. 18.

Translation of Pressure Loads For cases like the HWB, in which the center section has thick airfoils and large chord lengths, collapsing loads to a point like the previous method is not an option - a more detailed load distribution is needed. In this case, the pressures calculated from a panel method or higher order computational fluid dynamics (CFD) model are applied directly to the structural mesh. However, an interpolation scheme is needed because aerodynamic meshes are typically generated with a much higher resolution than structural loads model meshes.

Next, the material properties must be defined so that realistic load paths through the structure can be identified. This process is coupled with the structural sizing because the stiffness of the structure determines how much load is passed through a particular component or section of the structural model. Stiffness is not completely defined until the detailed structure design variables, $\mathbf{X}_T$, are determined.

The solution method for structural analysis is dependent on how the model is set up. Some potential solutions include: linear elastic, nonlinear elastic, buckling, aeroelastic, and more. The implementation of these methods is fairly simple in a

FEM approach, where it is a matter of switching a command, so long as the elements and properties are consistent with the method. In the case of analytical solutions, the equations must also fit with the representation of the structure.

Structural Sizing

Once the internal loads have been developed through structural analysis, the structure needs to be sized so that failure does not occur within the load cases defined in the previous step. Typically, structural sizing is posed as an optimization problem in which the lightest weight solution is the most optimal. However, this is not universally true, as some problems call for optimization toward a target compliance (stiffness) [48] or target weight. In this research context, weight minimization is the objective of structural sizing and is posed as:

For all c Sizing Elements, C_i,

$$\begin{aligned}
\text{Minimize :} \quad & W_{S,i} \\
\text{with respect to :} \quad & \mathbf{x}_{T,i} \in \mathbf{X}_{T,i} \\
\text{Subject to :} \quad & g_j\left(\mathbf{x}_{T,i}\right) \leq 0 \qquad && j = [1, \ldots, m] \\
& h_k\left(\mathbf{x}_{T,i}\right) = 0 && k = [1, \ldots, l] \\
& \mathbf{X}^l_{T,i} \leq \mathbf{x}_{T,i} \leq \mathbf{X}^u_{T,i} && i = [1, \ldots, n]
\end{aligned} \tag{10}$$

where $\mathbf{x}_{T,i}$ is a vector set of design variables within the detailed structural design space $\mathbf{X}_{T,i}$, g and h represent functional constraints, and side constraints are given by the inequality in the last line of Eqn. 10. This formulation highlights the combinatorial problem of degrees of freedom for the sizing process, since $DOF = c \cdot n$. For instances in which analytical equations have been developed for weight based on first principles [5, 45, 36], an analytical solution of $\mathbf{x}_{T,i}$ may exist for the satisfaction of constraints. For example, for a qausi-analytical method (Class II 1/2) developed by Elham [22], equivalent plates are used to model the upper and lower skins, and the thickness is

determined by:

$$t_{s_i} = \frac{M/\sigma_{max_i}}{\eta_t t_{max} S_i} \tag{11}$$

where $i \equiv [upper, lower]$, M is the bending moment defined at the span station, σ_{max_i} is the stress allowable for each plate material, and $\eta_t t_{max}$ is the effective distance, which is a fraction of the maximum airfoil thickness t_{max}. For FEM approaches and other more detailed structural analyses, numerical optimization is most appropriate. Semi-analytical approaches have also been developed for unconventional configurations like the BWB [109] and strut-braced wing [31].

Gradient-based algorithms [97], linear programming, and genetic algorithms (GA) [96] have been shown to be effective for weight minimization, where GA is beneficial for optimization problems in which discrete laminates and other discrete variables are being optimized. The benchmark approach within the structural sizing software, Hypersizer [88], uses an enumeration, or grid search, method in which design variables $\mathbf{x}_{T,i}$ must be defined by lower bound, upper bound, and a desired number of permutations. Lower bounds are most often defined by minimum gauge constraints, which represent either a manufacturing constraint or a damage/lightning constraint for skin surfaces. Upper bounds are defined by limitations of materials and manufacturing. The total number of discrete designs are collected for each component and ordered from the smallest weight to the largest weight. Starting with the smallest weight, each design is then checked for applicable failure constraints based on the component and loading conditions. As soon as all minimum required safety margins are met, where margin of safety is defined by:

$$M = \frac{g\left(\mathbf{x}_{T,i}\right)_{\text{allow}}}{g\left(\mathbf{x}_{T,i}\right)} - 1 \tag{12}$$

where $g\left(\mathbf{x}_{T,i}\right)_{\text{allow}}$ is a failure constraint equation defined with allowable material properties, then the design is considered optimal. There are some constraints and allowables that are defined for the design limit load (DLL) case and some that are

defined for design ultimate load (DUL). The difference between the two is defined by the factor of safety:

$$\text{DUL} = \text{DLL} \cdot \text{FS} \tag{13}$$

where the factor of safety (FS) typically takes a value of 1.5 for aerospace applications.

The constraints $g\left(\mathbf{x}_{T,i}\right)$ are defined by failure modes for both strength and stability. Stability based failures typically occur in compression, where slight imperfections, or out-of-plane loads cause divergence in the out-of-plane deflections for the structure. Buckling can occur for a skin-stiffened panel locally (between stiffeners), globally (full panel), or in the webs of the stiffeners themselves. Another stability failure mode is divergence of the entire wing, or flutter. These failures are checked either 1) within the structural analysis tool itself, 2) a third-party structural sizing tool, or 3) using offline empirical equations. The most typical strength failure check is through von Mises yield criteria, where the general form is defined by:

$$f_{VM} = \sqrt{\frac{\left(\sigma_{11}-\sigma_{22}\right)^2 + \left(\sigma_{22}-\sigma_{33}\right)^2 + \left(\sigma_{33}-\sigma_{11}\right)^2 + 6\left(\sigma_{12}^2+\sigma_{23}^2+\sigma_{31}^2\right)}{2}}. \tag{14}$$

where σ is the stress defined for each of the six degrees of freedom. This is a common failure check for metallic structures, but composite laminates, which are more prone to limits on strain, are commonly checked with the the Tsai-Hill or Tsai-Wu failure equations. The Tsai-Hill failure criterion is an anisotropic extension of the von Mises criteria defined at the composite ply level as:

$$\begin{aligned} f_{TH,F_{1,a}\geq F_{2,a}} &= \frac{\sigma_{11}^2}{F_{1,a}^2} - \frac{\sigma_{11}\sigma_{22}}{F_{1,a}^2} + \frac{\sigma_{22}^2}{F_{2,a}^2} + \frac{\tau_{12}^2}{F_{12,a}^2} \geq 1 \qquad \text{if } F_{1,a} \geq F_{2,a} \\ f_{TH,F_{1,a}<F_{2,a}} &= \frac{\sigma_{11}^2}{F_{1,a}^2} - \frac{\sigma_{11}\sigma_{22}}{F_{2,a}^2} + \frac{\sigma_{22}^2}{F_{2,a}^2} + \frac{\tau_{12}^2}{F_{12,a}^2} \geq 1 \qquad \text{if } F_{1,a} < F_{2,a} \end{aligned} \tag{15}$$

where σ is axial stress, τ is shear stress, 1 represents the axial panel direction, 2 represents the lateral panel direction, and F_a is the allowable defined for each direction. Implementation of the Tsai-Hill criterion is dependent on the sign of σ_{11} and σ_{22} because composite materials typically have two separate strength allowables for

tension and compression, respectively. The Tsai-Wu failure criterion sets up a single relationship that accounts for tension and compression directly:

$$f_{TW} = \left(\frac{1}{F_{1,a(t)}} - \frac{1}{F_{1,a(c)}}\right)\sigma_{11} + \left(\frac{1}{F_{2,a(t)}} - \frac{1}{F_{2,a(c)}}\right)\sigma_{22} + \frac{\sigma 11^2}{F_{1,a(t)}F_{1,a(c)}} + \frac{\sigma 22^2}{F_{2,a(t)}F_{2,a(c)}} + \frac{\tau_{12}^2}{F_{12,a}^2} \geq 1 \tag{16}$$

This criterion was developed with classical lamination theory and a ply oriented in a single direction [104]. Hypersizer contains a method in which these failure checks can be used without setting up discrete plies for a laminate. An "effective laminate" can be defined by a specific ply layup in which its thickness can be implemented as a continuous variable with orthotropic properties.

Allowables for these failure checks are typically defined by material properties, construction techniques, active load sets, etc. They are also generally defined as different values depending on the magnitude of load, i.e. tension or compression. Knockdown factors on allowables are used to account for phenomena that are not modeled in the structure, such as stress concentrations due to cutouts, etc. The final allowable implemented in structural sizing is generically defined as:

$$F_{final} = F_{nom}\prod_{i=1}^{n} q_i \tag{17}$$

where q is the knockdown factor that accounts for a specific phenomena (i) and n is the totaly number of knockdowns considered. These knockdowns have an adverse effect on weight By definition, $q \in [0, 1]$, where a value of 1 represents no change to the allowable and 0 would be complete and utter catastrophic degradation of the structure, similar to likening the structure to tissue paper. For example, a feature like stitched composite structure's ability to arrest damage would have a larger value for q than a SoA pre-preg composite with no such mechanism.

, but some unmodeled effects are accounted for through non-optimal weight penalty factors directly applied to the output weight. These penalties must be added to the

sized structural weight to account for some of the following: material added to prevent flutter and fatigue (if it is not directly accounted for), local increases in thickness at joints, non-optimum skin taper, discrete material layups and gauges, fasteners, cutouts, fillets, landing gear and engine mounting, etc. Airframers have a traceable process to account for these penalties either in the form of non-optimal weight factors and knockdowns on material allowables within the sizing process. To determine final predictions for "as-built" structural weight, it is a matter of enumeration:

$$W_{S,total} = \sum_{i=1}^{c} V_i \rho_i \left(1 + K_1 + K_2 + \cdots + K_n\right) \tag{18}$$

where i represents the component, V is the volume of the component that has already been structurally sized, ρ is the effective density of the material (direct or smeared), K defines the set of non-optimal weight penalties for component i, and c is the total number of components. These two factors, q and K, are mechanisms for the implementation of structural technology assumptions in structural weight estimation models.

If fixed weight is known for secondary structure like control surfaces and LE/TE structure, it can be added to the W_{total} as well [101]. This is represented by:

$$W_{adj} = \left(W_{est}\right)\left(M_{at}\right)\left(M_{si}\right) + W_{inc} \tag{19}$$

where W_{est} is the estimated weight, M_{at} is an advanced technology multiplier, M_{si} is a special impact multiplier, and W_{inc} is the constant weight increment. This approach is similar to the implementation of structural technologies in conceptual design, where M is equivalent to the k factors defined in the TIES method. Although through manipulation, it is potentially a method by which to estimate technology performance in the case that the actual weight W is known, and W_{est} is a reliable estimate for non-technology infused weight:

$$M_{at} = 1 - \sum_{i=1}^{n} \left(\frac{W}{W_{est}}\right)\left(M_{at}\right)\left(M_{si}\right) + W_{inc} \tag{20}$$

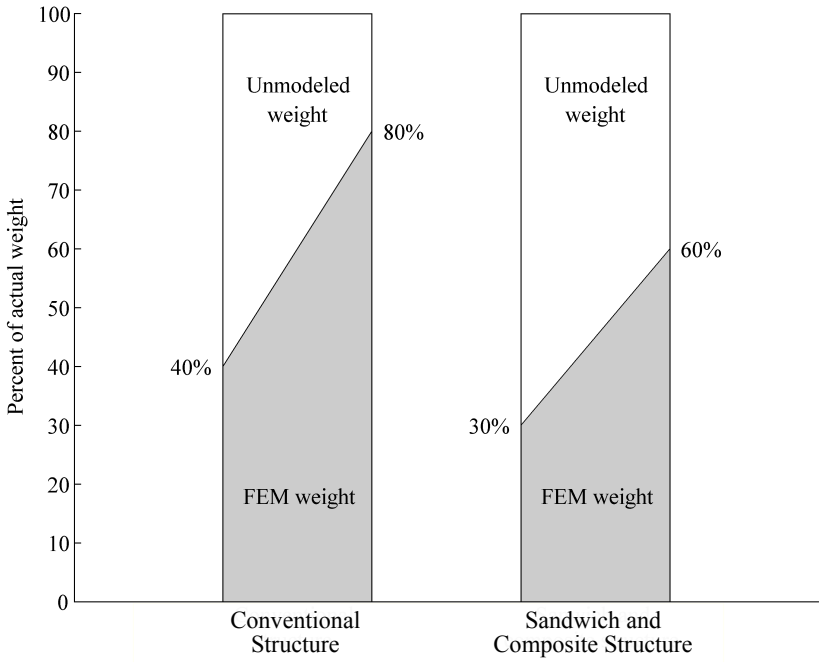

Figure 19: Trends of FEM sized weight compared to "as-built" structural weight [101]

This tuning parameter can then be applied to the conceptual design process similarly to References [112, 66].

Much of the more advanced optimization research in weight estimation has been in the field of multidisciplinary design optimization (MDO) [47], whereas weight estimation for the conceptual phase is more simplistic in nature. Structural sizing formulations for the conceptual phase can be drawn from these approaches because they are often required to be computationally efficient for the large number of function calls required for optimization [8, 110]; however, they are also limited in design variable ranges and most appropriate for preliminary design applications in which more design variables are locked for the configuration.

The physics-based approaches in this section were described somewhat generically. This was done as an attempt to survey methods that would potentially be applicable for any structural technology. Benchmark implementation of structural technology

performance estimation through SWE is discussed in the last section of this chapter. The next subsection discusses design characteristics of the PRSEUS technology in detail for a better understanding of its impact on structural weight and the structural weight estimation process. This technology is the foundation on which the benchmark implementation of structural technology performance estimation is built. For design characteristics of other structural technologies to assess their impact on structural weight, see the references listed in Table 1.

2.3.2 Design Characteristics of PRSEUS

The Pultruded Rod Stitched Efficient Unitized Structure (PRSEUS), as previously mentioned, was identified as a potential alternative for structural implementation on the HWB centerbody integrated skin-shell configuration. Thick sandwich composite structure was initially identified as a solution to withstand loading conditions on this HWB section because fatigue sensitive metallic materials were not a viable option. However, traditional pre-impregnated composites were not ideal due to potential of fastener pull-through failures and inadequate repair techniques. As an alternative, co-bonded and co-cured composites were investigated but required too many through-the-skin fasteners for structural viability [105]. A departure from these composite concepts, PRSEUS is a fully integrated stitched structure and can be seen in Fig. 6. The laminate used in the skin, stringer, and frame designs is a warp-knit fabric with directionally balanced AS-4 fibers, with the largest percentage in the direction of of the largest load, e.g. spanwise due to the bending loads in the upper and lower skin panels of the HWB centerbody. Rather than conventional pre-impregnated "pre-preg" composites, these laminates are assembled and stitched into a self-sustaining preform and then infused with resin with a process called Controlled Atmospheric Pressure Resin Infusion (CAPRI). Current PRSEUS laminates are built completely from AS-4 fibers simply to reduce fabrication costs in the development stages, but it

was acknowledged that other materials like higher performing IM-7 fibers could be used in sections dominated by tension loads [107, 59].

A foam core frame is used in the spanwise direction of the upper and lower centerbody skins to counteract the bending loads introduced from wing lift and pressure over the centerbody bay width. The longitudinal stringer has a composite pultruded rod dominated with 0° fibers to increase stiffness in that direction. This stringer passes through a slot in the frame, as shown in Fig. 6, for load path continuity and unitization. Laminates are stitched together through the web of the stringer and along the edges through the stringer tear strap, attaching the sub-assembly to the skin. Similarly, the frame is attached to the skin through stitch lines that run through a frame cap. This structure is used for all pressure containing surfaces in the HWB centerbody, whereas the ribs and bulkheads designed to carry shear and bending loads but not contain pressure are typically, but not exclusively, designed with traditional sandwich composite structure. For the vertical pressure containing surfaces, the orientation of PRSEUS panels can be in either direction [57, 105].

The PRSEUS design has characteristics which are beneficial to both structural performance and manufacturing, making it categorically both a configuration and manufacturing structural technology [107]. Although the scope of this research is limited to performance assessments, the manufacturing benefits will also be discussed here, because they drive certain design characteristics.

2.3.2.1 Stitching and Unitization

For skin stiffened panels, large in-plane and out-of-plane loads typically produce significant bending and shear stresses at the interface. It was found in the ACT program that stitching the stiffeners to the skin suppressed debonding and delamination failures at these interfaces while also suppressing damage propagation [32]. Velicki [105] identified that damage arrestment as “the single most important breakthrough

needed to realize the full load-carrying potential of carbon fiber based materials for large primary structures." While composite materials are less prone to fatigue than aluminum, an added benefit from stitching is the ability to use damage tolerant and fail-safe design philosophies rather than safe-life design that is required of traditional integral and bonded composites. To take advantage of this philosophy, redundant load paths needed to be implemented and proven through PRSEUS testing. If a local failure occurred or the a component suffered from barely visible impact damage (BVID), then the structure would continue to carry load and arrest damage propagation [35, 13]. If these mechanisms do not exist, more material is required in areas that are typically prone to damage. The suppression of laminate pull-off and delamination failure modes through composite stitching is another mechanism for weight reduction, as these constraints are less likely to be active for PRSEUS in typical loading conditions.

The unitization aspect of PRSEUS enables continuous load paths at stiffener-to-stiffener interfaces and decreases the stress concentrations at these intersections, further enabling weight reduction performance. A unitized structure also requires a smaller number of fasteners, decreasing the need for knockdowns on design allowables due to stress concentrations at fastener holes in addition to the added weight of the fasteners themselves. The unitized and stitched stiffener construction also creates a panel that can operate locally in the post-buckling regime. Therefore, local skin buckling is no longer a means of critical failure since the load is transmitted efficiently through the stiffeners [105, 108, 42, 7].

For the manufacturing side, the stitching method developed at Boeing enables one sided stitching and in turn, one sided inner mold line (IML) tooling. Stitching also allows for a self-sustaining dry preform, where only OML tooling is required to maintain shape during curing.

2.3.2.2 Warp-Knit Fabric and CAPRI

Carbon fiber composite materials have much higher stiffness-to-density and strength-to-density ratios compared to conventional aluminum aircraft materials [79]. This attribute, without other considerations of the design process, allows for more weight efficient design. Therefore, composite construction that behaves like damage arresting conventional aluminum construction takes full advantage of these better performing ratios. The design of the warp-knit fabric enables stitching and the benefits associated with it, and the CAPRI process eliminates the need for autoclave curing. Without the need for an autoclave, much larger panels can be fabricated, which saves weight through decreasing the number of required panel joints, and a reduction of manufacturing costs can also be achieved [105].

2.3.2.3 Foam Core Frame

The frame acts similarly to a hat stiffener, increasing the moment of inertia of the cross section to counteract bending. A foam core is used for both manufacturing and performance functionality. The foam expands during cure, providing an inner surface to contain resin and maintain shape. Vacuum bagging on the outer surface contains the resin on the outer frame surface. The foam core also helps maintain the shape of the preform before resin infusion by providing support to the rod stringer through the keyway slot. A secondary function is to provide stability to the frame web by resisting inward deflections during loading.

2.3.2.4 Rod Stringer

The rod stringer provides significant bending stiffness compared to traditional integral blade stiffeners or J-stiffeners. Its pultruded rod is dominated by 0-degree fibers to increase stiffness and strength in the stringer direction, and the pultrusion process ensures straightness of the rod to aid in stability by maintaining stringer shape. The stitching on the web of the stringer helps arrest damage and preserve preform shape

along with the frame keyway.

2.3.3 Benchmark Technology Performance Estimation

The elements that have been discussed in this section are now synthesized into a process that becomes the benchmark for comparison of structural technology weight reduction performance estimation. The formulation of this process is shown in Fig. 20, and it is built on the approach used to perform trade studies on the PRSEUS technology [105] – the core of which is the structural sizing process shown in Fig. 7. Because of the detailed structural characteristics of PRSEUS that contribute to weight which were discussed in the previous section, the physics-based Finite Element Model global-local structural sizing approach is an appropriate fidelity to assess how detailed characteristics manifest into changes in structural weight. The process begins with the information sent from conceptual design. Section 2.2.1 explained that during the TIES method, the benchmark technology selection approach, a baseline vehicle is determined through the desirability function for surrogate models of the conceptual design space. This baseline vehicle is the configuration portion of the data sent from conceptual design. It consists of a single point OML design $\mathbf{x}^*_{OML} \in \mathbf{X}_{OML}$, and it is assumed that a structural layout configuration $\mathbf{x}^*_{SL} \in \mathbf{X}_{SL}$ already exists.

Generating a *Structural Model* is the first step in the benchmark process, and this can be performed with any finite element model pre-processor, e.g. Altair HyperMesh [37] or MSC Patran [99]. That step is broken down in Fig. 21. First a geometry is required, which may need to be built from scratch or could already be provided in terms of a CAD model or previously generated FEM for the vehicle configuration. In the benchmark process used by Boeing, it is not evidently clear how the BWB-5-200G FEM was generated or what drove its structural layout. It is assumed that this configuration was the result of some previous study where the structural topology was optimized. Details of this model can be found in Reference [105] in Section 1.1.

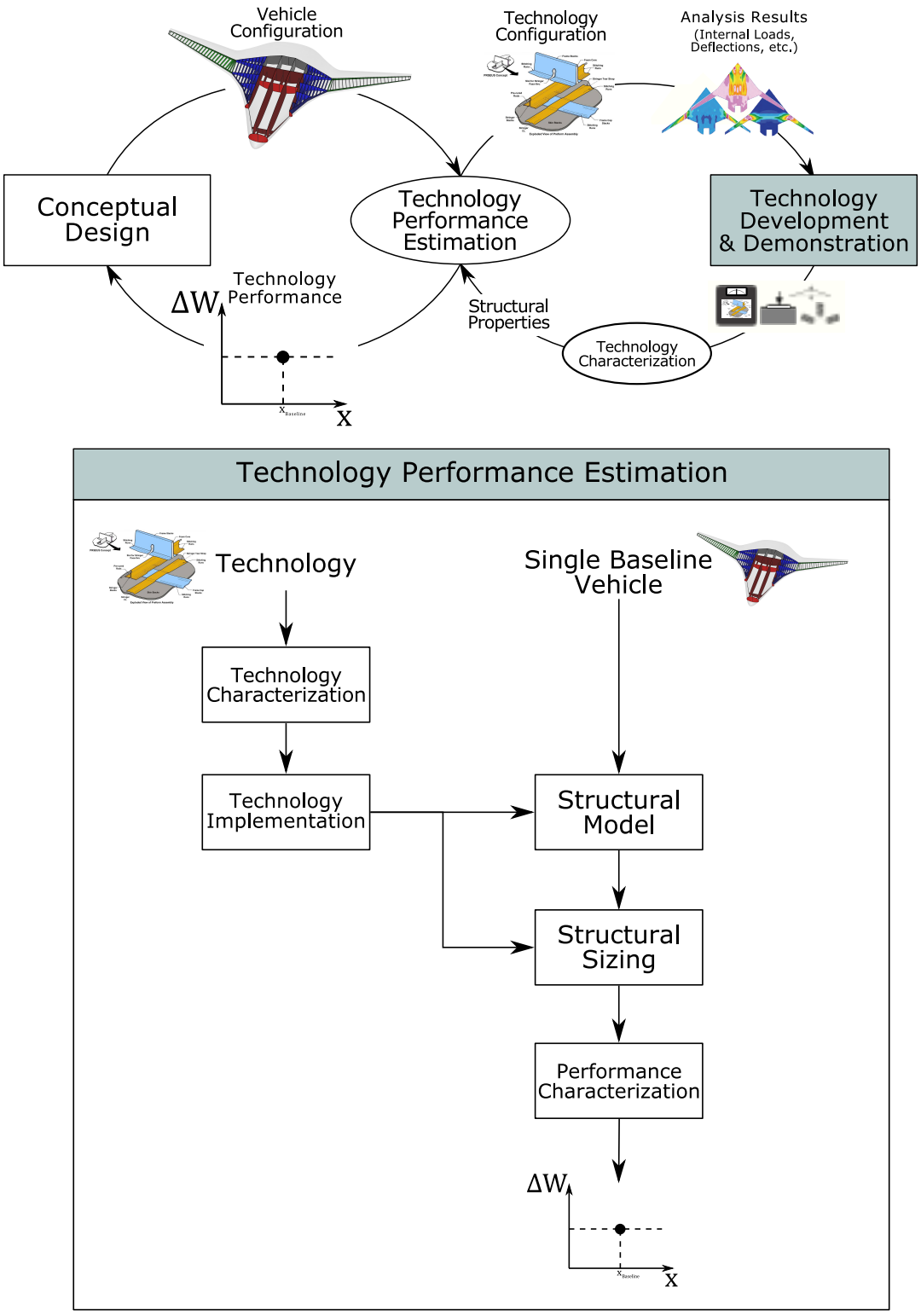

Figure 20: Formulation of benchmark process for technology performance estimation

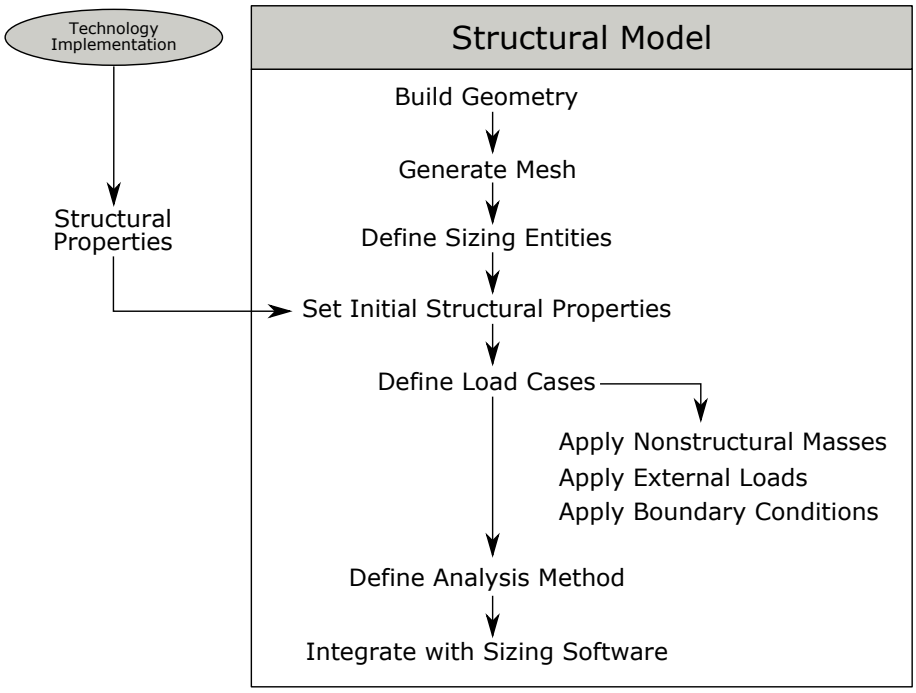

Figure 21: Benchmark structural model

Since most airframe load-bearing primary structure is configured as stiffened panels, in which the thickness of the structure is much less than the other panel dimensions, then surfaces are an appropriate representation of the primary structural components for a full aircraft loads FEM.

If a mesh is not already included in the model, then one must be created in the FEM pre-processor. The mesh resolution is important because a tradeoff exists between accuracy and computational speed as a function of the number of elements in a model. For an HWB configuration, see Laughlin [54] for a study in convergence as a function in mesh resolution. Then, an architecture must be chosen for the definition of sizing entities. There are multiple approaches in which this task can be performed, but the two most generally used in full vehicle aircraft models are a fully-stressed sizing scheme or component sizing. Fully-stressed sizing means that the *Sizing Elements*, C_i, from the optimization formulation are defined as each and every element in the model. The component sizing approach groups elements into logical

components based on boundaries, manufacturing expectation, etc. These components are then scaled together based on failure methods specified by the user, e.g. von Mises or Tsai-Hill. Since the benchmark structural sizing is a global-local approach with a third party structural sizing software, i.e. separate from the main analysis tool, the component sizing formulation must be used. This approach is described later in this subsection.

Next, an initial set of aggregate or "smeared" structural properties must be applied to the FEM. This takes the configuration of skin-stiffened panels, e.g. thicknesses and materials of skin and stiffeners, shape of stiffeners, and computes a unit density, unit stiffness, unit strength, etc. for each component. This information comes from the *Technoloogy Implementation* element of the architecture, which makes use of the structural sizing software Hypersizer to calculate these properties and update the global FEM, or in this instance, provide initial property estimates. Next, the load cases are defined for application to the structural model. Nonstructural masses for fuel and payload, externally applied loads from cabin pressurization or aerodynamics, and boundary conditions must be calculated and applied for each load case. This is where the other information from the *Conceptual Design* element of the architecture is required. The load cases and their required elements are determined by applicable regulations of the aircraft, the mission analysis, and other assumptions.

Finally, the structural model is complete when an analysis method is defined and it is integrated with the third party structural sizing software. In the Boeing process, MSC Nastran [70] was used for the global FEA portion of sizing. An optimization algorithm within Nastran was used that implements a static, linear elastic analysis method. Integrating the FEM with the Hypersizer sizing software is a fairly straightforward process, so long as components and properties were defined during FEM pre-processing with integration in mind. With a structural model set up, the benchmark process moves to the *Structural Sizing* step. This element is represented as

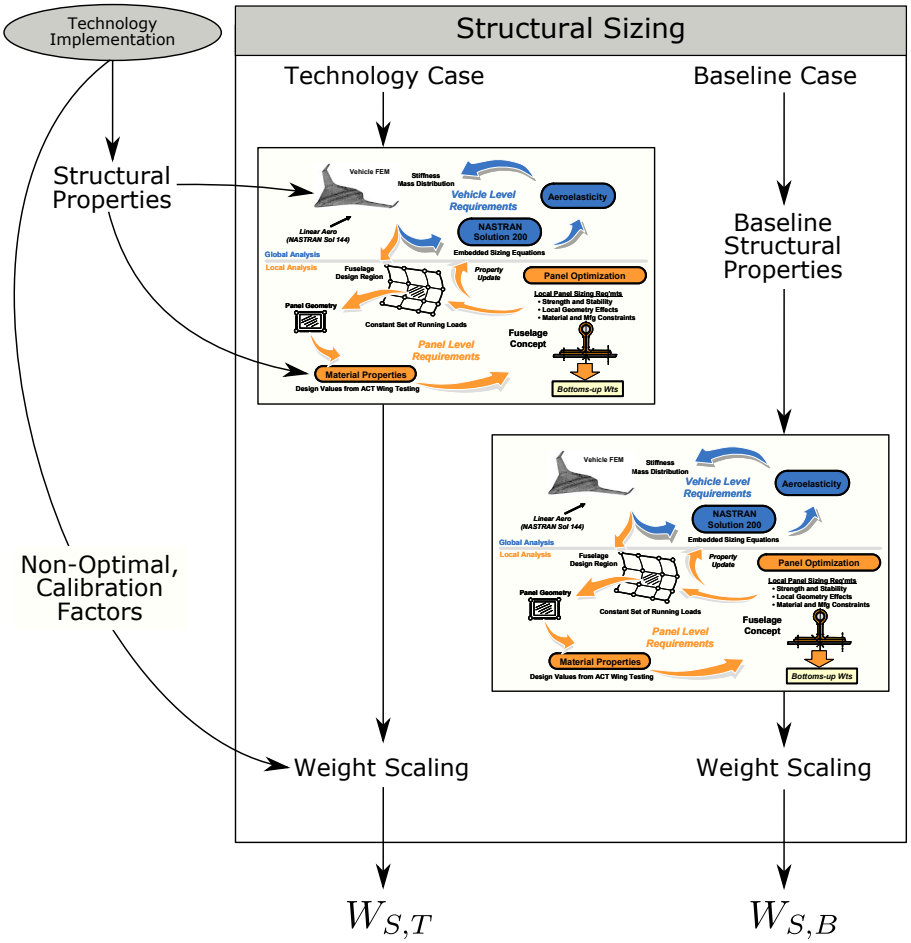

Figure 22: Benchmark structural sizing

one step for simplification, but it includes the processes mentioned in the *Structural Analysis* description in Sec. 2.3.1.3.

Figure 22 shows the Boeing benchmark structural sizing process from Fig. 7 in the context of creating structural weight estimates for both the technology and baseline structural concept configurations [57]. The structural properties that must be implemented in the sizing process come from the *Technology Implementation* element of the process and from literature for the structural technology and baseline, respectively. The same sizing process is used for both configurations, which starts with a function call of the global FEM. In this instance, the internal aerodynamic loads solver in MSC Nastran was used for calculations and loads transfer. A global weight

optimization is performed in Nastran, with static aeroelasticity accounted for. Once convergence of the global FEM occurs, an iteration of the local sizing is performed.

The internal loads of the converged global FEM are extracted within Hypersizer for each sizing component, and each component is defined by the "Panel Geometry" element. Detailed material properties are used for the local sizing portion of the process, which like the global FEM, are defined by the *Technology Implementation* element of the process and from literature for the structural technology and baseline, respectively for each sizing component. The "Panel Level Requirements" denoted in Fig. 22 are a set of failure criteria, for both strength and stability, defined in Hypersizer by applicable methods based on the geometry of the panel, stiffener arrangement, materials, and the local loading conditions of the panel. Local loading conditions refer to axial forces (N_x), lateral forces (N_y), bending moments (M_x, M_y), out-of-plane pressures(P), etc. Hypersizer definitions for constraints translate the failure criteria into margins of safety, M. For example, the Tsai-Hill condition shown in Eqn. 15 is implemented in Hypersizer as:

$$\begin{aligned} M &= \frac{1}{f_{TH,F_{1,a} \geq F_{2,a}}} - 1 && \text{if } F_{1,a} \geq F_{2,a} \\ M &= \frac{1}{f_{TH,F_{1,a} < F_{2,a}}} - 1 && \text{if } F_{1,a} < F_{2,a} \end{aligned} \tag{21}$$

A grid search approach, or enumeration method, which was mentioned in the previous section, is used for local structural sizing. This approach depends on a sufficient definition for upper and lower bounds and number of permutations for each technology level design variable, x_T. Once all components have been optimized, the estimated weight must be translated to "as-built" weight, listed as *Weight Scaling* in the last step of the process. This step is simply the implementation of non-optimal weight factors, K, and calibration factors, CF, to both technology and baseline structural concept. Each structure has its own assumptions that are used for this step and they are attributable to either literature or results from the technology development

process. For example, a non-optimal weight factor for stitched composite will be less than a metallic structure with bolted on stiffeners because less fasteners are required for the former, which can add a significant amount of structural weight.

The outputs of the structural sizing element, in terms of performance, are structural weights of both the technology- and baseline-configured airframes. These are also compiled in terms of the aircraft section, e.g. outboard wing and centerbody, for by-section performance definitions. Returning to Fig. 20, once *Structural Sizing* has been accomplished, then *Performance Characterization* occurs. In the benchmark approach, this is a very direct process in which Eqn. 4 is used for the total aircraft and for each aircraft section for selection and implementation in the *Conceptual Design* portion of the architecture, respectively. Although this performance is the main objective of the *Technology Performance Estimation* element, it is not the only valuable output data. The structural weight estimation model contains a multitude of relevant structural data on full-aircraft, aircraft section, and component bases. This data includes: weight breakdowns, weight per design load case, failure modes, technology design variable configurations, internal loads, etc.

On the technology side of *Technology Performance Estimation*, *Technology Implementation* through Hypersizer has been discussed. However, where does the information used in this element originate from? The *Technology Characterization* task takes the responsibility of translating lower level technology details to inputs relevant to the structural weight estimation model. The sizing process in Fig. 22 eluded to the source of initial technology characterization. From 1985 to 1997, a program existed at NASA Langley Research Center called the Advanced Composites Technology (ACT) program that performed research on textile composites in the context of airframe structures [19]. As part of this program, a stitched composite wing was fabricated for full-scale testing. Results from this research endeavor were used as the basis for material properties and design values for PRSEUS composites, although

their derivation is not directly addressed in the NASA contractor report [105]. This report, however, does provide values for knockdown factors on allowables and non-optimal weight penalties. These values represent the lessons learned in the ACT Wing program and the design assumptions that can then be allowed by PRSEUS. Therefore, it is accepted that *Technology Characterization* is an expert-driven process that takes results from technology development experiments and translates them to useful parameters in structural weight estimation.

2.3.4 Summary of Observations

Compared to other methods, a number of advantages and disadvantages exist by using this benchmark process to estimate structural technology weight reduction performance. The global-local structural sizing approach for weight estimation is particularly beneficial because it enables a significant amount of detail to be considered for the technology that would be otherwise unattainable for finite element modeling. This approach, however, increases the run-time of each function call because of the convergence loop required for internal loads. Additionally, the grid search approach for optimization at the structural component level is tedious and user intensive for defining the bounds and number of permutations for each technology level design variable. These parameters do not scale well with the global vehicle. For example, upper bound definitions of $\mathbf{x}_T$ for a particular passenger class may not be sufficient to create a feasible design for a larger passenger class, generating a structural design that is projected to fail. A grid search may also not find the true optimum, which can lead to artificial variability in technology performance estimation.

What the sizing approach lacks in resolution, it gains in traceability for technology development. While performance characterization is the objective output of this process, each sized structural component contains results useful in experiment design: technology design values, failure margins, local loading conditions, etc. This data is

particularly beneficial downstream in the more detailed design and analysis phases for the sructure. Also, even though the grid search may not find the true optimum, it does not risk converging to local minima. In the context of weight estimation for conceptual design, potential adverse effects due to a discretized sizing approach are limited and the approach tends to offer an added flare of conservatism for the early phase design process.

The "smeared" approach for implementation of a structural technology is a useful modeling assumption that simplifies the structural sizing process. However, if this assumption was implemented for global-only structural sizing, then scaling the thickness of a "smeared" component with aggregate structural properties loses traceability to the detailed technology design parameters, $\mathbf{x}_T$. In this formulation, the only design variable in the optimization defined by Eqn. 10 is the effective thickness of each sizing element, C_i, and this would be the only parameter that could be recalled from the design, slightly reducing the fidelity of the model. The ability to extract sized values for the detailed technology variables $\mathbf{x}_T$ for all components, as well as specific failures for each of the specific technology subcomponents, is important because it is one of the data sources that enables decision-making for experimentation at the technology development level. Also, these aggregate properties, e.g. effective density, effective stiffness, and effective strength, are derived from a nominal single point technology design configuration, $\mathbf{x}_T^*$. These effective parameters potentially vary in relationship to $\mathbf{x}_T^*$, which would have an impact on the structural weight and other sizing results.

One of the other potential disadvantages of the benchmark process is the definition of technology performance in terms of the structural layout. The structural layout remains constant between the baseline and technology configurations, but is this missing some potential of the technology to enable a more weight efficient structural topology? As discussed, the challenge of generating structural finite element models for an entire vehicle in an automated fashion is most likely what drove this

treatment of the structural layout. Generating one-off derivative models is still very time consuming even for a design parameter like rib spacing of a traditional two-spar wingbox. The mesh and surfaces must be completely discarded and regenerated from the underlying geometry definitions, which can become a very tedious, user-intensive process.

Setting up load cases and defining governing design weights for each load case is another challenge with this process for an unconventional concept like the HWB. Since traditional design models for the conceptual phase rely on historical data, how are weight breakdowns generated for these advanced concepts? Aerodynamics, structures, and stability all play a role in the convergence to a gross weight for a particular aircraft mission. Can conventional tube-and-wing empty weight fractions be used for the HWB in these types of models to provide an estimate? How are drag polars obtained to generate required thrust and fuel weight?

From the technology perspective, standards of design practices exist for the treatment of structural properties for given assumptions, e.g. knockdowns on allowables in the presence of cutouts, etc. However, for new types of structural features, like composite stitching of the ACT program and PRSEUS, an expert-driven process for characterization of technology implementation is required. In the benchmark process, that implementation is achieved through parameters like non-optimal weight penalties, Q, and technology weight reduction impact factors, k, but it requires some expert and/or experimental data input to configure.

Once the technology has been characterized and implemented in the benchmark weight estimation model, a performance value is obtained through comparison with a baseline structure. Is this scalar performance value applicable for any operating conditions the structure can be placed in? Do other assumptions regarding the model also affect performance? Considering the statistical structural wing weight relationship presented in Eqn. 9, conceptual design parameters, $\mathbf{X}_{OML}$, have an influence on the

total weight of this aircraft section. If two structural concepts are being considered, baseline and technology configurations, is the impact of $\mathbf{X}_{OML}$ on W_S the same for each? Combining this equation with structural technology performance definition in Eqn. 4,

$$\begin{aligned}\Delta W_S &= W_{S,B} - W_{S,T} \\ &= C_{sd,B}\left(W_{dg,B}N_z\right)^{n_{1,B}} S_w^{n_{2,B}} AR^{n_{3,B}} \Lambda^{n_{4,B}} \left(t/c\right)_r^{n_{5,B}} - \\ &\qquad C_{sd,T}\left(W_{dg,T}N_z\right)^{n_{1,T}} S_w^{n_{2,T}} AR^{n_{3,T}} \Lambda^{n_{4,T}} \left(t/c\right)_r^{n_{5,T}}\end{aligned} \tag{22}$$

where the subscripts B and T on the tuning parameters designate the configurations of baseline structure and structural technology, respectively. If all the hyperparameters in this equation with subscripts B and T are equivalent, e.g. $n_{1,B} = n_{1,T}$, then they effectively cancel each other out in the relationship with $\mathbf{X}_{OML}$ and ΔW_S. If the hyperparameters are not equivalent, then the relationship between $\mathbf{X}_{OML}$ and W_S does not necessitate the same relationship between $\mathbf{X}_{OML}$ and ΔW_S. Factors to consider in this supposition are: 1) how much of the regressed weight function is driven by conceptual design parameters themselves and how much is driven by the variation in structural configurations of the historical data points and 2) what the physical representation is of the tuning parameters marked with "B" and "T" subscripts in Eqn. 22. If a relationship does exist between $\mathbf{X}_{OML}$ and ΔW_S, and if that relationship between performance and OML is different across aircraft sections, is the functional form of structural technology performance significant enough to create risk in the conceptual design and technology selection process? Practical implementation of the weight reduction performance in conceptual design occurs for each section, i.e. HWB centerbody and wing, and therefore the identification of the existence of risks and their quantification are important to the design process.

2.4 Structural Technology Development

From the inception of an idea for an airframe structural technology, the single most important objective for its development is to be chosen for the design of an aircraft. Throughout development, demonstration, and certification stages, it is the role of the technology development team to advance the structural technology toward this objective by increasing its knowledge base and improving confidence in the estimates of its performance. The mechanism for the development team in achieving these is experimentation. In technology development, experimentation is a somewhat generalized term that incorporates simple thought experiments, computational experiments, and physical experiments. For structural technologies, the physical experiments can be assessments in performance, fabrication, assembly, repair, etc. This section examines the potential goals for experimentation, the elements of a structural technology experiment, and describes the benchmark process for designing/selecting a structural technology experiment.

2.4.1 Objectives for Structural Technology Experiments

There are multiple factors that help define the role that an experiment plays in the development process of a technology. Some examples include its current maturity (TRL), available models, previously performed experiments, parameter uncertainty, assumptions made regarding its composition and architecture, etc. A general framework for designing technology development activities was synthesized through a literature review by Jacobs [38]. This framework was comprised of three phases with increasing complexity of models and architecture:

Thought Experimentation This phase is a mental exercise in characterization which is argued logically and substantiated by literature, and it benefits from working through the details in the imagination before deciding to exert resources for execution. Information can be found on the philosophy of this type

of experiment in References [28, 67, 100].

Detailed Definition of Activities In this phase of the framework, all the details of the degrees of freedom for an experiment should be characterized and decided. The process follows again the top-down decision support process shown in Fig. 15. Parameters needing defined include independent variables that can be controlled by the technology team, dependent variables that need to be measured, and extraneous variables that need to be decided but have no effect on the metrics being observed.

Statistical Design of Experiments The last phase is the generation of a set of values that are of interest for the independent variables of the previous phase. Resources required to control these variables hold high regard in the design of these experiments, and the overall goal of this phase is to obtain the largest amount of information for the objective of the program in the most efficient manner. [69]

Within a framework and process to guide experimentation, what are some of the reasons experimentation is desired for a particular system?

Gatian [27] describes a taxonomy of generic potential objectives for experiments, tailored to the development of technologies and adapted from Reference [9]. Each component is described and given an example in the context of the PRSEUS test case:

System Characterization This first objective is a qualitative or quantitative assessments and observations of technology phenomena. It represents a general fundamental research approach to characterize how a technology behaves and if causality can be determined for particular phenomena that are observed. *Example: the fabrication of a small scale PRSEUS panel placed in tension to observe trends in strain, deflection, and failure.*

Model Construction This research activity deals with determining the governing physics of an observed phenomenon and determining if models are available to represent the physical relationship. *Example: testing a similar PRSEUS panel with damage initiation to identify parameters required to construct a progressive failure finite element model.*

Model Calibration Once a physics-based model has been constructed, this type of experiment helps determine appropriate settings for parameters. These parameters can be physical or non-physical, but the experiment reduces model error and model uncertainty. *Example: a compression test for a PRSEUS panel to determine an appropriate allowable margin of safety on local buckling.*

Model Validation A similar experiment objective to model calibration, a model validation experiment assesses the accuracy of the current models, whether it has been calibrated or not. *Example: the same compression experiment can be performed on a different panel configuration to assess the sizing capability with the current value for allowable margin of safety on local buckling.*

Uncertainty Reduction Even if a model has been properly calibrated and validated, sources of uncertainty are likely still present in its physics representation or parameter values that have not been assessed. This experiment objective seeks to determine more exact values for these characteristics or the technology's performance. *Example: a linear elastic structural model has been developed for PRSEUS, but there is uncertainty in the calibration parameters for it predicting nonlinear behavior for design, and a nonlinear FEM is generated and placed under multiple loading conditions to find a more exact value of that calibration parameter.*

Feasibility Study A feasibility experiment is analogous to a late-phase system characterization, in which the technology or concept is tested . It is, in a sense, a

validation experiment of the concept or technology itself rather than the model representing it. A specific subset of this category would be "Certification" experiments, which examine a technology or concept under realistic operating conditions to qualify it to be implemented in operation. *Example: an assembly of PRSEUS panels containing internal pressure to ensure this concept can withstand the design limits for an application.*

Any of these objectives can be achieved through computational or physical modeling and analysis, and thought experimentation is a mechanism by which to enable the construction of the actual experiments.

2.4.2 Elements of a Structural Technology Experiment

To perform a structural technology experiment, the following features are needed: 1) a test article, 2) operating conditions (e.g. loading and boundary conditions), 3) metrics of observation, and 4) required devices and instrumentation. The first two elements represent the independent variables of experimentation and values must be chosen for the implementation of the test. Examples of these elements include structural skin thickness (1), material (1), stiffener spacing (1), force magnitudes (2), test article fixture (2). It is these variables that will be included in the third phase of *Statistical Design of Experiments*. Metrics for a structural test include strain, deflections, loads, etc., while the required devices and instrumentation could be a finite element model for computational study, combined load apparatus like the one used at the COLTS facility at NASA Langley for the MBB experiment [91, 41], or simply deflection transducers and strain gauges.

The experiment design process proposed by Gatian [27] also acknowledges a morphological readiness analysis in which the elements of a structural technology experiment can be categorized:

Test Environment The test environment represents the mechanism for testing and

the operating conditions for the technology. Options include computational simulations, a lab environment, and in-situ. For structural technologies, the operating conditions are the loads and boundary conditions in which the structure is to be tested in.

Fidelity of Test Environment The fidelity of the environment represents the physics captured by the mechanism of testing and the operating conditions, e.g. how complex are the loading conditions, etc.?

Fidelity of Test Article Depending on the type of model or physical test article, are simplifications made regarding its implementation? How many features are considered?

Scale of Test Article Is the test article able to be modeled or fabricated to full-scale or is the test occurring at a sub-scale?

Level of Test Article Level refers to the system in which the technology is represented, e.g. single technology, technology assembly, the technology implemented on a full system with other subsystems and/or technologies, etc.

Setup for a structural technology experiment is similar whether it is a computational or physical. One of the key differences is in planning for measurements. A physical experiment requires a sensing mechanism [34] whereas a computational finite element model simply requires a node be present at the location of interest and a command is used to elicit the desired output information from the analysis.

2.4.3 Benchmark Experiment Design for Structural Technologies

A wealth of information is available regarding structural testing of the PRSEUS technology. The technology development activities for PRSEUS combine both computational and physical experimentation. An initial trade study of performance was discussed earlier in this chapter and is the basis of much of the following efforts

[57, 105]. A "building-block" physical testing approach was synthesized from this trade study to test feasibility of PRSEUS for the HWB centerbody structure [106]. The approach decoupled the combined loading environment and had a sequential build-up of tests. Simple compression and tension panel tests were performed first [108, 114]. Then, pressure testing was performed on a single panel [63] and a simple cube assembly comprised of PRSEUS panels [61, 113]. The final physical test article that was representative of an 80% scale HWB centerbody based on the initial trade study was referred to as the "multi-bay box" [43, 92, 41].

Along the way, structural modeling and analysis was performed for physical test preparation [39], post-test correlation [84, 33], optimization studies for materials [55, 56], and development of higher fidelity representations of the composite stitching [40]. Other activities included investigations of characteristics for full implementation and certification of the technology, including repairs [82, 83] and assembly joints [62]. Information regarding the fabrication process and manufacturing can be found in References [42] and [59]. These activities were experiments in and of themselves because the performance of the technology hinged on the ability to create large-scale panels using the CAPRI and curing process. Processes also needed to be in place to examine the physical structures after testing, and therefore, non-destructive evaluation techniques were researched as well [7].

What all these studies and experiments have in common is that they stem from the initial characterization of the technology through a full aircraft trade study. In a sense, this is the first experiment performed in the technology development process, which follows the first objective in the taxonomy presented in Sec. 2.4.1. This trade study experiment sets up the information for the rest of the experiments to be derived. Corresponding to the overall program objective, which is to characterize the feasibility of PRSEUS as a solution to the HWB centerbody structural challenges, the objectives of all subsequent experiments obtain settings for the elements mentioned in Sec. 2.4.2

Some of the research activities, e.g. curved panel testing, showed the interest of the development to move beyond the HWB centerbody section and into more conventional structure. What if the overall program objective took a more general focus rather than specifically for the HWB centerbody? Would the trade study that was performed be sufficient to derive a wider array of potential experiment objectives and experimental designs?

Figure 23 shows the interpretation of the benchmark experiment design process for structural technologies, synthesized from the information in the PRSEUS and other literature. This simple approach enumerates all the potential objectives that could align with the overall program objective and performs an initial characterization of the technology in full aircraft operating conditions. The data resulting from this initial performance quantification enables the subject matter expert (SME) to perform an *Experiment Characterization* for each of the potential objectives. *Experiment Characterization* represents the second phase of the generic framework discussed in Sec. 2.4.1 - the "Detailed Definition of Activities." The independent, dependent, and other experimental parameters are decided for each potential experiment, and an assessment is performed by the SME to address the utility for advancement of each potential experiment. For the PRSEUS test case example, the experiments developed during ERA Phase II were focused on examining the feasibility of this structural concept for the HWB centerbody. Therefore, the following data was retrieved from the vehicle level structural model that was used to assess performance: 1) results of the technology design parameters ($\mathbf{x}_T$) for each of the panels in the HWB centerbody section, 2) internal loads of the centerbody section, and 3) critical failure modes of the centerbody. The characterization step must connect these inputs to the experiment elements that were described in Section 2.4.3. Based on the advancement criteria of the structural technology, a decision is made for which experiment is the "best" within the scope and resources of the program. The decision for PRSEUS was the

"building-block approach" of physical experiments shown as the output in Fig. 23 and also referenced in Fig. 9.

2.4.4 Observations

Since the experiment design process is highly expert-driven, there is limited traceability to the decisions that are made in experimentation. This research benefits from the breadth of knowledge gained through research activities of the PRSEUS technology. The performance characterization trade study from which all technology development activities were derived was carried out on a single outer mold line and structural layout configuration (BWB-5-200G). What level of risk exists in this process by neglecting how a technology scales or the impact of varying the global operating conditions in this initial performance characterization? What are the consequences and are they able to be quantified?

2.5 Synthesized Benchmark Process

This benchmark process is an instantiation of the framework presented in the first section of this chapter. Each of the detailed elements that have been discussed in this chapter are synthesized together in a process for structural technology characterizations, which is shown in Fig. 24. At the beginning of this process are three elements, shown at the top of Fig. 24, the technology of interest, the experiment objective, and the baseline aircraft. The synthesized benchmark process stems from the single vehicle trade study implementation, which is influenced by the technology development program objective and in turn the experiment objective. The structural weight estimation core of the physics-based weight estimation process is shown via the Structural Model, Structural Sizing, and Technology Implementation tasks, and this creates the data for performance and experiment characterizations. The technology performance is then characterized as a scalar value and implemented in conceptual

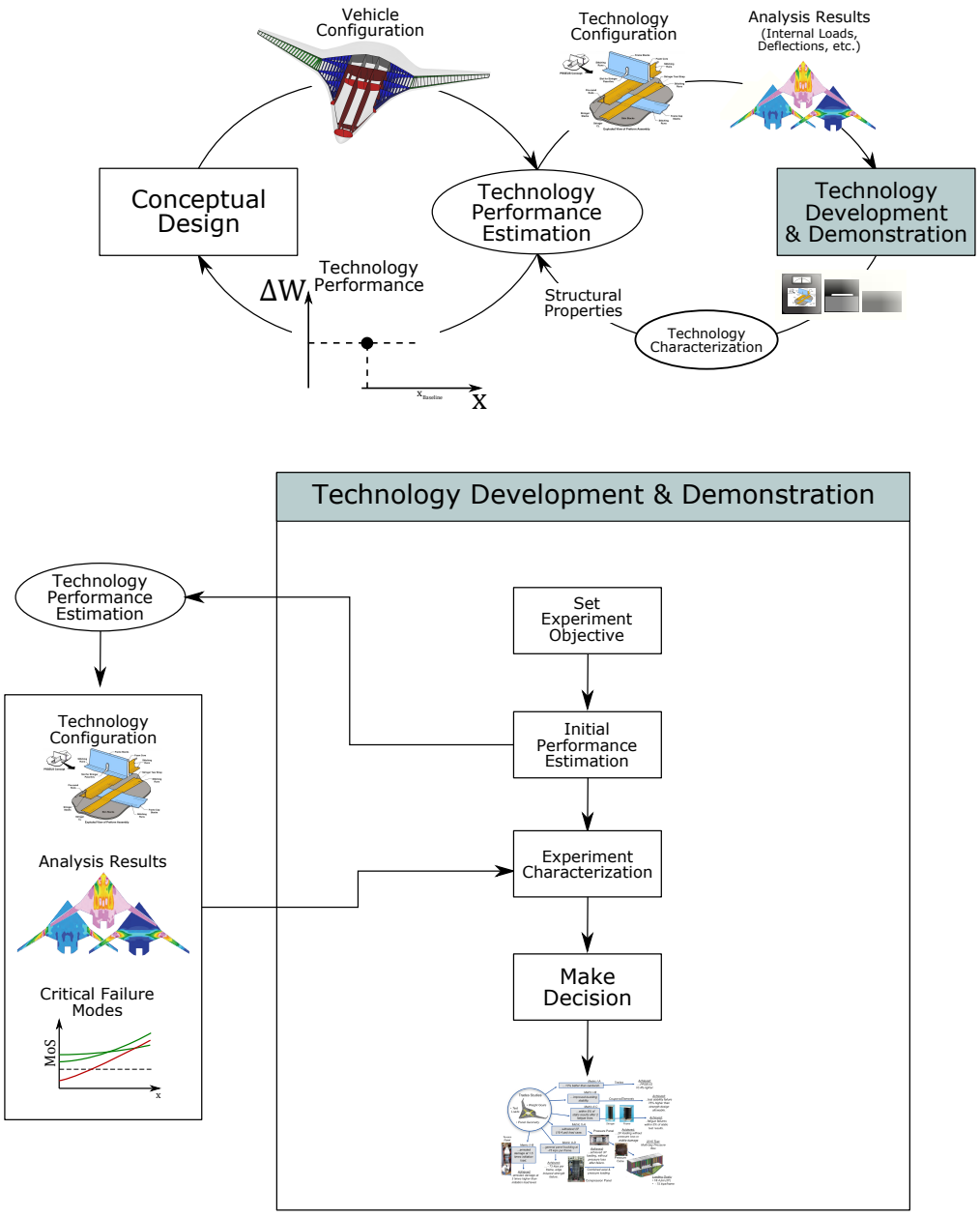

Figure 23: Overview of benchmark process for structural technology experiment design

design, shown in the bottom left portion of Fig. 24. Given available resources, an experiment or experiments are selected based on a decision made from the supporting elements of the experiment characterization. This benchmark approach will be the basis of comparison for the research presented in the following chapters.

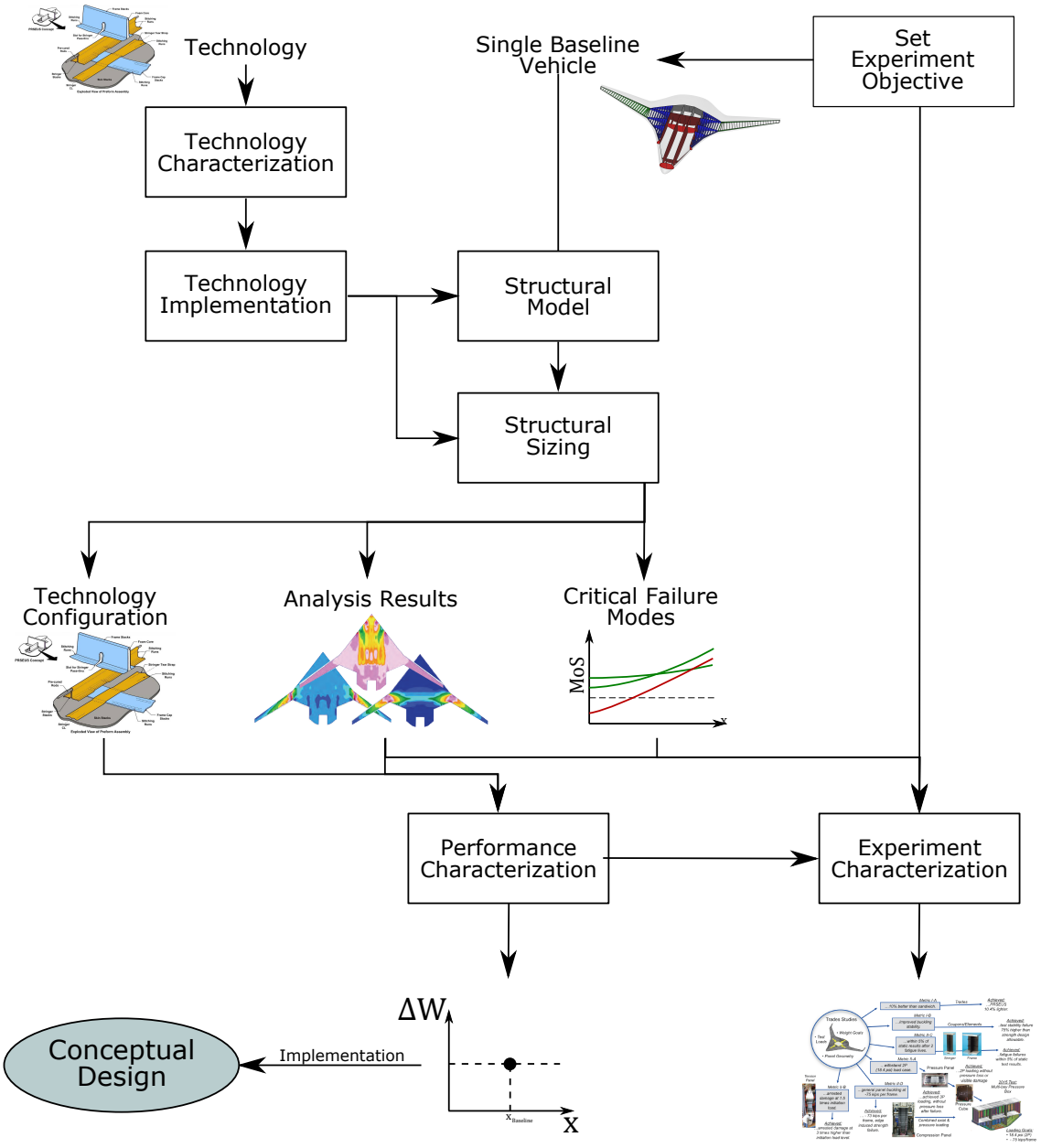

Figure 24: Benchmark process for structural technology performance estimation and experimental design

CHAPTER III

RESEARCH FORMULATION

An architecture for the problem of characterizing structural technology performance and a benchmark approach within that architecture were introduced in the previous chapter. The research presented in this thesis is in response to gaps in that benchmark process that could present potentially significant consequences in the structural technology selection process, the conceptual design implementation of structural technologies, and the decision-making process of structural technology experiment design. This chapter first identifies those gaps and presents hypotheses regarding the ability to close those gaps.

3.1 Identification of Research Gaps

Of all the observations made in Chapter 2, there is one that has the greatest proliferation through the problem architecture in Fig 11: incomplete characterization of structural technology performance in terms of OML and structural geometries. It was shown that only one baseline aircraft was considered in the benchmark process for structural technology performance estimation, i.e. a single design for outer mold line ($\mathbf{x}^*_{OML} \in \mathbf{X}_{OML}$) and a single design for structural layout ($\mathbf{x}^*_{SL} \in \mathbf{X}_{SL}$). The reasoning behind this benchmark characteristic is likely either: 1) an initial objective of the program for a single configuration to be used as a stepping stone for further research or 2) the cumbersome process of manually generating full vehicle structural models with only conceptual design knowledge.

Equation 9 shows that through historical data, the structural weight of a wing is functionally dependent on the conceptual design variables of the aircraft, X_{OML}. This functional relationship means that these parameters should have a quantifiable

effect on the structural sizing process that was explained in Section 2.3.3. Is this effect different for a structural technology than it is for a baseline structure, and will it in turn make structural performance a function of the conceptual design space, $\mathbf{X}_{OML}$?

Gap 1: The characterization of structural weight reduction performance of a structural technology is potentially incomplete if the impact of the outer mold line is neglected.

What are the consequences of not characterizing performance as a function of this relationship if it exists? To examine the potential significance this incomplete characterization of performance, a series of preliminary thought experiments is presented. Then, the impacts on the problem architecture will be discussed.

3.1.1 Thought Experiments

Structural technology performance is defined by Eqn. 4, and it was shown that the $W_{S,B}$ and $W_{S,T}$ estimates are generated through physics-based structural sizing in the context of this research. Are the results from this structural sizing process dependent on $\mathbf{X}_{OML}$ and $\mathbf{X}_{SL}$? First, the functional relationships of the three design spaces of interest are are examined. At the highest level exists the outer mold line design space ($\mathbf{X}_{OML}$), which coincides with technology selection and implementation in the conceptual design phase, which was discussed in the motivation section and problem architecture. The design parameters in $\mathbf{X}_{OML}$ can be considered purely independent.

One level below the OML is the structural layout design space ($\mathbf{X}_{SL}$), which is representative of design tasks that occur in the late conceptual phase and early preliminary phase. While these structural layout design parameters are defined independently of the OML design variables, the actual shape of the resulting structure is dependent on OML design point. For example, a traditional two spar wingbox configuration is defined by a front spar location, a rear spar location, and spacing of

the ribs, which are independent variables. However, the upper and lower skin panels that result from this structural definition follow the curve of the upper and lower OML surfaces, respectively. Similarly, each spar is defined by a percentage of the chord length of the wing per span, and therefore the height of the spar is defined by the thickness of the airfoil, an independent OML design parameter, at that chord location.

Finally, the lowest level of the design spaces is the technology level ($\mathbf{X}_T$), which is representative of the later phases of preliminary design. The variables in $\mathbf{X}_T$ are technology specific and their dependence needs to be examined on a case-by-case basis. For the test problem, $\mathbf{X}_T$ design variables are listed in Table 11 in Chapter 4. If a high fidelity geometry model was created of the technology, in which stiffeners were modeled discretely, then few of these design variables could actually be considered independent due to assembly challenges for load path continuity. However, the global-local sizing approach enables the user to define the desired level of dependence, e.g. linking stringer spacing as a function of span. In the context of a full vehicle structural model, the only variables that are not independent are contained in the "Panel Global" group, because they represent the geometry of the sizing components, C_i. The previous paragraph discussed the dependence of structural component shape on $\mathbf{X}_{OML}$ and $\mathbf{X}_{SL}$, and therefore, the functional relationship of global panel variables at the $\mathbf{X}_T$ level will be designated by:

$$\begin{aligned} \mathbf{x}_{T,\text{panel}} &\in [l_{\text{panel}}, w_{\text{panel}}, r_{\text{panel}}, \ldots] \\ &\sim f\left(\mathbf{x}_{OML}, \mathbf{x}_{SL}\right) \end{aligned} \tag{23}$$

where $\mathbf{x}_{OML} \in \mathbf{X}_{OML}$, $\mathbf{x}_{SL} \in \mathbf{X}_{SL}$, and l, w, and r represent the length, width, and curvature of the structural component, respectively. An example of this dependence is shown in Fig. 25 with a planform view of the tip section of a traditional wingbox. The figure shows how changes in front and rear spar location and sweep can change

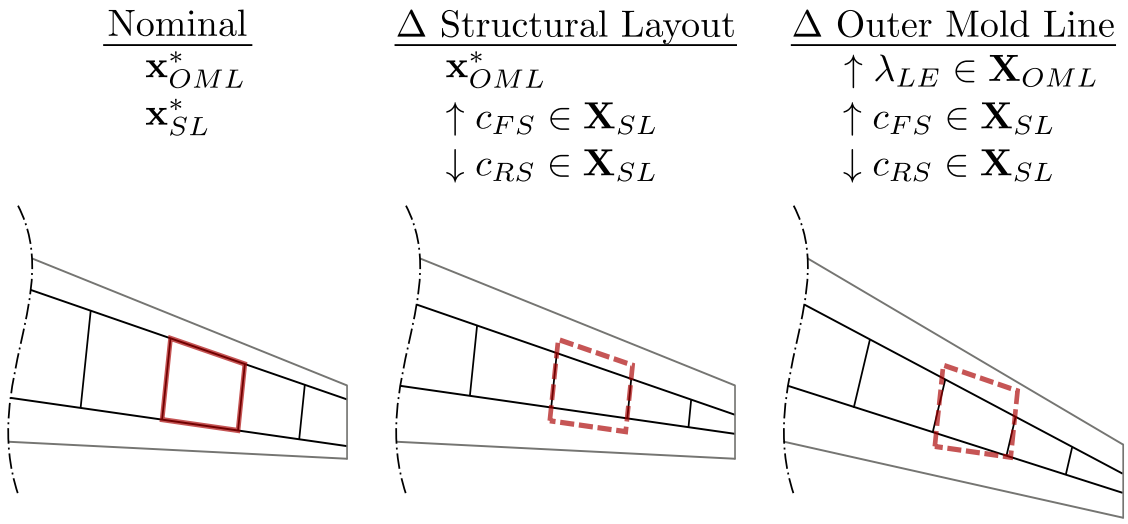

Figure 25: An example effect of X_{OML} and X_{SL} on component dimensions

the skin panel geometry definition.

What other characteristics of technology performance estimation change as a function of $\mathbf{X}_{OML}$ and $\mathbf{X}_{SL}$? The technology design level is first discussed, because this is the level in which optimization takes place for the benchmark structural sizing approach. The optimization formulation for structural sizing mentioned in Eqn. 10 is visually depicted in Fig. 26. For simplicity in visualization, each of the design spaces in Figs. 26, 27, and 28 is collapsed to a single dimension in the x-axis, although this represents the entire design space. Fig. 26 is a visual representation of the constrained minimization problem for each component, C_i, described in Eqn. 10. The solution to this optimization problem is defined as the design variable vector, $\mathbf{x}_{T,i}$ with the minimum structural weight, $W_{S,i}$, that satisfies all constraints.

The weight function, $W_{S,i} = f(\mathbf{x}_T)$, is shown in green and described first. Structural weight for a component is simply the summation of the volume of all the technology features, e.g. skin, stiffener, etc. multiplied by their densities. Therefore, the relationship can be defined by:

$$W_{S,i} \sim f(\mathbf{x}_T, \rho_T, \mathbf{x}_{T,\text{panel}}) \tag{24}$$

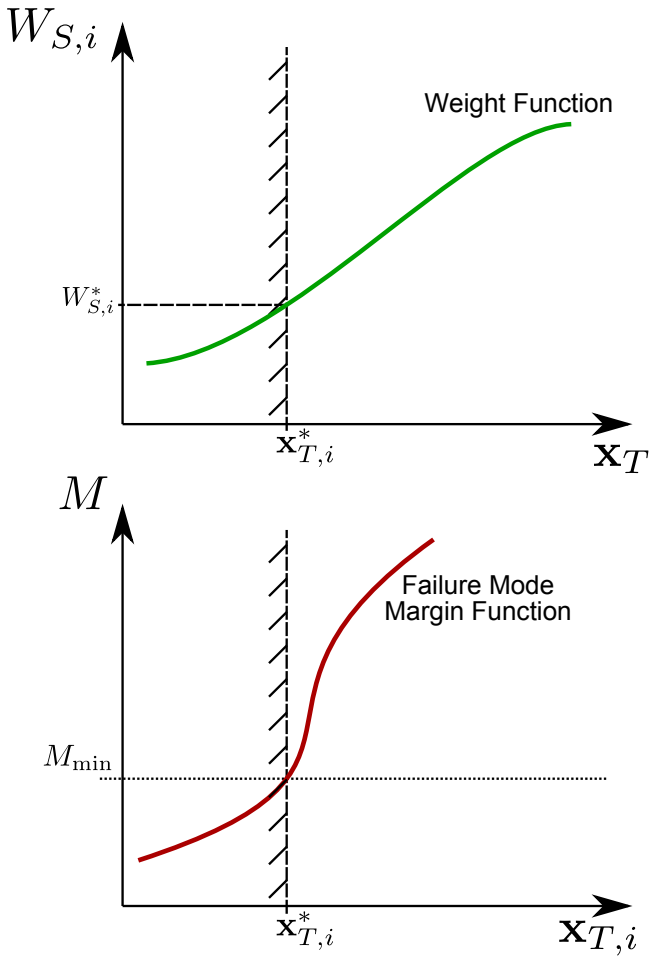

Figure 26: Structural sizing at the technology component level

where $\mathbf{x}_T$ represents the geometry technology design variables, ρ_T represents the material densities of all technology features, and $\mathbf{x}_{T,\text{panel}}$ is the global panel geometry defined in Eqn. 23. The material density term, ρ_T, however, does not need to be separated from the total technology design vector $\mathbf{x}_T$; this was only done to show the explicit relationship of volume and density. By substituting this equation into the previous, the following is obtained:

$$\begin{aligned} W_{S,i} &\sim f\left(\mathbf{x}_T, f\left(\mathbf{x}_{OML}, \mathbf{x}_{SL}\right)\right) \\ &\sim f\left(\mathbf{x}_T, \mathbf{x}_{OML}, \mathbf{x}_{SL}\right) \end{aligned} \tag{25}$$

This relationship shows that at the technology level for each component, structural weight is an implicit function of the SL and OML design spaces when considering it independently of constraints.

How do the constraints affect the structural weight function? The side constraints are simply user defined or regulation defined, e.g. minimum gauge constraints. Other constraints can be defined globally, such as maximum deflections or flutter checks. At the technology level, the most applicable constraints, along with side constraints, are the failure modes that were discussed in Ch. 2. For each of the j failure modes considered in the sizing process, the benchmark process formulates constraints in terms of safety margins, defined by the relationship:

$$M_j \sim f\left(\mathbf{x}_T, \mathbf{L}_{\text{panel}}, F_{T,j}\right) \tag{26}$$

where M is the margin, $\mathbf{L}_{\text{panel}}$ is the appropriate set of local panel loading conditions for failure mode j, and $F_{T,j}$ is the appropriate design allowable for failure mode j.

The local loading conditions for each C_i are equivalent to the internal loads that are determined by structural analysis for every global load case. Specific external aircraft loads, $\mathbf{L}_{a/c,k}$, are calculated for k global load cases and applied to the structure, so

the following relationship is defined:

$$\begin{aligned}\mathbf{L}_{\text{panel},k} &\in [N_x, N_y, N_{xy} M_x, M_y, P, \ldots] \\ &\sim f\left(\mathbf{L}_{a/c,k}, \mathbf{x}_{\text{panel}}, s_T, \rho_T\right)\end{aligned} \tag{27}$$

where s_T and ρ_T are the stiffness and density properties of the technology panel, respectively. Both of these parameters are either contained in or calculated using the technology geometry and material design variables, $\mathbf{x}_T$, but they are noted here separately for clarification. In the following equations, s_T and ρ_T will be represented by $\mathbf{x}_T$.

The next thought experiment is to develop a functional relationship for aircraft loads. Looking at the $\mathbf{X}_{OML}$ first, if any of design parameters changed within this space are changed, does it have a significant effect on the global aircraft loads, $\mathbf{L}_{a/c}$? Basic principles shows that the aerodynamic lift and moment distribution of a wing are dependent on the shape of the wing and the total lift is scalable through wing area, $S_w \in \mathbf{X}_{OML}$. Considering other forms of external aircraft loads, if scale parameters like HWB center section length, or shape parameters like centerbody leading edge sweep or thickness-to-chord ratio are changed, then this changes the definition of the passenger cabin. The pressure differential is then acting over a different surface area, changing the resultant load. Similarly, since some structural layout parameters like spar location are defined as a normalization of an outer mold line design variable like chord length, then changing the chord changes the wingbox definition, and in turn the bounding surfaces of the fuel tanks. The location of the resultant inertial force due to fuel weight will then change, similar to adjusting the sweep angle for the wing, creating an alternate bending moment that the wing structure must withstand.

Moving to the structural layout design space, $\mathbf{X}_{SL}$, design variables within this space can also create differences in the inertial and pressure loads that are applied to the aircraft structure. Even if the OML is held constant, deviations in $\mathbf{x}_{SL} \in \mathbf{X}_{OML}$

affect the internal loads that the structure must be sized to. Internal loads can either be defined as a force per unit area, similar to stress, or a force per unit length. Take, for example, an upper surface skin panel on a simple two spar wing box in a positive maneuver load. If the front and rear spar were redefined like the middle configuration in Fig. 25, then that panel would be receiving a greater compressive force per unit width, because the effective width of the panel (in the chord direction) is decreasing. These thought experiments show that:

$$\mathbf{L}_{a/c,k} \sim f\left(\mathbf{x}_{OML}, \mathbf{x}_{SL}, LC_k\right) \tag{28}$$

where LC is each of the k global load cases defined by the mission analysis, requirements, and regulations in conceptual design.

The final term in Eqn. 26 is $F_{T,j}$, or the allowable(s) for each j failure mode. These allowables were discussed in Section 2.3.1.2 and represent:

$$F_{T,j} \in \left[\epsilon_{\text{allow},j}, \sigma_{\text{allow}}, \delta_{\text{allow}}, F_{\text{cr},j}, \ldots\right] \tag{29}$$

depending on whether the failure mode is strength- or stability-based, the type of material the structure is comprised of, and the technology level structural configuration $\mathbf{x}_T$.

Through substitution of the functional relationships of each of the components in Eqn. 26, the representation of safety margins becomes:

$$\begin{aligned} M_{j,k} &\sim f\left(\mathbf{x}_T, f\left(\mathbf{L}_{a/c,k}, \mathbf{x}_{T,\text{panel}}, \mathbf{x}_T\right), F_{T,j}\right) \\ &\sim f\left(\mathbf{x}_T, f\left(f\left(\mathbf{x}_{OML}, \mathbf{x}_{SL}, LC_k\right), f\left(\mathbf{x}_{OML}, \mathbf{x}_{SL}\right), \mathbf{x}_T\right), F_{T,j}\right) \end{aligned} \tag{30}$$

which shows that the constraint function represented notionally in Fig. 26 is an implicit function of the outer mold line and structural layout of the aircraft. Simplifying the terms, margin of safety takes the form of

$$M_{j,k} \sim f\left(\mathbf{x}_T, \mathbf{x}_{OML}, \mathbf{x}_{SL}, LC_k, F_{T,j}\right). \tag{31}$$

Figure 26 also represents the case in which the bounding constraint for the weight function is the safety margin, rather than being a natural minimum or side constrained. This means that the structural weight for component C_i is defined by the critical load case and critical failure mode, taking the functional representation of structural weight at the technology level to:

$$\begin{aligned} W_{S,i} &\sim f\left(\mathbf{x}_T, \mathbf{x}_{OML}, \mathbf{x}_{SL}, M_{j,k}\right) \\ &\sim f\left(\mathbf{x}_T, \mathbf{x}_{OML}, \mathbf{x}_{SL}, f\left(\mathbf{x}_T, \mathbf{x}_{OML}, \mathbf{x}_{SL}, LC_k, F_{T,j}\right)\right) \\ &\sim f\left(\mathbf{x}_T, \mathbf{x}_{OML}, \mathbf{x}_{SL}, LC_k, F_{T,j}\right) \end{aligned} \tag{32}$$

Finally, technology performance at the technology level can be defined by the following representation:

$$\begin{aligned} \Delta W_{S,i} &= W_{S,B,i} - W_{S,T,i} \\ &= W_{S,B,i}\left(\mathbf{x}_{T,B}, \mathbf{x}_{OML}, \mathbf{x}_{SL}, LC_k, F_{T,B,j}\right) \\ &\qquad - W_{S,T,i}\left(\mathbf{x}_{T,T}, \mathbf{x}_{OML}, \mathbf{x}_{SL}, LC_k, F_{T,T,j}\right) \end{aligned} \tag{33}$$

showing that technology performance at the component level, while using the benchmark approach in which $\mathbf{x}_{OML}$ and $\mathbf{x}_{SL}$ remain constant in the performance estimation process, is driven by the differences between technology level variables and allowables of the baseline structure and structural technology. This examination raises the following questions. If the structural layout or outer mold line were to be treated as design spaces rather than single design points, what affect would it have on component level technology performance? Is it possible that the sources for each respective change in weight for the baseline and technology cancel each other out? Is technology performance at the component level, $\mathbf{X}_T$, any indication of performance for the total aircraft or specific aircraft sections?

These aircraft level assessments are more appropriate for the structural layout and outer mold line design spaces. Traversing to the next level, $\mathbf{X}_{SL}$, a summation of the

component level weights, specified in Eqn. 18 is needed to translate the component weights to the aircraft level weights.

$$W_S = \sum_{i=1:c} W_{S,i} \tag{34}$$

Using Eqn. 34, performance with the benchmark process is estimated as

$$\Delta W_S = \sum_{i=1}^{c} (W_{S,B,i} - W_{S,T,i}) \tag{35}$$

However, if the SL changes, then a 1:1 panel comparison may not be possible for the entire aircraft. A different number of components may exist entirely; for example, if rib spacing of the outboard wing is increased, a smaller number of ribs, and therefore smaller number of skin panels exists. Therefore, as a function of a different structural layouts, the summations must be executed independently in performance characterization

$$\Delta W_S = \sum_{i=1}^{c_B} W_{S,B,i} - \sum_{i=1}^{c_T} W_{S,T,i} \tag{36}$$

where c_B and c_T are the number of components in the baseline and technology configurations, respectively. These independent summations can create ambiguity in the direct causes of technology performance, potentially affecting the ability to design effective structural technology experiments. Vehicle level technology performance (ΔW_S) is presented notionally as a function of the structural layout in Fig. 27. This also shows the benchmark estimate, which is generated through the benchmark performance weight estimation process using a single baseline vehicle configuration, which includes a single point baseline structural layout design, $\mathbf{x}^*_{SL}$. What would the consequence be if the baseline structural design was at a different point along the notional curve?

In this stage of the discussion with vehicle level performance, it is helpful to reiterate the objectives of technology performance characterization. They are to enable: 1) conceptual design phase structural technology selection, 2) conceptual design phase

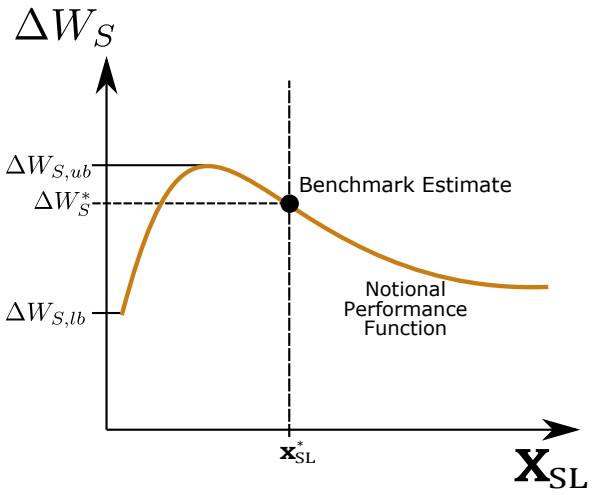

Figure 27: Structural technology performance at the structural layout design level

structural technology implementation, and 3) design and selection of experiments for technology advancement. For objectives 1 and 2, it was shown that only $\mathbf{X}_{OML}$ design variables are considered in the exploration of the conceptual design space and technology selection because traditional conceptual design models do not contain inputs for lower level structural layout design variables. Therefore, it is assumed that some structural layout exists for each design point $\mathbf{x}_{OML} \in \mathbf{X}_{OML}$. What structural layout design should be used? Should it be the same for every $\mathbf{x}_{OML}$ design point? Should it be constant for both baseline and technology configurations, as in the benchmark performance estimation process? These questions represents an additional gap in the benchmark process.

Gap 2: For a given conceptual design point, $\mathbf{x}_{OML} \in \mathbf{X}_{OML}$, estimating structural technology performance with a constant structural layout design, $\mathbf{x}_{SL}^*$, cannot account for the ability of the technology to enable a more weight efficient structural layout.

If the structural layout is not constant between baseline and technology structure

configurations, is traceability lost from the vehicle level to the technology level to determine causality of estimated performance changes through experimentation?

The last design space to examine is at the conceptual design level, or $\mathbf{X}_{OML}$. Performance is depicted notionally as a function of this design space in Fig. 28. This figure also shows the benchmark estimate that is propagated from the structural layout design space, which is representative of the data presented in the benchmark trade study in performance characterization [105]. This study quantified the potential structural weight reduction of PRSEUS solely for the centerbody section of a single point HWB aircraft design, the BWB-5-200G, and found it to be 10.3%. It was recognized that PRSEUS, or more generally S/RI composites, could also be used in the construction of other aircraft sections. However, the lack of any other references or performance data points necessitated the use of a 10.3% weight reduction in trade studies that included PRSEUS for other aircraft sections, vehicle scales, and aircraft concepts, all with different scales and different design variables [94, 74, 75, 44]. This scalar representation of performance throughout the OML design space is depicted by the blue dotted line at the constant ΔW_S^* in Fig. 28, showing the notional benchmark implementation in the conceptual design space. For both $\mathbf{X}_{SL}$ and $\mathbf{X}_{OML}$, weight reduction technology performance is shown notionally as a continuous function of the respective design spaces, reflecting the thought experiments mentioned in this section. If performance were quantified compared to this notional representation, would the function be continuous as shown or can discontinuities exists for scenarios like changing rib spacing and in turn changing the number of total ribs in the outboard wing, for example? Additionally, is there a process by which the performance function in Fig. 28 can be quantified and does it have consequences for the objectives mentioned in the previous paragraph?

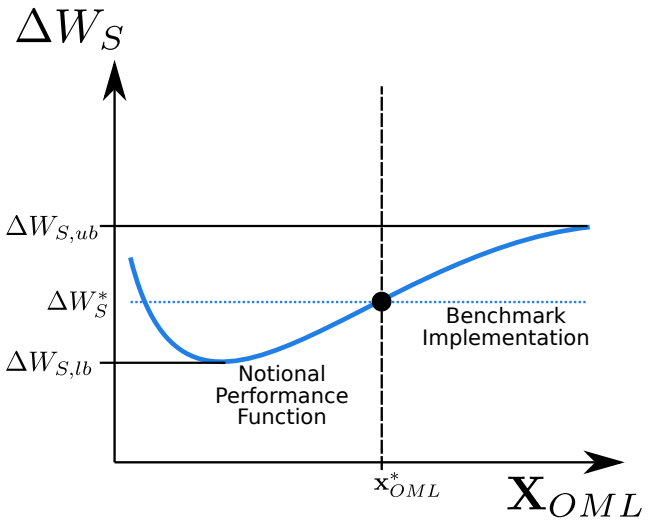

Figure 28: Potential error in performance implementation using the benchmark approach is shown notionally as a function of the OML deign space

3.1.2 Effects on the Problem Architecture

In the previous subsection, gaps were identified in the benchmark process for failure to consider the outer mold line and structural layout in characterizations of structural technology performance. How do these gaps affect the rest of the problem architecture in Fig. 11? From a conceptual design perspective, i.e. technology selection and implementation, Fig. 29 shows notionally that quantifying performance as a function of the OML design space can reveal potential error in the scalar implementation of performance derived from the baseline OML design point, $\mathbf{x}_{OML}^* \in \mathbf{X}_{OML}$. Error in the benchmark estimated performance is maximum at:

$$\varepsilon_{\max}\left(\Delta W_S^*\right) = \max\left(\left|\Delta W_S^* - \Delta W_{S,lb}\right|, \left|\Delta W_S^* - \Delta W_{S,ub}\right|\right) \tag{37}$$

where ΔW_S^* is benchmark estimated performance and the bounds of the actual quantified performance function are $[\Delta W_{S,lb}, \Delta W_{S,ub}]$. This maximum error is important to technology selection and implementation, because it presents potential risk for both tasks, which introduces another gap:

GAP 3: An incomplete characterization of structural technology performance introduces error in the selection and implementation of the structural technology in the conceptual aircraft design phase.

For example, assume a previous trade study was executed for a structural technology, like the benchmark [105], that characterized performance at a single point design in the OML space, and this study publishes weight reduction performance for the structural technology as ΔW_S^*. At a later point in time, another technology development program with a different set of objectives wants to invest in the advancement of a technology for advancement to meet those objectives The baseline aircraft concept design ($\mathbf{x}_{OML}^*$) which is being used for technology selection in this program, however, is equivalent to the OML design point that corresponds to the lower bound of weight reduction performance $\mathbf{x}_{OML}|_{\Delta W_{S,lb}}$. Error in the technology impact factor becomes:

$$\varepsilon_{k_{ST}} = \Delta W_S^* - \Delta W_{S,lb} \tag{38}$$

and this presents a risk to the technology development program in meeting their objective(s). For technology implementation in conceptual design, the entire area between the benchmark implementation line and the notional performance line represents a distribution of error for the aggregate design space, and therefore risk in meeting conceptual design requirements. Reiterating the importance of a solution to this problem, is there a process by which these risks can be characterized and quantified?

Revisiting the problem architecture in Fig. 11, another manner in which the *Conceptual Design* element must respond to Gaps 1 and 2 is to send extra data to the performance estimation and technology development. If the entire conceptual design space is relevant to technology performance estimation, then design space limits must be an output of this architectural element, while other information like load

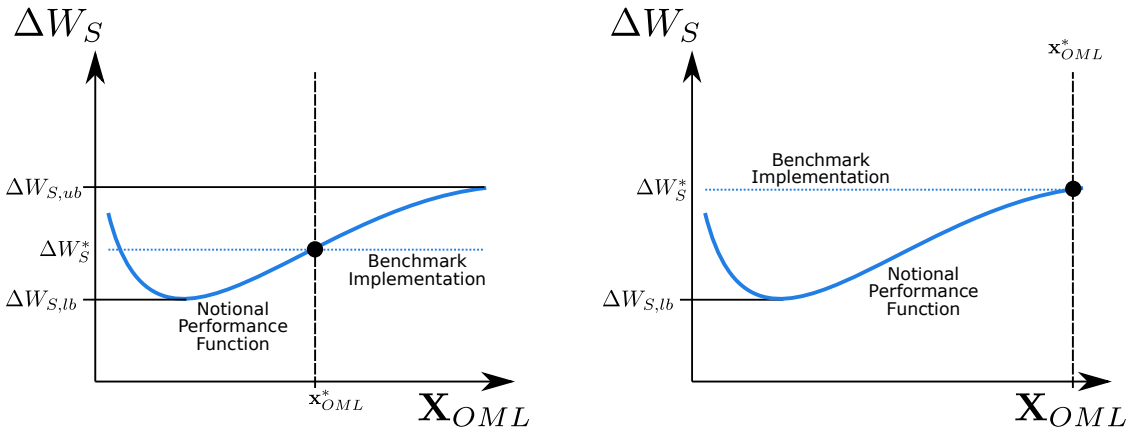

Figure 29: Change in notional error when different baseline design point, $\mathbf{x}^*_{OML}$ is chosen

cases defined from the mission analysis and conceptual level assumptions can remain the same.

On the technology development and demonstration side of the architecture, only the data that supports the technology development objective is technically required as an input. However, the data available to decision makers at this level drastically exceeds that of the benchmark approach with the formulation of an entire OML design space rather than the benchmark single OML design point. As an expert-driven process, how should the technology experiment characterization task respond to the increased data, and how can this data be processed in a pragmatic fashion? Data management was a challenge identified in Section 1.2.3, and a comparative example will highlight this issue. The NASA/Boeing N2A HWB configuration with a nominal structural layout defined by Laughlin contains 200 structural components contained in the centerbody, rear centerbody, trapezoidal wing, and outboard wing that can be constructed with the PRSEUS technology [53]. Considering the data that can be used in structural technology experiment design, each of the components contains:

- **1**: structural weight, $W_{S,i}$,
- **1**: critical failure mode and corresponding safety margin, M_i^*,
- **81**: total number of applicable failure modes that can be applied in Hypersizer for PRSEUS structure, covering skin, stringers, and frames and their corresponding margins of safety, $M_{k,i}$,
- **1**: critical load case, LC_i^*, that governs the internal panel loads,
- **8**: internal panel loads, $\mathbf{L}_{\text{panel},i}$, and
- **21**: optimal technology design variable settings, $\mathbf{x}_{T,i}^*$.

This results in a total of 113 parameters for each 200 components that are of potential use in experiment design for the PRSEUS structural technology based on the N2A. Decision makers for experiment design may also wish to use technology performance and its component weights, i.e. $W_{S,B}$, $W_{S,T}$, and ΔW_S, for the entire aircraft or each individual aircraft section, adding another six degrees of freedom for the HWB: 1) total aircraft, 2) centerbody, 3) rear centerbody, 4) total wing, 5) trapezoidal wing, and 6) outboard wing. The combination of trapezoidal and outboard wing sections into a total wing is considered because it is basis of implementation for conceptual design tools like FLOPS. For the N2A, this results in a total of $(113 \cdot 200 + 18) = 22,618$ parameters that could be required to design structural technology experiments based on one configuration. In the ERA development program, this data was already focused to the particular objective surrounding the HWB centerbody, which reduced the total number of data points to $(113 \cdot 27 + 3) = 3,054$.

Expanding experiment characterization to an entire design space requires that some of these parameters be treated as a function of the OML design space, e.g. critical failure mode margin of safety $M_i^*(\mathbf{X}_{OML})$. Depending on the mathematical representation of the functional form of these parameters or aggregation distributions

of these parameters, the total number of degrees of freedom available to experiment design SMEs may only increase by a small combinatorial factor This factor would be equivalent to the number of hyperparameters of an appropriate approximation function for each parameter. However, to fit (or train) the approximation function, e.g. linear model, neural network, radial basis function, etc., a design of experiments within the $\mathbf{X}_{OML}$ design space must be executed.

As an additional example, characterization of a design space that is expected to be nonlinear requires a sampling plan beyond 2-level full factorial. Model generation DOEs sometimes account for this with a 3-level full factorial or a combination of central composite and space filling designs like a Latin Hypercube. Considering a characterization of just a limited subset 5 parameters of the OML design space, a total of $3^5 = 243$ would need to be performed to account fully for second order effects. The total number of potential data points that can be used by the technology development team is $22,618 \cdot 243 = 5,496,174$. Thousands more are possible if parameters within $\mathbf{X}_{OML}$ and/or $\mathbf{X}_{SL}$ are useful for the technology development team. This represents an additional gap in the expert-driven benchmark experiment design and selection process.

Gap 4: The current benchmark structural technology experiment design process relies heavily on subject matter expertise, and a repeatable process does not exist which can 1) manage the increase in data input from the technology performance characterization or 2) assess the impact of an experiment on other conceptual aircraft designs beyond the single point OML design from which the experiment was derived.

As mentioned, the technology development team operates under the influence of specific objectives and decision-making is typically performed by subject matter experts.

The goal of this research is not to make the decision of which experiment is the best for the advancement of the technology, rather it is to enable decision making for experiment design and selection through a robust characterization of technology impacts at the three different levels of design spaces discussed in this section. Allowing experiment designers to answer questions like:

- *Do results from the experiment influence confidence in performance estimates for a different loading condition or other section of the aircraft?*
- *Are results from a scaled test still relevant to the full-scale structure or operating conditions?*
- *Which regions of the conceptual design space should efforts be focused to ensure the experiment will have the greatest impact on advancement of the technology?*

drives a portion of the structural technology performance characterization efforts. A summary of the gaps identified in this section and the portions of the architecture they relate to is shown in Fig. 30. Each gap is color coded for ease of identification throughout this chapter. Gaps 1 and 2, relating to the OML and SL design spaces, directly affect the process of *Technology Performance Estimation* and are shown over this element. Gap 1 is also shown in smaller boxes in the data that is affected being passed from element to element. Gap 3 relates to the error in Conceptual Design, and Gap 4 refers to the drawbacks of an expert-driven experiment characterization process for traceability, repeatability, and the ability to deal with large amounts of input data. A research formulation is presented to address these gaps in each of the subsequent sections.

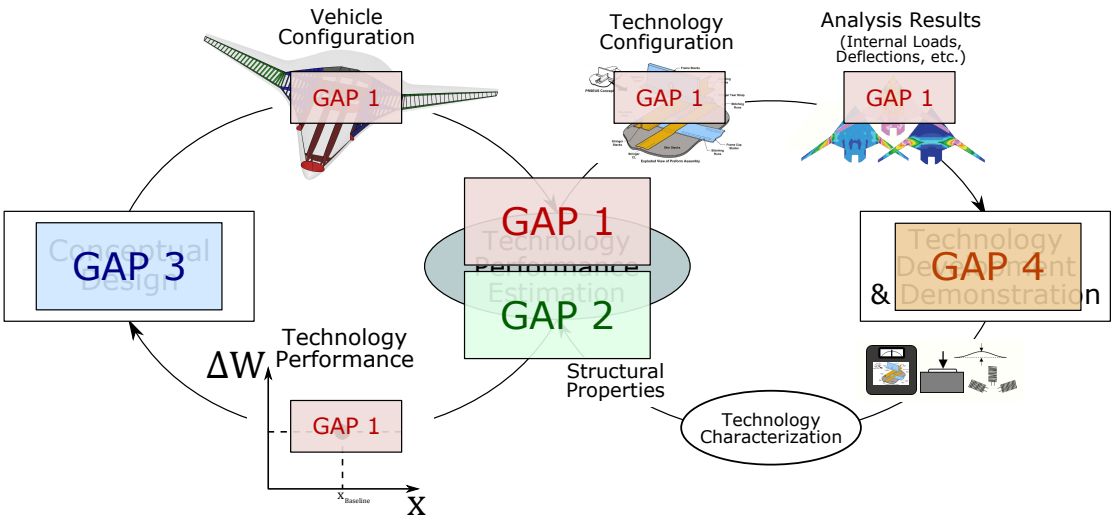

Figure 30: Gaps identified in the benchmark structural technology performance framework

3.2 Characterization of Structural Technology Performance

The research formulation begins with the central focus of the architecture and the source of the problem that was identified: structural technology performance estimation. The informal questions that were posed as a result of hypothetical thought experiments are intended to guide the formalization of a research approach in this chapter. These questions are entirely dependent on the notion that performance trends actually exist as a function of the $\mathbf{X}_{OML}$ design space. The historical contention that structural weight of an aircraft has a functional relationship with the OML, as shown in Eqn. 9, does not necessitate technology performance to the same dependency. At any design space level, the possibility exists that the source of that weight dependence affects both the baseline and technology structure in the same manner and those sources effectively cancel each other out by definition in Eqn. 4. However, the logic behind the thought experiments provides enough substantiation for further assessments.

The main goal for this research is to understand if it is possible to quantify the functional impact of the OML on structural technology performance and to determine

if that impact is significant enough to warrant its characterization in the estimation process. This is addressed with an overarching research question:

Overarching Research Question: If observations lead to the identification of a significant relationship between structural technology performance, ΔW_S, and the outer mold line design space, $\mathbf{X}_{OML}$, is there a process that can systematically quantify this functional impact and assess the consequences of failing to recognize this impact?

This question is somewhat of a reiteration of the research objective, but it identifies key characteristics that must be addressed in the research. First, the statement that $\Delta W_S(\mathbf{X}_{OML})$ must be a significant relationship is somewhat ambiguous but becomes clearer throughout this chapter. It is assumed, however, that the characterization of this performance relationship is of little interest to decision makers if it only results in a potential error in performance estimates of a few percentage points. This magnitude of error, or uncertainty, is expected for a developing technology of $TRL \leq 5$. Moreover, if the characterization of this performance relationship requires a computationally taxing structural weight estimation process like the benchmark approach, the slight reduction of error may not be worth the resource investment. Another observation of this research question is the identification of a systematic process that is needed for performance characterization. This process should maintain traceability in performance to the three design space levels mentioned in the previous section, i.e. $\mathbf{X}_{OML}$, $\mathbf{X}_{SL}$, and $\mathbf{X}_T$, to enable decision-making in technology selection, technology implementation, and technology experiment design.

To begin the development of an approach, the ability must exist to make observations that support the significance of the performance function, $\Delta W_S(\mathbf{X}_{OML})$. The benchmark performance estimation process was described in Section 2.3.3 and is shown in Fig. 20. The manner in which the research gaps affect that process is

presented in Fig. 31. Gaps 1 and 2 both directly impact the generation of a structural model because they require the ability to change outer mold line and structural layout geometries to examine their effect on performance. Because of the challenges and tedious process of manually generating structural models, a modeling environment that can parametrically vary these geometries in an efficient manner is therefore required. Additionally, the *Performance Characterization* step is affected by Gap 1, and this is due to the benchmark approach only requiring a scalar value be output from this step. What is the form of that functional relationship and how is it quantified?

The development of a structural model, like the thought experiments in the previous section, can be decomposed into the three design space levels of the characterization problem. This decomposition can be represented by a Vee diagram in systems engineering, in which a functional decomposition is performed to define the problem, and then the problem is synthesized from the bottom level up to construct a set of experiments to test hypotheses made at each level. At the highest level is the $\mathbf{X}_{OML}$ design space, which is characteristic of conceptual design. Once the OML is defined, the structural layout takes shape within the confines of the OML geometry. This design space, $\mathbf{X}_{SL}$, is typically examined in the late conceptual or early preliminary design phase. If the full aircraft is defined at the systems level, then the structural layout can be considered at the subsystem airframe level. The lowest level is the technology design space, $\mathbf{X}_T$, or the component level, in which the constrained optimization of structural sizing takes place. At the modeling and analysis fidelity discussed in the benchmark process, this level can be considered part of the late preliminary design phase. While detailed technology design variables are modeled, detailed characteristics like cutouts, fittings, and such are not considered.

A schematic that represents the Vee diagram formulation is shown in Fig. 32, which is structured to support the first overarching hypothesis.

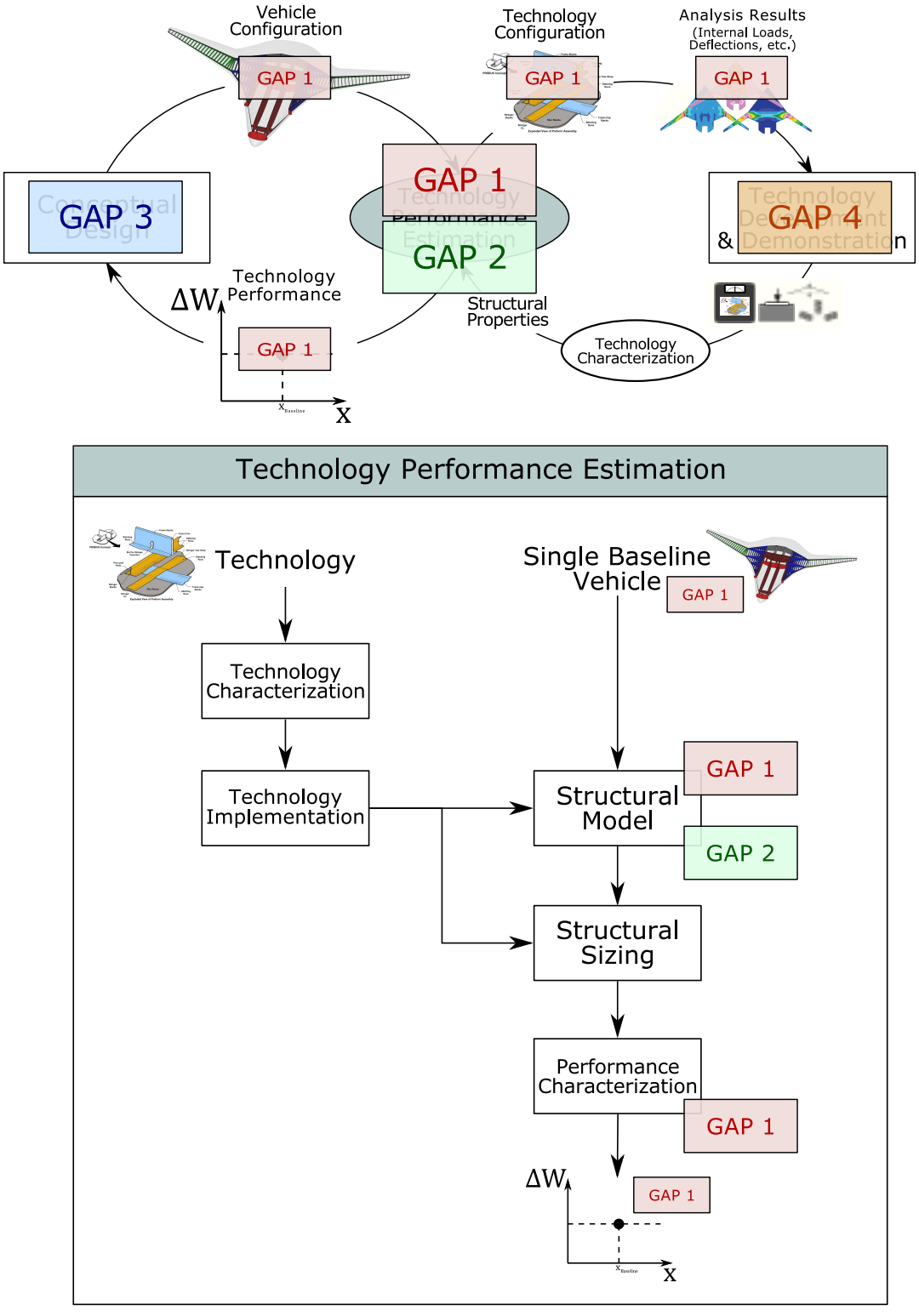

Figure 31: Gaps identified in the benchmark structural technology performance estimation process

---

Overarching Performance Hypothesis: Beginning at the technology level, if the characteristics of structural technology performance, ΔW_S, at a given design space level indicate a potentially significant relationship with the conceptual design space, $\mathbf{X}_{OML}$, then performance should be characterized at the next higher level.

At first glance, this statement might seem nuanced or repetitive, but it sets up a framework to test the first contention raised by the Overarching Research Question: a relationship exists between performance and the conceptual design space and it cannot be ignored in the characterization process. This is the first step in developing a systematic, traceable, and repeatable process to characterize performance for any weight-reducing structural technology. The hypothesis that the OML has a significantly influential impact on technology performance is being tested at each level in terms of the functional relationships that were established through thought experiments. Evidence supporting or refuting hypotheses at each design space level is built on results generated at the current design space level and all those below it. The Overarching Performance Hypothesis establishes a tollgate formulation for a structural technology of interest to mitigate unnecessary modeling and to generate observations which help decide at each step if moving forward is appropriate. For example, at its lowest design space level, $\mathbf{X}_T$, the PRSEUS technology can be implemented in Hypersizer through a simplified, non-FEM panel that is assessed through analytical equations for weight and constraints. Investigating this design space requires much less effort in setup and less computational time than a conceptual design space exploration of a full-aircraft FEM that needs to iterate between global and local models.

The research was also formulated in this manner in an attempt to enable traceability and allow for a decoupling of potential effects when moving from one design

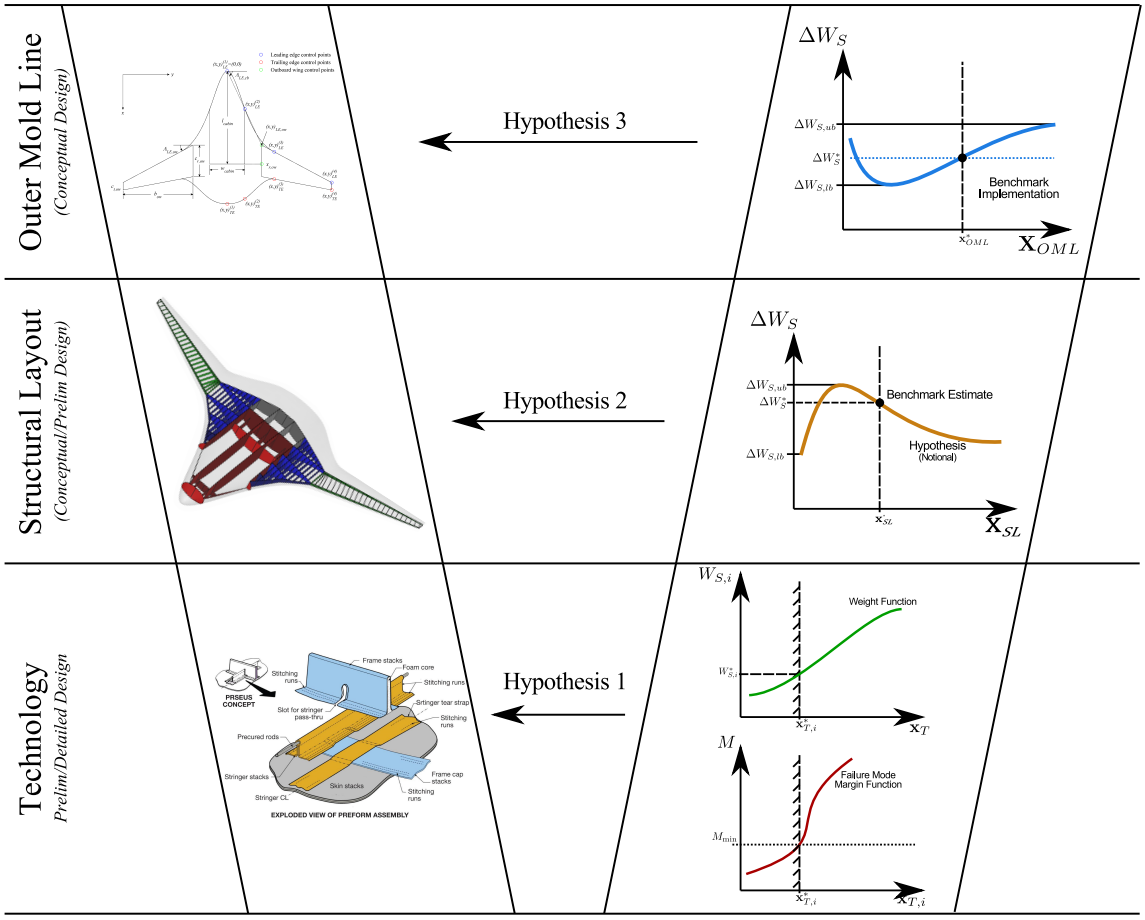

Figure 32: A Vee diagram representing the sequential testing of hypotheses to support Overarching Performance Hypothesis

space level to the next. For example, when examining the impact of structural layout level design variables, $\mathbf{X}_{SL}$, on W_S or ΔW_S, the weight and performance metrics are the result of a summation of effects from all considered structural components in the entire aircraft or a particular aircraft section. Unless the structural layout is held constant between the baseline configuration and the technology-infused configuration, then single-panel effects cannot be compared between configurations because of the issues presented in the discussion of Gap 2. Additionally, local loading conditions cannot be explicitly controlled in a full aircraft model - they are a function of the global aircraft load cases and structural properties. This is important for the experiment design process in the *Technology Development & Demonstration* element of the problem architecture. Returning to the actual process of weight reduction performance estimation, however, the technology level is the first to address Gaps 1 and 2 within the Vee diagram framework.

3.2.1 Technology Level

For the technology design space level, $\mathbf{X}_T$, examples have been discussed regarding its importance as the initiation point to a tollgate framework. The ease of technology modeling – using the benchmark model – at this level makes design space exploration a simpler undertaking, and there is potential to efficiently consider a larger number of design variables and loading conditions. Also, it has a potentially important role in providing traceability for technology experiment design. Identifying performance trends as a function of the technology design space sets a precedent. If the process began with investigation of performance directly at the higher levels, the root source of some trends may be muddled through the summation defined by Eqn. 36. For example, if an observation was made for an OML design point, $\mathbf{x}_{OML}^{(1)}$, that showed no change in structural weight when the structural layout design space, $\mathbf{X}_{SL}$, was explored, does that constrain other OML design points to the same observation?

Information learned at each design space level propagates up the right side of the Vee diagram to better inform the characterization at that level. Continuing with the example, consider that a large sensitivity was observed for $\Delta W_{S,i}(N_x)$ at the technology level, then it suggests the higher level observation of constant $\Delta W_S(\mathbf{X}_{SL})$ at OML design point 1, $\mathbf{x}_{OML}^{(1)}$, may be an isolated effect. As shown by the functional relationships in Eqns. 27 and 28, the internal load N_x is an implicit function of the structural layout. Leveraging this technology level information, it would be logical to assume through the chain rule that the structural layout would have a significant impact on technology performance. Therefore, the decision would likely be made in the 2^{nd} tollgate, i.e. the structural layout design space level, to explore $\mathbf{X}_{SL}$ for multiple OML design points $\mathbf{x}_{OML}^{(i)}$ before making a decision to traverse to the next higher level.

With the consequences of performance characterization addressed, what observations can be made at the technology level to warrant investigation at the $\mathbf{X}_{SL}$ and potentially $\mathbf{X}_{OML}$ levels?

Hypothesis 1: If a non-zero relationship exists between structural technology performance at the technology level, $\Delta W_{S,i}$, and 1)the global panel geometry parameters, $\mathbf{x}_{\text{panel},i} \in \mathbf{X}_T$, or 2) local load, $\mathbf{L}_{\text{panel},i}$, for one or more local loading conditions, then structural technology performance at the upper level design spaces, $\mathbf{X}_{OML}$ and $\mathbf{X}_{SL}$, must be examined.

This hypothesis stems from the functional relationship of structural weight reduction, $\Delta W_{S,i}$, to local loads and global panel dimensions at the technology level, addressed in Sec. 3.1.1. These parameters were identified through thought experimentation as those that connect the higher level design spaces to the technology level. Because the technology level is the furthest removed from the OML and because component performance trends are additive, very relaxed requirements are placed on observed

trends to support the hypothesis. Only a non-zero relationship is needed to substantiate exploration at the next level.

What other observations, besides the need to explore $\mathbf{X}_{SL}$ and $\mathbf{X}_{OML}$, can be drawn from exploring the technology level design space that help characterize structural technology performance? Does the point of best technology performance coincide with the most desirable, i.e. minimum weight, configuration for a given design load? Do local loading conditions exist that are more conducive to structural weight reduction through technology infusion? What failure modes drive the design of the structural technology and under what operating conditions? These questions will be further examined in Chapters 4 and 5.

3.2.2 Structural Layout Level

At the structural layout design space level, the research goal is to twofold: 1) generate data to make observations that indicate technology performance is a significant function of $\mathbf{X}_{OML}$ and 2) determine an appropriate treatment of the structural layout in the performance characterization process. To generate data at the $\mathbf{X}_{SL}$ level, this design space must be appropriately explored; however, observations made from structural layout DSE for a single $\mathbf{x}_{OML}$ are not sufficient to make a generalized statement regarding the appropriate treatment of the structural layout for a full-scale performance characterization. Information synthesized at this level is used to augment technology level observations to determine whether or not it is beneficial to pursue a full quantification of $\Delta W_S\,(OML)$.

Hypothesis 2: If the range of $\Delta W_{S,p}\,(\mathbf{X}_{SL})$ for any p outer mold line design point, $\mathbf{x}_{OML}^{(p)}$, exceeds an appropriate threshold, then a full characterization of $\Delta W_S\,(OML)$ should be pursued.

The range of structural technology performance as a function of the chosen structural layout design space refers to:

$$\mathrm{R}\left(\Delta W_S\right) = \left|\Delta W_{S,ub}\left(\mathbf{X}_{SL}\right) - \Delta W_{S,lb}\left(\mathbf{X}_{SL}\right)\right| \tag{39}$$

Observations of the phenomenon introduced in this hypothesis must still consider lower level technology results. For instance, an appropriate threshold is purposefully vague, because it gives the decision maker the ability to assess trends at the technology level to determine what an appropriate threshold actually is. If an extremely weak, but still non-zero, relationship was witnessed between the indicative technology level parameters and metrics, then a somewhat larger threshold for $\mathrm{R}\left(\Delta W_S\right)$ could be set by the decision maker at the structural layout level. This would be the result of increased confidence of a small likelihood that there is some phenomena not captured by observations at both levels, so long as $\mathbf{x}_{OML}^{(p)}$ are sufficiently different from each other. Conversely, a relatively smaller threshold may be more appropriate with very strong technology level relationships.

If the modeling capability exists and a design space exploration is being performed at the $\mathbf{X}_{SL}$ level, what trends are pursued to determine what the setting for $\mathbf{x}_{SL}^*$ should be in a full characterization of $\Delta W_S\left(\mathbf{X}_{OML}\right)$? It was not explicitly stated how $\mathbf{x}_{SL}^*$ was developed for the benchmark approach, but it is assumed that some structural topology optimization was performed to obtain the BWB-5-200G structural model. For quantification of performance as a function of the OML, the easiest modeling and analysis implementation for the structural layout is to choose a default configuration, $\mathbf{x}_{SL}^*$ and keep it constant throughout the OML design space for both the technology and baseline structure configurations, i.e.

$$\mathbf{x}_{SL}^* = \mathbf{x}_{SL,B} = \mathbf{x}_{SL,T} \tag{40}$$

Once again, for a generalized process, the baseline weight can also be generated through empirical weight relationships and the structural layout is inconsequential.

However, under the assumptions of the HWB, in which both baseline and technology weights need to be generated with physic-based approaches, the following hypothesis is made:

Hypothesis 2.1: If variation in $W_{S,B}\left(\mathbf{X}_{SL,B}\right)$ and $W_{S,T}\left(\mathbf{X}_{SL,B}\right)$ causes significant error in technology performance, ΔW_S, then the structural layout cannot be held constant in the performance characterization process.

This hypothesis means that an "Uninformed" treatment of structural layout, i.e. setting a default $\mathbf{x}^*_{SL}$ representative of Eqn. 40 for any given OML design point, could not be used in a structural technology performance estimation process, because performance would be justifiably dependent on $\mathbf{X}_{SL}$. Since structural technology performance is a function of both structural layout and outer mold line in this case, i.e. $\Delta W_S \sim f\left(\mathbf{X}_{OML}, \mathbf{X}_{OML}\right)$, the resulting impact on the characterization process is that a larger number of design variables and more cases will need to be considered.

The literature would suggest that respective structural layout optimization of both the baseline and technology configurations to be the most "correct" approach, because weight optimization of any configuration should be performed using all influential structural design variables. As previously mentioned, there are cases, however, in which minimization of weight is not necessarily the objective in structural design. For example, later in preliminary and detailed design, other approaches are used since the global vehicle design has been locked – like optimizing to target weights or compliance – because all components and subsystems at this point in the design process are interdependent. Therefore, any independent structural design at this level has to keep in mind the integration of the full vehicle. Unless the structural layout was chosen for manufacturing concerns or other requirements than performance, then structural weight should be the overall objective.

In the benchmark approach, a "Benchmark" treatment of the structural layout is implemented. It is assumed in this treatment that structural layout of the aircraft with baseline structure has been optimized through minimization of $W_{S,B}\left(\mathbf{X}_{SL,B}\right)$, and then this same layout is used to estimate the structural weight of the technology configuration. Following Eqn. 40, this weight would be $W_{S,T}\left(\mathbf{x}^*_{SL,B}\right)$. Comparatively, this is a simpler implementation than more "correct" approach because a smaller number of function calls for the weight estimation environment is required compared to topology optimization for both the baseline and technology aircraft configurations. However, under the challenge of a computationally expensive function call, is it sufficient to follow Eqn. 40 and only optimize the baseline structural layout?

Hypothesis 2.2: If significant error exists between estimates in structural technology performance when 1) optimizing only the baseline structural layout and 2) optimizing both the baseline and technology structural layout separately, then the structural layout cannot be held constant at the optimized baseline, $\mathbf{x}^*_{SL}$, in the performance characterization process for each and every OML design point.

Mathematically, this hypothesis can be built up by defining:

$$\Delta W_S\left(\mathbf{x}^*_{SL,B}\right) = W_{S,B}\left(\mathbf{x}^*_{SL,B}\right) - W_{S,T}\left(\mathbf{x}^*_{SL,B}\right) \tag{41}$$

$$\Delta W_S\left(\mathbf{x}^*_{SL,B}, \mathbf{x}^*_{SL,T}\right) = W_{S,B}\left(\mathbf{x}^*_{SL,B}\right) - W_{S,T}\left(\mathbf{x}^*_{SL,T}\right) \tag{42}$$

where $\mathbf{x}^*_{SL,B}$ represents the optimized structural layout for the baseline structure configuration and $\mathbf{x}^*_{SL,T}$ is the optimized structural layout for the technology configuration. Equations 41 and 42 represent the "Benchmark" structural layout treatment and what is for now referred to as the "Proper" structural layout treatment. The error associated with using the Benchmark treatment instead of the Proper is defined

as:

$$\varepsilon_{\Delta W_{S,B\rightarrow P}} = \left|\Delta W_S\left(\mathbf{x}^*_{SL,B}\right) - \Delta W_S\left(\mathbf{x}^*_{SL,B}, \mathbf{x}^*_{SL,T}\right)\right| \tag{43}$$

and if that error is above some threshold of significance, or

$$\varepsilon_{\Delta W_{S,B\rightarrow P}} \geq \varepsilon_{\Delta W_{S,B\rightarrow P,\text{threshold}}} \tag{44}$$

then Hypothesis 2.2 and the Proper treatment of the structural layout is supported in performance characterization.

The hypotheses at the $\mathbf{X}_{SL}$ level present metrics for a research approach to determine 1) the appropriate treatment of the structural layout in structural technology performance estimation and 2) if observations can be made that suggest full characterization of $\Delta W_S\left(\mathbf{X}_{OML}\right)$ should be executed, i.e. another tollgate step. Are there additional observations that could be made regarding the implementation of structural layout in a full characterization? If evidence is provided that supports moving to the next tollgate, should all design variables in $\mathbf{X}_{SL}$ be considered in performance characterization since the structural weight estimation function calls are computationally expensive, especially for two structural concepts? Can additional observations also be made to potentially support the technology experiment design application?

3.2.3 Outer Mold Line Level

The last level for the Overarching Performance Hypothesis is outer mold line and it represents another tollgate in the process. Ultimately, the importance of the OML impact on technology performance is assessed by the metrics of the applications of this problem: conceptual design technology selection, conceptual design technology implementation, and technology experiment design. However, as part of this tollgate approach, are there indications at the OML level that the quantification of $\Delta W_S\left(\mathbf{X}_{OML}\right)$ adds enough value to the overall characterization of performance that this functional relationship is worth implementing in these applications? At this

stage, the characterization process has gotten to the OML level because of observations made in the lower levels that showed the potential significance of the $\Delta W_S \mathbf{X}_{OML}$ function. Just because the functional relationship was developed, is it necessary to carry it through to the problem applications?

Hypothesis 3: If a characteristic is observed which is indicative of substantial information gained over the benchmark performance estimation process, then the characterization of aircraft level structural technology performance as a function of the outer mold line design space, $\Delta W_S(\mathbf{X}_{OML})$, should be implemented in suitable applications.

This hypothesis is contains the phrase "substantial information gained" as the active metric, but what does it refer to?

"Substantial information gained" generally means a compelling trend was observed which shows benefit of using the functional $\Delta W_S(\mathbf{X}_{OML})$ rather than the benchmark scalar ΔW_S. For example, if technology performance changes from positive to negative anywhere in the OML design space, it is by definition an indication of adding weight to the aircraft, which automatically raises a red flag. This indication of significance is especially true for technology selection: a technology will not be chosen for development or implemented in a design if it adds structural weight if that is its main proposed benefit. Another means of "substantial information gained" could be the result of a comparison of aggregate design space performance, e.g. histogram of $\Delta W_S(\mathbf{X}_{OML})$, to a nominal distribution of performance based on TRL. Technology Readiness Level accounts for uncertainty in technology performance based on immaturity, currently unobserved phenomena, and effects unknown. Therefore, if the probabilistic performance distribution $\Delta W_S \sim f(\mathbf{X}_{OML})$ represents a larger amount of "uncertainty" than should be expected of the probabilistic performance distribution $\Delta W_S \sim f(\text{TRL})$, then the effect of $\mathbf{X}_{OML}$ is statistically significant. This can

be tested by comparing values of the two distributions at specified confidence levels. An additional option for "substantial information gained" is the translation of performance to terms of gross weight. This metric, however, would require information from the designer or decision maker. Reference [78] states that the addition of one pound of empty weight can translate to an extra ten pounds of gross weight. If there is risk in adding gross weight by over-predicting structural technology performance, then some threshold of an acceptable increase in W_{TO} can be set that indicates to the designer that the relationship is significant.

Similar to the lower levels, performance characterization at the OML design space level can help the experiment design application as well. What other trends can be learned by investigating $\mathbf{X}_{OML}$? For experiment design, can the cause of these trends be determined through the characterization approach developed through this research? Are there certain aircraft sections, structural configurations, or loading conditions in which a structural technology performs better or worse compared to a baseline structure?

Technology performance is not a surrogate for structural weight and assertions about the design space cannot be made by independently examining technology performance. Simply because a technology performs well in a particular region of the design space does not make that the best configuration for the aircraft. Is there a possibility that the best technology performance occurs at a point in the design space where the airframe is far too heavy for technology performance to be relevant?

Hypothesis 3.1: The design region of $\mathbf{X}_{OML}$ that corresponds to the best structural technology performance will not coincide with the most optimal aircraft design in terms of W_S.

For the test case, preliminary research indicated that PRSEUS generally performs well for structural designs that are weight inefficient for the baseline. These findings,

however, were generated using the Benchmark treatment of the structural layout. Further information on the applications of the performance characterization problem is presented in the following sections. The last section of this chapter discusses the effect of the Hypotheses 1-3 on Gaps 1 and 2 that influence changes to the benchmark technology performance estimation process, seen in Fig. 31.

3.3 Implementation and Selection in Conceptual Design

Gap 3, which was identified in Section 3.1.1, states that error is introduced in the conceptual design applications of structural technology performance estimation, i.e. structural technology selection and implementation, as a result of an incomplete characterization of performance. Failure to consider the functional relationship $\Delta W_S\left(\mathbf{X}_{OML}\right)$ can introduce risk in the conceptual design process.

Hypothesis 4: The structural technology selection risk and implementation risk due to an incomplete characterization of weight reduction performance is greater than the standard risk due to technology immaturity.

The two parts to this hypothesis, representing the two conceptual design applications, are somewhat interwoven, and it requires multiple scenarios to fully capture the impact of the functional performance relationship.

To assess Research Gap 3, the TIES method and steps that are potentially affected by Gap 1 (neglecting the $\Delta W_S\left(\mathbf{X}_{OML}\right)$ relationship) are first considered. The beginning steps of the TIES method that reflect conceptual design space exploration up to the point of selecting a baseline OML configuration, $\mathbf{x}^*_{OML}$, remain unaffected. Step 6, however, is the point in which alternate scenarios must be examined. Three scenarios that require technology performance estimates are considered in addressing research Gap 3. They are described in this section and depicted along the TIES steps that they affect in Fig. 33. Scenario 1 follows the benchmark approach in which

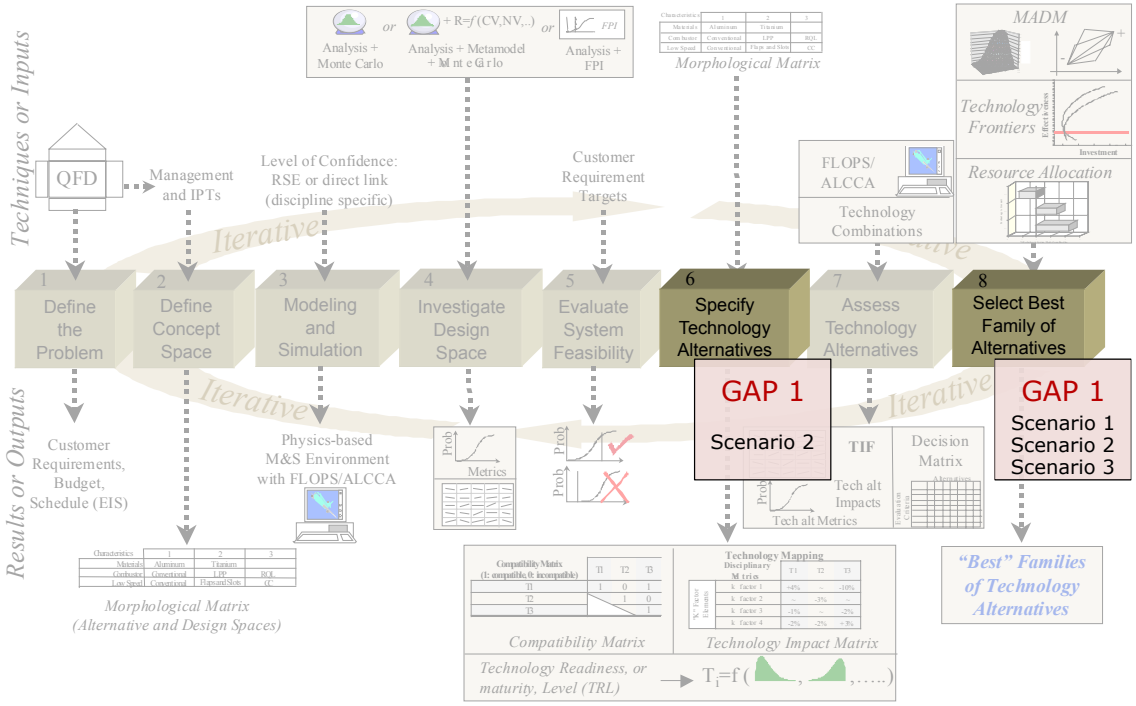

Figure 33: The steps in the TIES technology selection method affected by Research Gap 1 and their applicable scenarios

technology performance estimates do not yet exist. These estimates, ΔW_S, must be generated for the first time by the technology development program to be included in the technology impact matrix (TIM) and therefore assessed with other technology alternatives. The separation of Scenario 1 with the benchmark process occurs during Step 8 of TIES. In this step, assuming the structural technology has been selected as a part of the portfolio, technologies are implemented back in the conceptual design space to see if another $\mathbf{x}^{*2}_{OML}$ design point can achieve better performance than $\mathbf{x}^{*1}_{OML}$ considering all technology impacts. At this point in Scenario 1, both formulations of technology performance impact, scalar k_{ST} and functional $k_{ST}\left(\mathbf{X}_{OML}\right)$, can be applied to conceptual design to compare their respective results for $\mathbf{x}^{*2}_{OML}$ and $\mathrm{R}\left(\mathbf{x}^{*2}_{OML}\right)$, where R represents a response of interest.

Scenario 2 follows a similar approach, except the assumption is made that technology performance has been previously characterized as a scalar using the benchmark

approach for another technology development program. In this scenario, multiple baselines can be chosen in Step 6 to represent varying objectives of multiple programs. The new technology development program would most likely default to using the value of technology performance previously published in the literature by the benchmark, i.e. $\Delta W_S\left(\mathbf{x}^*_{OML}\right)$. For each of the potential OML baselines, what would the error be in implementing this value rather than an appropriate value drawn from the functional $\Delta W_S\left(\mathbf{X}_{OML}\right)$?

The last scenario, Scenario 3, deals with general implementation of the technology within the conceptual design space. In this scenario, a conceptual designer has interest in the structural technology and performs trade studies in $\mathbf{X}_{OML}$ with the technology in mind. To compare the effect of the benchmark performance estimation approach and the functional performance characterization, the technology performance impact k^*_{ST} is treated first as a scalar, estimated at baseline $\mathbf{x}^*_{OML}$, and then examined as a function, $k_{ST}\left(\mathbf{X}_{OML}\right)$. Risk, in this scenario, is determined by 1) calculating the probabilistic distribution of a conceptual design response, $\mathrm{R}\left(k_{ST}\left(\mathbf{X}_{OML}\right)\right)$, then 2) subtracting that distribution from the value of the response generated with scalar impact k^*_{ST}:

$$\mathrm{P}\left(\varepsilon_{W_{\mathrm{fuel}}}\right) = \mathrm{R}\left(k^*_{ST}\right) - \mathrm{P}\left(\mathrm{R}\left(k_{ST}\left(\mathbf{X}_{OML}\right)\right)\right) \tag{45}$$

and 3) setting a desired confidence interval (CI) for risk and assessing the value of $\mathrm{P}\left(\varepsilon_{W_{\mathrm{fuel}}}\right)\|_{CI}$. Through these scenarios, observations can be made from a comprehensive assessment of conceptual design metrics in terms of $k_{ST}\left(\mathbf{X}_{OML}\right)$ to determine support for Hypothesis 4.

3.4 Experiment Design and Selection

The other application of the structural technology performance characterization problem is the design and/or selection of technology level experiments. These experiments

are executed to advance the structural technology and enhance confidence in the inputs and assumptions of structural technology performance estimation models. A limited characterization of technology performance also limits the number of objectives that can be considered in structural technology experimentation. There are four different levels at which technology performance is assessed in this research approach: 1) technology level, 2) structural layout level, 3) conceptual design parameter level, and 4) conceptual design metric level. At each of these levels, if an interesting observation is made regarding performance characterization, the first question that is asked is most likely "why?" Experimentation is an investigation in causality, and it provides the chance to determine whether the observed phenomena is real or if it is a result of inadequate/faulty modeling or assumptions.

The gaps that affect the benchmark experiment design process are shown in Fig. 34. This schematic shows that Gap 1 has an influence in the data that is sent to the *Technology Development & Demonstration* element, and this phenomenon was discussed in the development of Gap 4. Gap 4 represents the lack of traceability and potential inability to manage the massive amount of data that is generated with a higher fidelity structural weight estimation model for an three levels of design spaces, $\mathbf{X}_{OML}$, $\mathbf{X}_{SL}$, and $\mathbf{X}_{T}$. As shown in the example of Section 3.1.2, there are upwards of over 5 million potential data points for the OML level alone, and more results are generated at each of the lower levels as well. How can this data be processed to show causality in trends and can it enable additional potential experiments and experiment objectives?

Hypothesis 5: If performance of the three design space levels, $\mathbf{X}_{OML}$, $\mathbf{X}_{SL}$, and $\mathbf{X}_{T}$, can be connected through similar aggregate parameters in the experiment characterization process, then a larger number of objectives can be considered for experiment design.

Development of the experiment characterization process is dependent on the results of structural technology performance characterization and the inputs and outputs at each level. As mentioned, if Hypothesis 2.2 is supported and performance for the baseline structure configuration and technology configuration are estimated with different structural layouts, the one-to-one component comparison is lost. Therefore, a direct comparison cannot be made for internal loads, design variables like skin thickness, etc. If the various levels can be bridged by examining aggregate values of appropriate inputs and metrics of each design space, then it is hypothesized that a causality relationship can be achieved.

There are additional considerations that should be made in that are not necessarily addressed by this research but should be accounted for in assumptions nonetheless. For example, can results obtained from technology experimentation be applied back into the performance estimation model, even if the objective of the experiment is not directly related to model development, calibration, or validation? Do the results scale, i.e. are the results of a particular experiment valid for different scale of design, or more generally a different $\mathbf{x}_{OML}$ design point? This is extremely important in the realm of physical experimentation. Physical experiments can be expensive, and with limited resources, a program may choose to perform an experiment on a particular configuration at a smaller scale. If results obtained from this experiment are not applicable beyond the small scale configuration, is that particular experiment useful for the advancement of the technology?

Additionally, one of the main assumptions for the experiment design application of this problem is that limited resources are available to the technology program, and therefore, the single best experiment for technology advancement should be determined. However, do the results from this experiment influence the development of the next experiment, i.e. should experiment design be performed serially? In the benchmark process, a "building-block" approach was designed all at once. There are

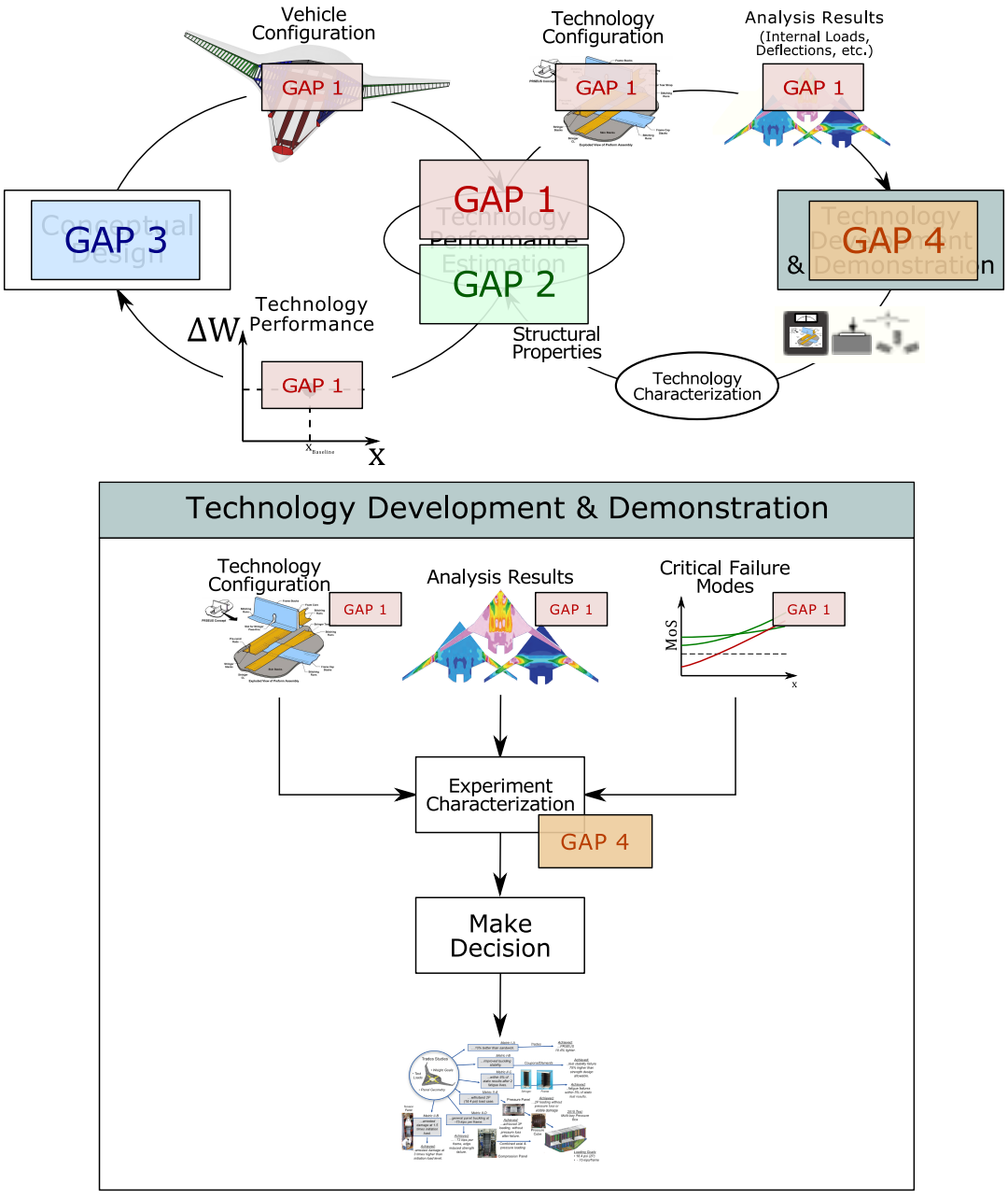

Figure 34: Gaps in structural technology experiment design

instances within this approach that small changes were made as a result of lessons learned. For example, the frame spacing for PRSEUS changed in the design of the multi-bay box (MBB) to ensure continuous load paths when the panels were assembled. Aside from minor changes like this, would the experiments have been designed different if the experiment design process was implemented serially? These notions may be areas of future research, but are considered in the implementation of the research plan developed in this chapter.

3.5 Summary

This chapter has presented the formulation of research for the problem of structural technology performance characterization. The Overarching Performance Hypothesis was focused on the development of a process to assess whether or not the effects of quantifying structural technology performance as a function of the outer mold line, $\Delta W_S\left(\mathbf{X}_{OML}\right)$ are significant enough to pursue a full characterization. The impact of this characterization on conceptual design and technology development applications can be synthesized into another overarching hypothesis, representing the entire thesis:

Thesis Statement: Aircraft level structural technology performance, i.e. structural weight reduction ΔW_S, should be quantified as a functional relationship to the conceptual design space, $\mathbf{X}_{OML}$, because the failure to do so could potentially introduce additional risk in technology selection and implementation in the conceptual aircraft design phase as well as experiment design and selection for technology development. This will be demonstrated with the process developed in this research.

Assessments based on this thesis statement and its corresponding lower level hypotheses are compared against the benchmark approach presented in Chapter 2. Practical implementation of a full characterization of $\Delta W_S\left(\mathbf{X}_{OML}\right)$ requires significant effort

because of the challenges addressed thus far. As mentioned, the overall objective is to determine at design space each level and each application if the impact of this characterization is significant enough to substantiate the added effort. If the hypotheses developed in this chapter are supported or rejected, how does it translate to changes in the benchmark approach?

Figure 35 shows how each of the gaps affect the synthesized benchmark process of Sec. 2.5. This is a summation of effects of each research gap discussed in the previous sections of this chapter. Through the hypotheses, a process is synthesized to fill the gaps. The thesis process is shown in Fig. 36, and the changes from Fig. 35 are explained hereon. It provides a framework by which hypotheses can be tested. Gap 1's effect on data passing for the vehicle configuration, shown at the top of Fig. 35, was identified because the *Conceptual Design* element of the framework would be required to send information about the entire design space to the characterization process. Its next effect is on the generation of a structural model, along with Gap 2. These two gaps necessitate the ability to define geometries parameterically, for both the outer mold line and structural layout, before a structural model can be created. To explore each of these design spaces, $\mathbf{X}_{OML}$ and $\mathbf{X}_{SL}$, a sampling approach is required, which translates to an iterative loop through cases. A decision point is then required after the structure is sized to cycle through all the sampling cases.

Once all cases are examined for a particular sampling plan, then the structural technology performance characterization takes place. This characterization is now a function of the OML and SL design spaces. Extra data is generated by addressing Gap 1 in the Structural Sizing outputs in Fig. 35, and it is driven by the designer's sampling plan. The output of performance characterization is now a functional $\Delta W_S\left(\mathbf{X}_{OML}\right)$, which is implemented back into *Conceptual Design*. The last step, in the bottom right of Fig. 35, is *Experiment Characterization*. In the benchmark, this was an expert-driven process with little transparency, but through the hypotheses made, is now also

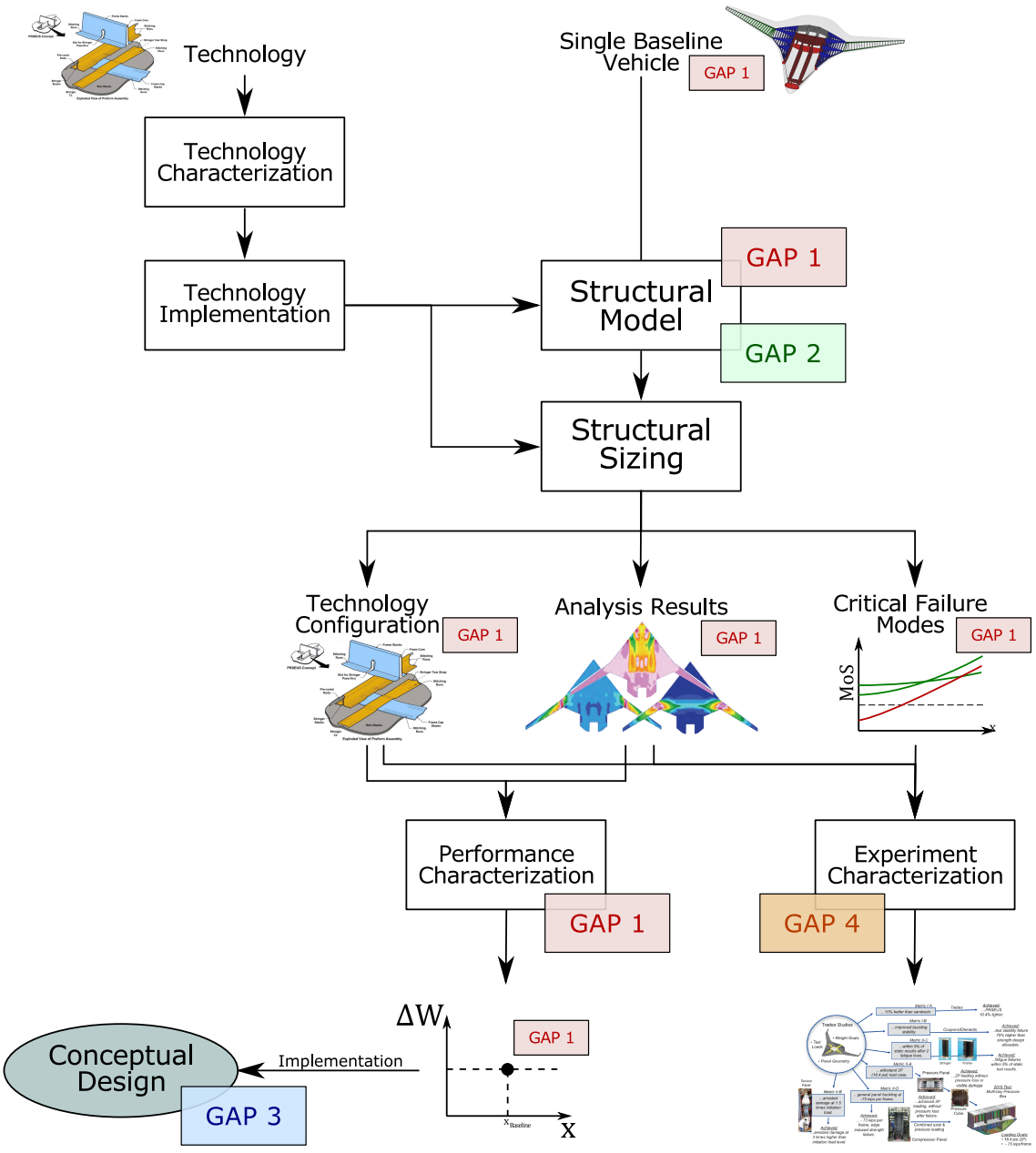

Figure 35: Gaps in the benchmark process

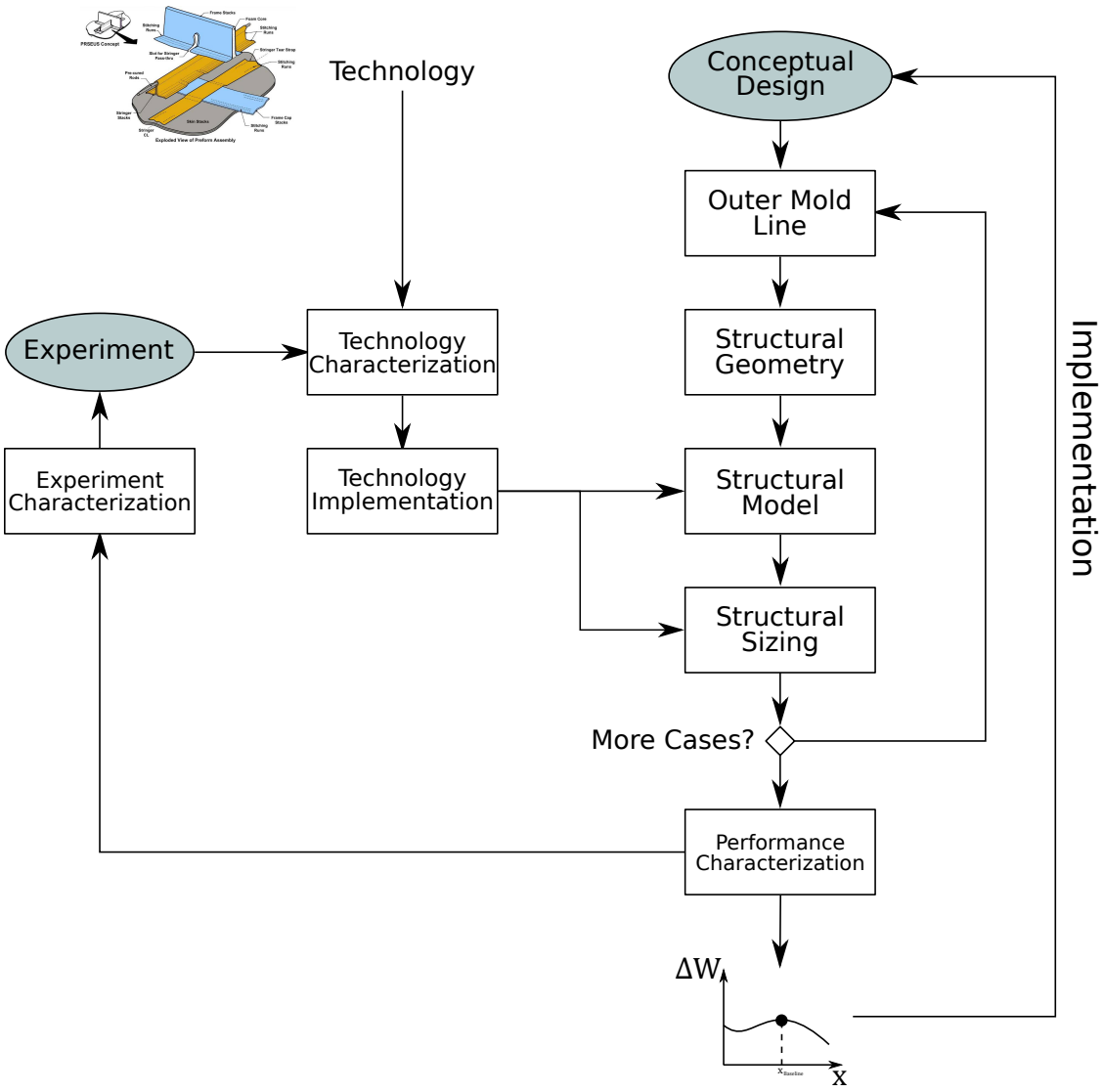

Figure 36: Synthesized approach to fill gaps presented in this chapter

function of the technology performance characterization itself to enable repeatability and traceability in the process. Experiment characterization enables a decision to be made for experiment design, and then the experiment is performed. Results from this experiment should feed into the expert-driven *Technology Characterization*, and then the technology is implemented back into the structural weight estimation model. Although the serial process of experimentation is not addressed within this research, the process shown in Fig. 36 is the framework on which this thesis research is built.

CHAPTER IV

IMPLEMENTATION OF RESEARCH PLAN

To investigate structural technology performance as a function of the design space levels discussed in the last chapter, a set of models that captured appropriate technology effects needed to be synthesized for a test case. The scope of the test case is defined by aircraft concepts, configurations, structural technologies, and design variables within each level of design space that are considered. Because an uncommon amount of non-proprietary data regarding the PRSEUS structural concept is available to academia, the test case is centered around this technology. This subset of stitched, resin infused composites is applicable to any airframe structure that can be built in a skin-stiffened configuration, e.g. conventional wingboxes, circular fuselages, non-circular HWB centerbodies, etc. However, the design intent for PRSEUS through experimentation in the ERA program was focused on the HWB centerbody section. It is shown in this chapter that a parametric weight estimation model with features appropriate for PRSEUS characterization was built around the HWB aircraft configuration. These two factors made the HWB an appropriate configuration for the test case.

This chapter discusses the various models that were considered and implemented in this research plan for characterizing performance of the PRSEUS structural technology. It also discusses the configurations, design parameters, etc. that were considered in the characterization and application of structural technology performance. Within the framework presented in Fig. 36, the thesis method "Structural Technology Evaluations for Experimental Design" (STEED) is introduced. Specific attributes of this generic approach are established through testing the hypotheses of the research

formulation in the following chapters.

4.1 The STEED Approach

The success of this research is dependent on the ability to systematically identify whether the conceptual design space has a consequential impact on structural technology performance and, in turn, determine whether that impact introduces risk in conceptual design studies and experiment design for technology development and demonstration. Development of this systematic approach follows the top-down decision support process shown in Fig. 15. This was found to be an appropriate framework because the research formulation is set up as a series of decision points, e.g. the decision to move forward to a more comprehensive characterization of structural technology performance. For technology experiment design, however, providing support to enable decisions was just as important as the decision itself. The characterization details at each design space level were also important to establish a line of traceability to determine causality in technology performance trends.

The first steps in the top-down process were presented through the motivation of the technology performance characterization problem, the discussion of the benchmark process, and also the formulation of research. For steps 1 and 2, need and value were established through reduction of risk in conceptual design technology selection and implementation, as well as increasing the support to technology development. The problem was well defined for step 3 in terms of how to generate performance estimates and the various design space levels associated with that estimation process. In the context of the tollgate approach established by hypotheses in the research formulation, the alternatives at each level are 1) push forward with structural technology performance characterization in the framework established in Fig. 36, or 2) characterize structural technology performance with the benchmark process of Fig. 24. The Structural Technology Evaluation for Experimental Design approach is built on the

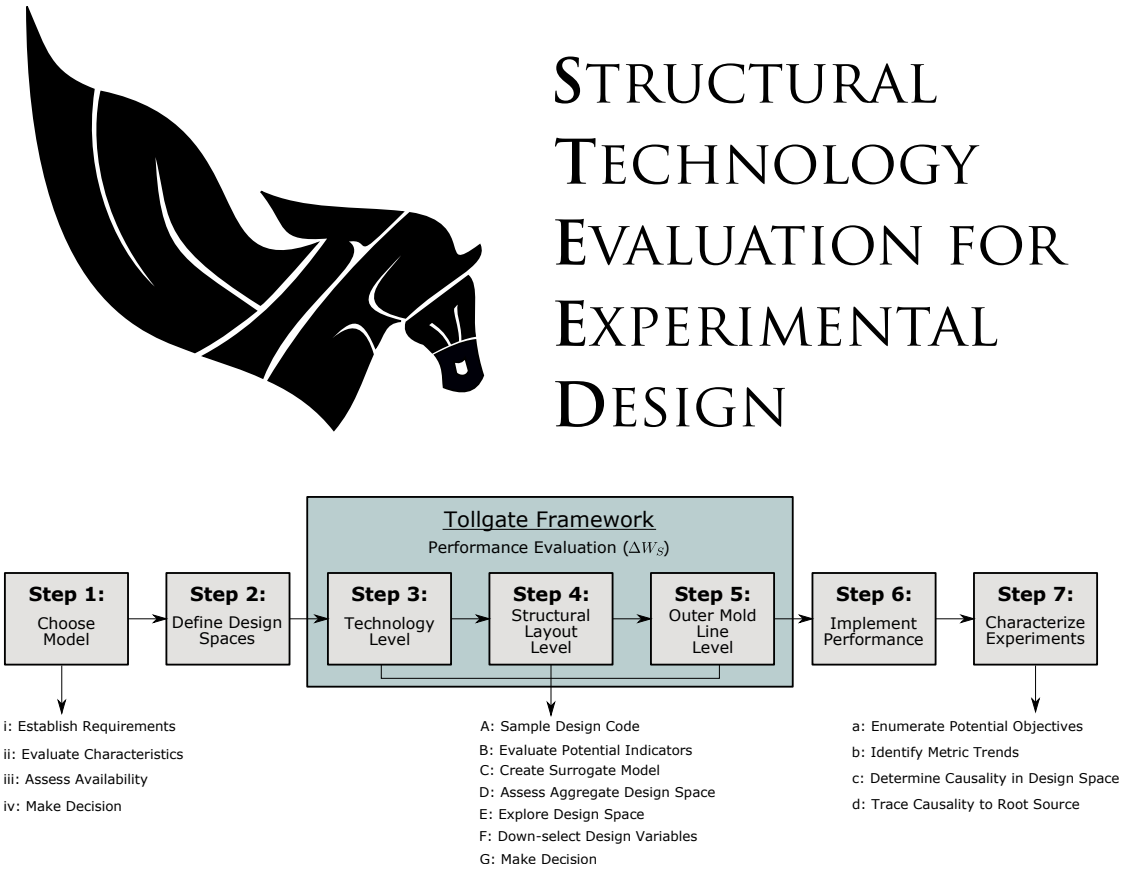

Figure 37: The STEED approach for structural technology performance characterization and implementation

tollgate process to enable decision making at each step of the way and is shown in Fig. 37. The steps of this process are discussed in the following subsections.

4.1.1 Step 1: Choose a Modeling Platform

The most important step in this process is in the setup of the approach. Depending on the goal of development and the structural technology's stage of maturity, an appropriate model is paramount in the ability to predict performance phenomena. Also, it is critical for this approach that the modeling platform have the ability to generate structural models in a parametric and automated manner. Therefore, before choosing a set of design variables for each level of the design space in the performance characterization problem, it must be determined if the ability to represent particular

parameters exists within a modeling platform. One of the challenges associated with the benchmark process is the tedious setup for manual generation of the structural model. On the other hand, the implementation of a single structural model enables the ability to include features that would otherwise be difficult for an automated process. Therefore, it is likely that assumptions must be made for a parametric environment.

To determine which model is most appropriate for generating structural technology performance assessments as a function of the conceptual design space, the following general steps should be followed:

i: Establish Requirements This step gives the user the chance to formulate which inputs, outputs, and features are most important to a successful characterization of structural technology performance. The capability of creating parametric high fidelity structural models to be used in the early phases of design is a significant research thrust at the NASA Aeronautics Mission Research Directorate (ARMD). The Transformational Tools and Technologies (TTT) project included this capability in a research solicitation which is underway. Limitations exists in current approaches, however, and they need to be accounted for when making requirements.

ii: Evaluate Characteristics The order of computational analyses, complexity of geometry, applicable failure modes, etc. should be considered against requirements when evaluating the characteristics of a modeling platform. A matrix of alternatives [24] is a useful tool when enumerating each of these characteristics to evaluate against each other.

iii: Assess Availability In academics, the most potentially influential characteristic is the availability of a particular code due to the proprietary nature of the aerospace industry. If it is found that a sufficient code does not exist, the user may find it best to develop his or her own modeling platform through the

integration of available tools.

iv: Choose Model A simple qualitative assessment is most likely sufficient for a decision in this first step based on the number of requirements or desired characteristics met for a modeling platform. If a more formal technique is required, one of the MCDM methods mentioned in Section 2.2.1 can be implemented.

These steps should be followed not only for a structural weight estimation platform for performance characterization but for the conceptual design model as well. In the latter, the user needs to decide if a simple assessment based on first principles and analytical equations, e.g. the Breguet Range equation, is sufficient or if a more complete conceptual design tool like FLOPS is required to assess risk. Once the models are chosen, the STEED approach moves to defining the design variables that will be investigated at each of the levels.

4.1.2 Step 2: Define the Design Spaces at Each Level

With models established, the design spaces need to be defined at each level of the problem: Technology, Structural Layout, Outer Mold Line, and Conceptual Design. Considering the limitations of the design environments, be it the parametric definitions or computational expense, a subset of the design space at any given level may need to be examined. Each design variable within $\mathbf{X}_{OML}$, $\mathbf{X}_{SL}$, and $\mathbf{X}_{T}$ should be enumerated with nominal values and limits.

4.1.3 Step 3: Evaluate Performance at Technology Level

This step in the STEED approach is pivotal. It is the point in the process that switches from design setup to implementation of the models and assessment of performance. Keeping in mind one of the most significant challenges, the extensive computational run-time for a higher order structural weight estimation model, if the relationship between technology performance and the OML design space, $\Delta W_S\left(\mathbf{X}_{OML}\right)$,

can be determined to be insignificant early in the process, then a portion of effort can be saved for the technology team. As the process traverses from this lowest level to the OML, the characterization efforts become larger. However, it was also mentioned in Hypothesis 1 that the threshold of "significance" for observations is much lower at this level because of the implicit relationship between low level indicators and the $\mathbf{X}_{OML}$ design space.

While function calls at the technology level, depending on the fidelity of the model, may be computationally cheap, they are not instantaneous. For example, interacting with Hypersizer at this level in an automated way takes on the order of hundredths or tenths of seconds. For the definition of an entire design space, loading conditions, etc., this time is not negligible. Additionally, decisions regarding indications of $\Delta W_S\left(\mathbf{X}_{OML}\right)$ significance are supported through aggregation of the design space. Although specific performance trends for particular design variables certainly play a role in the decision, assessments of the entire design space are the first indication that the OML can have a substantial effect on structural technology performance. The ability to evaluate both is required for each design space level and the computational expense affects how that can be achieved.

Since the goals of performance characterization are similar, if not the same, at each design space level, a generic set of steps can be followed in the tollgate process. These steps can be amended for specific characteristics, but the general process is to first determine ΔW_S in a measure of the total design space and then examine particular trends, and these steps reflect that notion.

Generic Sub-process:

A: Sample the Design Code This step is performed with the goal of creating a surrogate model of the design space for each applicable metrics, e.g. ΔW_S, $W_{S,B}$, $W_{S,T}$, etc. A DoE sampling plan must be generated and is dependent on the anticipated nonlinearities, allowable computational time, and expected

contribution to variance of each design parameter.

B: Evaluate Potential Indicators If enough information is presented to make a decision in the tollgate framework simply through the data generated by sampling the design code, and if no other assessments are needed at the particular design level, then the user can skip to the last step. *For example, if a 30% difference was witnessed between performance of two different technology designs,* $\Delta W_{S,i}(\mathbf{x}_{T,1})$ *and* $\Delta W_{S,i}(\mathbf{x}_{T,2})$*, then the threshold for a Hypothesis 1 has been exceeded. However, it is particularly important to characterize the design space at the technology level for eventual use in experimental design. Therefore, in Step 3, Hypothesis 1 would be supported, but the conditions to move forward have not yet been met.*

C: Create a Surrogate Model An approximation function should be built between the inputs and desired outputs for the data generated in Step A. The mathematical form of this model and the fitting or training algorithm are dependent on the characteristics mentioned in Step A as well. Artificial neural networks are versatile options for any of the design space levels because they can act like interpolating functions or can smooth through the data, depending on the user's objective and hyperparameters of the model, e.g. number of layers, number of nodes, activation function, etc. *For the technology level, nonlinearities and discontinuities may exist, depending on the configuration, due to stiffener drop-offs as a function of spacing, the transition of critical failure modes, and such. ANNs are therefore suggested as the model form at this level.*

D: Assess Aggregate Design Space Now that a mathematical form exists of the design model that can be run near instantaneously, a probabilistic approach can be easily implemented to assess performance for the entire design space. Monte Carlo simulation is a high fidelity form of probabilistic analysis, and is appropriate for generating distributions with surrogate models. Histograms at

this step will help quantify risk in terms of specific confidence levels, and other indications of $\Delta W_S(\mathbf{X}_{OML})$, such as the bounds of a distribution existing on both sides of the $\Delta W_S = 0$ performance mark.

E: *Explore the Design Space Surrogate models also enable a visual rapid design space exploration capability. This capability can augment aggregate values of performance by identifying trends in correlation of performance between design variables, i.e. changes in sensitivity for $\Delta W_{S,i}(\mathbf{x}_{T,1})$ when $\mathbf{x}_{T,1}$ is varied, or unique trends in one of the weights comprising performance, $W_{S,B}$ or $W_{S,T}$. This step can also help assess the functional form of the surrogate model if unexpected trends occur in the design space.

F: Down-select Design Variables At each subsequent design space level that is investigated in this bottom-up formulation, greater resources are required to perform trade studies. To mitigate the number of setup and computational hours required to sample the design code, down-selection from the design space $\mathbf{X}$ should be performed.

G: Make Decision The last step in this sub-process is to make a decision to expend additional resources for a more comprehensive performance characterization at the next design space level. Guidelines have been set up through hypotheses and other indicating factors; however, these guidelines are not a catch-all. If a decision is traceable to a supporting evidence-based indication factor, then this factor warrants the move to the next tollgate step.

The design space exploration step is marked with an asterisk because, as mentioned, it may not directly contribute to the tollgate framework of STEED, but it can potentially provide a traceable route of causality to enable experiment design.

The full sub-process described in this section should be followed for Step 3 of the STEED approach. Design parameters to be examined in $\mathbf{X}_T$ are defined as

$\mathbf{X}_{T\sim f(OML,SL)}$, i.e. those that map to the upper level design spaces, and include global geometry of the technology level component and local loading conditions. Any design parameters not directly identified in one of the design space relationships presented in Section 3.1.1 will be included in a weight optimization for each point in $\mathbf{X}_{T\sim f(OML,SL)}$, e.g. skin thickness, stringer spacing, etc. Realistically, a statement of non-zero is still made with some threshold. While the user is free to interpret and prescribe this threshold, the author suggests an upper limit of $\delta\left(\Delta W_{S,i}\right) = {}^{+}/_{-}5\%$, depending on the technology, its design characteristics, its weight reducing mechanisms, and the assumptions made in the technology model.

4.1.4 Step 4: Evaluate Performance at Structural Layout Level

If evidence warrants the examination of performance at the structural layout design space level, Step 4 begins with sampling $\mathbf{X}_{SL}$ and recording outputs of structural weight, component design values of $\mathbf{x}_{T,i}$, internal loads, failure modes, and any other pertinent data for characterization. This step has the additional burden of determining an appropriate manner of handling the structural layout for each OML design point if a full characterization is required, and this should be kept in mind when determining an appropriate DoE. If any nonlinearities are expected in the relationship between structural weight and the structural layout design space, then a sampling plan that accounts for nonlinearity should be chosen, eg. a n-level full factorial where $n > 2$, central composite design, space filling method like Latin Hypercube, or any combination of these options. The sampling should be repeated for at least one additional OML design point to 1) ensure the trends are not simply local to the initial baseline design point and 2) provide evidence to the supposition of the significance of $\mathbf{X}_{OML}$.

An example of the tests performed in Step 4 is shown in Section 5.3. The desired treatment for the structural layout in performance estimation is to specify some

default $\mathbf{x}^*_{SL}$ configuration and hold it constant throughout the OML design space. Referred to as the Uninformed approach, this treatment would require the least effort in setup and computational time. If it is observed that ΔW_S changes as a function of $\mathbf{X}_{SL}$, then the decision must be made to either perform optimization within the $\mathbf{X}_{SL}$ space to find a single estimate of $\Delta W_S|_{\mathbf{x}_{OML}}$ or the functional $\Delta W_S(\mathbf{X}_{SL})$ can be propagated to the OML level and a range of performance can be found at each $\mathbf{x}_{OML}$. This choice affects the sampling plan chosen in Step 5A, and the example in Section 5.3 shows the former case of structural layout optimization. Variation of the structural layout can also be considered a form of uncertainty for technology performance if confidence is lacking in results of the structural weight estimation model.

4.1.5 Step 5: Evaluate Performance at Outer Mold Line Level

Step 5 is the last tollgate in this framework that operates on ΔW_S as a metric. The same generalized process discussed in Step 3 is taken here, and the lessons learned from the previous design space investigations are implemented. Surrogate modeling is critical in investigating the OML design space, because, if Hypotheses 2.1 and 2.2 are supported, then a large number of design variables in both the $\mathbf{X}_{OML}$ and $\mathbf{X}_{SL}$ spaces must be considered in Step 5. Additionally, if the structural layout is properly accounted for in the Step 5A DoE, then structural layout optimization or variation can be implemented in the surrogate models. Using these function calls rather than calls of the structural weight estimation model take, on average, approximately 0.25 seconds compared to 1-2 hours – a reduction on the order of 10^{-6}.

Even though all indications from lower level design spaces support the identification of a significant relationship between outer mold line and structural technology performance, Step 5 acts as part of the tollgate framework because results at the $\mathbf{X}_{OML}$ level could still potentially indicate a weak functional performance relationship. In this case, even though the characterization has taken place, is any value

added in actual implementation of the $\Delta W_S(\mathbf{X}_{OML})$ function in the conceptual design model? Is the variation within the limits of standard TRL uncertainty or error due to model uncertainty? The decision is also dependent on the ease of implementation in the conceptual design model. If implementation is not a showstopper, the likelihood of a significant impact of $\Delta W_S(\mathbf{X}_{OML})$ on conceptual design metrics is extremely low.

4.1.6 Step 6: Implement Performance in Conceptual Design

Once the full $\Delta W_S(\mathbf{X}_{OML})$ characterization has been performed in Steps 3–5, this function is implemented in the conceptual design code to evaluate the technology performance impact on conceptual design metrics. The same generic sub-process for Steps 3-5 can be followed for conceptual design implementation despite characterization for a tollgate not being the end goal of Step 6. Depending on the form of the conceptual design model and the design parameters included in $\mathbf{X}_{OML}$, simple logic can be used to determine whether a particular step is applicable. For example, if a low order "model" like the Breguet Range equation is being used as the conceptual design performance representation, then there is no need to complete Sub-step A and sample the design space. Computational expense will not be an issue for an analytical equation.

If a higher order conceptual design tool like FLOPS is used in Step 6, then the DoE should include a design variable that accounts for structural technology performance. In FLOPS, design parameters for performance implementation are segmented between the wing and fuselage (or HWB centerbody) and also defined as a scale factor on each respective weight. The need for sectional performance estimates was established just for this reason, and the transformation from performance to conceptual design

implementation is translated from Eqn. 5 and defined as:

$$k_{ST,w} = 1 - \frac{\Delta W_{S,w}}{W_{S,B,w}} = \frac{W_{S,T,w}}{W_{S,B,w}}$$
$$k_{ST,cb} = 1 - \frac{\Delta W_{S,cb}}{W_{S,B,cb}} = \frac{W_{S,T,cb}}{W_{S,B,cb}} \tag{46}$$

where k is the scale factor implementation in FLOPS, and the last subscript for each term represents the aircraft section. In this case, the wing is accounted for as one section, so trapezoidal and outboard wing performance is combined. Assessment of conceptual design metrics as an aggregate of the OML design space enables the quantification of risk of neglecting the $\Delta W_S(\mathbf{X}_{OML})$ function rather than with a benchmark scalar implementation. This risk helps quantify the value in efforts spent to characterize the functional performance relationship. Additionally, it supports conceptual design and technology development program decision makers in determining if the value proposition for performance characterization is worth the effort for other structural technologies. Finally, design space exploration will enable analysis of trends that can be used in experiment design. If a technology development objective aligns with the conceptual design metric space, then the process in the next step can be followed to determine causality.

4.1.7 Step 7: Identify Trends for Experiment Design

Although *Conceptual Design* and *Technology Development* are both applications to structural technology functional performance characterization, $\Delta W_S(\mathbf{X}_{OML})$, experiment design for *Technology Development* is the last step in the process. Its placement here is because the technology team should use all available resources to determine the best experiment for technology advancement in the context of the overall program objective, even the conceptual design metric level. Step 7 is defined with a vague program objective in mind, where development is in the early stages and fundamental research is still being performed on the technology to characterize the system. In this instance, rather than a single experiment objective like the benchmark process,

the team can investigate the potential impact of an array of objectives. Available resources also needs to be considered in experiment design process, and without prior knowledge, the process of Step 7 is simply an approach to sift through the drastically increased amount of available data in comparison to the benchmark process.

The technology development team needs versatility in the ways they can examine data. Ultimately, the goal is to determine the configuration of a test article (component or assembly), loading conditions (local or global), boundary conditions, and important assumptions. To enable a versatile, repeatable, and traceable process to determine these characteristics, the following steps are followed:

a: Enumerate Potential Objectives Experimental objectives are discussed in Sec. 2.4.1, and the first step in this sub-process is to identify all potential experiment objectives that align with the overall technology development program objectives. These objectives will aid in establishing requirements that each any potential experiment must meet in terms of information gained for advancement of the technology.

b: Identify Metric Characteristics Throughout Steps 3-6, quantification of the relationship of weights ($W_{S,B}$ and $W_{S,T}$) and performance (ΔW_S) as a function of each level of design space has been developed. With aggregate distributions of the design space and interactive design point sensitivity analysis, the technology development team can search through each design space level as needed to identify specific metric characteristics, e.g. sensitivities, distribution variance, etc., that coincide with a particular experiment objective. These characteristics will initialize a study in causality to determine experiment design parameters.

c: Determine Causality in Design Space Within the design space level that a particular metric characteristic is identified, there are design parameter settings and loads at which that characteristic occurred, even if these variables are

distributions themselves. For example a filtering process could take place for experiment characterization in which investigation of bottom-line performance is desired at $\mathbf{X}_{OML}$. The metric space is then filtered to include all the cases from a Monte Carlo simulation with a performance below some threshold $\Delta W_{S,LB}$. Aggregate design variables such as $\mathbf{x}_{OML}$ and $\mathbf{x}^*_{SL}(\mathbf{x}_{OML})$ as well as detailed design variables and results for each structural component, e.g. internal loads, failure modes, $\mathbf{x}_T$ values, etc., can be determined for each of these cases. This sub-step is an exercise in determining causality in the specific design space level in which the metric characteristic was identified.

d: Trace Causality to Root Source The last step in this sub-process is to determine causality to the lowest applicable level. Regardless of the metric characteristics identified in sub-step (b), traceability exists between each design space level through loads, failure modes, and/or design variables. The lowest applicable level is not required to be the technology level. As previously mentioned, technology development experiments can be in the form of thought experiments, computational experiments, or physical experiments, and if an assumption in the design model is creating risk for the technology performance estimation, for example, then an experiment can be performed that uses higher order physics to mitigate that risk.

Determining causality is an inverse problem and therefore, the potential for non-uniqueness in the solution space exists. Step 7 presents the technology team with options, and the responsibility for decision-making relies on the SMEs rather than this enabling process. Example scenarios are provided in Chapter 7.

The following sections in this chapter present the first two steps of the STEED approach applied to the PRSEUS test case.

4.2 Choosing a Modeling Platform

4.2.1 Structural Weight Estimation

The research formulation introduced in the previous chapter hinges on one capability – the ability to create structural models with parametric outer mold line and structural geometries that fit into an appropriate structural weight estimation approach for technology performance. Development of a fully parametric geometry model for an entire aircraft structure can be a daunting undertaking, especially for higher fidelity structural analysis. A few parametric structural weight estimation models were considered for this research, and a discussion of these models is presented in the following subsection.

4.2.1.1 Potential Parametric Weight Estimation Approaches

Physics-based parametric modeling for structural weight estimation is difficult because a large amount of effort is required in geometry definitions and recognizing inappropriate or infeasible structural configurations in an unsupervised automated capability. Relationships between $\mathbf{X}_{OML}$ and $\mathbf{X}_{SL}$ can be problematic for parameter sweeps, especially in highly integrated configurations. These challenges increase directly with the desired level of complexity and fidelity.

Low order approaches have been attempted in the characterization of structural technology performance as a function of the conceptual design space. One such approach by Adams [1] is based on low order handbook equations and enumerates the material properties of advanced high performance structural materials to obtain a weight factor (k-factor):

$$WF = R\chi_{adv} + 1.0\chi_{Al} \tag{47}$$

where

$$R \equiv \frac{(\rho/\sigma)_{adv}}{(\rho/\sigma)_{Al}} \equiv \frac{(\rho/E)_{adv}}{(\rho/E)_{Al}} \tag{48}$$

and χ_{adv} is the fraction of aluminum structure to be replaced by advanced materials.

This method relies on statistical equations for weight estimates, listed in Reference [1], and the ratios of structural properties in the previous equations do not account for specific loading conditions or failure modes. The geometry configuration and other detailed characteristics of the technology are also not accounted for.

A more advanced low order approach is exemplified by a method by Elham [23], in which the skin, stringers, ribs, and spars are collapsed into equivalent plates for upper and lower surfaces. These equivalent plates are then sized for strength-based failures only using equivalent, or "smeared," properties. These two approaches have one thing in common, traceability to lower level detailed design parameters is lost. For structural technologies, these reduced order and analytical methods may not be appropriate because information and performance attributes of the structural technology may be lost in the aggregation of equivalent parameters. For example, key attributes that contribute to PRSEUS performance are mainly in the nonlinear region of structural characteristics. Ability to carry load past the point of local skin buckling, arrestment of damage propagation through composite stitching, mitigation of laminate pull-off failure mechanisms. If technology developers are to design and select experiments based on results from a trade study that target these phenomena, the simplifications of these low order approaches may not provide any insight.

Higher order approaches exist in industry [16], government [29], and academia [53], with the two former being somewhat less available to the latter. Parametric higher order structural FEM approaches specifically for the HWB have been a focus because: 1) performance typically calculted with empirical models of historical data are not available for this configuration and 2) it is a relatively simple geometry to model compared to a traditional T&W that requires complex integrations of the wing and body. An example is a code developed at NASA Langley Research Center called HCDstruct [29]. This tool was considered for this research, but it uses the same "smeared" property approaches as the lower order methods and applies them to a

full vehicle finite element model. Multiple load cases are considered in the structural sizing routine, but information about the technology design variables and sources of phenomena are lost in the optimization process. For example, trade studies have been performed that implement PRSEUS structure for direct weight estimation (not for estimating technology performance). The approach takes the nominal design of PRSEUS, shown in the 2nd column of Table 12, and develops an equivalent plate with the same orthotropic properties and a reference thickness of 1 in. This reference thickness is scaled for every element in a fully-stressed formulation. How does the new calculated thickness translate to the PRSEUS design parameters, especially when every element has a different thickness? Would the result be different if the nominal PRSEUS design variables from which the "smeared" parameters were calculated took different values than a nominal design, $\mathbf{x}_{T,nom}$?

PRSEUS, like other potential structural technologies, is a complex configuration with a large number of potential failure mechanisms. It needed to be modeled with higher fidelity, especially to enable technology experimentation; and therefore, the low order models are inappropriate for the test case of this research. Higher order structural modeling with HCDstruct has shown to be an asset for conceptual phase structural design and weight estimation [30, 76, 85, 86], but in terms of predicting structural technology performance, there are concerns with 1) applicability of equivalent "smeared" structural property modeling for the PRSEUS technology and 2) traceability to technology design parameters for experiment design. A HWB structural weight estimation environment developed by Laughlin [53] is integrated with Hypersizer and mimics the global-local benchmark sizing process. This environment also has the capability to produce parametric OML and SL geometries, and it was therefore chosen as an appropriate model for this research.

4.2.1.2 Structural Weight Estimation Implementation

Details of the weight estimation approach by Laughlin can be found in References [53] and [54]. This section outlines specific characteristics of how this environment was used for technology performance estimation within the approach framework in Fig. 36. The Laughlin method will be referred to as the Georgia Tech - Weight Estimation for Structures (GT-WESt) for brevity. With user and SME input, this environment encompasses five steps in the framework from Fig. 36: *Outer Mold Line*, *Structural Geometry*, *Structural Model*, *Structural Sizing*, and *Technology Implementation*.

Minor changes were made to this environment for technology performance estimation suitability compared to the version in Reference [53]. For instance, four global load cases were applied to the structural model: +2.5g maneuver, -1.0g maneuver, 2P cabin overpressurization, and a -2.0g taxi bump. These were four of the most critical load cases determined by the benchmark trade study [105]. Geometries and general structural modeling remained the same; however, the structural sizing implementation was slightly different.

While Laughlin accounted for conceptual design uncertainty, unmodeled structure, and lack of detailed geometry characteristics like cutouts and such with a scale factor on the estimated structural weight per HWB section, the implementation used in this research explicitly accounted for those effects when possible. For example, knockdown factors on allowables discussed in Sec. 2.3.1.3 increase the estimated weight by directly accounting for lack of geometry detail and uncertainty in material properties, which is important for traceability in technology performance. Non-optimal factors have the same traceability effect for unmodeled structural features like fittings, rivets, etc. These helped appropriately account for the benefit of PRSEUS unitization. Additionally, the estimated weight scaled by non-optimal factors is included in the iterative sizing process to converge on interal loads, and consequentially structural weight. The structure can therefore be appropriately sized considered the impact of

added weight on inertial loads.

Once the structural weight estimate is provided by Hypersizer, with the corresponding non-optimal weight penalty, it can then be scaled by a calibration factor as needed to produce a final estimated "as-built" structural weight:

$$W_S = W_{est}\left(\prod_{i=1}^{n} q_i\right)(1 + K_1 + K_2 + \cdots + K_n) \cdot K_{cal} \tag{49}$$

where K_{cal} can be incorporated with the other non-optimal factors, K, during the iterative process to converge on internal loads if it is known a priori. This process is taken for both the structural technology and baseline structure configurations, modeled in Hypersizer with values from Tables 12, 13, and 14, to obtain $W_{S,B}$ and $W_{S,T}$.

4.2.1.3 Calibration and Validation of SWE Environment

The Georgia Tech - Weight Estimation for Structures contains the appropriate mechanisms to model attributes of the technology performance characterization problem, but are the results obtained using this method accurate? Steps were taken by Laughlin to calibrate and validate GT-WESt [53], but these values could no longer be used in this research since the bookkeeping methods for weight scaling were changed. Separate calibration and validtion studies were performed as part of this research.

The first portion of the calibration was performed for the N2A configuration with a nominal structural layout and fitted with baseline structural concepts. This same process was performed by Laughlin using weight breakdown data in Reference [46]. Calibration factors determined from this data are listed in Table 3. Since this reference combined the weight of the outboard and trapezoidal wings, a combined calibration factor was found for both sections. The rear centerbody section is significantly larger than the other two sections because there are not sufficient loads applied to this section in the GT-WESt implementation. Loads from the engines and vertical tails were not considered as these models were not available. This section, however, accounts for

Table 3: HWB calibration factors for GT-WESt

HWB Section	$\mathbf{K_{cal}}$
Centerbody	1.075
Rear Centerbody	1.251
Wing	2.070

a small percentage of the total structural weight and was not a large focus of the PRSEUS implementation.

This full vehicle calibration effort uses the results from Reference [46] as a "truth model," the data in this report is the result of a computational study. It is assumed that industry models are superior to those available in academia and can rely on a wealth of detailed structural findings. Until a HWB aircraft is manufactured, computational studies will be compared and calibrated to computational studies for the full vehicle. To anchor the results obtained from this weight estimation environment, however, a smaller subset of physical test data was available for the PRSEUS experiments of the building block approach. Models of these physical test articles were generated manually using the same assumptions and methods as GT-WESt. The nominal PRSEUS configuration in Table 12 were used on each of the five configurations: 1) compression panel, 2) tension panel, 3) pressure panel, 4) pressure cube, and 5) multi-bay box (MBB) assembly. Relevant local loading conditions and boundary conditions were applied to each model, and the results compared to assess the capability of the weight estimation environment to accurately capture PRSEUS characteristics. This is also a supplement to the validation work done by Hypersizer directly [88]. The following sections show results for the compression panel and multi-bay box, because these two configurations were most applicable to the full aircraft weight estimation process.

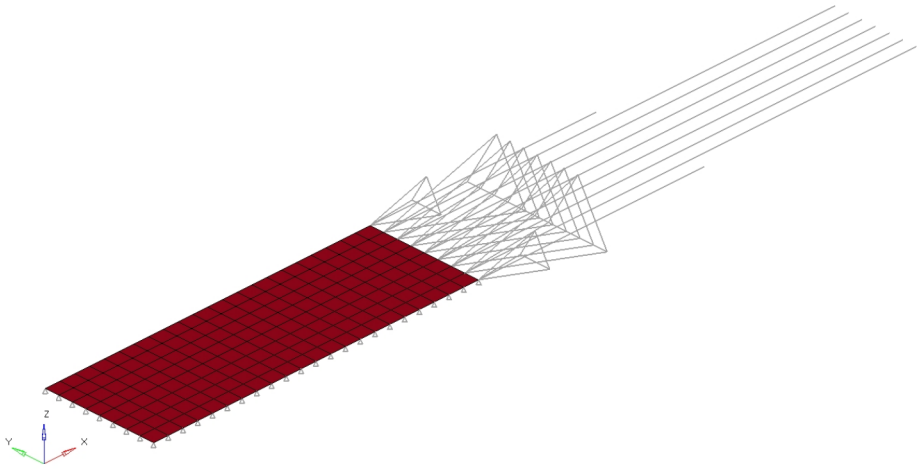

Figure 38: Compression Panel FEM

4.2.1.4 Compression Panel

The compression panel test was performed to assess post-buckling and damage arresting performance of the PRSEUS technology. An equivalent FEM was built using GT-WESt assumptions and is shown in Fig. 38. Information regarding this experiment can be found in Reference [114]. Table 4 lists significant events within the loading scheme of this experiment, and corresponding margins of safety due to failure checks with the weight estimation model is shown in Fig. 39. Two models were assessed for the compression panel because of the side restraints that were used in the physical test setup. The fixity of these side restraints were unclear and therefore one model treated them as pinned and the other used clamped boundary conditions, respectively.

Although there was some difference in the internal loads calculated by the global FEM, there was virtually no difference in the failure criteria calculations that were performed in Hypersizer for both models. The most important observation from this test is the value for limit margin of safety when local buckling occurs. Hypersizer models are conservative in their prediction for local buckling for PRSEUS because there is zero level of fixity that is implemented at the stiffener boundaries. In reality,

Table 4: Compression panel loading events

$\mathbf{N_{y,c}}$ (kip)	**Description**
30	Actual local buckling
59	FEM predicted local buckling
120	Local failures
147	Actual panel failure
200	FEM predicted frame buckling initiates
207	FEM predicted catastrophic panel failure

increased thickness due to the tear strap and added stiffness because both the stringer and framer would add a level of fixity to the boundary. This is accounted for by a further decreased margin of safety. The minimum margin of safety was found to be $M_{lim} = -0.47$ when local buckling occurred, shown in Fig. 39, and the compression panel continued to carry load beyond this point, confirming that this mode does not designate a critical failure.

4.2.1.5 Multi-Bay Box

A representative global FEM was generated using GT-WESt assumptions as well. This model was integrated with Hypersizer in a manner similar to the total aircraft model, in which sizing components are represented by nearly every intersected structural panel. The global FEM is shown in Fig. 40, and the load cases that the MBB was placed under are listed in Table 5. This experiment was the only test in which fabricated PRSEUS panels were weighed, and these weights were used as a validation of the GT-WESt structural weight estimation process given the current settings used in this research.

First, the MBB was placed under all design load cases, i.e. load cases $LC_1 - LC_8$, for both limit and ultimate level loads, and the model was analyzed in Hypersizer for corresponding margins of safety. Design variables were set at nominal values for all PRSEUS panels, and the corresponding results are shown for most panels in Figs. 41

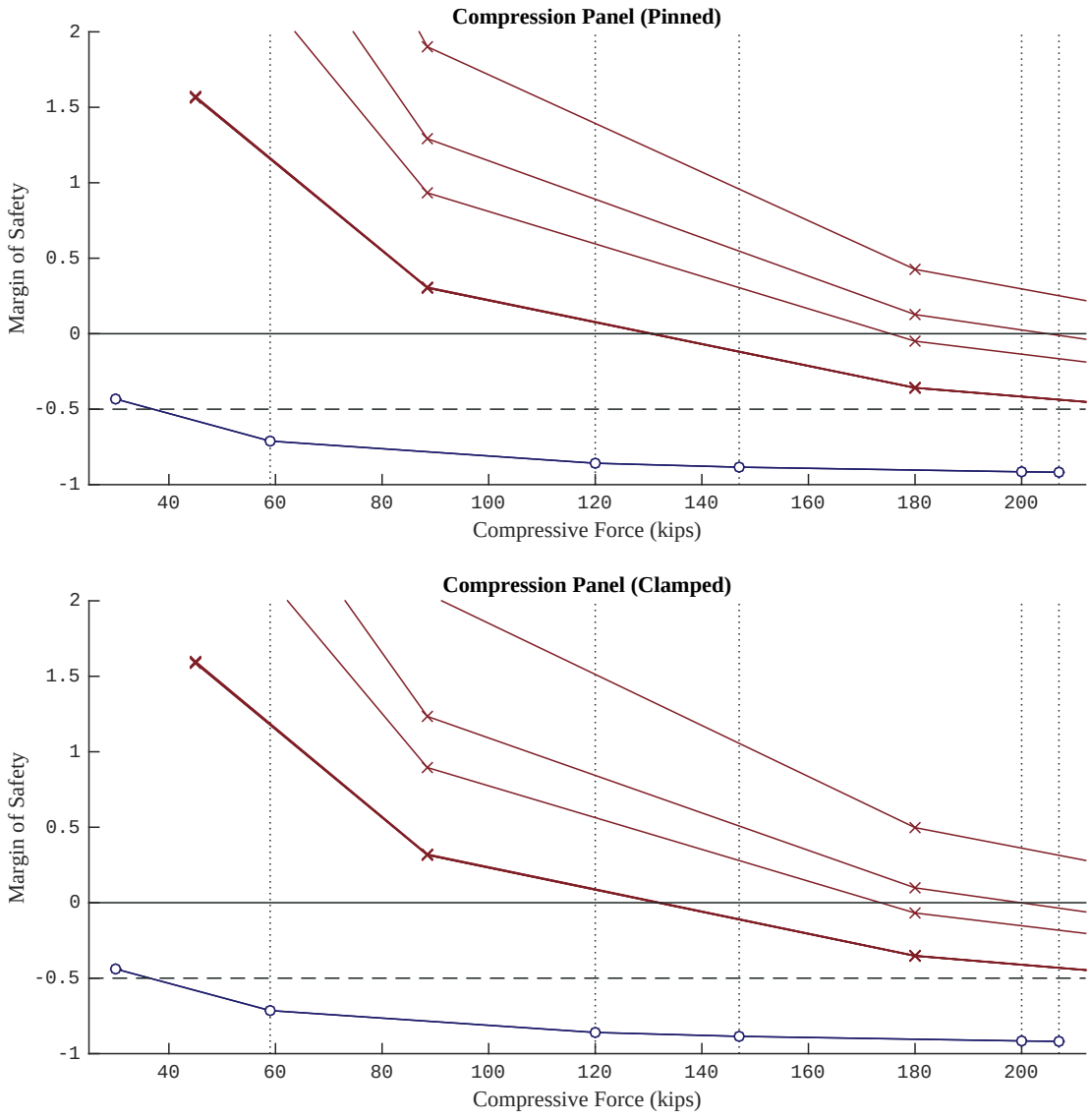

Figure 39: Compression Panel failure results for both pinned and clamped assumptions for side restraints

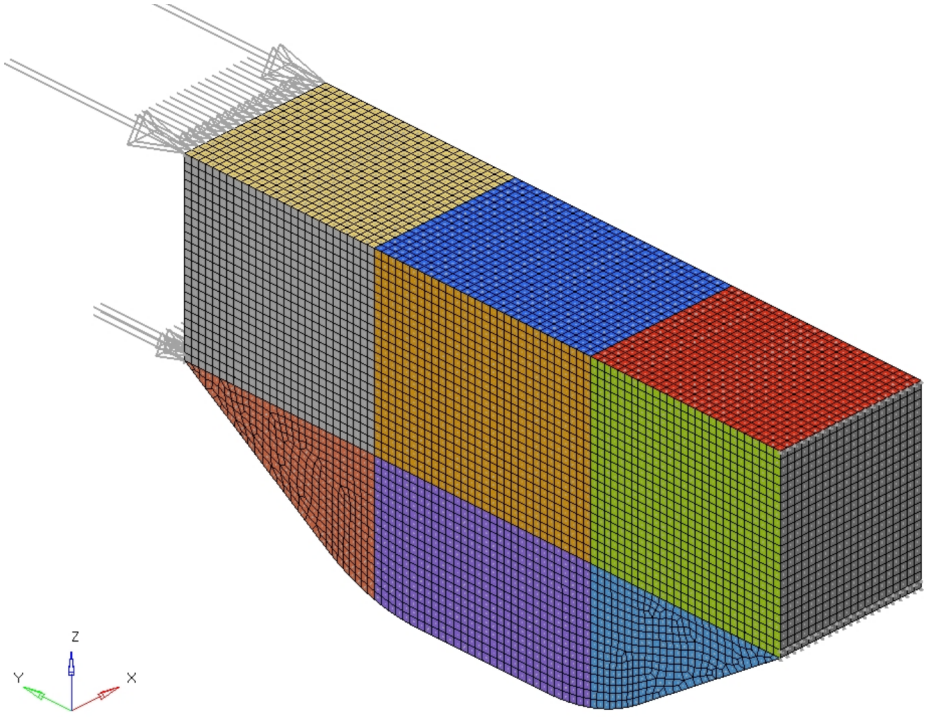

Figure 40: MBB FEM

Table 5: MBB Load Cases

Load Case	**DLL**		**DUL**	
	Man, n-G	*P (9.2 psi)*	*Man, n-G*	*P (9.2 psi)*
LC_1	-1.0	0	-1.5	0
LC_2	-1.0	1	-1.5	1.5
LC_3	0	1.33	0	2
LC_4	+2.5	0	+3.75	0
LC_5	+2.5	1	+3.75	1.5
LC_6	-	-	+3.75	0
LC_7	-	-	+4.125 (1.65DLL)	0
LC_8	-	-	+4.125 (1.65DLL)	1.5
LC_9	-	-	+5.0 (2.0DLL)	0

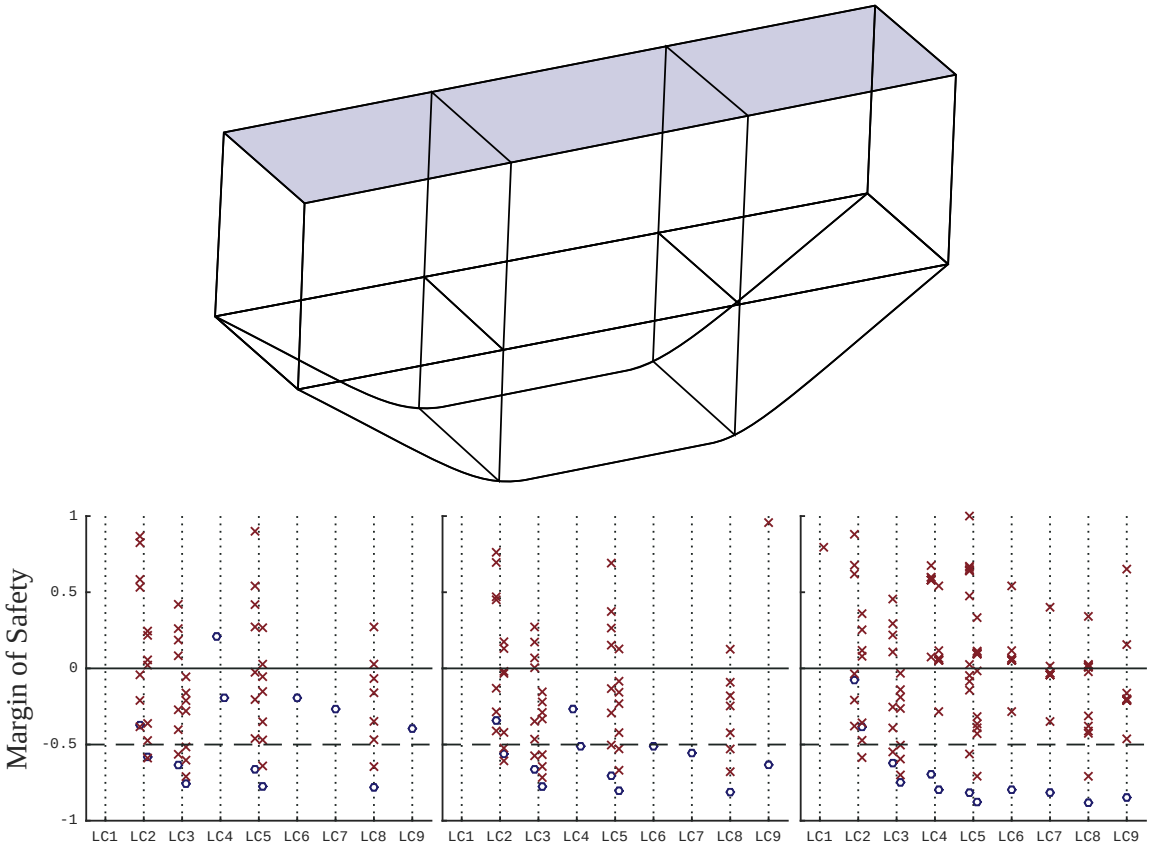

Figure 41: MBB Crown Panel Results

to 44. Only margins of safety for panels that were weighed before MBB assembly are shown. It can be seen in these figures that margins of safety are well under the allowable values, $M_{ult} = 0$ and $M_{lim} = -0.5$. Even though actual sizing using the GT-WESt model would only take place for load cases 1-5 for limit load values (Hypersizer has a built-in check for ultimate loads), all load values were examined for verification of trends. The failure plots for each panel show $LC_1 - LC_5$, and on the left side of $LC_1 - LC_8$ are the resulting margins for limit load values and to the right for all load cases is the corresponding ultimate load results.

Even for the limit load cases, safety margins were well into the failure indication ranges for nearly all panels. Additionally, using the nominal design parameter values for PRSEUS resulted in a severely underweight configuration. With pure Hypersizer

estimated weight, i.e. without knockdown or non-optimal factors, all predicted panel weights were less than half of the actual panel weight values. This phenomena was alarming, and detailed MBB panel drawings were obtained. One major feature missing from each of these MBB PRSEUS components was the integral caps used for assembly. These design features were included in the measured weights of the panels but were not considered in the GT-WESt model. Therefore, the global model was revised to include a Hypersizer equivalent to integral caps using the same material and laminate configuration as the other PRSEUS panels.

Results are shown in Table 6 that include integral caps. Another feature of the actual PRSEUS MBB panels compared to the nominal model is the inclusion of skin and stiffener pad-ups near joints, cutouts, and load-introduction fittings. The role of these material pad-ups was to deal with stress concentrations. In the GT-WESt modeling approach using Hypersizer, these detailed features were not accounted for directly. The manner in which they were treated was in the structural sizing process itself. If failures were predicted, then panel features were up-sized until all margins were above their minimum allowable values. Table 6 shows resulting panel weights from this sizing process, but no non-optimal factors are included, which are representative of the GT-WESt approach.

These results are sufficient to verify the trends of the weight estimation model. Physical testing of the MBB indicates that the assembly was likely oversized – withstanding all ultimate loads without any indication of failure. The MBB actually exceeded predicted performance and it took two times the ultimate load with a saw cut in the crown panel to cause catastrophic failure. Because of these observations, the predicted values in Table 6 are considered realistic at 20% underweight. However, the validation approach was taken one step further.

Since it was observed that the MBB was likely oversized, then the sizing routine in Hypersizer was performed again for the model, this time including the design

Table 6: Comparison of actual MBB panel weights to sized model with caps

Panel	W_{act}	$W_{mod,s}$	ΔW_s	$S.F._s$
Crown	751.0	602.3	19.8	1.25
Floor	588.0	466.9	20.6	1.26
Upper Bulkhead (Fwd)	645.0	515.6	20.1	1.25
Upper Bulkhead (Aft)	650.3	515.6	20.7	1.26
Outboard Rib	111.3	116.2	-4.4	0.96

Table 7: Comparison of actual MBB panel weights to super-sized model with caps

Panel	W_{act}	$W_{mod,ss}$	ΔW_{ss}	$S.F._{ss}$
Crown	751.0	784.6	0.3	1.00
Floor	588.0	616.3	-4.8	0.95
Upper Bulkhead (Fwd)	645.0	648.6	-0.6	0.99
Upper Bulkhead (Aft)	650.3	648.6	0.2	1.00
Outboard Rib	111.3	141.5	-27.1	0.79

ultimate load cases defined as limit loads. This formulation means that ultimate failures would be predicted at 1.5× the already ultimate design load, corresponding to the overseeing of the actual MBB configuration. The approach, referred to as the "super-sized" model, was also performed including the non-optimal weight penalties, representative of the full GT-WESt formulation. Predicted panel results are shown in Table 7, and confirm the weight estimation capability of GT-WESt. The crown panel and both bulkhead panels were nearly identical to the actual panel weights, whereas weights for the floor and outboard rib panel were only slightly over-predicted as a result of component configurations with faulty assumptions. These results consider the GT-WESt model validated for the PRSEUS technology and verified in terms of HWB weight.

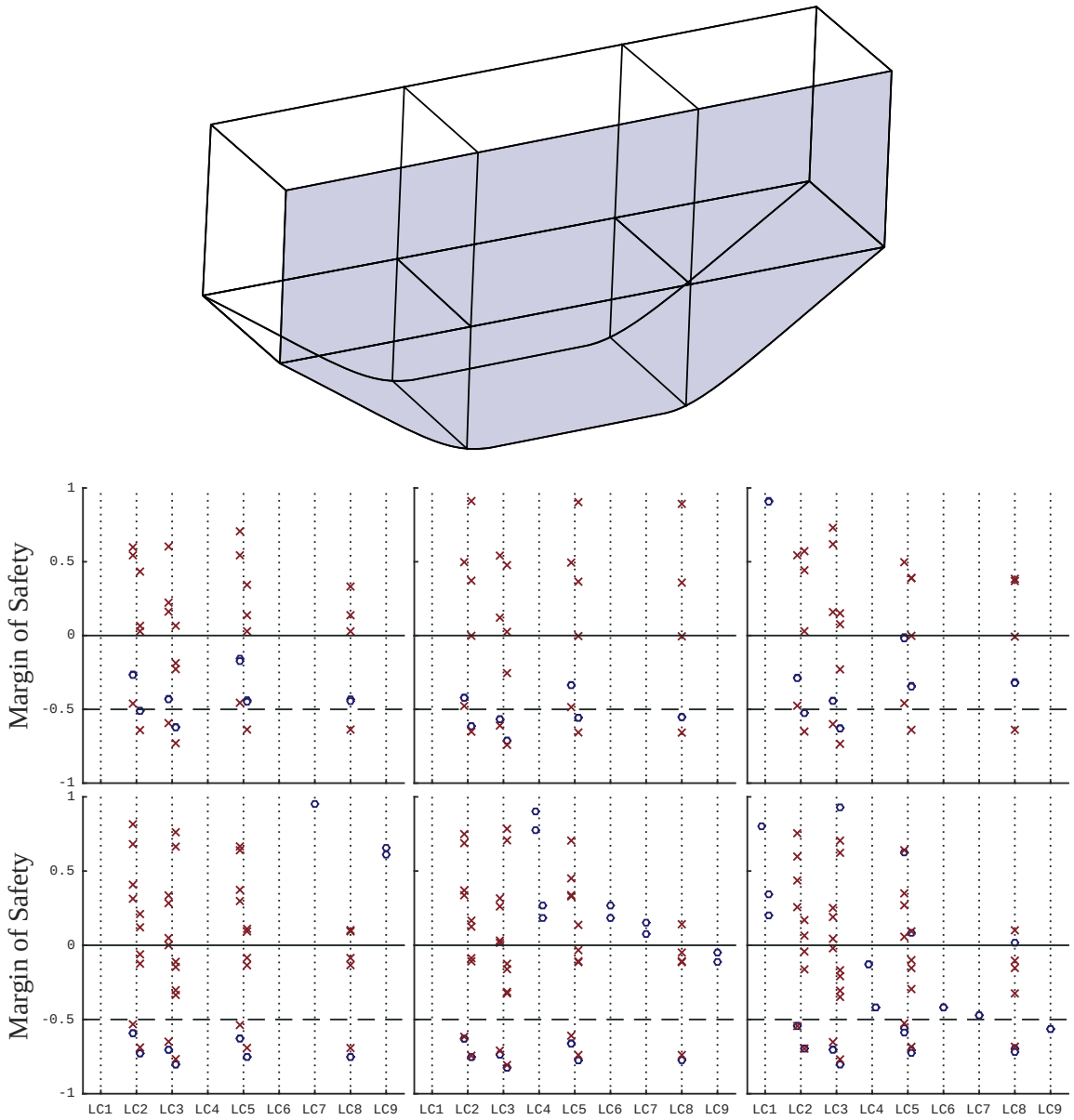

Figure 42: MBB Forward Bulkhead Results

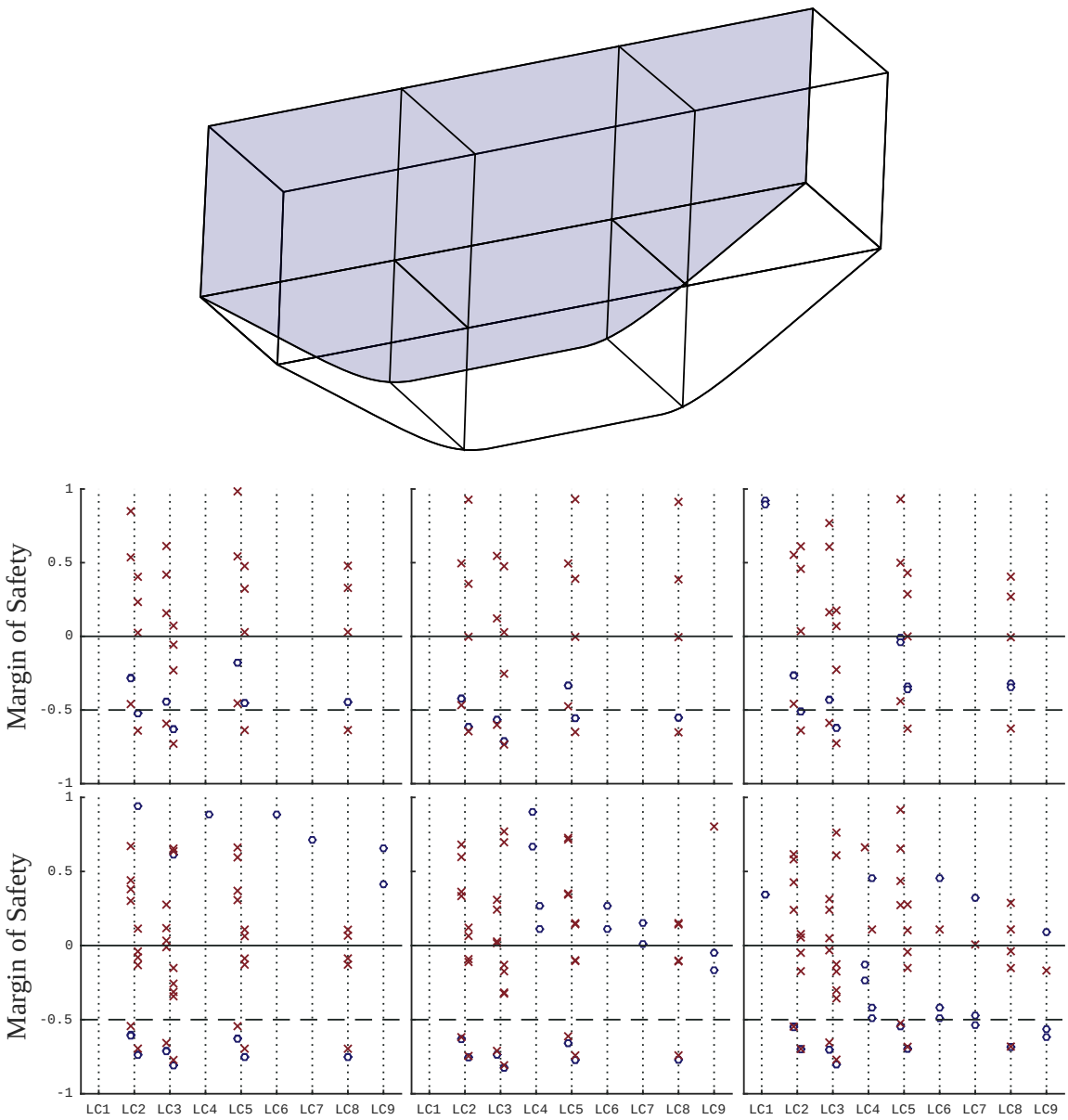

Figure 43: MBB Aft Bulkhead Results

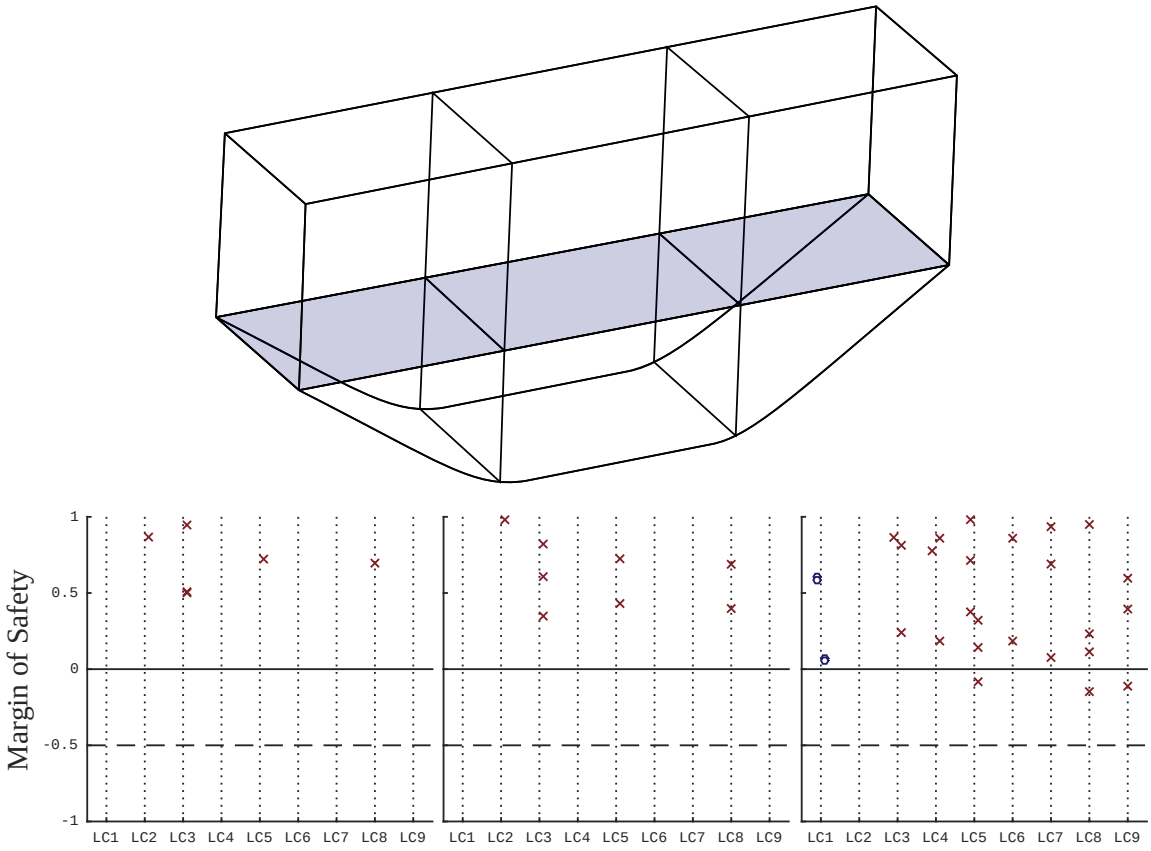

Figure 44: MBB Floor Panel Results

4.2.2 Conceptual Design

A transfer function was needed to test the effect of performance characterization on conceptual design metrics. Therefore, a surrogate model of the Environmental Design Space (EDS) [50], introduced in Section 2.2.1 and shown in Fig. 12, was created for rapid design space exploration of a 210-passenger HWB comparable to the N2A. Conceptual phase performance outputs were fuel burn, takeoff gross weight, and wing loading. The configuration was modeled with state of the art technologies representative of year 2010, and the effect of the structural technology was isolated from other technologies, i.e. it was alone applied to the conceptual design space through k_w and $k_c b$ for structural weight reduction of the wing and centerbody, respectively. To account for the functional relationship of $k_w\left(\mathbf{X}_{OML}\right)$ and $k_c b\left(\mathbf{X}_{OML}\right)$, the OML design space was also sampled. Variables that were considered are discussed in Section 6.1.

4.3 Defining Design Spaces

The HWB is broken down through each level of its design space in this section, and applicable parameters and assumptions are discussed for each.

4.3.1 Outer Mold Line

The shape of a hybrid wing body aircraft can essentially be defined in the same manner as a conventional multi-stage wing. Parameters that drive that definition, however, are much different. As shown in Fig. 4, there are four main sections of primary structure that are contained with a HWB. From inboard to outboard and forward to aft, they are the: 1) centerbody, 2) rear centerbody, 3) trapezoidal wing, and 4) outboard wing. Sections are organized in this manner as a result of either specific loading conditions, or significant change in the organization/layout of the structure, which can be seen in Fig. 47. Parameterization of the OML is not required to be cognizant of these sections, but it enables a more simplistic organization of

data and a relevant means of comparison, e.g. the outboard wing can be compared to other conventional wing configurations through common parameters.

Definition of the HWB OML begins with the centerbody section passenger cabin, and the number of passengers defines the scale of the vehicle. From a HWB planform view, Nickol discusses the manner in which the passenger cabin is configured for HWB aircraft is similar to "home plate" in baseball [73]. FLOPS contains cabin layout methods that translate the number of passengers to centerbody length and width values, but other parameters must also be defined to enable this method [68]. The full center section of the HWB is defined by: centerline chord length l_c, centerline passenger cabin length l_{cabin}, passenger cabin width w_{cabin}, center section leading edge sweep $\Lambda_{LE,cb}$, and centerbody side of body length $l_{sob,cb}$. This last parameter defines the length from the leading edge to the rear spar of the centerbody at a span defined by $0.5 \cdot w_{\text{cabin}}$. Laughlin uses a similar parameterization but also defines control points so that the planform geometry can either be blended or linear between each aircraft section [53].

The trapezoidal wing is the defined as the buffer zone between the centerbody side of body wall and the root rib of the outboard wing. The only parameter needed to define this section of the OML is the starting span of the outboard wing. From that span point, the outboard wing is defined like a conventional wing. Root chord, tip chord, sweep, and span complete the overall planform for the HWB, and the overall span from centerline to outboard wing tip has the option to be fixed or free. In the fixed configuration, the trapezoidal wing would shrink or expand in terms of span with the outboard wing span definition; otherwise, the tip span is free to vary.

Three-dimensional shape is added by airfoil stacks as a function of span, which considers thickness-to-chord ratio, dihedral, and washout. In this research, the same OML parameters were considered as in Reference [54], which are listed in Table 8. The control points for the planform with this approach are shown in Fig. 45. Also used

Table 8: HWB OML design parameters reproduced from [53]

Variable	Description
$LE_{sw_{cb}}$	Sweep angle of centerbody leading edge
l_{cabin}	Length of centerbody cabin
w_{cabin}	Width of centerbody cabin
toc_{rcb}	Thickness-to-chord ratio at root of centerbody
toc_{tcb}	Thickness-to-chord ratio at tip of centerbody
b_{ow}	Span of outboard wing section
$LE_{sw_{ow}}$	Sweep angle of outboard wing leading edge
$LE_{sw_{ow}}$	Sweep angle of outboard wing leading edge
cr_{ow}	Chord length at root of outboard wing
ct_{ow}	Chord length at tip of outboard wing
toc_{row}	Thickness-to-chord ratio at root of outboard wing
$twist_{ow}$	Twist angle at tip of outboard wing
dih_{ow}	Dihedral angle of outboard wing

in this research were two baseline $\mathbf{x}_{OML}$ single point designs for studies of structural layout: the Boeing/NASA N2A and the NASA HWB301.

4.3.1.1 Boeing/NASA N2A

The N2A HWB configuration is a derivative of the SAX-40 vehicle, developed as part of the Massachusetts Institute of Technology Silent Aircraft Initiative (SAI [111]). This configuration has two podded engines mounted at the rear centerbody section with horizontal stabilizers on each side providing noise shielding. The N2A was originally designed as a cargo freighter for a 6,000-nm range with a mission profile typical of a transport aircraft. Other requirements included a 103,000 pound payload weight, a minimal initial cruise altitude of 35,000 ft, a cruise Mach number of 0.8, and a maximum field length of 10,000 ft. A planform is shown compared to the NASA HWB301 in Fig. 45. The internal structure, shown in Fig. 47, was generated by Laughlin[54] and is consistent with original drawings[46] and typical HWB passenger cabin layouts[73].

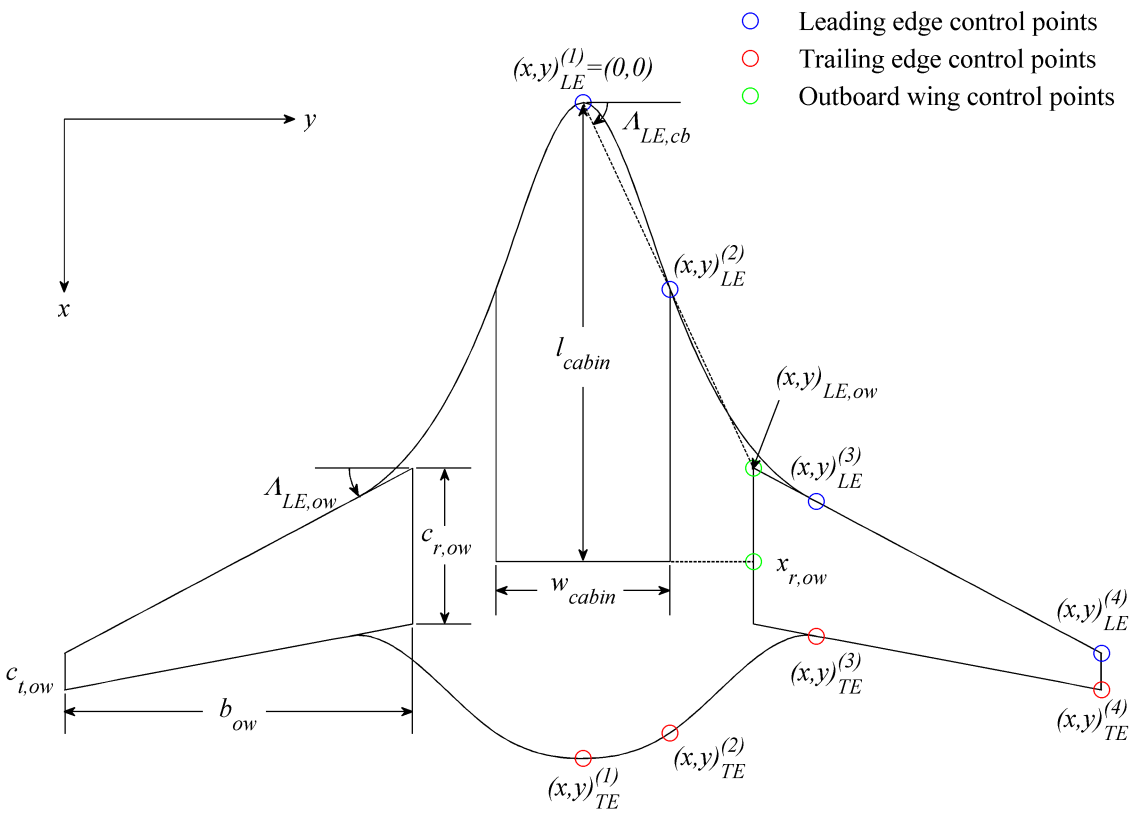

Figure 45: HWB OML control points implemented in Reference [54]

Table 9: HWB301 design attributes

Value	Attribute
118,100 lb	Payload
7,500 nm	Design Range
768,000 lb	Takeoff Gross Weight, W_{TO}
342,900 lb	Operational Empty Weight, W_e
0.84	Cruise Mach
279,800 lb	Block Fuel Burn, W_{fuel}

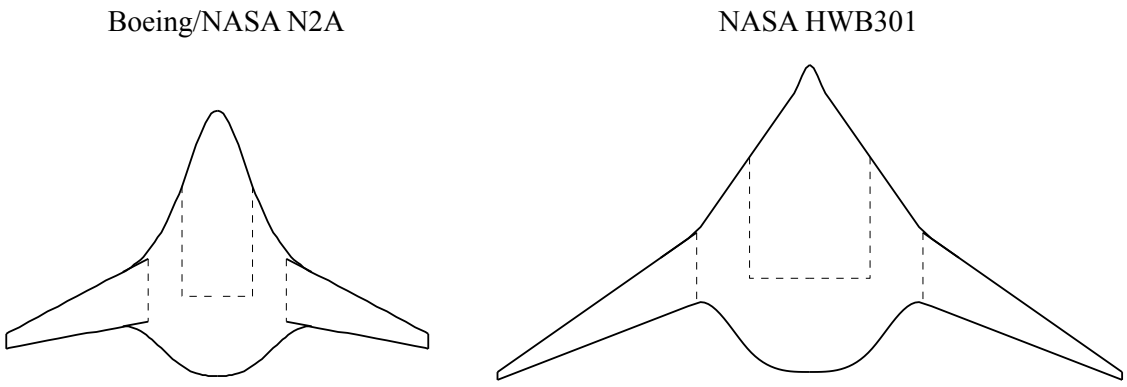

Figure 46: Boeing/NASA N2A and NASA HWB301 planforms

4.3.1.2 NASA HWB301

The HWB301 is a configuration that was used for HWB scaling studies [74], and therefore data was readily available for this design. It is a 301-passenger aircraft, comparing to a baseline large twin aisle (LTA) conventional tube-and-wing concept, similar to a 777-200LR. The HWB301 OML is shown in Fig. 46 in comparison to the N2A, and Table 9 lists some design characteristics for this configuration. Other information can be found in Reference [74].

4.3.2 Structural Layout

A full characterization of structural layout definition considered in this research can be found in Reference [53], but important characteristics will be described in this

section. HWB structure will also be descried from inboard to outboard and forward to aft of the configuration. The structural layout for the HWB is organized much in the manner of the OML for the center section, and since the structural layout is set up for load path continuity and best practices, design variables for a particular section often have an effect on other sections of the HWB. The centerbody passenger cabin is defined by the "home plate," and the outer walls of this section is fitted with pressure containing structure. Side of body rib walls are defined at a span location of $y = 0.5 \cdot w_{\text{cabin}}$, and the forward and aft chord locations are defined by centerbody front spar at $c_{FS,cb}$ and the centerbody aft bulkhead at l_{cabin}, respectively. The width and length of the centerbody passenger cabin section are determined in FLOPS as a function of the number of passengers, but these variables can be adjusted by defining a centerbody aspect ratio, $AR_{cb} = {}^{l_{\text{cabin}}}/_{w_{\text{cabin}}}$. The design variable that most affects the centerbody structure design, however, is the number of passenger cabin bays, $n_{\text{Bays},cb}$. Given a centerbody width, this parameter implicitly defines the gap between bay walls that the cabin pressure differential will act on.

The only parameter that needs defined for the rear centerbody structure is the rear bulkhead. While each of the structural layout design parameters can be defined in a number of ways, the most appropriate for the rear spar of the rear centerbody is a chord location at the centerline. As shown in Fig. 47, the rear spar is defined linearly from the root of the outboard wing to the innermost rear centerbody bay wall. For this reason, the rear spar for the trapezoidal wing is implicitly defined. The front spar of the trapezoidal wing is defined at a percent chord location and is split into sections that kink to follow the curvature or linear breaks in the leading edge of the HWB OML. Trapezoidal wing rib spacing is defined by the user, and a relationship is created with spar locations for the multi-spar configuration of this section. For load path continuity, spars coincide with the front and rear spar of the outboard wing, and they carry the load to centerbody bulkheads in the same chord location.

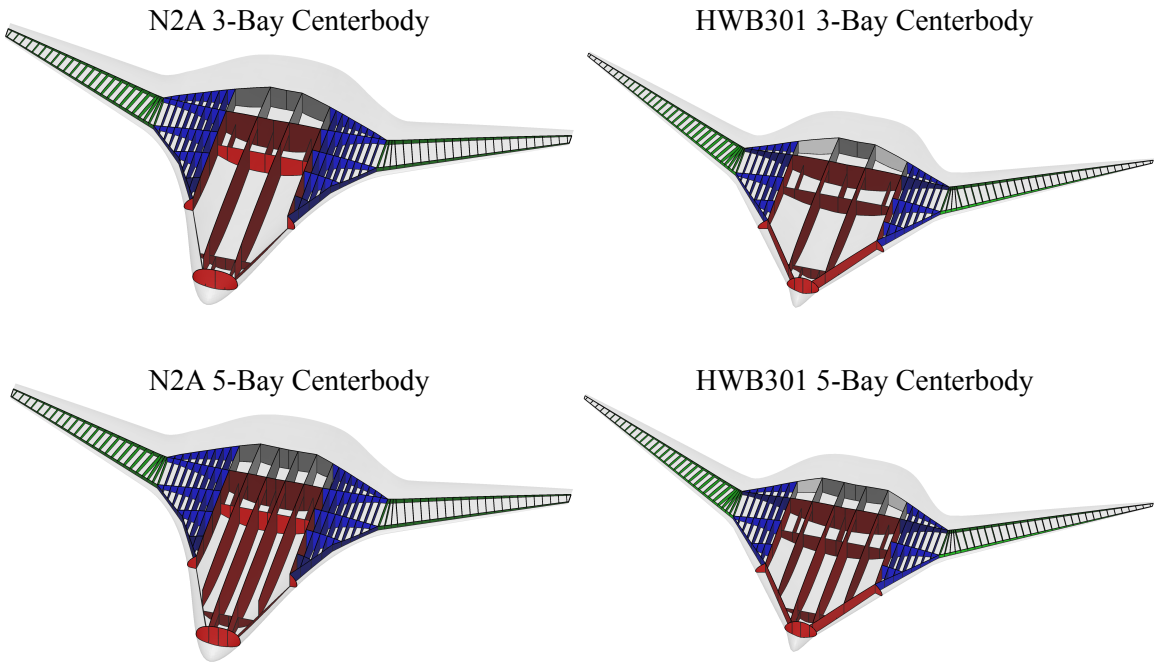

Figure 47: Nominal structural layout designs for the N2A and HWB301

The outboard wing is a simple two-spar wingbox configuration in which front and rear spars are defined as a percent chord and ribs are defined by a particular pitch, or spacing. There is also a parameter to perturb the span definition of the root rib of the outboard wing to account for planform curvature in the leading and trailing edges. Nominal structural layout designs are presented for the two baseline test vehicles in Fig. 47.

This comparison highlights some of the features mentioned in this section, but the most important is how the number of passenger cabin bays affects the centerbody structure. The top row of the figure shows a 3-bay configuration while the bottom row shows a 5-bay configuration for both vehicles. While at different passenger class scales, 216 vs. 301 for the N2A and HWB301, respectively, the aspect ratio of the centerbody is different for both aircraft. The relative impact on total surface area that the pressure differential is acting on can be seen between the two vehicles qualitatively. The HWB301 design with a smaller aspect ratio and larger number of passengers has

Table 10: HWB structural layout design variables, $x_{SL} \in \mathbf{X}_{SL}$

Variable	Description
$n_{\text{Bays},cb}$	Number of passenger cabin bays
$c_{B,rcb}$	Chord location of rear centerbody bulkhead
$c_{FS,tw}$	Chord location of trapezoidal wing front spar
$p_{Rib,tw}$	Spacing (pitch) for trapezoidal wing ribs
$c_{FS,ow}$	Chord location of outboard wing front spar
$c_{RS,ow}$	Chord location of outboard wing rear spar
$p_{Rib,ow}$	Spacing (pitch) for outboard wing ribs

wider bays and sizing for the centerbody is most likely be driven by cabin pressure load cases. A subset of the full $\mathbf{X}_{SL}$ design space was considered for this research and the design parameters are listed in Table 10. From experience, these parameters were shown to have the most significant impact on structural design metrics.

4.3.3 Technology

The technology level design space does not just refer to the variables that correspond to the structural technology itself; this is the level that the explicit differences between the technology and baseline structure are implemented. Therefore, the baseline structure at this level is referred to as $\mathbf{X}_{T,B}$ while the structural technology is defined as $\mathbf{X}_{T,T}$. Implementation of both these structural concepts is performed through Hypersizer. This software manages materials and knockdown factors on allowables, configuration and geometry design variables, and applicable failure modes.

Because this research considers the effects of PRSEUS on traditional structure as well as the flat panel pressure-containing structure that was investigated in ERA, two configurations for this structural technology are considered. As a result, there are two baseline structural configurations that are defined and are dependent on the section and component to which they are applied.

Table 11: PRSEUS Design Variables

Category	Design Variable, $\mathbf{X}_T$
Skin	– Thickness, $x_{T,st}$ – Material, $x_{T,sm}$
Rod Stringer	– Height, $x_{T,rsh}$ – Pitch (Spacing), $x_{T,rsp}$ – Web (Wrap) Thickness, $x_{T,rswt}$ – Web (Wrap) Material, $x_{T,rswm}$ – Flange* Thickness, $x_{T,rsft}$ – Flange* Width, $x_{T,rsfw}$ – Pultruded Rod Diameter, $x_{T,rsrd}$ – Pultruded Rod Material, $x_{T,rsrm}$
Foam Core Frame	– Height, $x_{T,fh}$ – Pitch (Spacing), $x_{T,fp}$ – Web (Wrap) Thickness, $x_{T,fwt}$ – Web (Wrap) Material, $x_{T,fwm}$ – Flange* Thickness, $x_{T,fft}$ – Flange* Width, $x_{T,ffw}$ – Foam Core Thickness, $x_{T,ffct}$ – Foam Core Material, $x_{T,ffcm}$
Panel Global	– Length, $x_{T,L}$ – Width, $x_{T,W}$ – Curvature, $x_{T,R}$
	* Flange variables include tear strap

4.3.3.1 PRSEUS Configurations

PRSEUS design characteristics were described in Sec. 2.3.2, and it was discussed that the unitization, stitching, damage arrestment properties, and warp-knit carbon fiber laminates influenced the reduction in structural weight. The total list of design variables for structural sizing is found in Table 11, except for the "Panel Global" set, which are defined by the $\mathbf{x}_{OML}$ and $\mathbf{x}_{SL}$. These variables hold different values depending on which aircraft section they are implemented in.

Table 12: PRSEUS Implementation in Hypersizer (All dimensions $\sim$ in.)

General		**Centerbody**		**Wing**	
Variable	Nominal	Limits	Perm	Limits	Perm
$x_{T,st}$	0.052	$[0.052, 0.408]$	4	$[0.052, 0.408]$	4
$x_{T,sm}$	AS-4 EL	AS-4 EL (r)	-	AS-4 EL	-
$x_{T,rsh}$	1.25	$[1.25, 3.75]$	4	$[0.75, 3.25]$	6
$x_{T,rsp}$	6.0	$[6.0, 6.0]$	1	$[6.0, 6.0]$	1
$x_{T,rswt}$	0.104	$[0.104, 0.208]$	3	$[0.104, 0.208]$	3
$x_{T,rswm}$	AS-4 EL	AS-4 EL	-	AS-4 EL	-
$x_{T,rsft}$	0.104	$[0.104, 0.208]$	2	$[0.104, 0.208]$	2
$x_{T,rsfw}$	3.37	$[3.37, 3.37]$	1	$[3.37, 3.37]$	1
$x_{T,rsrd}$	0.375	$[0.375, 1.0]$	3	$[0.375, 1.0]$	3
$x_{T,rsrm}$	AS-4 EL (0)	AS-4 EL (0)	-	AS-4 EL (0)	-
$x_{T,fh}$	6.0	$[4.0, 10.0]$	4	$[4.0, 8.0]$	3
$x_{T,fp}$	20.0	$[24.0, 24.0]$	1	$[36.0, 36.0]$	1
$x_{T,fwt}$	0.104	$[0.104, 0.312]$	4	$[0.104, 0.312]$	4
$x_{T,fwm}$	AS-4 EL	AS4 EL	-	AS-4 EL	-
$x_{T,fft}$	0.156	$[0.156, 0.312]$	3	$[0.156, 0.312]$	3
$x_{T,ffw}$	3.93	$[3.93, 3.93]$	1	$[3.93, 3.93]$	1
$x_{T,ffct}$	0.5	$[0.5, 0.5]$	1	$[0.001, 0.001]$	1
$x_{T,ffcm}$	R 110 WF	110 WF	-	R 110 WF	-

Table 12 highlights the changes in parameters between the centerbody and wing sections. Also listed are the nominal design values from Reference [105]. Within the structural sizing scheme in Hypersizer, a grid search approach, the variable bounds and number of permutations must be defined in a sizing scheme. Unless otherwise explicitly stated, these were the PRSEUS configurations that were used in all full vehicle structural weight estimation studies. Design variables can be seen visually on the PRSEUS technology in Figs. 48, 49, and 50.

One of the more important characteristics is the configuration of the laminate for the skin. All laminates were modeled in Hypersizer as "Effective Laminates", in which thickness can be considered continuous, and properties scale in direct relation to the nominal ply stack sequence. This is denoted by the "EL" for material variables. The laminate stack that was used in technology development during ERA was

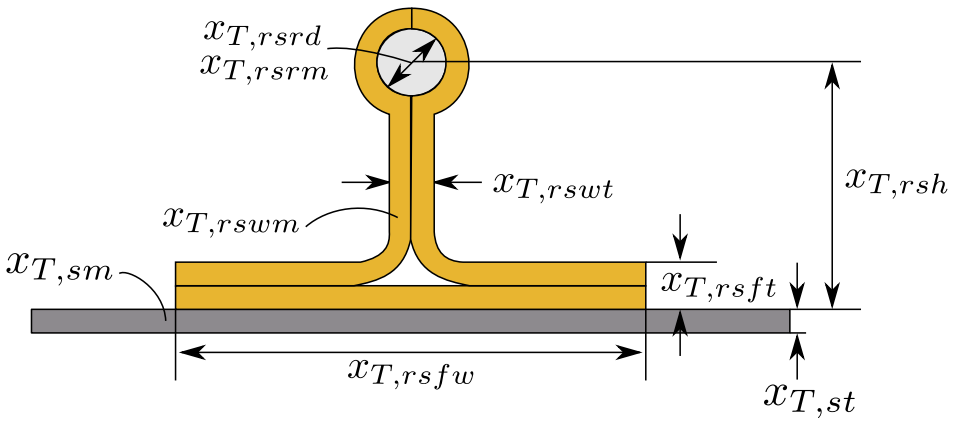

Figure 48: Design variables for sizing of PRSEUS rod stringer

balanced but slightly dominated by 0° fiber orientations. For the centerbody, since the combined loading of bending moments due to pressure and compression/tension due to aerodynamic load introduction from the wing were in the span direction, the laminate stack was turned by 90° in its local axis. This aligned with the foam core frame and provided extra strength and stiffness in the direction it was needed. For the wing, however, the 0° fiber domination corresponded to the local x-direction, in line with the rod stringer. Another characteristic of the carbon fiber materials was the knockdown factors on stress and strain allowables, q. Guidelines in Reference [105] were followed to properly account for design assumptions relating to PRSEUS damage arrestment and unitization for load path continuity characteristics. The frames in the wing configuration were rid of the foam core for safety concerns with wing fuel tanks, but because of requirements in Hypersizer, the foam core thickness was defined at a negligible value in the model, i.e. $x_{T,ffct} = 0.001in$. Frame structure for the wing section has the role of integral attachment structure for ribs and spars.

The last important assumption that is made regarding PRSEUS performance is its ability to continue to carry load post-buckling. Therefore, this is not considered a critical failure. Guidelines from Hypersizer state that the assumptions made regarding local buckling calculations for PRSEUS are somewhat conservative. It treats every

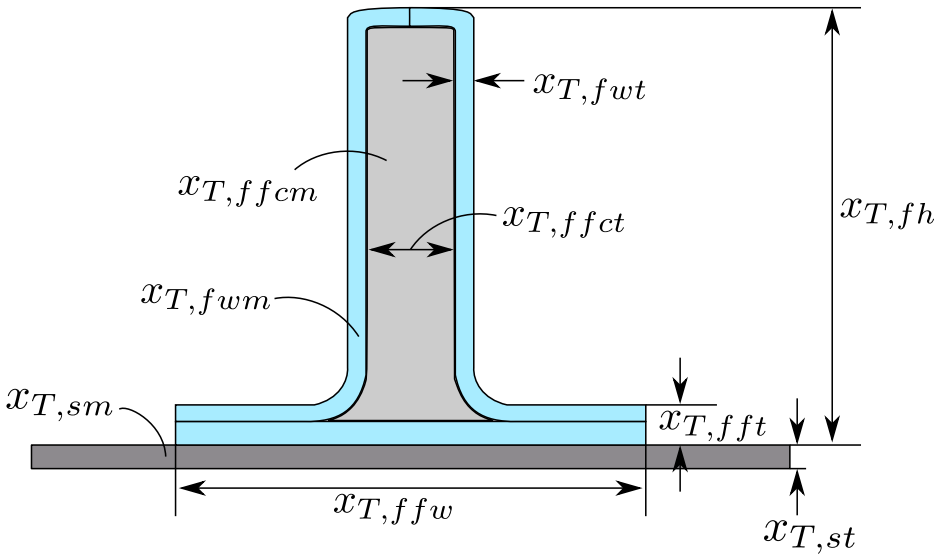

Figure 49: Design variables for sizing of PRSEUS foam core frame

local skin panel between stiffeners (shown in Fig. 50) as a pinned panel, meaning no fixity from the stiffeners is considered. A minimum margin of safety of $M = -0.5$ is the default value to account for both these parameters, but this value is further investigated later in the chapter.

4.3.3.2 Baseline Configurations

The baseline implementation for the technology design space, $\mathbf{X}_{T,B}$, considered both state of the art and suggestions by the authors of Reference [105]. In this section, notation is shortened to $\mathbf{X}_B$. The FEM approach in this benchmark trade study modeled frames in the centerbody spanwise direction discretely, increasing the complexity and number of elements of the model. Another solution was sought within Hypersizer that could mimic the stiffened sandwich structure considered in the benchmark trade study without the added burden that could be treated like PRSEUS in a fully global smeared element and local detailed sizing approach. An orthogrid stiffened sandwich structure was chosen as the baseline centerbody concept for comparison [11]. This concept, shown in Fig. 51, is stiffened in both the local axial and lateral directions,

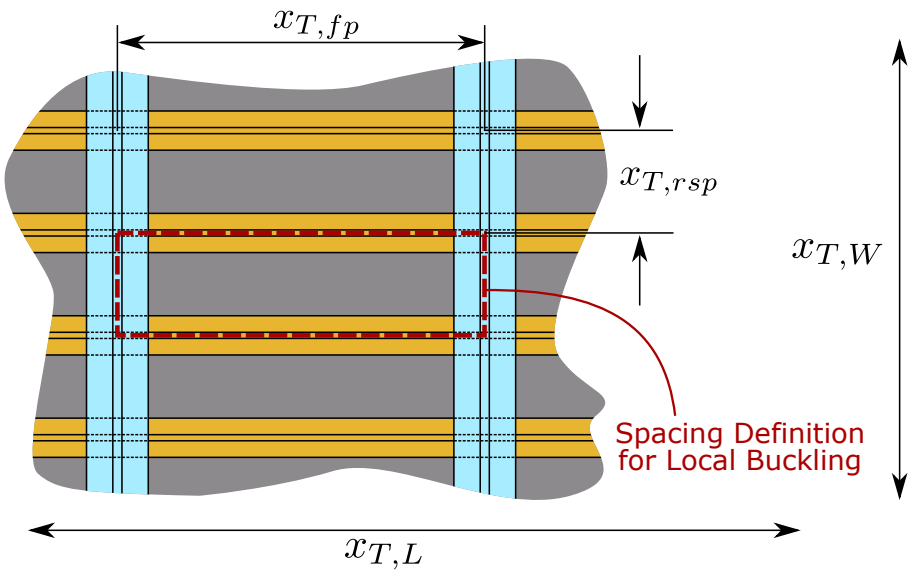

Figure 50: Global PRSEUS panel configuration with definition for local buckling

corresponding to the global streamwise and spanwise directions. All but the inner bay wall structures were modeled wtih the orthogrid concept; the these walls were comprised of unstiffened sandwich structure because they did not need to contain pressure, only withstand shear loads.

The orthogrid stiffened panels for the centerbody were modeled with the same materials and same ply layup as the PRSEUS laminates. However, the knockndown factors, q, were smaller to account for the lack of a damage arresting mechanism and less unitization. Material knockdowns were consistent with the benchmark trade study for the baseline as well. Table 13 shows the limits and number of permutations for the grid search optimization in Hypersizer that were used in this research. It is important to note that limits must be relative to the scale of the aircraft. The values listed for PRSEUS and baseline structures are applicable for approximately 200-300 passenger class HWB aircraft. Lower bounds correspond to minimum gauge constraints, but the upper bounds of thickness variables would potentially need to be increased with the scale of the aircraft. Preliminary tests for a larger scale aircraft, the HWB450, showed that many of the components had reached the upper limits of

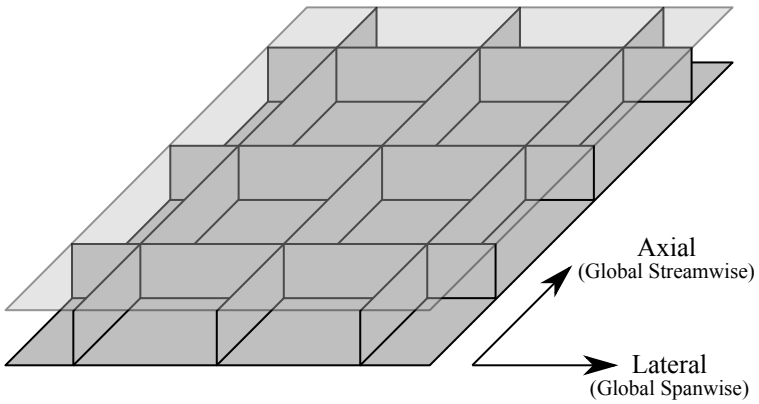

Figure 51: Orthogrid stiffened structural concept for baseline centerbody configuration

all design variables without finding a feasible solution. Expanding the design value ranges without increasing the number of permutations, however, leaves risk of the estimated "optimum" $\mathbf{x}^*_{SL,est}$ being further off from the actual optimum configuration, $\mathbf{x}^*_{SL}$.

The state of the art baseline structural configuration for the wing skin, spars, and ribs, were uniaxially integral blade stiffened composites, shown notionally in Fig. 52. Similar to the centerbody, the same materials were used but the knockdowns were representative of non-stitched pre-impregnated composite structure. Stringers were oriented in the direct spanwise direction for the trapezoidal wing and parallel to the rear spar of the outboard wing for the upper and lower skins. Ribs and spars also used this configuration, but the stiffeners were oriented in the vertical direction for added stability. Since no lateral stiffening structure was represented in the blade-stiffened configuration to account for attachments, e.g. spar caps, rib caps and clips, etc., beams were implemented in the model separately to account for them. The variables that define integral blade-stiffened composites for the wing are shown in Table 14.

Table 13: Centerbody baseline structure implementation

Variable	LB	UB	Perm
$x_{B,cb,stt}$	0.05	0.50	7
$x_{B,cb,smt}$		– AS-4 EL –	
$x_{B,cb,stb}$	0.05	0.25	7
$x_{B,cb,smb}$		– AS-4 EL –	
$x_{B,cb,ash}$	1	4	4
$x_{B,cb,asp}$	6.0	12.0	4
$x_{B,cb,aswt}$	0.10	0.50	6
$x_{B,cb,aswm}$		– AS-4 EL –	
$x_{B,cb,lsa}$	30°	30°	1
$x_{B,cb,lsh}$	2	8	4
$x_{B,cb,lswt}$	0.10	0.65	6
$x_{B,cb,lswm}$		– AS-4 EL –	

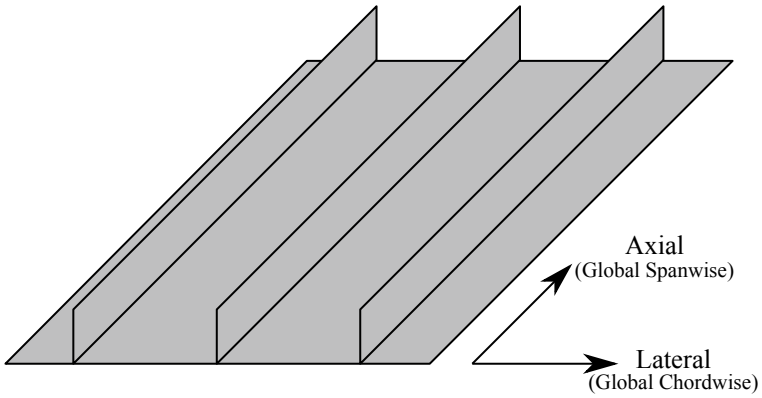

Figure 52: Integral blade stiffened structural concept for baseline wing configuration

Table 14: Wing baseline structure implementation

Variable	LB	UB	Perm
$x_{B,w,st}$	0.05	0.8	10
$x_{B,w,sm}$		– AS-4 EL –	
$x_{B,w,ash}$	1	6	8
$x_{B,w,asp}$	6.0	8.0	2
$x_{B,w,aswt}$	0.05	0.80	10
$x_{B,w,aswm}$		– AS-4 EL –	

CHAPTER V

STRUCTURAL TECHNOLOGY PERFORMANCE CHARACTERIZATION

The research formulation and STEED approach both focus heavily on determining the existence of a relationship between structural technology performance and the conceptual design space, i.e. the aircraft outer mold line. A test case was described in the previous chapter that is used to demonstrate the STEED process for the PRSEUS structural technology through OML variation of the N2A HWB aircraft. Steps 3-5 coincide with quantification of the $\Delta W_S(\mathbf{X}_{OML})$ functional relationship, and these relate back to Hypotheses 1-3 in the research formulation from which the approach was developed. This chapter explains the experiments which were performed to test these hypotheses within the design framework described in the previous chapter.

5.1 Experimental Plan

The experimental plan for performance characterization follows the right side of the Vee diagram setup of the first overarching hypothesis, shown in Fig. 32. These experiments were designed as a demonstration of the STEED process and to test Hypotheses 1-3 for PRSEUS. Some assumptions and limitations have been made to account for limited computational resources and setup time. It is acknowledged that the STEED approach in practice should be followed with full-scale characterization for a structural technology development program that wishes to characterize performance.

5.1.1 Experiment Set 1: Technology Level Characterization

The objective of the first set of experiments is to characterize performance in terms of the technology design space, $\mathbf{X}_T$, for both the PRSEUS technology and the baselines to which it is compared. Hypersizer contains a module in which single panel components can be examined without the need for iterating between the FEM in the global-local approach. This enables ease of examining technology level design variables under various loading conditions and quantifying the resulting panel weight and constraint functions that were discussed in Sec. 3.1.1. Following the STEED approach, two main experiments were performed at this level: Experiment 1A) a test of the aggregate design space, and Experiment 2B) a test of performance sensitivities to the technology design space.

First, surrogate models were built of all the metrics in this space. The process required sampling the Hypersizer panel environment for the technology level design variables that mapped to the structural layout and OML design spaces, denoted as $\mathbf{X}_{T\sim f(OML,SL)}$. These variables included panel length, panel width, and local panel loads. The panel loads considered in this experiment set were axial and lateral compression (N_x and N_y), axial and lateral positive bending moments (M_x and M_y), and positive normal pressure (P). A design of experiments was built using a 3-level full factorial for the global panel dimensions and four levels of each respective load. At each sample point, the technology design variables were optimized for weight within their bounds. Optimization variables for representative centerbody panels included: PRSEUS (skin thickness, stringer spacing, and frame spacing) and orthogrid sandwich composites (skin thickness, axial stiffener, and lateral stiffener). Wing representative panel optimization parameters were similarly defined: PRSEUS (skin thickness, stringer height, and stringer spacing) and uniaxial blade-stiffened composites (skin thickness, blade height, and blade spacing). These subsets were chosen following a more complete design space exploration, but due to the wealth of data generated

during these cases, it was more manageable to investigate the few to which panel weight $W_{S,i}$ showed the largest sensitivities and most unique trends.

For every sampled design point, results included structural weight and failure mode margins of safety. For PRSEUS, the number of failure modes was on the order of 80, while both baseline configurations were checked for failure with only about 30 methods. Therefore, filtering was required to determine only the particular failure modes which contained margins of safety for any given sampled point that fell below a threshold of $M = 2$. Because of Hypersizer's grid search optimization process, safety margins often never met the optimality condition of $M = 0$, and this is an identified drawback of the structural sizing tool. Experiment 1A used the surrogate models of $W_{S,i}\left(\mathbf{X}_{T\sim f(OML,SL)}\right)$ and $M_{j,k}\left(\mathbf{X}_{T\sim f(OML,SL)}\right)$ to perform a Monte Carlo simulation with uniform distributions applied to each design variable in $\mathbf{X}_{T\sim f(OML,SL)}$. The results are shown in Section 5.2.1.

Experiment 1B expanded on the first experiment to examine the whole subset of the design space for each panel configuration, including the variables that were optimized in Experiment 1A. The goal of this experiment was to supplement the aggregate results and determine if any significant trends could be shown that led to additional evidence that the next step in the STEED tollgate framework should be investigated. The same process was used to develop these surrogate models as well, where the three optimization variables for each configuration were added to the DoE at 3 levels each to account for potential nonlinearities. An interactive trade space was created for these variables, which included results from Experiment 1A for reference. Results are shown and discussed in Section 5.2.2.

5.1.2 Experiment Set 2: Structural Layout Level Characterization

Experiment Set 2 was performed to represent Step 4 in the STEED approach and test the set of hypotheses made under Hypothesis 2. This experiment follows the same

general tollgate process for characterization of structural technology performance related to the structural layout level. A 3-level full factorial DoE was generated to sample GT-WESt. Design variables that were considered were for the outboard wingbox structure only - the front spar location, rear spar location, and rib spacing, $\mathbf{X}_{SL} = [c_{FS,ow}, c_{RS,ow}, p_{rib,ow}]$. This sampling plan was implemented for both the baseline and technology-infused configuration, combining for a total 54 function calls to the full weight estimation environment. In order to account for potentially local effects, two OML design points were considered for Experiment 2A, the N2A and HWB301. Examining two configurations also helped provide additional evidence for the tollgate approach to move forward.

Experiment 2A was designed to test Hypothesis 2 and determine the maximum difference between structural layout designs. It also challenged the benchmark definition of performance in which the structural layout is held constant between baseline structure and technology configurations. This was a two step process in which observations were made for Hypothesis 2.1, which states that default values for the structural layout should not be used throughout the OML design space if error is injected into the process by doing so. To test Hypothesis 2.1, ΔW_S was calculated for each point in the 3-level full factorial DoE, and the optimal design point for the baseline was noted to coincide with the benchmark process. Secondly, the notion that the structural layout should be optimized for each configuration rather than optimized for the baseline only was tested. This approach identified the weights of each optimal point and found error between the two performance values in Eqn. 42. Two observations were created for the two baseline OML designs.

An additional experiment was performed to demonstrate the Step 4G in the STEED approach: design variable down-selection. The number of required cases for performance characterization as a function of the OML increases exponentially

with every new design variable that is considered. Experiment 2B considered an expanded set of design variables beyond the outboard wing, to see which parameters most greatly contributed to variability in performance. GT-WESt was sampled for this experiment using a 16-case Taguchi orthogonal array for eight structural layout design parameters: number of centerbody bays, rear spar chord location for the rear centerbody, front spar chord location and rib spacing for the trapezoidal wing, and for the outboard wing, front/rear spar chord locations, rib spacing, and the span location of the root chord for the outboard wing. Analysis of Variance was performed on the results of this DoE using a linear model.

5.1.3 Experiment Set 3: Outer Mold Line Level Characterization

The last set of experiments for direct characterization of weight reduction performance for the PRSEUS structural technology were at the OML design space level. Within the constraints of computational resources, this experiment was scoped to design parameters of the outboard wing of the HWB, using the N2A as a baseline. A 200-case design of experiments was used to generate structural weight estimates for each structural configuration: the baseline and PRSEUS technology. Although the $\mathbf{X}_{OML}$ and $\mathbf{X}_{SL}$ design variables were limited to the outboard wing, it was anticipated that effects of these changes would propagate to the centerbody section, and structural weights and performance were tabulated for each aircraft section separately and as a total for the full aircraft.

Depending on the results of Experiment 2A, there were likely three options moving forward for the OML: 1) carry multiple structural layouts forward for each design point and represent technology performance as a functional distribution, 2) optimize the structural layout through the GT-WESt model, or 3) sample GT-WESt using both OML and structural layout parameters to build a surrogate model. For option 3, the surrogate model could then be used to perform optimization of both the baseline and

structural technology aircraft configurations, and it could be done with fewer function calls to GT-WESt.

A GT-WESt function call is approximately 50 minutes for the 216-passenger N2A and approximately 100 minutes for the HWB301. The difference between the two is a result of the Hypersizer grid search approach and the number of candidate designs that need to be checked before an optimum is found for each component. If variable settings, i.e. bounds and number of permutations are tuned for each scale of aircraft, then a 40-50 minute runtime is achievable. However, making these function calls within a structural layout optimization process increases the computational expense to the point that only 2-3 cases can be analyzed on one machine. Therefore, option 3 was the obvious choice, and a sampling plan to account for nonlinearities in the structural layout and OML design spaces was required. The 200-case DoE used to generate results for Experiment Set 3 was comprised of a 143-case central composite design and 57-case Latin hypercube space-filling design, and the upper limit of the LH portion was based on available computational time.

The design variables considered for the outboard wing were

$$\begin{aligned} \mathbf{X}_{OML} &= [S_w, AR, TR, \Lambda_{LE}] \text{ and} \\ \mathbf{X}_{SL} &= [c_{FS}, c_{RS}, p_{rib}] \,. \end{aligned} \tag{50}$$

Artificial neural networks were fit to create surrogate models of aircraft section structural weights in relation to these design parameters, and those surrogates were in turn used to calculate structural technology weight reduction performance. With this capability, Experiment 3A was designed to examine the difference between handling the structural layout within the OML design space, augmenting the results obtained from Experiment 2. The structural layout could now be optimized for any given point $\mathbf{x}_{OML} \in \mathbf{X}_{OML}$ for the baseline structure, PRSEUS technology, or both. Multiple objectives for the weight optimization could be examined too.

Experiment 3A was designed with a number of goals in mind: 1) determine which optimization strategy for structural technology weight reduction performance was appropriate, 2) examine aggregate trends of weight and performance as a function of the OML to assess the significance of the relationship, and 3) generate the data required for the $\Delta W_S\left(\mathbf{X}_{OML}\right)$ to be quantified so it can be implemented in conceptual design and technology development applications. After observations were made regarding structural layout optimization, the final data was fit to a surrogate model for design space exploration. Experiment 3B used the final surrogate models to perform this design space exploration and observe trends from the parameter sweep. The goal of this experiment was to determine if any other indicators were present in the OML design space supporting the significance of the $\Delta W_S\left(\mathbf{X}_{OML}\right)$ or if other potential risks were found for the applications of performance characterization.

5.2 Technology Level Results

5.2.1 Experiment 1A: Aggregate Technology Level Design Space Results

The objective of the first technology level experiment was to assess structural technology performance as an aggregate of the technology level design space that was considered. Surrogates were developed for structural weight of each of four panels that were modeled at this level, single panel baseline and technology representations of the centerbody and wing, and performance for the representations of the wing and centerbody were calculated through:

$$\begin{aligned}\Delta W_{S,w} &= W_{S,blade}\left(\mathbf{x}_{T\sim f(OML,SL)}\right) - W_{S,PRSEUS,w}\left(\mathbf{x}_{T\sim f(OML,SL)}\right)\\ \Delta W_{S,cb} &= W_{S,orthogrid}\left(\mathbf{x}_{T\sim f(OML,SL)}\right) - W_{S,PRSEUS,cb}\left(\mathbf{x}_{T\sim f(OML,SL)}\right)\end{aligned} \tag{51}$$

respectively. A $50,000$-case Monte Carlo simulation was performed on each of the surrogates – $W_{S,blade}$, $W_{S,PRSEUS,w}$, $W_{S,orthogrid}$, $W_{S,PRSEUS,cb}$ – to represent performance distributions, $\Delta W_{S,w}$ and $\Delta W_{S,cb}$, for the $\mathbf{X}_{T\sim f(OML,SL)}$ design space. As previously mentioned, the functions represented in Eqn. 51 were generated with cases in which

the other technology level design variables for each structure concept were optimized for weight.

Aggregate results for the centerbody concept are shown in Fig. 53. Each histogram is labeled for the corresponding load that was applied to the panel, and from the top left going clockwise, the plots represent: N_x, N_y, M_y, P, and M_x. The first and obvious observation is that for each of these cases, the variation of weight reduction performance is decidedly non-zero. As discussed, the metric identified in Hypothesis 1 set the precedent that *any* variability in performance as a function of the technology parameters that mapped to the upper level design spaces warranted investigation of the next level. While the shape of performance distributions for each load on wing-representative structural configurations is somewhat different, as shown in Fig. 54, the same observation of variation, or spread of the distribution, can be made. This evidence supports Hypothesis 1 for PRSEUS technology, given the assumed baseline structures and loads considered. However, the hypothesis cannot be confirmed, i.e. show that the non-zero indicating factor was correct, under these conditions unless analysis at the $\mathbf{X}_{SL}$ or $\mathbf{X}_{OML}$ levels shows variation of performance within these respective design spaces.

Another observation for the centerbody-like structure is the shape of the distributions under bending moment loads, M_x and M_y. Using the definition of weight reduction performance, it is noted that the left side of each figure represents PRSEUS actually adding weight under specific conditions within $\mathbf{X}_{T\sim f(OML,SL)}$. If portions of the distribution are further away from $\Delta W_S = 0$, this means that performance becomes more extreme in either direction. For the bending moment loads applied to the centerbody structure, the distribution encapsulates the zero performance value. This phenomenon is significant because it presents a case in which higher level applications of performance characterization are affected. For instance, if technology selection in conceptual design defined some assumptions or mission analysis that replicated the

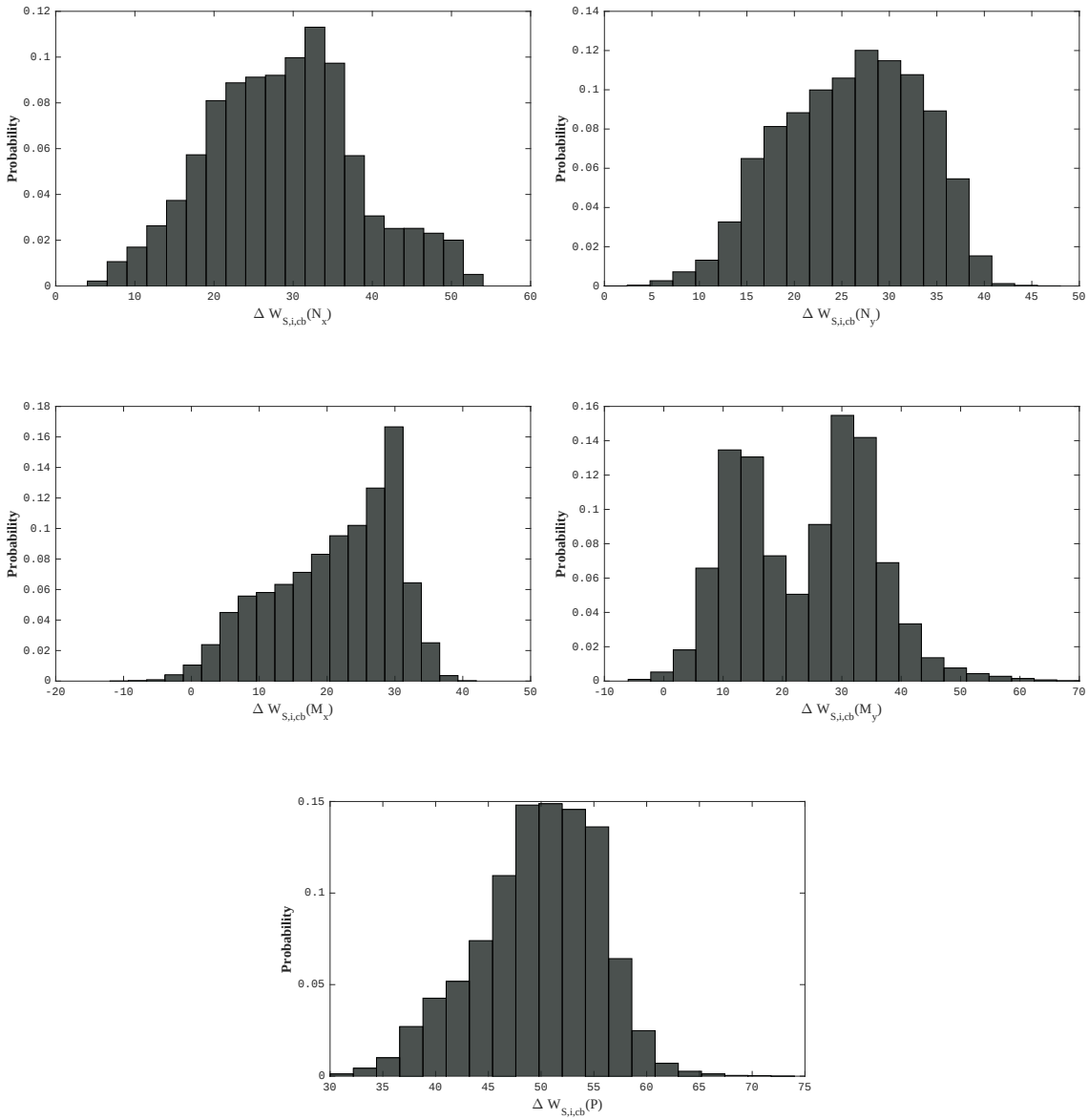

Figure 53: Variation of $\Delta W_{S,i}$ in terms of panel dimensions and local loads for centerbody structure

conditions in $\mathbf{X}_{T\sim f(OML,SL)}$ for the bulk of components in an aircraft configuration, then there is a chance that the technology team would be submitting negative performance values for consideration. Probabilistically, there is a very slim chance of this occurring, since the negative values of performance are predominantly in the tails of the distributions. However, a risk is presented to the technology development team nonetheless and it may need to be quantified to prevent such occurrences.

For the wing-like structure, one of the drawbacks in the model is the absence of a stiffening element in the y-direction for baseline blade stiffened composites. In full vehicle models, this is overcome with the addition of rib caps; however, this capability was not present for the technology level model. Therefore, loads acting in the lateral panel direction (y), which corresponds to the chord direction on the wing, are shown to have extremely advantageous performance for the PRSEUS technology. The PRSEUS frame is equivalent to a rib cap in the full vehicle model, and it increases stiffness in the chord direction. Increased stiffness in the frame results in less load being carried through the skin structure, and as a result, the skin can be sized normally under these loads. Blade stiffened composites on the other hand, lack this mechanism in the technology model and are oversized comparatively. The oversized skin is the reason the top right and middle right histograms in Fig. 54 are fully on the positive side of performance and at relatively large magnitudes.

Also noted is the large difference in variability when comparing moments and forces in the local axial x-direction, i.e. relating to span on the full vehicle model. N_x for this demonstration was applied as a compressive force to account for the more critical of the load cases for the outboard wing of the HWB aircraft – the 2.5G pull-up maneuver. Under this local compressive loading condition, representing the upper wing skin in this case, local and global panel buckling become a more critical failure mode for the structure. Because the PRSEUS stiffeners continue to carry load after local buckling occurs, this was shown to not be a critical failure mode.

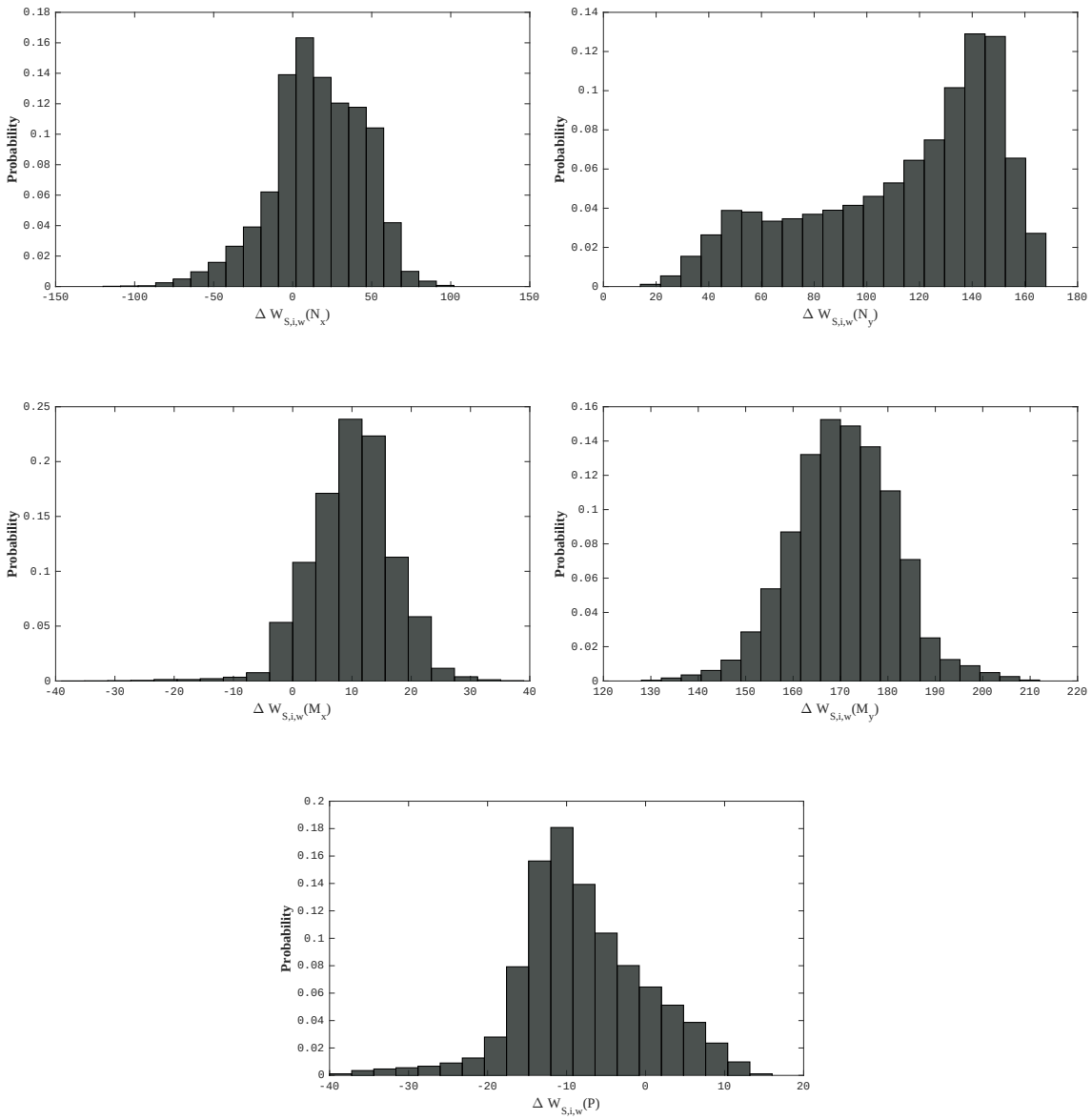

Figure 54: Variation of $\Delta W_{S,i}$ in terms of panel dimensions and local loads for wing structure

However, local buckling is still an active constraint for the baseline. More importantly, changing the global dimensions of the panel results in significant variation in the global buckling failure calculation. The design of experiments used to generate data for the surrogates contained cases which compared the upper bounds of panel size for the technology to the lower bounds of panel size to the baseline and vice versa. The global buckling constraint is most likely the reason for this large variation centered around zero performance, while there is a slight skew at the tail end of positive PRSEUS performance most likely due to post-buckling performance.

Determining causality in this manner is directly applicable to the technology development application – experiment design and selection. A detailed design space investigation was performed in Experiment 1B this reason; however, added clarity can be obtained through aggregate data from Experiment 1A being shown in terms of one-off variation of each design variable in $\mathbf{X}_{T\sim f(OML,SL)}$. Figures 55 and 56 show aggregate results in this manner for the centerbody-like structure and wing-like structure, respectively, under compressive local axial forces, N_x. Each histogram shows results from a Monte Carlo simulation with a uniform distribution of a single variable of the corresponding color: Red - panel length, Green - panel width, and Blue - local load magnitude. Each separate plot represents a different default value of the other two variables in $\mathbf{X}_{T\sim f(OML,SL)}$ corresponding to a percentage level of its respective range above its lower bound: Top - 25%, Middle - 50%, and Bottom - 75%.

Variation in centerbody performance remains relatively consistent for each level of the other defaulted parameters, shown in Fig. 55. Only a slight increase in spread of the histograms exists in the middle and bottom plots. Each plot also shows the green and red histograms skewed to the positive side of performance, meaning variation in global panel dimensions has a smaller probability in causing negative PRSEUS performance under compressive axial force conditions. Variation in the magnitude of the compressive force itself, however, is not skewed and only moves slightly to

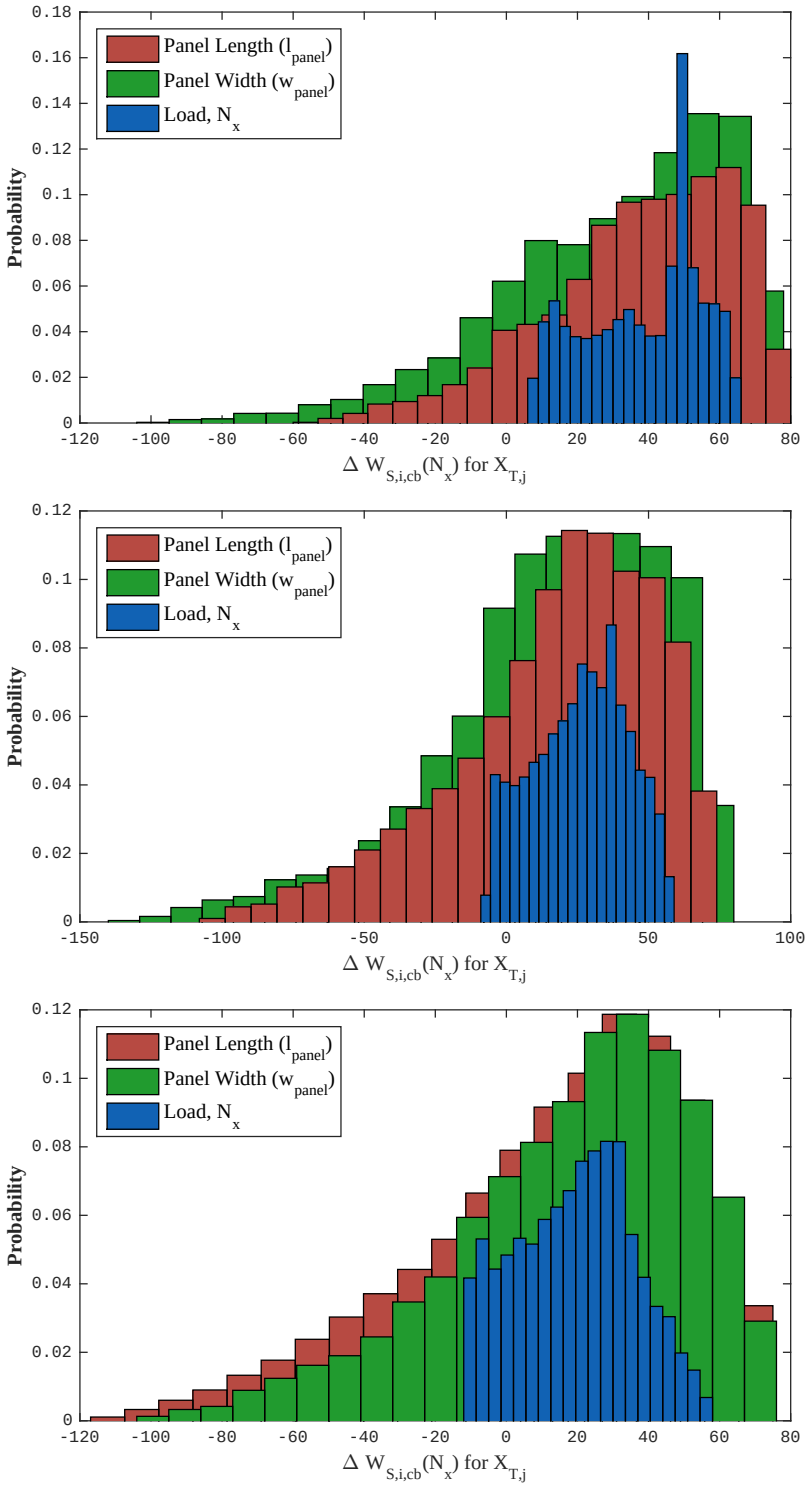

Figure 55: Variation of $\Delta W_{S,i}$ for centerbody structure for each $x_T \in [l_{panel}, w_{panel}, N_x]$

the left in the larger panel dimensions, e.g. the middle and lower plots. In the top plot, i.e. the smallest comparative global panel dimensions, the blue distribution fully exists in the positive side of performance. At this panel size, with the panel being optimized under each condition, many of the design variables likely remain at minimum gauge thicknesses due to less imminent stability failure modes. This trend then shows that under the assumptions on bounds for the detailed technology level parameters being used in sizing, $\mathbf{X}_{T,B}$ and $\mathbf{X}_{T,T}$, minimum gauge conditions benefit PRSEUS. An increased skewness toward positive performance for the green and red distributions of this top plot support this notion as well, meaning that for panels under comparatively small compressive loads, better performance exists for PRSEUS in the absence of failure constraints. It is important to note, however, that this observation is made *only* under the bounds that were applied for this demonstration case study. Some design parameters for each panel were defaulted, and those that were left to vary coincided with those in Experiment 1B.

The top left histogram of Fig. 54 for wing-like structure, which was the configuration with the greatest variability in performance of any considered, is broken down in Fig. 56. This figure is organized the same as the centerbody in Fig. 55. Observations that were made regarding the full distribution are confirmed by these plots. The variability in performed increases directly with the three variables in $\mathbf{X}_{T\sim f(OML,SL)}$, shown through an increased histogram spread from the top plot to the bottom plot. Global panel dimensions contributed to the greatest variability in the $\mathbf{X}_{T\sim f(OML,SL)}$ design space. Compressive force is shown to shift right from the top plot to bottom plot, showing that PRSEUS performs better under compressive loads for larger panel components compared to smaller components. Global buckling is less of a constraining failure mode for small panels, conditions in which post-buckling PRSEUS performance can be dominant. The red distribution in the top plot shows this effect, where variability in panel length – in the direction of load – creates a

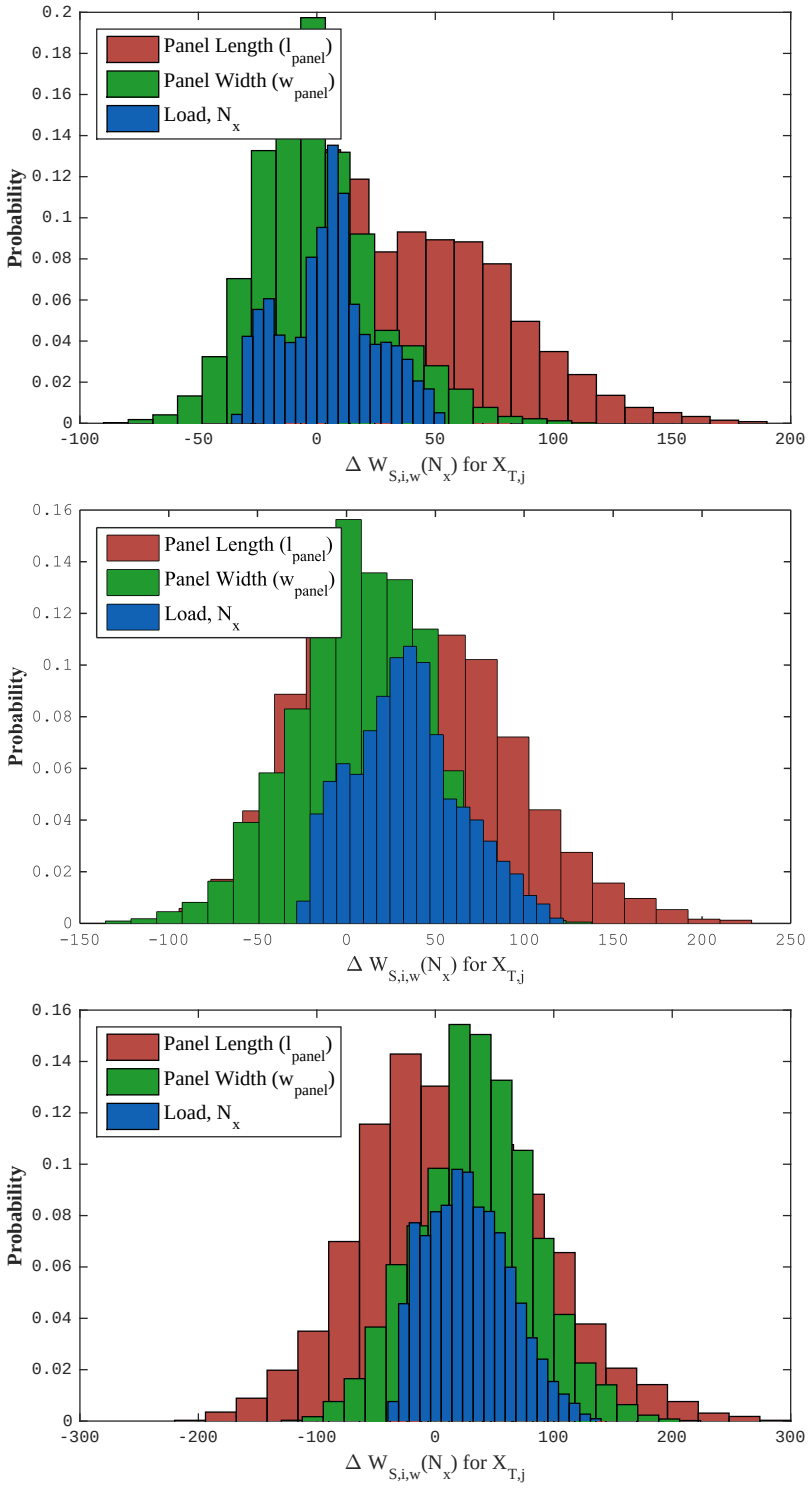

Figure 56: Variation of $\Delta W_{S,i}$ for wing structure for each $x_T \in [l_{panel}, w_{panel}, N_x]$

performance distribution that reaches further on the positive performance side. In the bottom plot, this distribution shifts left, meaning both blade stiffened composites and PRSEUS panel components are susceptible to buckling for larger components. This failure mode shifts and skews the blue histogram slightly to the right, which represents PRSEUS post-buckling performance at smaller force magnitudes.

5.2.2 Experiment 1B: Technology Level Design Space Exploration

To examine the technology design space in a more detailed fashion than aggregate histograms of random samples shown for Experiment 1A, sensitivity profiles are investigated for Experiment 1B. Sensitivities of weights, technology performance, and failure modes can be interactively assessed through environments like those shown in Figs. 57 and 58. Each plot represents a snapshot of a wealth of information regarding local effects within the technology level design space. Rows of the sensitivity matrix are the metrics at the $\mathbf{X}_T$ level: component technology performance $\Delta W_{S,i}$ (top row), component structural weight $W_{S,i}$ (2nd row), ultimate margins of safety M_{ult} (3rd row), and limit margins of safety M_{ult} (bottom row). Columns show the $\mathbf{X}_T$ design variables, in which columns 3-5 are not included in $\mathbf{X}_{T\sim f(OML,SL)}$.

The features in Figs. 57 and 58 are color coordinated for: structural technology performance (black), baseline structure (red), and PRSEUS structure (green). In each individual sensitivity plot, a thick solid line represents the design space exploration case, in which the three variables not contained in $\mathbf{X}_{T\sim f(OML,SL)}$ are left to vary. Their design settings are represented by the triangle along the x-axis in each column. Values of the $\mathbf{X}_{T\sim f(OML,SL)}$ parameters are set in the same way. The thinner dashed lines show the optimized case from Experiment 1A, and the optimized settings are represented for design variables in columns 3-5 by vertical dotted lines which are also color coordinated and labeled "B" for baseline and "T" for technology. In the bottom two rows, the optimized margin values for these cases are shown at their respective

optimized x_T value.

A total of ten environments like this were created, for each representative configuration (centerbody-like and wing-like structure) and for each of the five local loading conditions that was applied. Why is this capability needed and what is the goal of this experiment? It is recognized that Experiment 1A provided sufficient evidence for PRSEUS to move through the tollgate process to characterization of structural technology performance at the $\mathbf{X}_{SL}$ level. However, had this not been the case, the technology level design space would be need to be investigated for any local trends that would signify importance of the quantification of the $\Delta W_S\left(\mathbf{X}_{OML}\right)$ relationship. In addition, this interactive environment is an enabling capability for investigations in causality for technology experiment design.

The process used in Experiment 1B was a systematic parameter sweep of each of the design variables on the x-axis for each local loading condition. The objective of this parameter sweep is to observe any indicating factors which would have a significant impact on $\Delta W_S\left(\mathbf{X}_{OML}\right)$, including:

- a large degree in nonlinearity of the optimized or non-optimized:
  - performance function $\left(\Delta W_{S,i}\left(x_T \in \mathbf{X}_{T\sim f(OML,SL)}\right)\right)$,
  - baseline weight function $\left(W_{S,i,B}\left(x_T \in \mathbf{X}_{T\sim f(OML,SL)}\right)\right)$, or
  - technology weight function $\left(W_{S,i,T}\left(x_T \in \mathbf{X}_{T\sim f(OML,SL)}\right)\right)$,
- discontinuities in either the optimized or non-optimized functions of the previous bullet,
- instances in which the performance function crosses the "no impact" ($\Delta W_{S,i} = 0$) threshold,
- conditions which create large values of the optimized margin functions (dotted lines on the bottom two rows), e.g. $M_{ult} \gg 0$ or $M_{ult} \gg 0$, which indicate minimum gauge designs,

– conditions which create negative values of optimized margin functions, e.g. $M_{ult} < 0$ or $M_{ult} < 0$, which indicate an undersized structural configuration and the need to increase upper bounds of design variables, or
– instances in which the optimized values of respective $x_T \notin \mathbf{X}_{T \sim f(OML,SL)}$ for baseline and technology structure are exceedingly different.

Instances of these phenomena have direct implications if they are observed for any of the optimized functions, meaning that their existence is imminent at the next highest level. If these trends show for the non-optimized case in which $\mathbf{x}_T \notin \mathbf{X}_{T \sim f(OML,SL)}$ are left to vary, then the relationship is more implicit.

The first design space environment is shown in Fig. 57, and is a case of centerbody configurations for both baseline and PRSEUS structure under compressive lateral forces. This configuration is representative of the centerbody upper skin panels that exist between chord locations of trapezoidal wing load introduction for a positive-g pull-up maneuver. It can also represent a bulkhead in a similar maneuver. The fourth and fifth columns of this figure show the variable names for each concept designated with a "B" and "T." These design parameters show the same feature for each panel, but they do not necessarily have the same limits. For example, pitch for the 90° stiffener of the orthogrid baseline structure is an implicit design variable that is dependent on the axial stiffener pitch. By specifying an angle between the two stiffeners, where 45° defined equal spacing, the lateral stiffener pitch was determined. Therefore, the same lower bound exists for axial and lateral stiffener pitch, columns four and five, respectively; however, the lower bound for the PRSEUS configuration frame pitch is designated by the [symbol at $p_{fr} = 16$in.

Since this environment is meant to be interactive, the full scope of trends cannot be shown in this static instantiation. However, a few observations can be made at the current design variable settings. For instance, the dashed line in the top row for performance of the optimized configuration changes as a function of the $\mathbf{X}_{T \sim f(OML,SL)}$

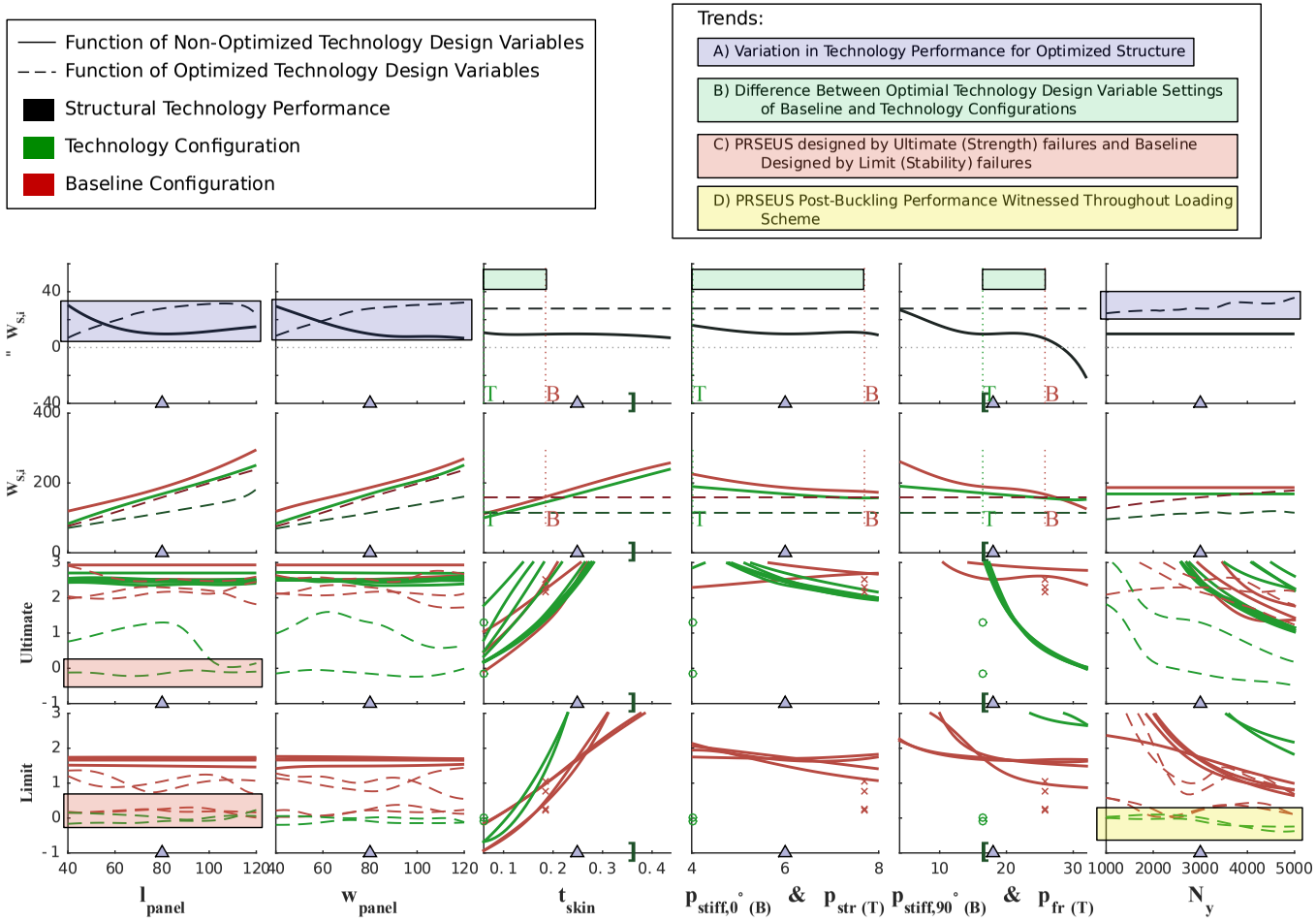

Figure 57: Technology design space for centerbody-like structure under compressive lateral force (N_y)

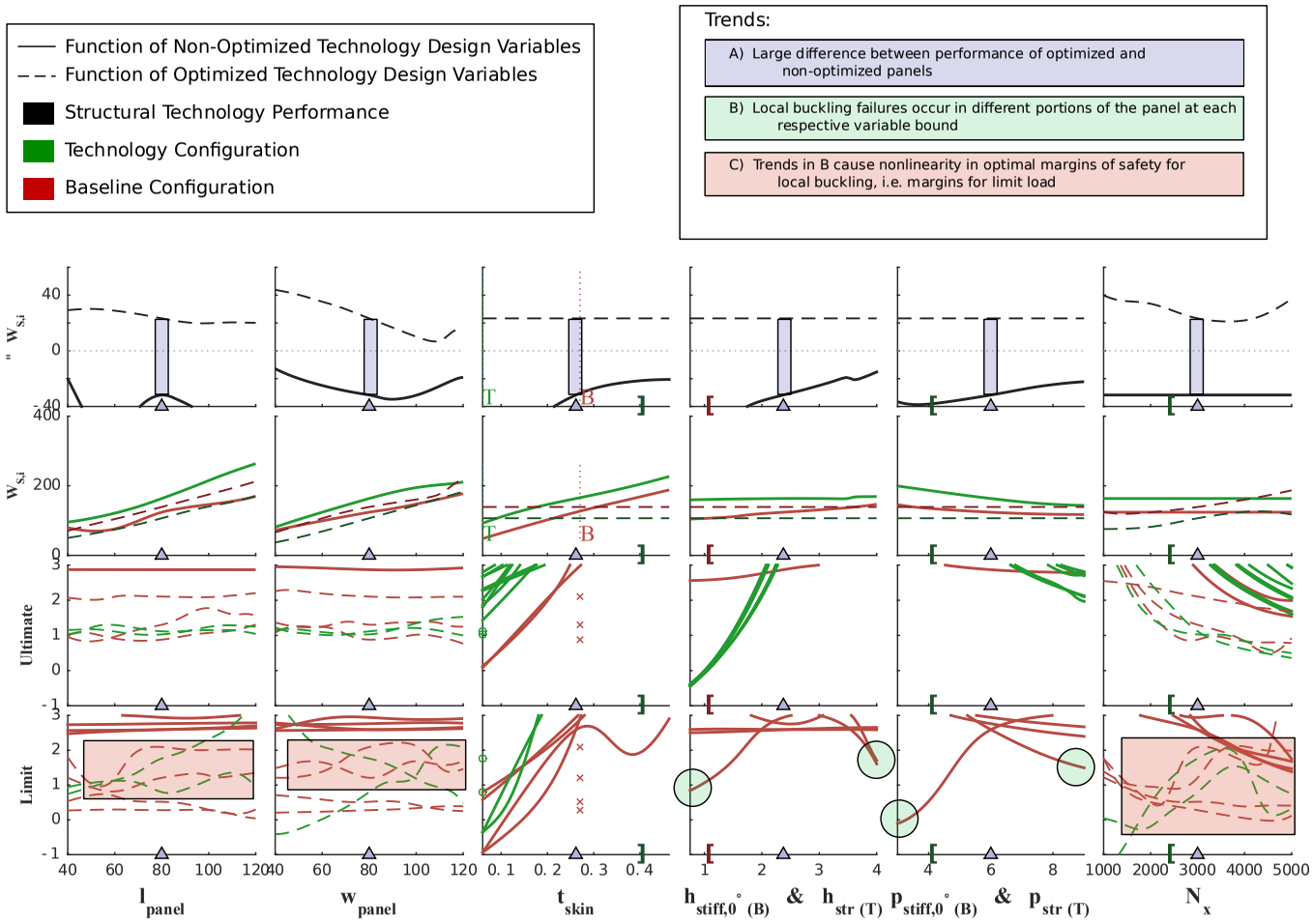

Figure 58: Technology design space for wing-like structure under compressive axial force (N_x)

variables (columns 1, 2, and 6), which further supports Hypothesis 1 and confirms the trend of variability in Experiment 1A for this specific configuration. This slope in performance is caused by the change in slopes from the green and red dashed lines of the 2nd row for each of the $\mathbf{X}_{T\sim f(OML,SL)}$ variables. Furthermore, optimized design variables in columns 3-5 are set to different values at the current global panel size and force magnitude, showing that these parameters effect sizing of each structure differently. Lastly, the bottom two rows represent the potential failure modes, and it is shown that at the current $\mathbf{X}_{T\sim f(OML,SL)}$ settings, the baseline structure in red is dominated by stability limit failure modes while PRSEUS is designed by strength-based ultimate failure modes. Although the limit level failures for PRSEUS in the green dashed lines are set to approximately zero, it is not designated a failure until $M \leq -0.5$ in this exercise.

A few characteristics in this figure also reflect assumptions of the Hypersizer technology level model. For instance, the solid lines for limit and ultimate margins of safety in columns 1 and 2 are constant as a function of the panel dimensions. Hypersizer calculates safety margins in terms of normalized loads and panel features, meaning all failures are checked relative to area and are scaled accordingly. The wavy nonlinearity of each of the dashed line sensitivities for these safety margins also reflects the optimization approach within Hypersizer. This discrete approach means that an optimized configuration is not always defined where the margin is equal to zero. In the load column to the furthest right, the "Ultimate" row shows an indirect relationship between ultimate margin and force magnitude, and this shows that there are configurations under minimum gauge constraints within this $\mathbf{X}_{T\sim f(OML,SL)}$ design space.

Some of the same trends can be seen in Fig. 58 for wing-like structural configurations. A large separation between optimized performance and performance under the current technology design parameter settings for t_{skin}, h_{stiff}, and p_{stiff}. Optimized

performance, in the dashed black line of the top row, is also nonlinear given the current $\mathbf{X}_{T\sim f(OML,SL)}$ settings. An interesting trend can also be seen for the limit failures of the baseline blade-stiffened configuration. These stability failure modes are calculated for both the skin and the stiffeners. Different failure modes, i.e. different solid red lines in the plot, are the most constraining at the upper and lower bounds, respectively for both stiffener height and stiffener pitch. This represents local buckling of the skin and stiffener at the lower bound and upper bound of stiffener height, respectively. The opposite trend exists for stiffener pitch, in which local buckling is the lowest value of any limit safety margin at $p_{\text{stiff},0^\circ,UB}$. Switching between these failures in the sizing cases results in the highly nonlinear margin functions of columns 1, 2, and 6.

5.2.3 Summary

Although Hypothesis 1 was solely established on variation in technology weight reduction performance, this is not the only significant characteristic to be observed at the technology level. The process by which performance assessments were generated provided a detailed insight into the sources and causes of structural weight reduction rather than solely the quantified values. The question of "why?" is just as important to the implementation of the technology in conceptual design as the performance values themeselves. Causality is determined in the last step of the STEED approach, which is associated with experiment characterization. However, causality and understanding why a technology performs the way it does and under what conditions, assumptions, etc. is critical in the implementation of the technology in conceptual design as well. For instance, some of the trends shown in this section advocate that blindly applying PRSEUS to all structural components may result in situations where structural weight is added to a particular configuration. PRSEUS may not be the solution for all loading conditions or all structural geometries, and it is likely the

same case for any other structural technology. However, this approach provides insight to a critical step in structural technology performance characterization to enable traceability and the capability to determine causality.

At the higher design space levels, question may arise regarding the trustworthiness of results or with artificiality of trends due to modeling assumptions. With Step 3 of the STEED approach, these questions can be brought to the source level of these concerns and the decomposition of the technology that occurs there. Important intangible lessons were learned in assessment process of these experiments as well. Initially, the technology level design space was sampled with a purely full-factorial DoE, and neural networks were used as the mathematical form of the surrogate models that enabled design space investigations like those in Figs. 57 and 58. This process was followed in anticipation of nonlinear trends with most of the functional relationships. Near-perfect model fits were obtained when regressing the data; however, observations were made that questioned the appropriateness of the surrogates.

Figure 59 shows an initial design space exploration enviroment that was generated (top) compared to a finalized version (bottom). The nonlinearities and discontinuities witnessed in the weight and performance functions, especially for the global panel dimension parameters (columns 1 and 2) are a complete artificiality of the neural networks. This process must be used with caution because discontinuities in the space could easily be attributed to discrete effects like stiffener drop-off as a function of panel size and stiffener spacing. However, Hypersizer "smears" these variables to an equivalent plate and all variables can be handled with pure continuity. If the user was unaware of this modeling assumption, false observations and a potentially unwarranted procession through the tollgate process could be made. A small space-filling sampling method was used to augment the full-factorial DoE, and the models smoothed to greater the greater accuracy shown in the bottom plot of Fig. 59

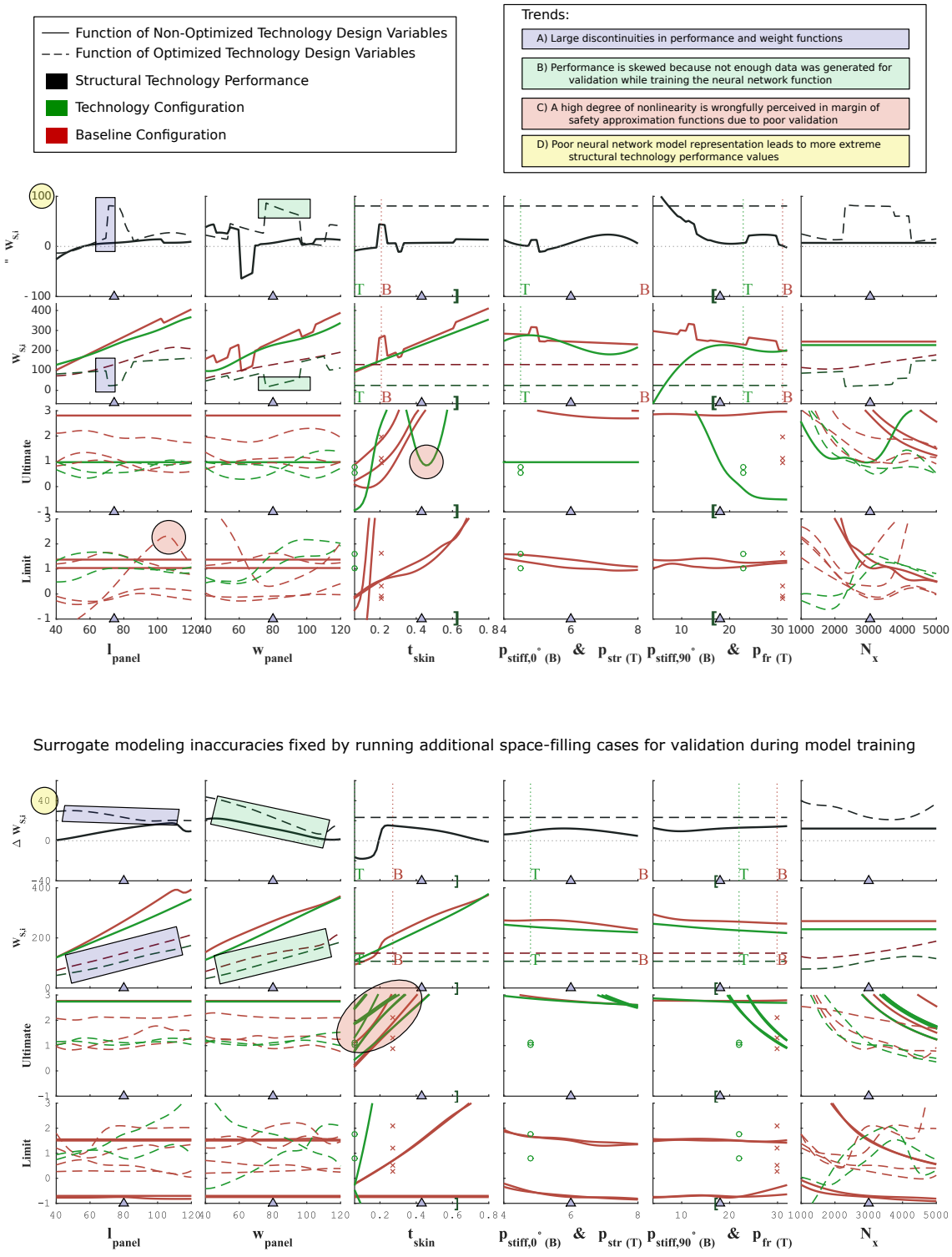

Figure 59: Artificial discontinuity and nonlinearity in the technology design space due to surrogate modeling

5.3 Structural Layout Level Results

A pivotal point in the tollgate framework of the STEED approach is Step 4, coinciding with the $\mathbf{X}_{SL}$ design space. In addition to providing support for the first overarching hypothesis, the results from the experiments performed at this level should answer one of the fundamental questions regarding structural technology performance: should structural weight reduction due to enabled topology optimization be attributed to the aircraft level performance of the structural technology, ΔW_S? Recall the benchmark approach treatment of $\mathbf{X}_{SL}$ in performance estimation, in which a baseline structural layout $\mathbf{x}^*_{SL}$ was implemented on a single OML for both the baseline structural concept and the technology of interest. This process does not account for the enabling effects of the technology, e.g. a more efficient structural layout, or perhaps a more efficient OML that can meet the same design objectives and mission with a resized configuration that further saves structural weight. Experiment 2A initializes investigations in the appropriate treatment of the structural layout in the performance estimation process. Experiment 2B addresses one of the challenges associated with using a higher fidelity structural model for performance estimation - the increased run time and limited number of design points that can be tested with limited computational power.

5.3.1 Experiment 2A: Benchmark definition of $\Delta W_S(\mathbf{X}_{SL})$

Experiment 2A was performed using the Georgia Tech - Weight Estimation Environment to assess the impact of structural layout design on structural technology performance. A subset of the total number of structural layout design variables was applied to the structural model for this experiment 1) for demonstration purposes, and 2) so that resources could be used for a design of experiments that enabled the assessment of nonlinearity in the design space for $W_{S,B}(\mathbf{X}_{SL})$, $W_{S,T}(\mathbf{X}_{SL})$, and $\Delta W_S(\mathbf{X}_{SL})$. For a single OML configuration, a variability assessment for these metrics could only be achieved using the benchmark definition of performance of $\Delta W_S(\mathbf{x}_{SL,B})$ rather than

the proposed definition in which the structural layouts are considered separately, $\Delta W_S\left(\mathbf{x}_{SL,B}, \mathbf{x}_{SL,T}\right)$. Two test case OML designs were therefore considered in Experiment 2A, which provided two data points for the latter case and the ability for a limited assessment for $\mathbf{X}_{OML}$ impact on ΔW_S for the tollgate approach.

First, GT-WESt was sampled using a 3-level full factorial DoE on the following parameters for the N2A outboard wing: front spar chord location c_{FS}, rear spar chord location c_{RS}, and rib pitch p_{rib} (ft). The outboard wing was used as a test bed for this experiment because of its ease of implementation and applicability to both unconventional and conventional aircraft configurations. Results from the full factorial sampling were used to test Hypothesis 2.1, shown below for reference, first for the benchmark definition of performance.

Hypothesis 2.1: If variation in $W_{S,B}\left(\mathbf{X}_{SL,B}\right)$ and $W_{S,T}\left(\mathbf{X}_{SL,B}\right)$ causes significant error in technology performance, ΔW_S, then the structural layout cannot be held constant in the performance characterization process.

The set of figures in this section show results obtained from Experiment 2A to either support or refute this hypothesis. Each plot shows front spar and rear spar location plotted along the x-axis and y-axis, respectively, and each surface shows a different rib spacing: $p_{\text{rib}} = 2$ ft (blue), $p_{\text{rib}} = 3$ ft (green), and $p_{\text{rib}} = 4$ ft (red). Values of the design variable ranges for this experiment were chosen to reflect the conventional wing structure reviewed in Reference[95].

Beginning with reduction of total N2A structural weight, results are shown in Fig. 60. This plot shows a total range of performance from 13.1% structural weight saved by PRSEUS to a potential 21.4%, resulting in a potential difference of $15,207$ lbs using the benchmark definition of performance. Weight reduction at the nominal design point was estimated at $16,371$ lbs, and therefore, the total range of difference throughout the design space is nearly 67.5% of benchmark predicted performance

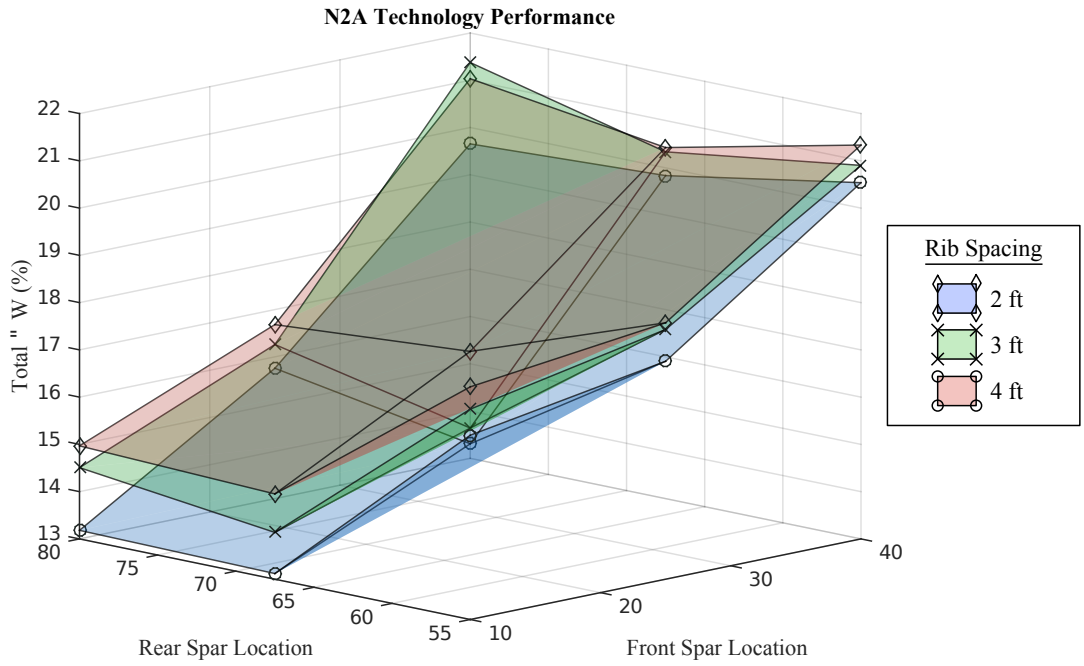

Figure 60: Total $\Delta W_S\,(\mathbf{X}_{SL} = \mathbf{X}_{SL,B} = \mathbf{X}_{SL,T})$ for N2A configuration enabled by PRSEUS

value. An error of this magnitude is significant and supports Hypothesis 2.1 in the need to consider variation in structural layout for structural technology performance estimation. Slight nonlinearity is also witnessed in the performance space, with the overall lowest estimate in performance being achieved at the midpoint of rear spar location. From this plot, it is also observed that front spar location seems to have the greatest impact on performance variability among outboard wing structural layout variables. It is also noted that the surfaces are layered in order throughout nearly the entire design space; however, the nominal setting of rib pitch at 3 ft slightly exceeds the others at $c_{RS} = 80\%$ and $c_{FS} = 40\%$, and performance at this point is near the midpoint of the range of technology performance in the design space.

Baseline and PRSEUS total structural weights are shown in Fig. 61 to provide further insight into why performance looks the way it does in the design space. These plots are normalized by the nominal total baseline structural weight, $W_{S,B}\,(c_{FS} = 25\%,$

$c_{RS} = 67.5\%,\ p_{rib} = 3$ ft) for ease of comparison. The same general trend is witnessed for weight functions as the performance function itself. PRSEUS total structural weight, however, shows a higher degree of nonlinearity, and the surfaces cross at multiple points in the design space, signifying further nonlinearity as a function of rib pitch. Also noted is the minimum weight design point among any configuration considered in Experiment 2A for both baseline and technology-infused N2A aircraft: the PRSEUS configuration with $\mathbf{x}_{SL,T} = [c_{FS} = 10\%, c_{RS} = 55\%, p_{rib} = 4$ ft]. PRSEUS performance for the total aircraft structural weight at this point is $\Delta W_S = 17.9\%$. In this case, the technology enabled a better performing structural layout compared to the most optimal baseline configuration of $\mathbf{x}_{SL,B} = [c_{FS} = 10\%, c_{RS} = 67.5\%, p_{rib} = 2$ ft]. Under the assumptions of the model, both configurations seemed to show better performance for the technology and lower structural weight for the entire aircraft at a front spar location of 10% chord.

The other OML design point considered in Experiment 2A was the HWB301, and the same set of results are shown in Fig. 62 and 63, respectively. The most obvious first observation of the performance surfaces is the separation of surfaces at the point $\mathbf{x}_{SL,T} = [c_{FS} = 10\%, c_{RS} = 80\%]$. This point is also the design with the smallest reduction in weight for the PRSEUS technology on the HWB301. Nonlinearity in performance is slightly less for this concept, but the overall range, upper bound, and lower bound for total aircraft weight reduction is nearly to the N2A. Initially, this might suggest that $\mathbf{X}_{OML}$ has no effect on the variability of performance, but the different overall shape of the surfaces is cause for further investigation. Similar to the N2A, the next step is investigation of the component weights of the performance calculation.

A significant difference exists between the HWB301 and the N2A for both baseline and PRSEUS configurations - the shape of the weight function is nearly opposite. The shape of the weight function is nearly opposite, where generally the bottom left corner

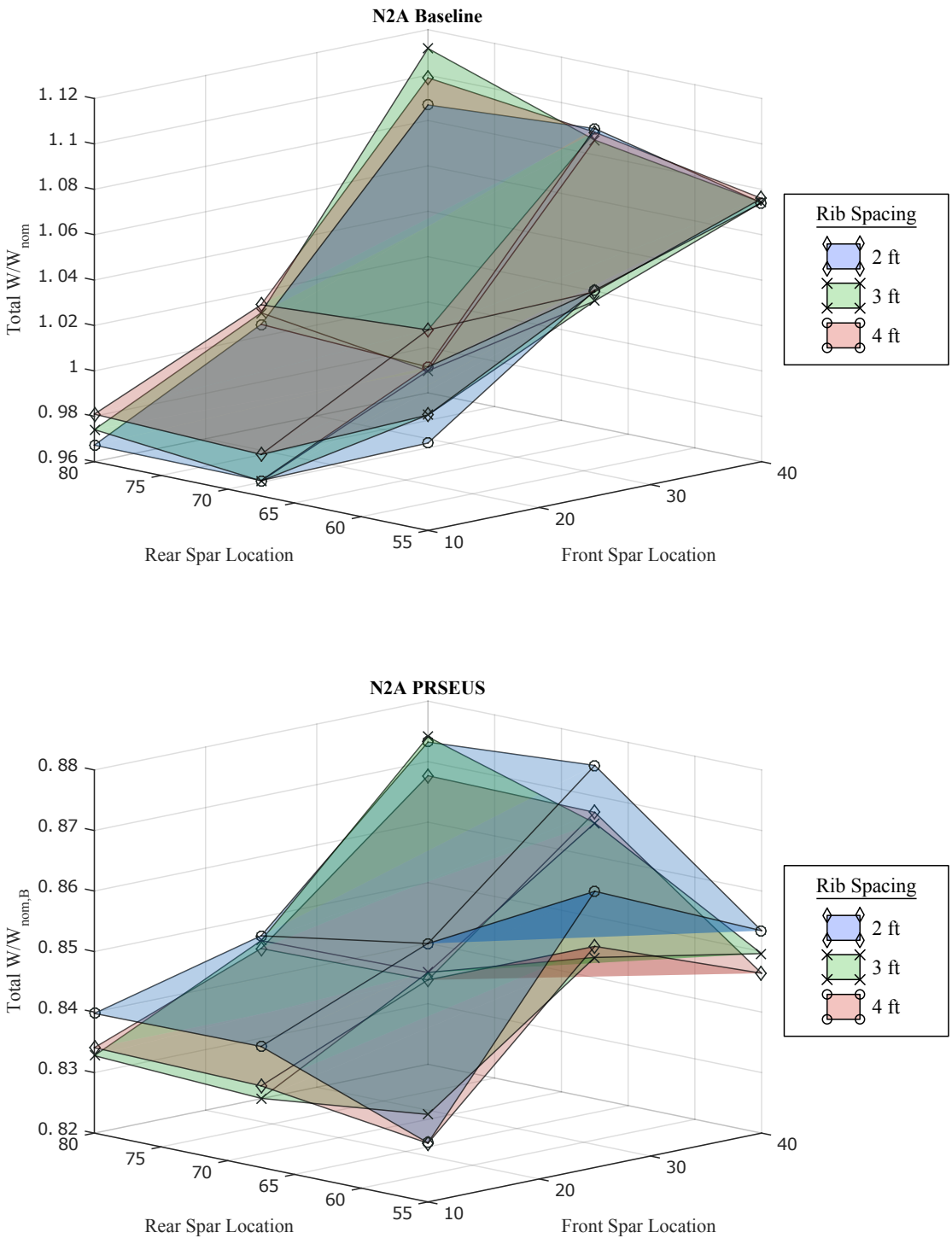

Figure 61: Total $W_{S,B}\left(\mathbf{X}_{SL,B}\right)$ and $W_{S,T}\left(\mathbf{X}_{SL,T}\right)$ for N2A configuration

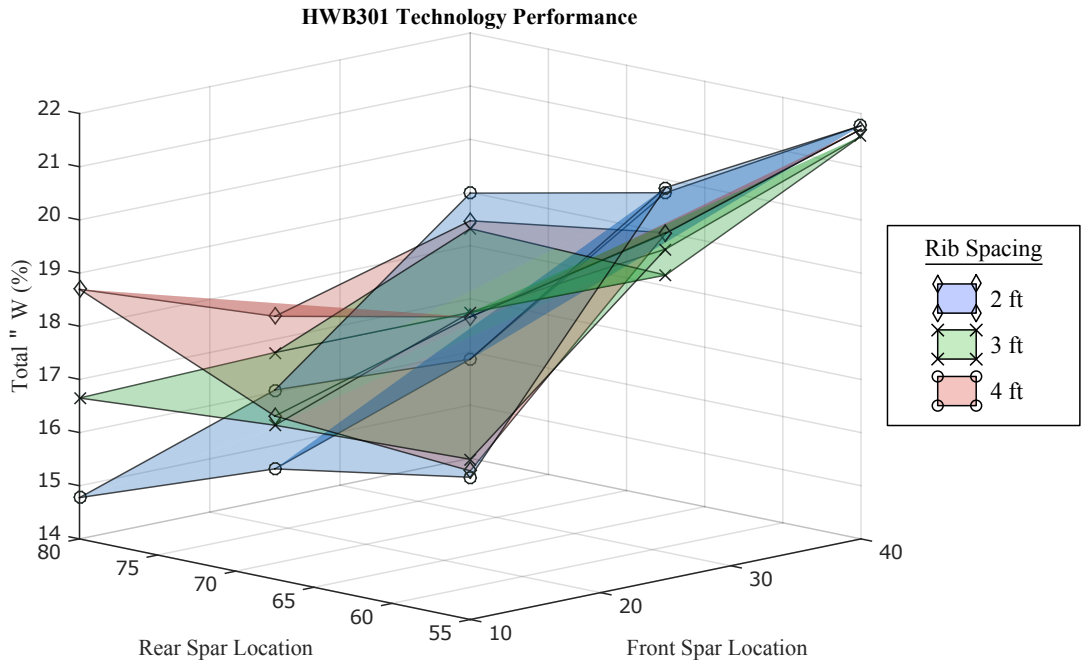

Figure 62: Total $\Delta W_S\,(\mathbf{X}_{SL} = \mathbf{X}_{SL,B} = \mathbf{X}_{SL,T})$ for HWB301 configuration enabled by PRSEUS

at $\mathbf{x}_{SL,T} = [c_{FS} = 10\%, c_{RS} = 80\%]$ was the most weight efficient structural layout for the N2A, it is the heaviest for the HWB301. Since the scale of the HWB301 is larger, the weight of the upper and lower outboard wing skin panels might be driving this trend, since they possess the largest defined surface area with the furthest forward front spar and the furthest aft rear spar. The opposite configuration is the most weight efficient for the HWB301, which is the configuration with the smallest surface area skin panels. Global stability of the wing might be a concern in this type of configuration, especially since comparatively, the average chord of the outboard wing of the HWB301 is smaller than the N2A. However, flutter calculations and other aeroelastic effects have not been implemented in the GT-WESt model.

The minimum weight solution for the HWB301 exists at the point of greatest PRSEUS performance, similar to the N2A. The difference between HWB301 and N2A, however, is that both the baseline and PRSEUS configuration have the same

weight optimum structural layout. Using the benchmark approach in this case, so long as topology optimization was performed in designing the structural layout, would generate the same estimate as an approach in which the effort was take to optimize both baseline and technology configurations separately. For how many OML design points would this observation hold true? Should the optimization objective for structural layout be the total weight, W_S, or the structural weight of one of the aircraft sections, and does it make a notable difference if so? Implementation of structural technologies in traditional conceptual design tools like EDS/FLOPS occurs for each aircraft section, and it is therefore dually beneficial to examine performance and weight trends by section for this experiment.

For each section, $\Delta W_{S,\text{sect}}$, $W_{S,B,\text{sect}}$, and $W_{S,T,\text{sect}}$ results are shown side-by-side for comparative purposes between the two test case configurations. This provides a direct contrast of the effect of outer mold line. In FLOPS, the k-factor implementation occurs for the HWB centerbody and the total wing, and these are the two sections shown first. Although none of the centerbody structural layout design variables were included in Experiment 2A, the outboard wing design parameters still have an implicit effect on the sizing process for this section. For load path continuity, the main landing gear front lower bulkhead is forced to the same global x-location as the front spar at the outboard wing root location. Therefore, variation in this parameter slightly effects the structural layout of the centerbody, which is why it is the source of largest variation in weight and performance of the outboard wing design parameters considered in this experiment. Additionally, if internal load distributions are changed as a function of the outboard wing structural layout, then load introduced to the centerbody also changes with the $\mathbf{X}_{SL,ow}$ design variables.

The trends shown in Fig. 64 reflect this relationship. This figure presents $\Delta W_{S,\text{sect}}$, $W_{S,B,\text{sect}}$, and $W_{S,T,\text{sect}}$ for the N2A and HWB301 in the left column and right column and top to bottom, respectively. Little variation exists in PRSEUS performance for

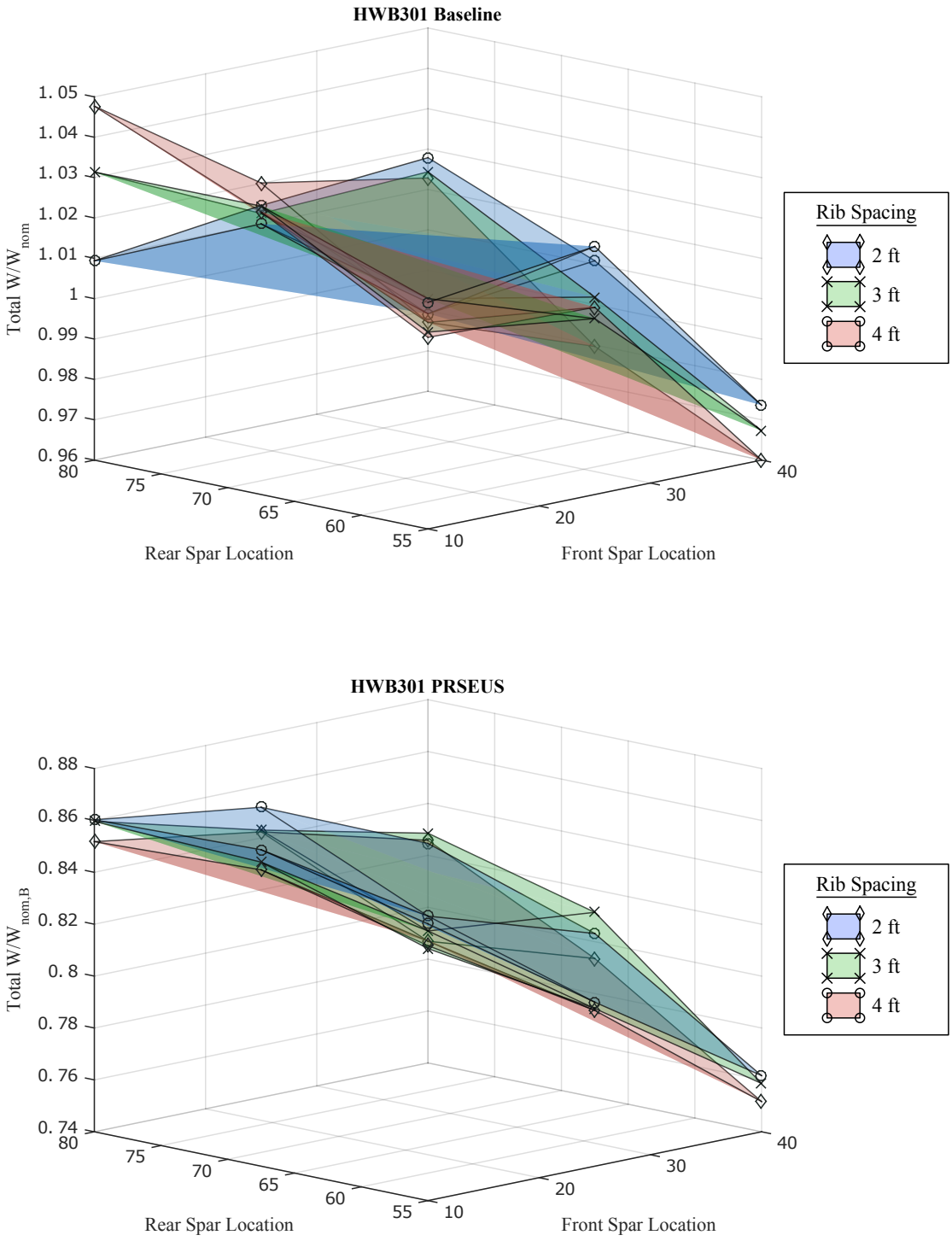

Figure 63: Total $W_{S,B}\left(\mathbf{X}_{SL,B}\right)$ and $W_{S,T}\left(\mathbf{X}_{SL,T}\right)$ for HWB301 configuration

either configuration, which is to be expected; however, the shapes of the performance functions are noteworthy. PRSEUS performance for the N2A centerbody is a bowl-like function in which the nominal settings in the design space (center design point) exhibit the worst performance, albeit still a significant weight reduction. The shape of the performance function for the HWB301 matches the shapes of its component weights, showing that the best performance exists at the most weight-inefficient design point for the outboard wing. Within the 3-D representation for the N2A, the baseline and PRSEUS configurations have opposite curvature, resulting in the bowl-shaped performance function. For both configurations, the rib spacing has very little impact on the centerbody weight or performance, which is why all three surfaces are nearly equivalent. These plots, however, show the significance of the airframe as a full system that cannot be completely decoupled, especially for structural connectivity of the HWB. The trends also show that sections in the aircraft may not follow the exact weight and performance trends of the entire airframe structure.

Next, results of the total wing (combined outboard and trapezoidal wing sections) are examined in Fig. 65. This is the first instance in Experiment 2A in which a negative performance value exists in which PRSEUS is actually adding weight to a portion of the structural configuration. Coincidentally, that design point is the optimal point for structural weight for the baseline configuration. In the benchmark approach, without optimizing the technology configuration separately, the wing performance would be implemented in conceptual design, potentially for the technology selection process, as $k_{ST,w} > 1$. The optimized point for PRSEUS, shown in the bottom left plot of Fig. 65, is actually $16,420$ lb less than the optimized design point for the baseline, or equivalently a 14.2% reduction of structural weight for the total wing. This observation leads to the next part of discussion regarding performance estimates considering the structural layout.

It has been recognized that the potential error given the benchmark approach

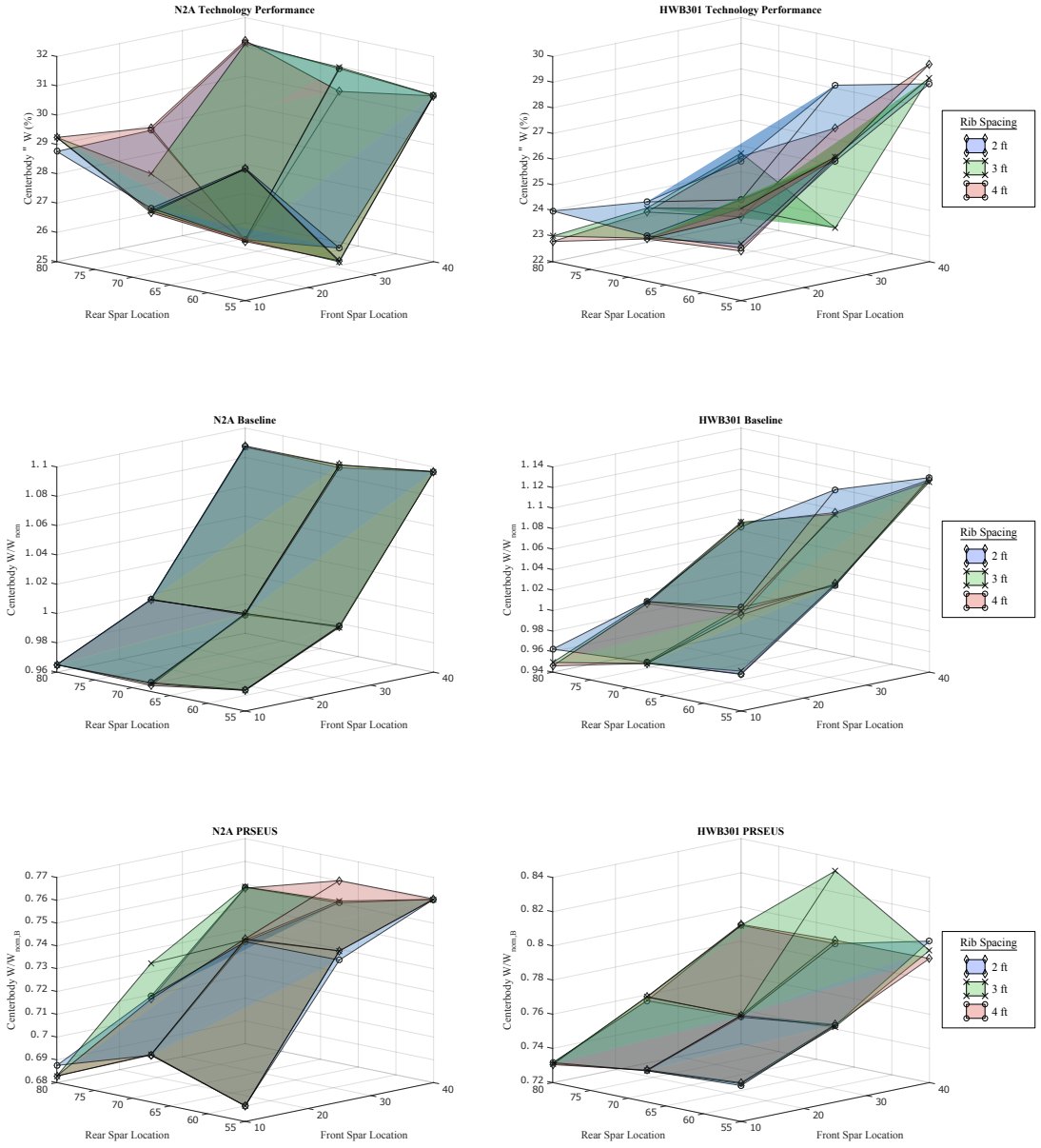

Figure 64: PRSEUS performance and structural weights for centerbody of N2A and HWB301 as a function of $\mathbf{X}_{SL}$

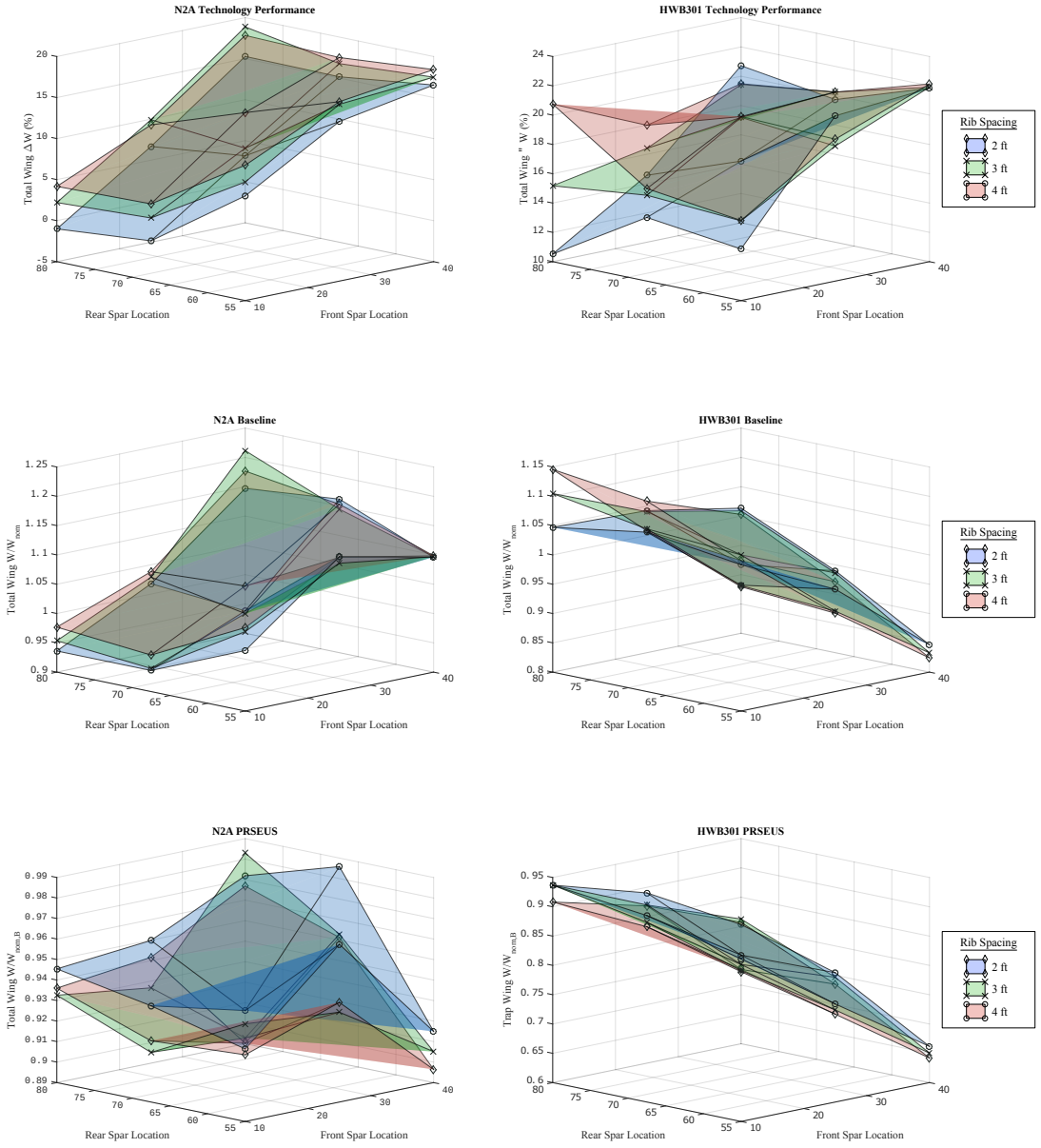

Figure 65: PRSEUS performance and structural weights for outboard wing of N2A and HWB301 as a function of $\mathbf{X}_{SL}$

Table 15: Ranges of ΔW_S ($\mathbf{X}_{SL} = \mathbf{X}_{SL,B} = \mathbf{X}_{SL,B} = [c_{FS}, c_{RS}, p_{rib}]$)

Section ΔW_S	Lower Bound	Upper Bound	Range
N2A:			
Total Aircraft	15,207 (13.1%)	28,489 (21.4%)	13,282 (8.3%)
Centerbody	13,502 (21.8%)	17,265 (26.4%)	3,763 (4.6%)
Total Wing	−434 (−1.0%)	10,527 (18.9%)	10,961 (19.9%)
Trapezpoidal Wing	−384 (−1.5%)	5,473 (16.2%)	5,858 (17.7%)
Outboard Wing	−688 (−4.0%)	7,401 (29.5%)	8,090 (33.5%)
HWB301:			
Total Aircraft	19,894 (14.8%)	29,111 (21.8%)	9,217 (7.0%)
Centerbody	9,720 (17.5%)	14,291 (24.0%)	4,571 (6.5%)
Total Wing	6,861 (10.5%)	14,810 (22.1%)	7,949 (11.6%)
Trapezpoidal Wing	2,556 (8.9%)	6,972 (21.9%)	4,416 (12.9%)
Outboard Wing	3,680 (9.5%)	11,723 (26.0%)	8,043 (16.5%)

of holding structural layout constant between structural configurations is significant, and therefore cannot be ignored or defaulted in the performance estimation process. Ranges of performance for each section of the N2A and HWB301 are shown in Table 15 to support Hypothesis 2.1. Moving to Hypothesis 2.2, which challenges the benchmark definition of performance that holds the structural layout constant between configurations, what is the appropriate approach to determine the design point for each structural concept, the baseline and technology, from which performance will be quantified? Hypothesis 2.2 is recalled here:

Hypothesis 2.2: If significant error exists between estimates in structural technology performance when 1) optimizing only the baseline structural layout and 2) optimizing both the baseline and technology structural layout separately, then the structural layout cannot be held constant at the optimized baseline, $\mathbf{x}^*_{SL}$, in the performance characterization process for each and every OML design point.

With only two test case outer mold lines considered in Experiment 2A, a limited number of data points can be observed. Important considerations in this analysis are:

1. How should the objective be defined for topology optimization?

2. Does full aircraft ΔW_S dictate whether both structural layout design spaces, $\mathbf{X}_{SL,B}$ and $\mathbf{X}_{SL,T}$, should be optimized, or should sectional performance predictions influence the decision?

3. What if, in a practical sense, multiple global minima exist, e.g. multiple configurations within $\sim 1\%$ of each other?

Results from a test case scenario in which the objective function for optimization was based on the total aircraft structural weight. This table lists performance and weights for each aircraft section as a result of each definition: **Benchmark** - structural layout optimization of the baseline configuration and holding it constant for the technology configuration $\left(\Delta W_S\left(\mathbf{x}^*_{SL,B}\right)\right)$, and **STEED** - separate structural layout optimization of the baseline and technology separately, $\left(\Delta W_S\left(\mathbf{x}^*_{SL,B}, \mathbf{x}^*_{SL,T}\right)\right)$. The exception to these definitions, designated with a $(^*)$, is for the Baseline configuration near the bottom. In this portion of the table, the "Benchmark" method defines a nominal design without topology optimization and compares it to an optimized structural layout for the baseline configuration in the "STEED" column. This segment was to compare uninformed to informed structural layout design, since the benchmark approach was somewhat ambiguous in the design of the structural model that was used. Additionally, the term "optimization" is used loosely here, because the most optimal point for each case is defined as the minimum weight solution that was sampled in the 3-level full factorial for this experiment. Therefore, this "optimization" process is representative of an extremely coarse grid search method.

Table 16: Comparison of N2A performance metrics for Benchmark and STEED approaches to structural layout optimization

Parameter	Benchmark	STEED	Δ (%)
PRSEUS Performance (%):			
ΔW_S	14.0	17.9	21.9
$\Delta W_{S,T,cb}$	39.9	41.7	4.4
$\Delta W_{S,T,w}$	6.8	25.0	72.7
$\Delta W_{S,T,tw}$	-0.4	4.8	109.0
$\Delta W_{S,T,ow}$	7.3	20.2	64.2
PRSEUS Weight (lb):			
$W_{S,T}$	99,679	99,472	-0.2
$W_{S,T,cb}$	46,634	45,902	-1.6
$W_{S,T,w}$	42,084	42,466	0.9
$W_{S,T,tw}$	25,798	25,853	0.2
$W_{S,T,ow}$	16,287	16,613	2.0
PRSEUS Optimized Design:			
c_{FS}	10.0	10.0	0.0
c_{RS}	67.5	55.0	-22.7
p_{rib}	3.0	4.0	25.0
Baseline(*) Weight (lb):			
$W_{S,B}$	119,890	115,892	-3.5
$W_{S,B,cb}$	62,032	60,825	-2.0
$W_{S,B,w}$	46,035	43,249	-6.4
$W_{S,B,tw}$	27,815	25,688	-8.3
$W_{S,B,ow}$	18,220	17,561	-3.8
Baseline(*) Optimized Design:			
c_{FS}	25.0	10.0	-150.0
c_{RS}	67.5	67.5	0.0
p_{rib}	3.0	3.0	0.0

It was shown that optimizing the baseline and technology configurations separately had a slight impact on changing the estimated performance. Total aircraft structural weight of the PRSEUS configuration for $\mathbf{x}^*_{SL,T}$ was only 0.2% less than the structural weight at the $\mathbf{x}^*_{SL,B}$, likely well within the uncertainty of the model predictions. However, the results were slightly more significant for the various aircraft sections, even switching from an estimated negative performance to positive for the trapezoidal wing. Changes in the optimal design point were on the order of 20% different for the rear spar location and rib spacing, but this may not be the case had a higher resolution grid search been used for optimization, or if a gradient-based approach had been used. For the design points sampled, three other objectives were investigated for separate optimization of the baseline and PRSEUS configurations: minimization of N2A outboard wing structural weight, minimization of HWB301 total structural weight, and minimization of HWB301 outboard wing structural weight. All of these objectives found no difference between the optimal benchmark design point and the optimal PRSEUS design point. The goal of this experiment, however, was simply to identify that weight optimization for the structural layout may be warranted so that efficient means could be determined for the computationally expensive weight estimation function. Even though the coarse approach in this experiment did not find significant advantages to separate optimization of configurations, the difference in structural weight functions $W_{S,B}\left(\mathbf{X}_{SL}\right)$ and $W_{S,B}\left(\mathbf{X}_{SL}\right)$ between the N2A and HWB301 is an indication that the effect should be further explored.

The lower "Baseline" portion of Table 16 shows additional support that a default structural layout design should not be used in the estimation of structural technology performance. The difference between weight of the most optimal design point and the weight of the default design point is significant and this is true for all considered studies mentioned in the previous paragraph. Table 16 shows these results.

Table 17: Comparison of HWB301 performance metrics for Benchmark and STEED approaches to structural layout optimization

Parameter	**Benchmark**	**STEED**	$\Delta\,(\%)$
HWB301 Baseline(*) Weight (lb) for $\min(W_S)$ & $\min(W_{S,ow})$:			
$W_{S,B}$	$133,388$	$128,055$	-4.2
$W_{S,B,cb}$	$54,434$	$59,505$	8.5
$W_{S,B,w}$	$62,290$	$51,342$	-21.3
$W_{S,B,tw}$	$28,389$	$32,043$	11.4
$W_{S,B,ow}$	$33,901$	$19,299$	-75.7
HWB301 Baseline(*) Optimized Design for $\min(W_S)$ & $\min(W_{S,ow})$:			
c_{FS}	25.0	40.0	37.5
c_{RS}	67.5	55.0	-22.7
p_{rib}	3.0	4.0	25.0
N2A Baseline(*) Weight (lb) for $\min(W_{S,ow})$:			
$W_{S,B}$	$119,890$	$128,997$	7.1
$W_{S,B,cb}$	$62,032$	$65,989$	6.0
$W_{S,B,w}$	$46,035$	$50,577$	9.0
$W_{S,B,tw}$	$27,815$	$33,846$	17.8
$W_{S,B,ow}$	$18,220$	$16,731$	-8.9
N2A Baseline(*) Optimized Design for $\min(W_{S,ow})$:			
c_{FS}	25.0	40.0	37.5
c_{RS}	67.5	55.0	-22.7
p_{rib}	3.0	4.0	25.0

5.3.2 Experiment 2B: Down-selection of $\mathbf{X}_{SL}$ Parameters

Function calls in the Georgia Tech - Weight Estimation Environment (GT-WESt) are computationally expensive, and additional design variables for performance characterization translate to an exponential increase in the number of sample points required. The exponential increase is the result of observed nonlinear trends between weight metrics and a subset of structural layout design variables shown for Experiment 2A. Because of this nonlinearity, either a full factorial design of three levels or a central composite design should be used as the foundation sampling plan for the design space. Therefore, it is suggested to attempt to down-select from the full structural layout design space to mitigate the computational burden.

A linear model was fit to data generated using the Taguchi orthogonal array mentioned in Sec. 5.1.2. Analysis of Variance (ANOVA [25]) was used to assess if the contribution of each design variable was statistically significant in the variation of structural weight. Probability values were calculated first using structural weight reduction performance of the total aircraft as the metric for each the N2A and HWB301. This metric formulation was desired because it is the direct trend that the research is searching to obtain, i.e. does each design parameter significantly contribute to variation in performance? However, structural technology performance can only be implemented in this ANOVA formulation using the benchmark definition which holds the structural layout constant between baseline and technology configurations. Results for the N2A and HWB301 are shown in Fig. 66.

Using the p-value criterion, a design parameter is considered statistically significant if $p \leq 0.05$. Therefore, the area in these figures above this value is shaded red for rejection. ANOVA testing was performed on all aircraft sections, and the bar graphs are color coordinated to match the section for each design parameter listed on the x-axis. For the N2A, each design variable has at least one section in which the p-value is outside the rejection zone. The manner in which each parameter influences

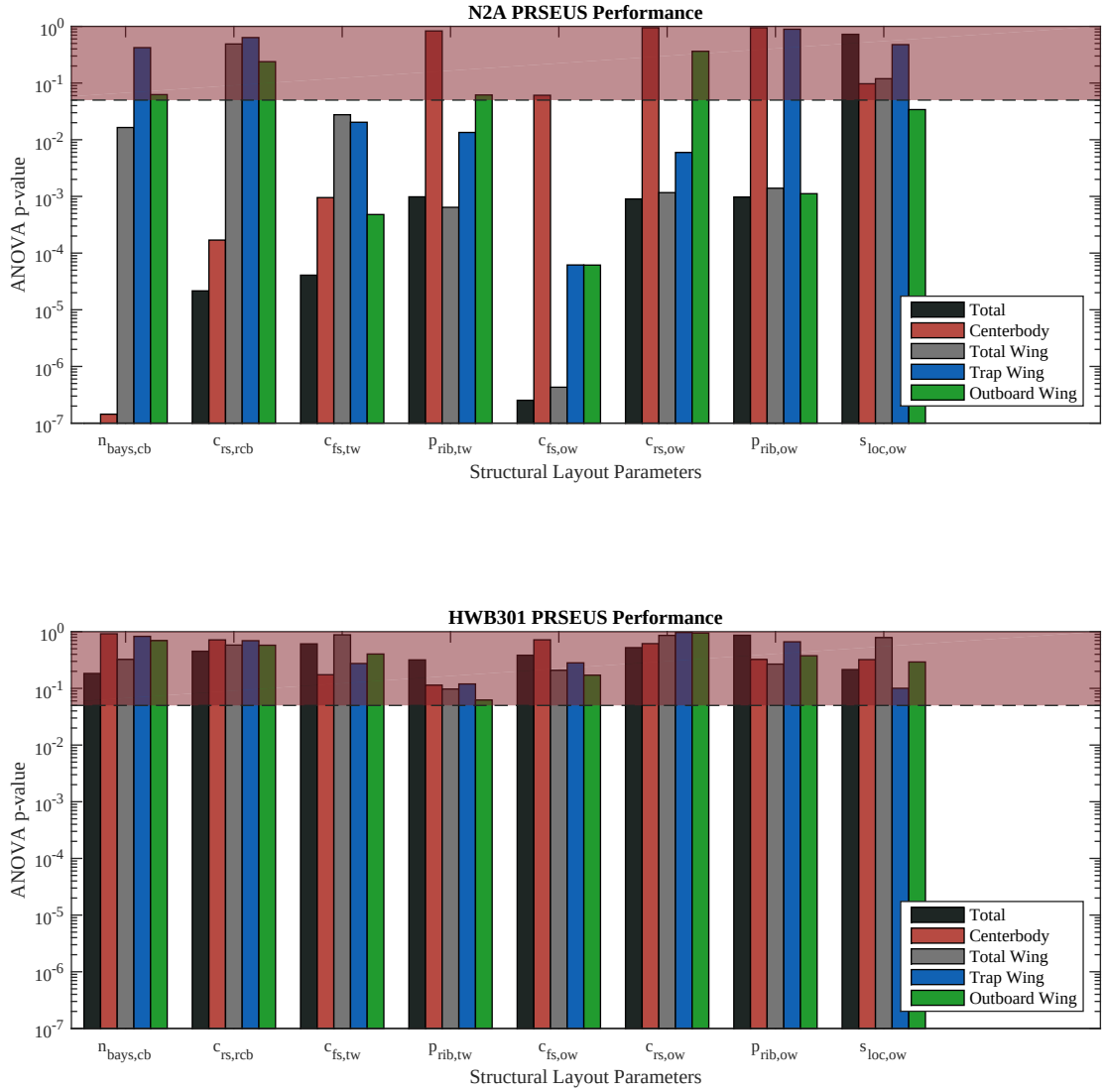

Figure 66: ANOVA for N2A (top) and HWB301 (bottom) $\mathbf{X}_{SL}$ variables using PRSEUS performance as variation metric

variability in the total aircraft is important because this metric is typically listed as the overall performance value in published results. Other important sections include the centerbody and total wing structural weight reduction performance because these parameters are used for implementation of the technology in conceptual design models. The only design parameter with a p-value over the threshold in all three sections is $s_{loc,ow}$, which defines the span value for the outboard wing root.

Results for the HWB301 are also shown in Fig. 66, which are significantly different than the data shown for the N2A. Using PRSEUS performance as the metric of variability shows that all structural layout design variables can be rejected for all sections These results are problematic because surface plots for the HWB301 shown in the previous section for a subset of structural layout design variables clearly indicates a sufficient variability to warrant inclusion. Design points selected in the Taguchi orthogonal array happened to coincide with points of little variation in structural technology performance, meaning that a larger number of cases should be considered. On the other hand, is performance necessarily the appropriate metric to be assessing impact of design parameters on variability, especially using the benchmark definition?

The benchmark definition was required at this stage in the STEED approach because structural layout optimization would have to be performed using GT-WESt for a large number of OML design points to obtain enough result data. A more appropriate implementation of ANOVA in this case is analyzing the components of the performance definition in Eqn. 4, $W_{S,B}\left(\mathbf{X}_{SL}\right)$ and $W_{S,T}\left(\mathbf{X}_{SL}\right)$. Topology optimization will be taking place using these metrics as the minimization objectives, and therefore, their variation is important for the formulation addressed by Hypothesis 2.2. These ANOVA results are shown for the N2A in Fig. 67.

The trends are relatively the same using structural weight for each configuration of the N2A compared to technology performance. Using all three metrics to set up the ANOVA criterion show a more complete picture of which design parameters are

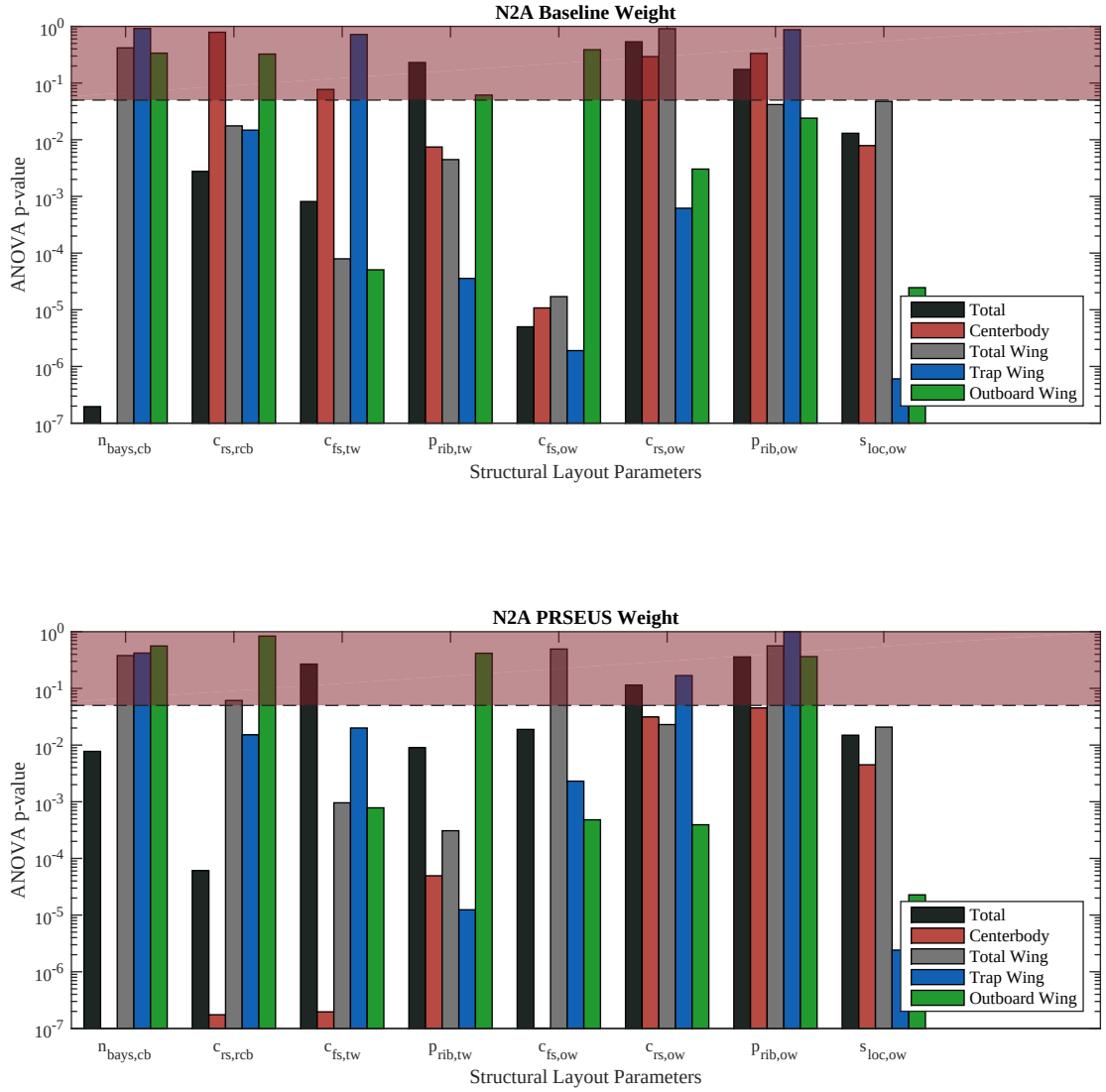

Figure 67: ANOVA for N2A $\mathbf{X}_{SL,B}$ and $\mathbf{X}_{SL,T}$ variables using $W_{S,B}$ and $W_{S,T}$ as variation metrics, respectively

important to the baseline and technology configurations. In some instances, like the outboard wing rear spar location and rib spacing, the relative importance to variation of weights does not match up with the relative importance to variation in weight reduction. Given these trends, if computational resources were not a factor, all design parameters would be recommended for inclusion in performance characterizations at the OML level. If a subset was necessary, the number of centerbody bays and front spar locations for both the outboard and trapezoidal wings would be recommended to carry through to the next level. For the HWB301, results using baseline and technology structural weights are shown in Fig. 68. The same recommendations would be made for parameter treatment, with the addition of rear spar location of the outboard wing being included in the structural layout design space considered at the next level.

5.3.3 Summary

One of the benefits of using the STEED approach for characterization of structural technology performance is that no step stand alone. It is a process which builds a knowledge base, and in each step the breadth of knowledge grows. Suggestions have been made in terms of hypotheses at the structural layout level for indications of movement within the tollgate framework of STEED. More importantly, the information at the technology level can be combined with the structural layout level for substantiation in moving to the $\mathbf{X}_{OML}$ design space level.

Assessing the results from Experiments 2A and 2B independent of the results from the technology level do not provide much support that the OML has a significant impact on structural technology performance. There are slight indications of potential significance, including the different shapes of structural weight functions between the N2A and HWB301, as well as the ranges of variation of performance as a function of structural layout design space for a given OML design point. Alone, there could be

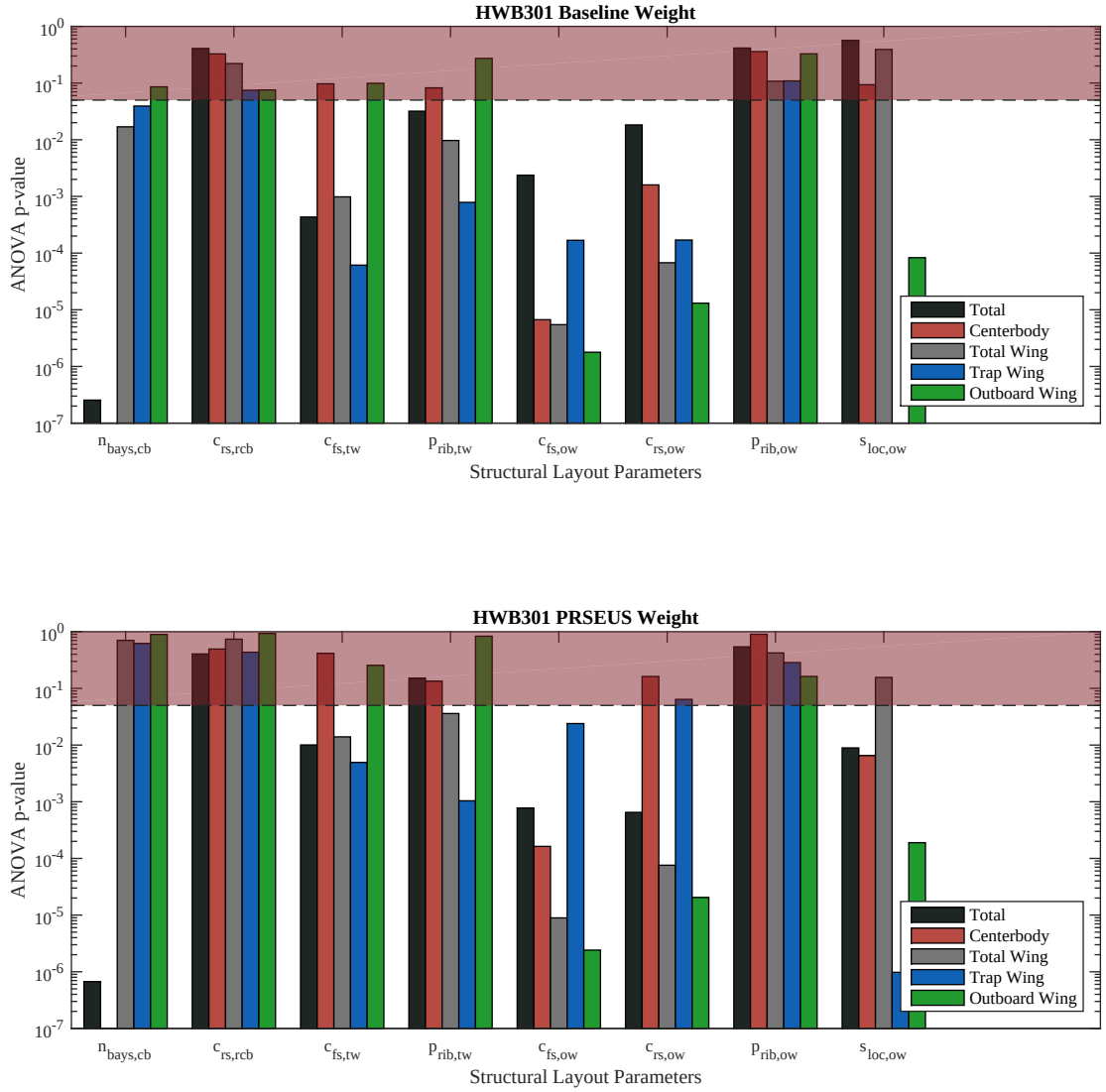

Figure 68: ANOVA for HWB301 $\mathbf{X}_{SL,B}$ and $\mathbf{X}_{SL,T}$ variables using $W_{S,B}$ and $W_{S,T}$ as variation metrics, respectively

some call to question whether or not the effort of a full-scale structural technology performance characterization is worth the effort it would take at the $\mathbf{X}_{OML}$ design space level. When considered with the significantly large spread of performance distributions as a function of the technology design space, there is a wealth of evidence that characterization is warranted at the next level.

Hypothesis 2.1 was supported by the results and variation in the structural weight function for $\mathbf{X}_{SL}$ parameters showed that a default setting $\mathbf{x}^*_{SL}$ is not representative of performance across the entire structural layout design space. However, what is the probability that the optimized layout for the baseline is equivalent to the optimized layout for the technology, i.e. $\mathbf{x}^*_{SL,B} = \mathbf{x}^*_{SL,T}$? This was the case for three out of the four investigated optimization objectives under the assumptions of Experiment 2A. With a limited number of design data points, however, further assessment is required to either support or refute Hypothesis 2.2. If there was no evidence that supported advancement to Step 5 in the STEED approach, then it could safely be assumed that the benchmark performance definition in which the structural layout remains constant for both the baseline and technology configurations would be sufficient in performance characterization, so long as the baseline configuration was optimized. However, evidence supported advancing through the Step 4 tollgate as a result of the data presented in the previous paragraph, and therefore, further assessment can be performed on structural layout optimization at the $\mathbf{X}_{OML}$ design space level.

5.4 Outer Mold Line Level Results

5.4.1 Experiment 3A: Aggregate Trends

The first experiment in Set 3 follows the global trend of the STEED approach: effort expended for performance characterization should increase only if indicated by supporting evidence. The approach described in Sec. 5.1.3 created a design and performance assessment environment that had a substantially decreased execution time

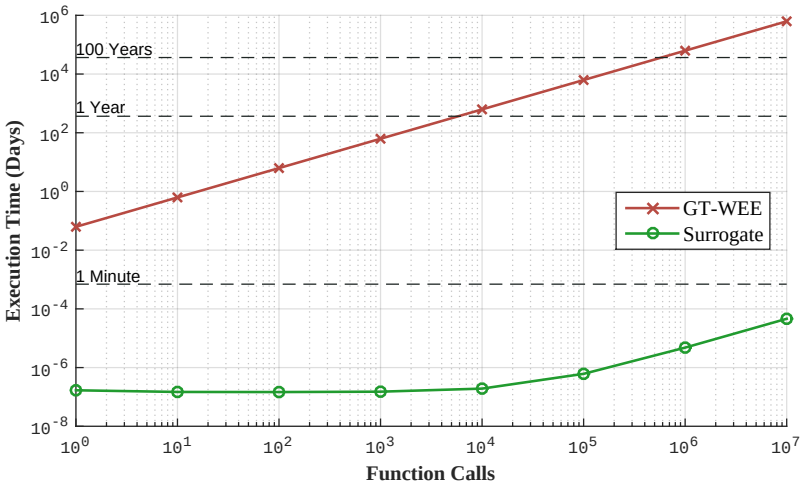

Figure 69: Comparative execution times of W_S surrogate models and GT-WESt

compared to GT-WESt. Figure 69 shows a comparison of total run time for a single function call to 100,000,000 function calls. With this enabling capability, a large number of trends could be investigated, and attributes could be assessed for the entire design space with a Monte Carlo simulation. This probabilistic assessment could be executed with minimal effort, and the aggregate design space results are shown in this section.

The first assessment was regarding treatment of structural layout optimization – a follow-on from the previous section. For demonstration purposes, the design variables that were investigated in Experiment Set 3 were a subset of the total in $[\mathbf{X}_{OML}, \mathbf{X}_{SL}]$. Only outboard wing design variables from each level were considered, for a total number of 7 design parameters. The neural network surrogate models of baseline structural weight and technology structural weight enabled structural optimization studies of a large number of design points. For each Monte Carlo case, three different variations treatment for structural layout design parameters, $[c_{FS,ow}, c_{RS,ow}, p_{rib,ow}]$ were considered:

Uninformed Structural layout parameters were left to vary randomly in their design

space, and performance was calculated as:

$$\Delta W_S = W_{S,B}\left(\mathbf{x}_{OML}, \mathbf{x}_{SL}\right) - W_{S,T}\left(\mathbf{x}_{OML}, \mathbf{x}_{SL}\right) \tag{52}$$

Benchmark Optimization was performed on structural layout design parameters for a specific objective for the baseline configuration and performance was estimated as:

$$\Delta W_S = W_{S,B}\left(\mathbf{x}_{OML}, \mathbf{x}^*_{SL,B}\right) - W_{S,T}\left(\mathbf{x}_{OML}, \mathbf{x}^*_{SL,B}\right) \tag{53}$$

STEED Both the baseline and technology configuration structural layouts were optimized and performance was estimated as:

$$\Delta W_S = W_{S,B}\left(\mathbf{x}_{OML}, \mathbf{x}^*_{SL,B}\right) - W_{S,T}\left(\mathbf{x}_{OML}, \mathbf{x}^*_{SL,T}\right) \tag{54}$$

Two objectives for optimization were considered for the Benchmark and STEED approaches: total aircraft structural weight minimization and outboard wing structural weight minimization. Because early implementations of this design space had shown sever nonlinearity of the structural weight function with multiple local, a particle swarm optimization technique was used to determine minimum weight. This approach, however, was actually more computationally expensive than a random search optimization method, and the latter yielded more consistent results for minimum weight. Therefore, each $\mathbf{x}_{OML}$ design point sampled in the Monte Carlo simulation also performed a random search optimization of 100,000 structural layout design points. The entire process was completed in less than 20 seconds on one machine.

The goal of this first assessment was to determine if a substantial difference in performance was witnessed between each of the approaches of increasing investigative effort. While the most appropriate definition, following the literature for topology optimization, is generated with the STEED approach that optimizes both baseline and technology configurations, the most simplistic was the uninformed approach, where any default structural layout can be implemented for all OML design points

and no extra cases need to be executed. Using the surrogate modeling approach of Experiment Set 3, there is actually little difference between implementation of the Benchmark approach and the STEED approach due to the execution times shown in Fig. 69.

Figure 70 shows three histograms of PRSEUS performance for total structural weight of the N2A as an aggregate of the OML design space. Each histogram is shown with some transparency so the full extent of each distribution can be seen. The trends assessed in Experiment 2A that supported Hypothesis 2.1 are further supported here. It is shown that simply by shifting from uninformed treatment of the structural layout to optimizing the baseline configuration, the tails of the distribution are cut off and the variation in performance also shrinks. The conclusion, then, is that structural layout optimization for the baseline is a manner in which risk can be reduced for structural technology performance estimates. Furthermore, comparing the yellow distribution to the blue distribution, aggregate technology performance using Benchmark and STEED definitions result in relatively the same distribution shape and spread. However, the shift to the right of the STEED (yellow) distribution shows that using the performance definition in Eqn.53 suppresses an enabling characteristic of the technology. This yellow distribution is shifted in the positive direction of better performance, increasing the bottom line by approximately 5% weight reduction. Moreover, a process is now in place to quantify this phenomenon and show the reduction in risk by considering structural layout optimization in performance characterization. Figure 71 shows the same formulation in terms of the structural weights that comprise each performance equation.

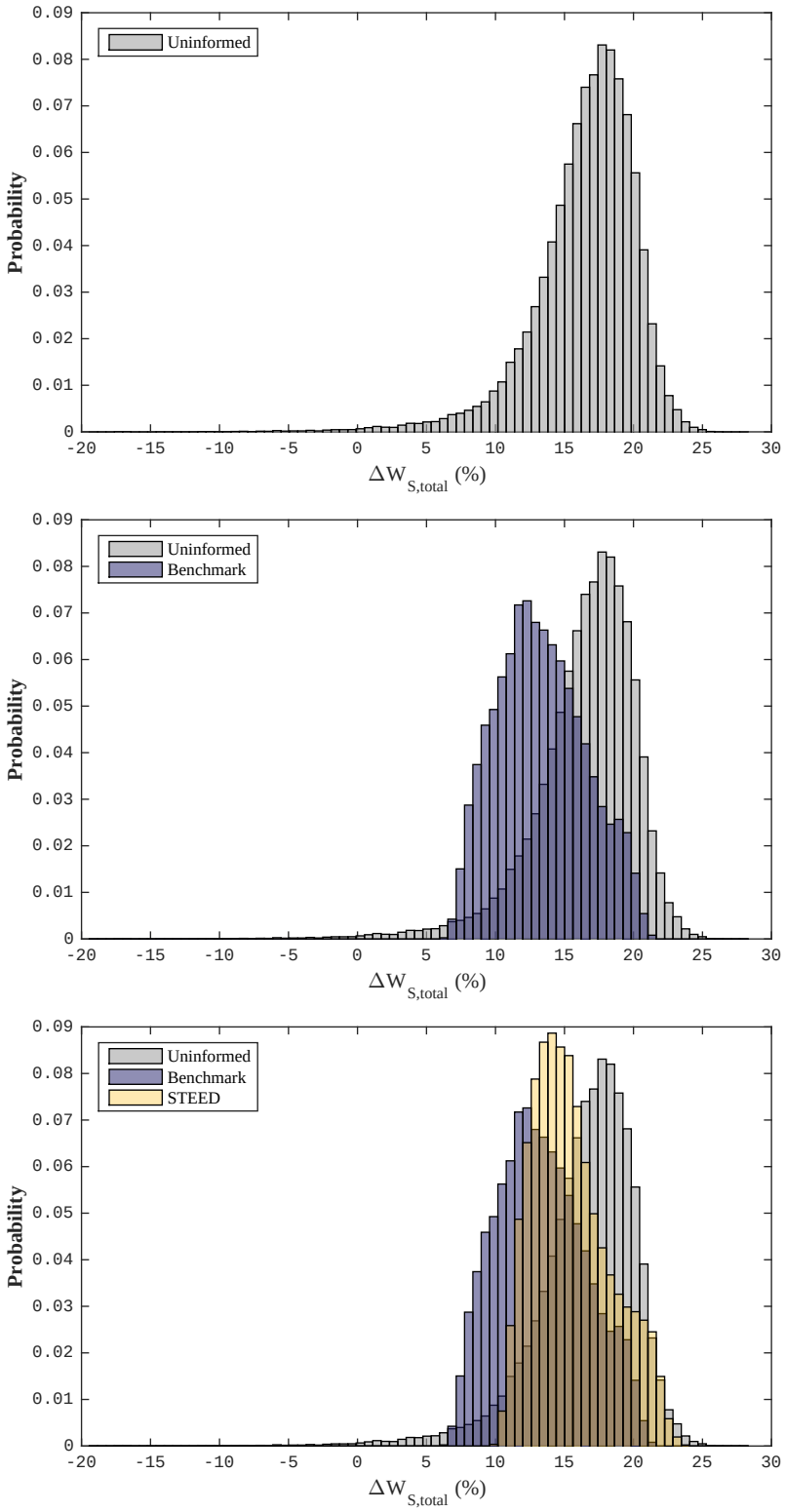

Figure 70: PRSEUS performance aggregate for the Uninformed (grey), Benchmark (blue), and STEED (yellow) approaches

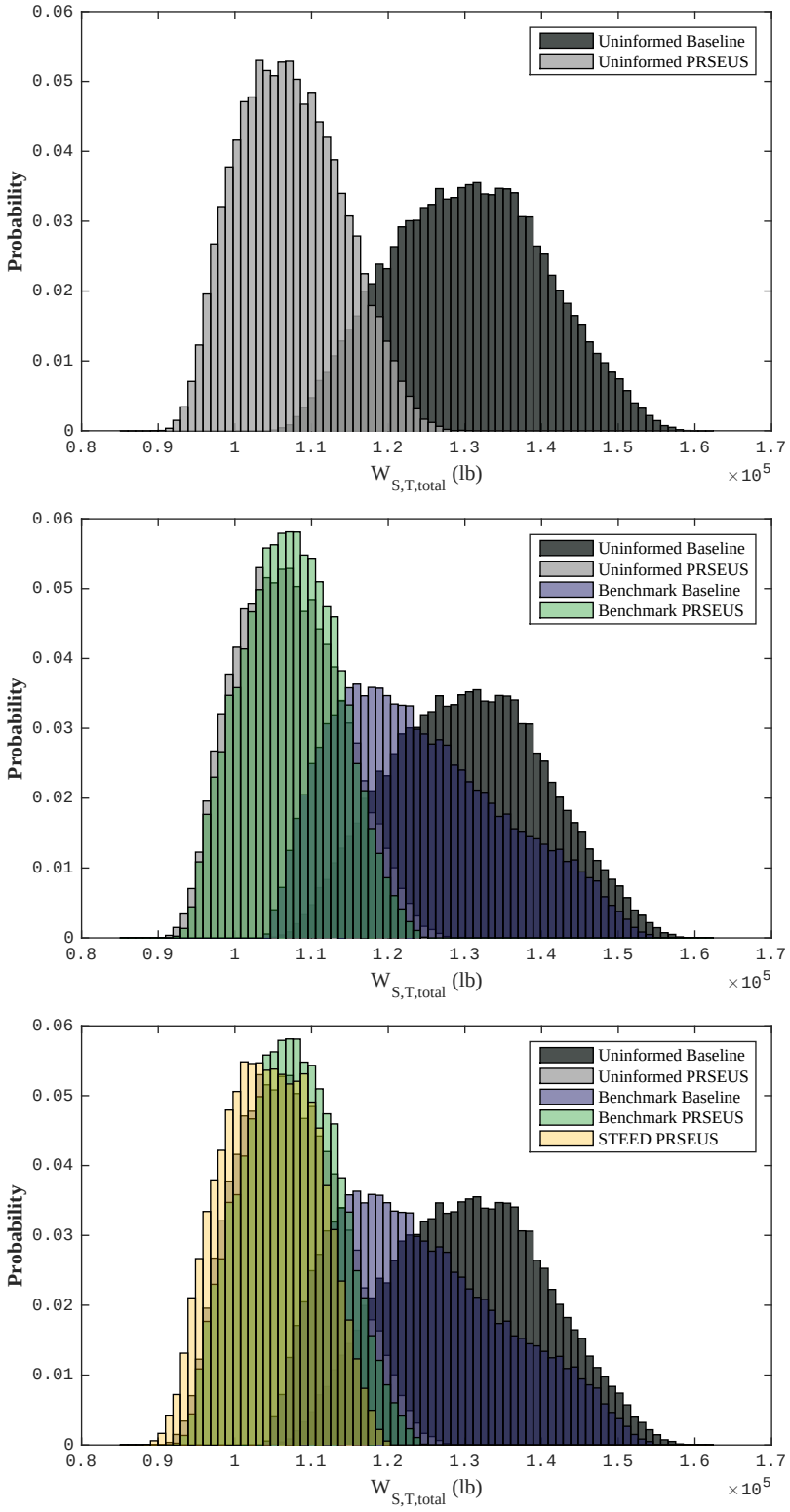

Figure 71: Baseline and PRSEUS structural weights before and after each structural layout optimization approach

With aggregate performance results for the $\mathbf{X}_{OML}$ design space obtained, Hypothesis 3 is revisited:

Hypothesis 3: If a characteristic is observed which is indicative of substantial information gained over the benchmark performance estimation process, then the characterization of aircraft level structural technology performance as a function of the outer mold line design space, $\Delta W_S(\mathbf{X}_{OML})$, should be implemented in suitable applications.

One characteristic shown in results thus far is the potential range of structural technology performance as a function of the design space. For reduction of total aircraft structural weight estimated with the STEED approach, values ranged from approximately 10% to 24%. Compared to a scalar value, this is a significant improvement in the ability to quantify technology performance.

Histograms of aggregate performance presented in the previous figures showed the theoretical performance values had each point in the conceptual design space been optimized for structural layout. These values were also generated under the assumption that performance was actually quantified at each one of the OML design points that was generated in the Monte Carlo simulation, representative of the Benchmark treatment of structural layout optimization. The potential error throughout the design space relating to performance under these assumptions is shown in Fig. 72. In practical implementation, however, benchmark performance was generated for only one OML design point. The actual N2A OML geometry was used for this nominal design point, and a practical comparison of the potential error throughout the OML design space of using the benchmark approach rather than the STEED approach is shown in the bottom plot of Fig. 72. Error was calculated in terms of the more correct

STEED definition of performance as:

$$\epsilon_{\mathrm{U}}\left(\mathbf{X}_{OML}\right) = \Delta W_{S,\mathrm{STEED}}\left(\mathbf{X}_{OML}\right) - \Delta W_{S,\mathrm{Bench}}\left(\mathbf{x}^{*}_{OML}\right) \tag{55}$$

$$\epsilon_{\mathrm{B}}\left(\mathbf{X}_{OML}\right) = \Delta W_{S,\mathrm{STEED}}\left(\mathbf{X}_{OML}\right) - \Delta W_{S,\mathrm{Bench}}\left(\mathbf{X}_{OML}\right) \tag{56}$$

where $W_{S,B,Bench}$ is the structural weight of the baseline structural configuration using benchmark topology optimization. Both these error distributions provide further evidence that consequential risk is associated with neglecting the $\Delta W_S\left(\mathbf{X}_{OML}\right)$ relationship. The consequence is an over-predicted performance value for implementation of the technology in conceptual design, where: 1) the structural technology can be selected under pretenses of false performance estimates for a particular OML design point or 2) a HWB can be designed with the technology in mind and costly later phase redesigns are required because weight targets cannot be met.

One other aggregate performance trend of interest is the relationship between performance and structural weight itself. Is implementation of the technology enabling more weight efficient configurations or does technology performance not have an impact on the lightest weight solutions within the conceptual design space. Results for these trends were generated under a significant assumption of the conceptual design space, i.e. $\mathbf{X}_{OML}$, which presents a potential area of future research. The $\mathbf{X}_{OML}$ design space under consideration in this experiment was not directly defined by a conceptual design tool, or in other words, the upper and lower bounds were not defined with conceptual design feasibility having been confirmed – they were, however, set with the mission analysis and trends in literature in mind. Therefore, some structural weights represent configurations that may not meet mission requirements, and the objective of this analysis is simply to understand the trend rather than the actual values themselves. In the next chapter, feasibility will be assessed for the $\mathbf{X}_{OML}$ design parameters.

Figures 73 and 74 show the performance trends as a function of structural weight

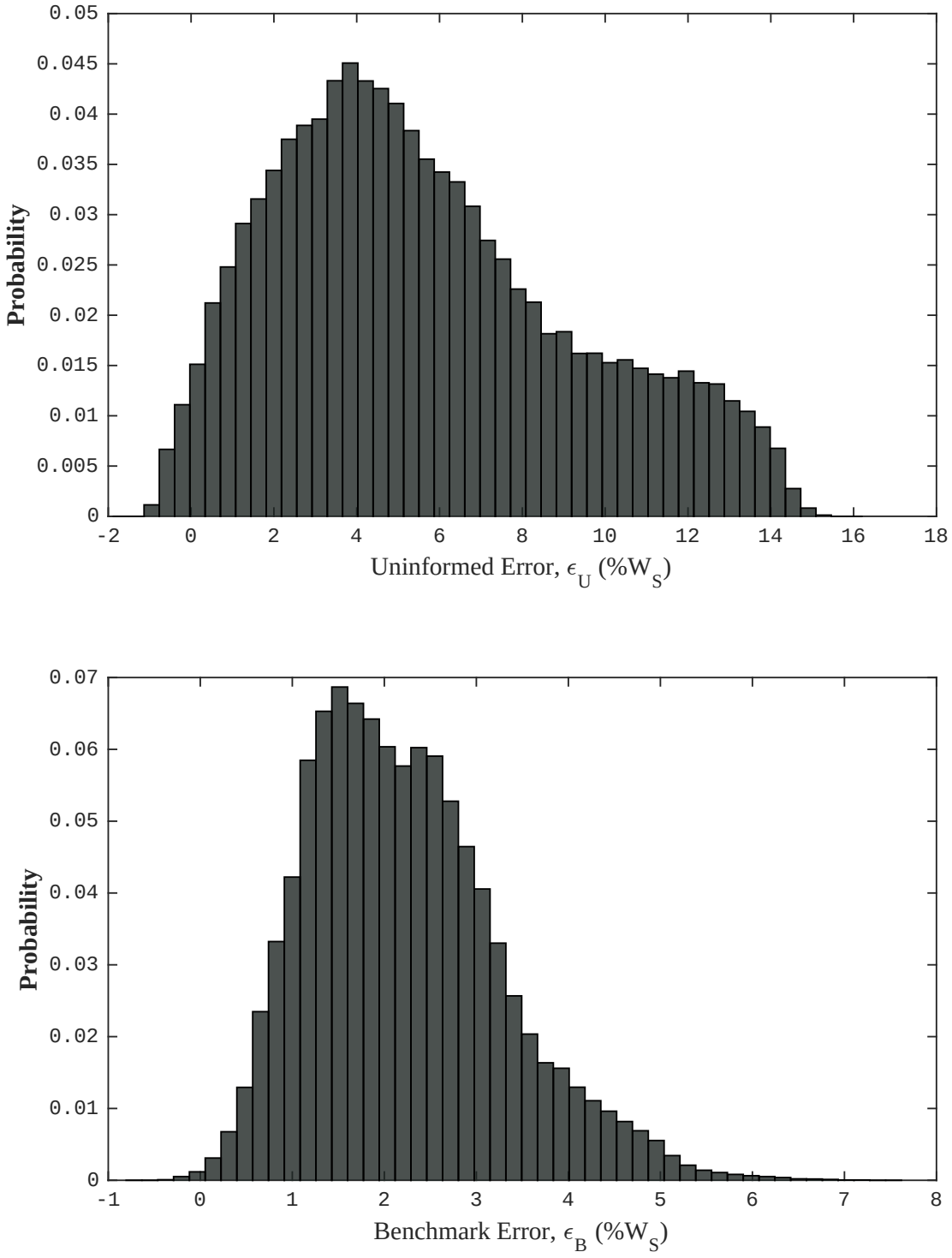

Figure 72: Error in PRSEUS performance estimates as a result of neglecting the $\Delta W_S\left(\mathbf{X}_{OML}\right)$ relationship

for the total aircraft, wing, and centerbody, respectively. The structural weight shown in these figures is for the PRSEUS configuration, and the three sections are representative of how performance is published (total structural weight reduction) and how it is implemented in conceptual design (wing and centerbody weight reduction estimates). Considering that weight is a demonstrable function of the conceptual design parameters as well, performance trends are shown as cloud-like shapes, and each point is representative of a different $\mathbf{x}_{OML}$.

The grey squares show the benchmark definition of performance with the structural layout being able to vary to any point within the $\mathbf{X}_{SL}$ design space. A high density bulk of these points is shown at a fairly constant range among all total structural weights in Fig. 73, and there are values of negative performance toward the higher end of structural weight. This trend is expected because negative performance is adding weight to the configuration. With performance defined by the benchmark approach but structural layout optimization takes place for the baseline configuration (shown as red $\times$'s), the cloud of performance points tightens between approximately $10 - 15\%$ structural weight reduced. For larger total structural weights, there is a slight upward shift in performance. This indirect relationship is witnessed with the STEED definition of performance too (blue $\circ$'s), which shows that the most weight inefficient OML design points are the ones that benefit most from a more effective structural technology performance. There is also a shift left to smaller total structural weights through each progressive step of structural layout optimization, which is also to be expected.

In assessing these trends, Hypothesis 3.1 is revisited,

Hypothesis 3.1: The design region of $\mathbf{X}_{OML}$ that corresponds to the best structural technology performance will not coincide with the most optimal aircraft design in terms of W_S.

The indirect relationship witnessed for weight reduction performance of the total aircraft structure, $\Delta W_{S,total}$, and total structural weight, $W_{S,T,total}$, confirms this hypothesis for a full implementation of the structural technology. It is vital to state that confirmation of the hypothesis exists only for the PRSEUS technology. For a generalized form, Hypothesis 3.1 would need to be tested with multiple structural technologies before it could be supported or refuted.

These same trends are seen in Fig. 74 for wing (left) and centerbody (right) structural weight, and there is a slight discrete shift in pattern for the wing that occurs above $W_{S,T,wing} = 50,000$ lb. PRSEUS performance makes a slight jump from a max 10% weight reduction to approximately 20% for the benchmark structural layout optimization approach, and this trend occurs at nearly $47,000$ lb for the STEED approach to an even larger 30% weight reduction. This is consistent with the change in inflection of the yellow and blue histograms shown in Fig. 70, but it is now known that this is a trend not only for performance but it is a trend for structural weight as well. An interesting observation, however, is the negative performance that exists for the most minimum weight $\mathbf{x}_{OML}$ design points. This is an indication that these design points are likely the smallest wing areas with optimized structural layouts that contain front spars furthest aft and rear spars furthest forward.

Centerbody trends are also shown on the right side in Fig. 74, which is the aircraft section affected least by variation in outboard wing design parameters. As a result, performance values shown on the y-axis have the smallest range, and there is also comparatively little variation in the actual centerbody weight on the x-axis as well. The grey points show a significant direct trend between performance and weight, which is smoothed to a more constant value with each layer of structural layout optimization. There is also a significant spread of points for STEED treatment at larger centerbody structural weights. Also observed is the generally increased weight between Benchmark structural layout optimization and STEED optimization,

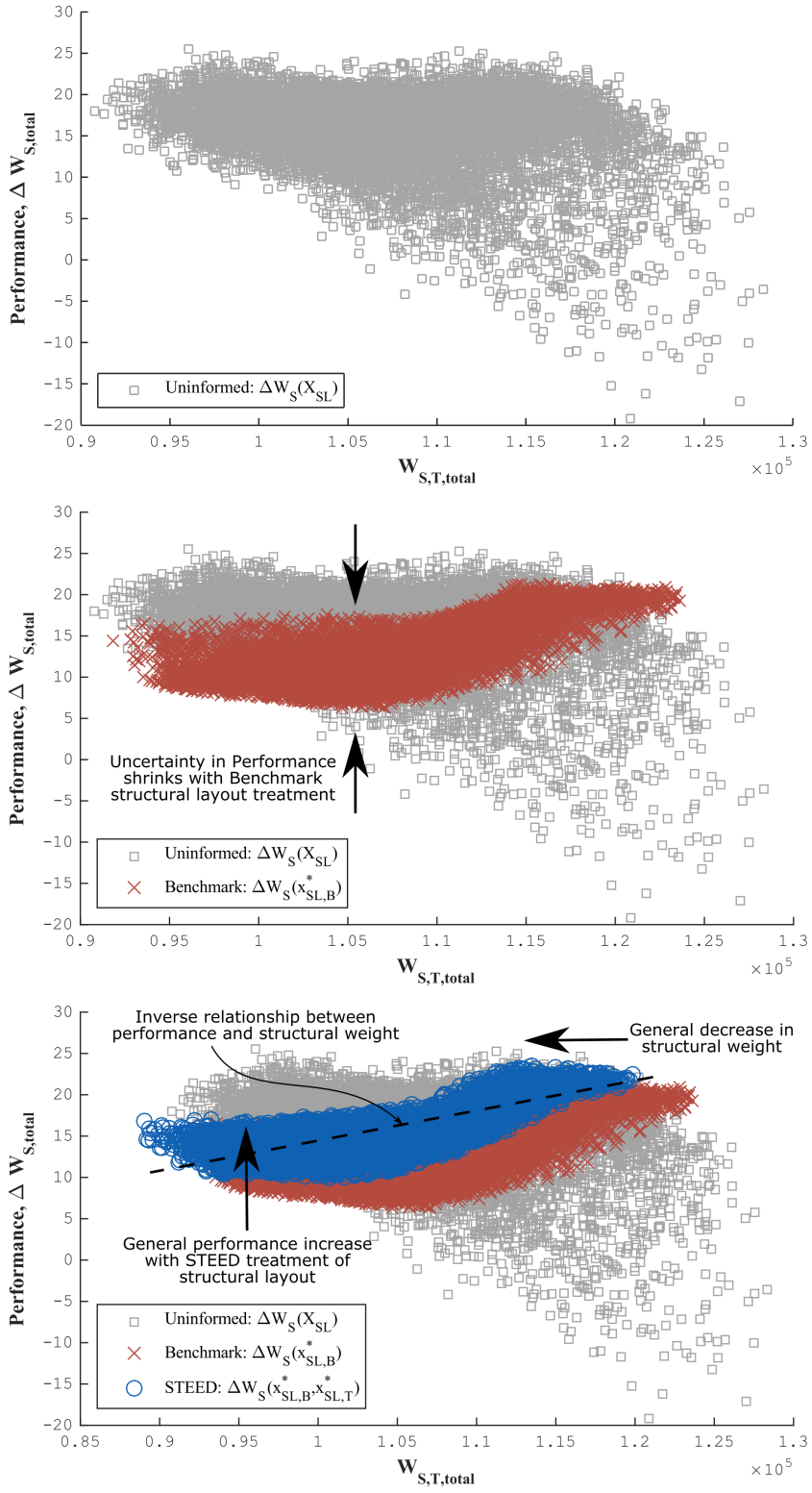

Figure 73: Technology performance as a function of structural weight for the total aircraft

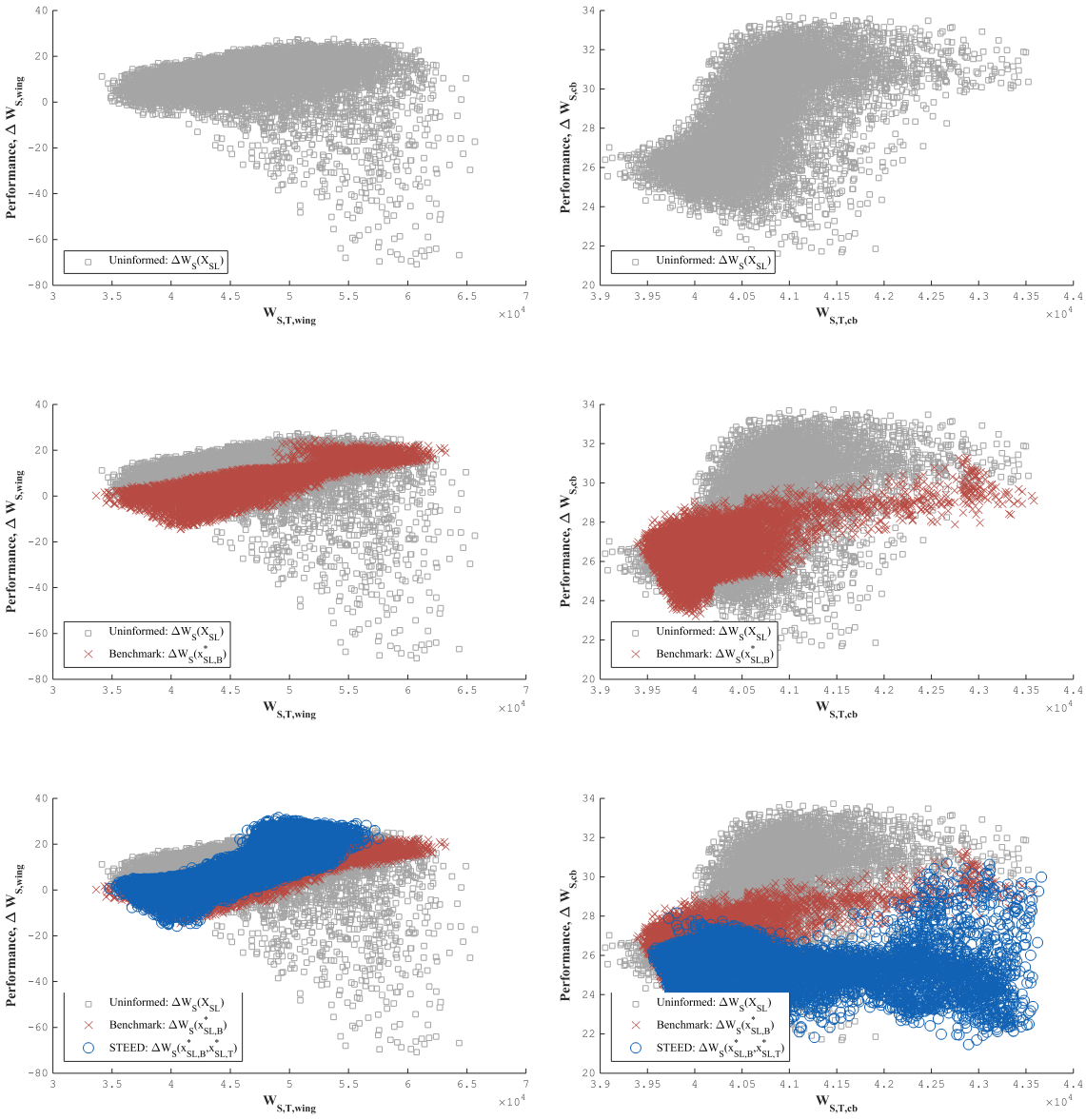

Figure 74: Technology performance as a function of structural weight for wing and centerbody sections

adding another potential explanation of the change in inflection for the performance histograms.

5.4.2 Experiment 3B: $\mathbf{X}_{OML}$ Design Space Trades

The same approach was taken at the OML level as the technology level – assessing aggregate trends first before exploring the design space in greater detail. Three data sets were used to create interactive sensitivity plots like those featured at the technology level. These sets were described in Experiment 3A as an *Uninformed*, *Benchmark* with baseline structural layout optimization and a constant structural layout design between baseline and technology configurations, and *STEED* which includes separate structural layout optimization of both configurations. Figure 75 shows a snapshot of sensitivities for the entire design space, including the three structural layout design variables for both the baseline structure configuration (top) and the PRSEUS structure configuration (bottom).

At the OML design point settings shown in this figure, indicated by the triangular sliders on each x-axis, there are competing trends in structural weights of various aircraft sections for front spar and rear spar locations, while rib spacing has a relatively low impact on structural weight of any section. The PRSEUS configuration shows the same trend, with the difference being in influence of the total wing weight. Structural weight of the baseline total wing matches the sensitivity trend for the trapezoidal wing while the total wing weight for the PRSEUS configuration matches the trend of the outboard wing. Trapezoidal wing weight is overall heavier for the baseline, showing that blade stiffened composites are less efficient for this type of structural layout, i.e. a multi-spar lattice-like structural configuration.

Another observation for both baseline and PRSEUS structure is the effect of sweep on structural weight for all sections. The N2A mission analysis defines a cruise Mach number of 0.84, and therefore wave drag may be an issue if the outboard wing were

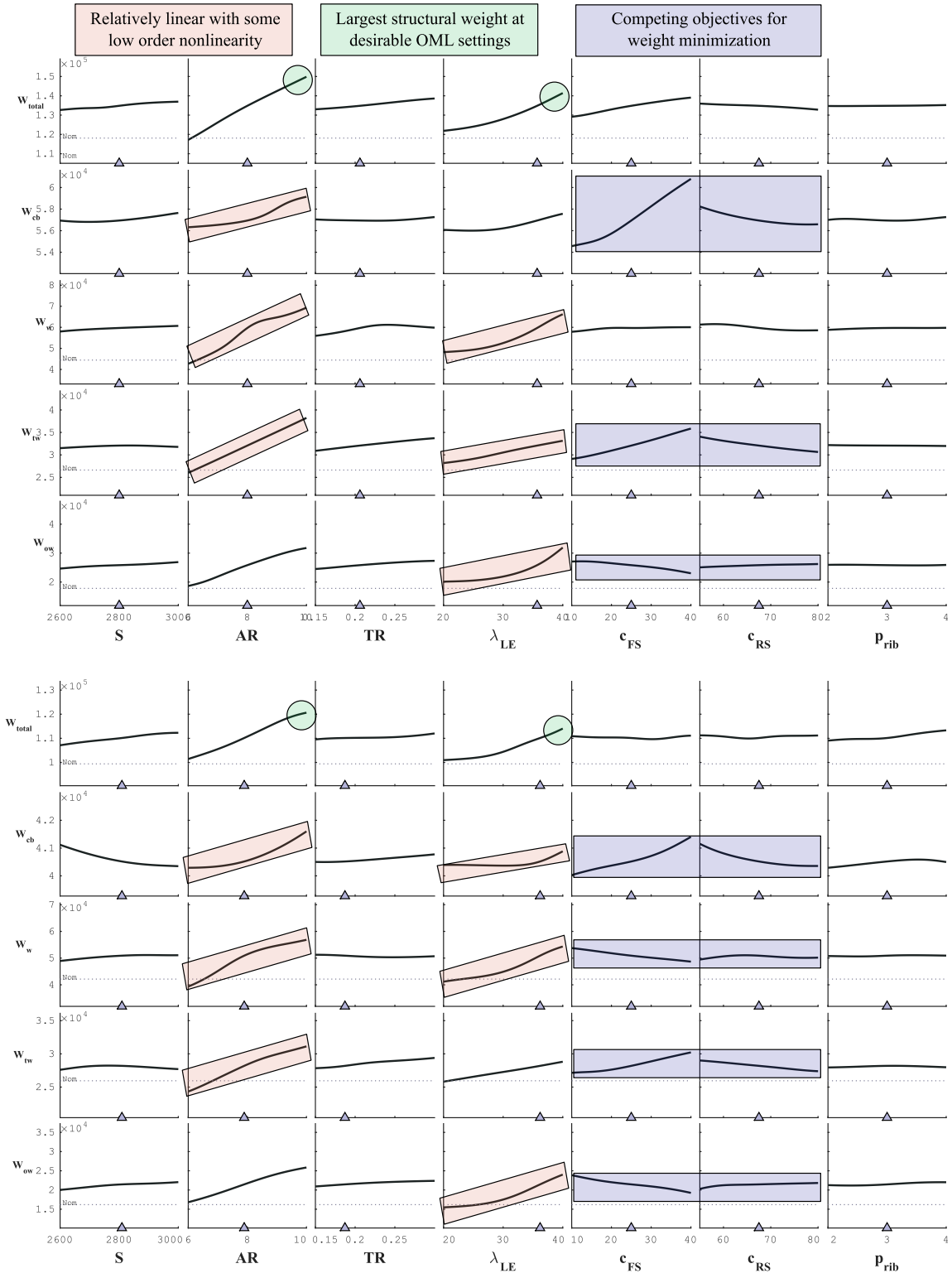

Figure 75: OML design space for Baseline (top) and PRSEUS (bottom) structural weights

to pass outside the shock cone. Higher angles of sweep, typically defined at quarter chord for aerodynamics, are generally preferred for transonic cruise conditions, and this presents an issue for structural weight. From the two plots shown in Fig. 75, it seems that the PRSEUS configuration increases at a smaller rate in terms of leading edge sweep, which was the structural definition of sweep for GT-WESt.

How do these trends translate to structural layout optimization? Figure 76 shows the resulting sensitivities for each of the OML design parameters in terms of both treatments of structural layout optimization. The benchmark treatment is shown in red and the STEED treatment shown in green for the PRSEUS configuration (bottom) while the baseline configuration (top) is unaffected by the STEED treatment and therefore is only shown in red. Additionally, optimization for these test cases was performed using total structural weight as a metric.

For the baseline configuration, the design region with the highest sensitivity nonlinearity was for high aspect ratio and large sweep angles. A these design parameter settings, it can be seen that for both large and small wing areas, the structural layout optimizes to a much heavier configuration. When checking the accuracy of the surrogates for these settings, the effect was shown to be purely physical as surrogate model accuracy was unaffected near the wing area bounds. This trend confirms the root cause of the inflection points in performance histograms toward positive performance, because a tradeoff exists between outboard wing structural weight and trapezoidal wing and centerbody structural weight for structural layout design parameters. The PRSEUS configuration, shown in the bottom of Fig. 76, suffers from this same tradeoff as well. Using the STEED approach for structural layout optimization shows a more limited design region in which minimization of trapezoidal wing and centerbody weight is favored over outboard wing weight. Baseline and PRSEUS weight sensitivities translate to performance sensitivities shown in Fig. 77.

Overall, total aircraft PRSEUS performance remains relatively stable as a function

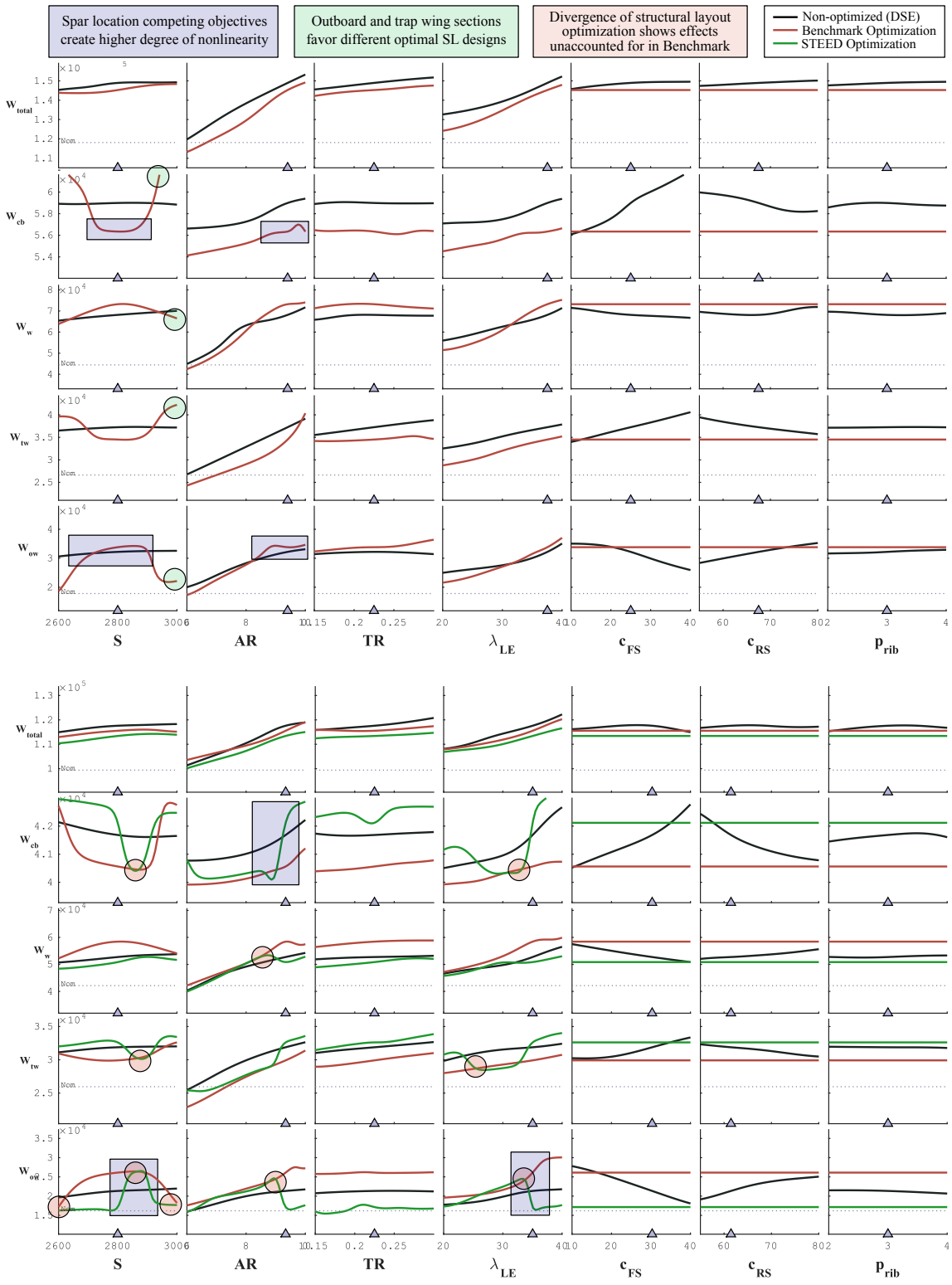

Figure 76: Comparison of weight sensitivities with Benchmark SL optimization (red) for Baseline (top) and STEED SL optimization (green) for PRSEUS (bottom)

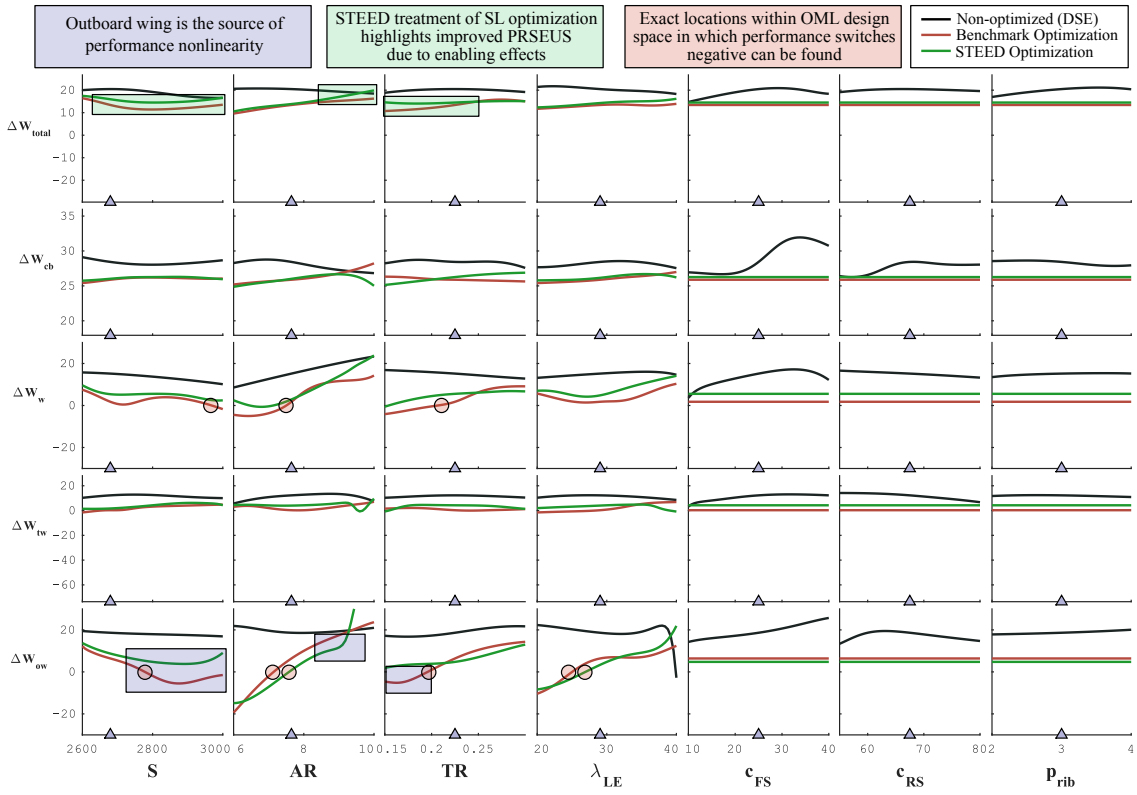

Figure 77: PRSEUS sensitivities for performance as a function of different SL optimization approaches

of the OML design space. Nonlinear effects are witnessed for most aircraft sections as a function of wing area S, aspect ratio AR, and leading edge sweep Λ_{LE}. These nonlinearities are most prevalent in the outboard wing section. Important observations relating to Hypothesis 3, however, are made for instances which indicate superior performance of the STEED approach compared to the benchmark. In this case, "performance" of the approach relates to better information obtained in the structural technology performance characterization or knowledge and trends that can be quantified with this process that were previously unavailable to the technology team. For instance, design points in which performance crosses the $\Delta W_S = 0$ threshold, large separations between the green and red performance sensitivity lines, etc. are significant indications that better information is being provided to the technology development team. The performance functions themselves are a significant contribution in the characterization of structural technology performance.

5.4.3 Summary

Step 5 of the STEED approach represents an important capability in structural technology performance estimation. With this approach and the parametric structural modeling environment of GT-WESt, the ability to quantify a functional relationship between the outer mold line and structural technology performance now exists. Its existence is not the only contribution, this highest level of Overarching Performance Hypothesis helps confirm the lower level hypotheses as well. Indicating factors that were mentioned at the $\mathbf{X}_T$ and $\mathbf{X}_{SL}$ design space levels were proven to support the existence of a significant relationship between HWB aircraft OML and PRSEUS structural weight reduction. It is noted that these hypotheses are confirmed only for the PRSEUS technology, but the success of the method up to Step 5 supports that the hypotheses made at each step are an appropriate systematic manner to characterize generalized structural technology performance.

With this approach, aggregate design space trends for both weight and performance indicate that scalar treatment of technology performance presents a potential risk for technology applications and in the development of the technology itself. It was also shown that allowing the structural layout of the technology configuration can have significant impacts on performance in the design space, showing upwards of $5-10\%$ improvement in performance by enabling more efficient structural layouts for a given OML design point. This information was previously non-existent with the benchmark approach. Additionally, the design space exploration environments that were created for assessing sensitivities in structural weights and technology performance provide an important connection with conceptual design and the lower level design spaces to ensure traceability in performance estimates. Using this capability, a source of significant performance influence and baseline configuration design influence was identified – the tradeoff between sectional weights for structural layout design parameters. The following chapters examine applications of technology performance estimation presented in this chapter, which represent the final steps of the STEED approach.

CHAPTER VI

CONCEPTUAL DESIGN IMPLEMENTATION

If a structural technology has made it through Steps 3-5 of the tollgate approach of STEED, then a functional relationship has been quantified for structural technology weight reduction performance in terms of conceptual design variables, i.e. $\Delta W_S(\mathbf{X}_{OML})$. Step 6 of the STEED approach represents the implementation of that relationship in the conceptual design process, particularly for technology selection and technology-enabled design space exploration. Quantifying conceptual design metrics in terms of structural technology performance either supports or refutes the efforts expended in the process of performance characterization up to this point. If observations can be made that support substantial information gained with this approach compared to the benchmark, then value is witnessed in STEED implementation. This chapter discusses the process by which observations were made to test Hypothesis 4 of the research formulation.

6.1 Experimental Plan

The test bed used for experimentation in the conceptual design applications was the Environmental Design Space (EDS) shown in Fig. 12. Integrated with FLOPS, this design tool allowed for calculations of conceptual design metrics with inputs of OML design variables, $\mathbf{X}_{OML}$, and structural technology performance impact, k_{ST}. While it has been shown that EDS is adept in exploring large portfolios of technologies [44, 94, 93], the goal of this set of experiments was to isolate the effects of PRSEUS in the conceptual design space for relevant metrics. Therefore, surrogate models were created for fuel burn (W_{fuel}), takeoff gross weight (W_{TO}), and wing loading ($^{W_{TO}}/_{S}$) as a function of the outboard wing OML design parameters investigated in Experiment 3.

Surrogate models enabled rapid design space exploration, similar to the studies performed in the previous chapter, and efficient assessment of the aggregate design space was enabled, allowing for an extremely large number of design points to be examined with the low order approximation equations, which took the functional form:

$$\begin{aligned} W_{fuel}, W_{TO}, {}^{W_{TO}}/_{S} &\sim f\left(\mathbf{X}_{OML}, \mathbf{X}_{k_{ST}}\right) \\ \mathbf{X}_{OML} &= [S_w, AR_{ow}, TR_{ow}, \Lambda_{LE,ow}] \\ \mathbf{X}_{k_{ST}} &= [k_{ST,w}, k_{ST,cb}] \end{aligned} \tag{57}$$

To develop these relationships, EDS was sampled with a 216 passenger HWB aircraft, the same scale as the N2A, that was implemented with technologies representative of 2010 state of the art. A design of experiments (DoE) was generated with 1,500 design points within the OML and technology space defined in Eqn. 57. This DoE was a blend of an 77-case face centered central composite design to ensure examination of the extents of the design space, and the baseline design point, $\mathbf{x}^*_{OML}$, was included in the DoE to enable estimates of fuel burn reduction and emissions reductions as a result of implementing PRSEUS on the aircraft. The rest of the cases were randomly generated to fill the design space for enhanced validation of the models. Each case was sized to a design mission payload, for passengers, crew, and baggage, as well as range, $6,000$nm, comparative to a 767-300ER. The mathematical representation of each surrogate was generated by fitting artificial neural networks with a network structure of one hidden layer with 7 nodes each to build the transfer function. This simplistic architecture helped avoid data over-fitting errors that plagued early models for the technology design space. Each node contained the function form of a log-sigmoid activation function, and all transfer function forms in Eqn. 57 were fit to $R^2 \geq 0.9999$.

There were three scenarios discussed in the research formulation for the conceptual design application of structural technology performance characterization. Experiments 4A, 4B, and 4C make observations for those three scenarios, respectively, to determine whether a $k_{ST}\left(\mathbf{X}_{OML}\right)$ characterization significantly reduces risk and improves the ability to make decisions at the conceptual design level. Figure 78 shows two snapshots of the conceptual design space. At this level, it is still important to delineate the Benchmark and STEED performance characterization approaches and definitions. The relationships between conceptual level metrics and each conceptual design variable in $\mathbf{X}_{OML}$ are shown in the left 4 columns, where conceptual design implementation of technology performance for the wing and centerbody is shown in the right 2 columns, defined by Eqn. 46. In this sensitivity environment, the capability exists to vary these technology impacts freely, but the actual performance of the PRSEUS technology is shown by vertical lines, color coordinated to the approach used for performance characterization. Red lines represent the benchmark treatment of structural layout and green lines represent the STEED treatment of structural optimization. The dashed lines show performance for outboard wing weight minimization as the structural layout optimization objective whereas solid lines reflect minimization of the total weight for definition of the structural layout. Two different OML design points are shown in Fig. 78, the top representing a design in which difference in estimated technology performance for each method is somewhat large (top), and a case in which all technology performance, regardless of performance definition or optimization objective, are the same.

This environment is shown before assessment of Experiment Set 4 to show one particular trend. A tradeoff exists between the wing loading metric and the other two metrics. The conceptual design process is full of design parameters that display impacts of competing objectives for metrics; however, this demonstration is being performed a very limited scope. Therefore, inclusion of the wing loading metric and

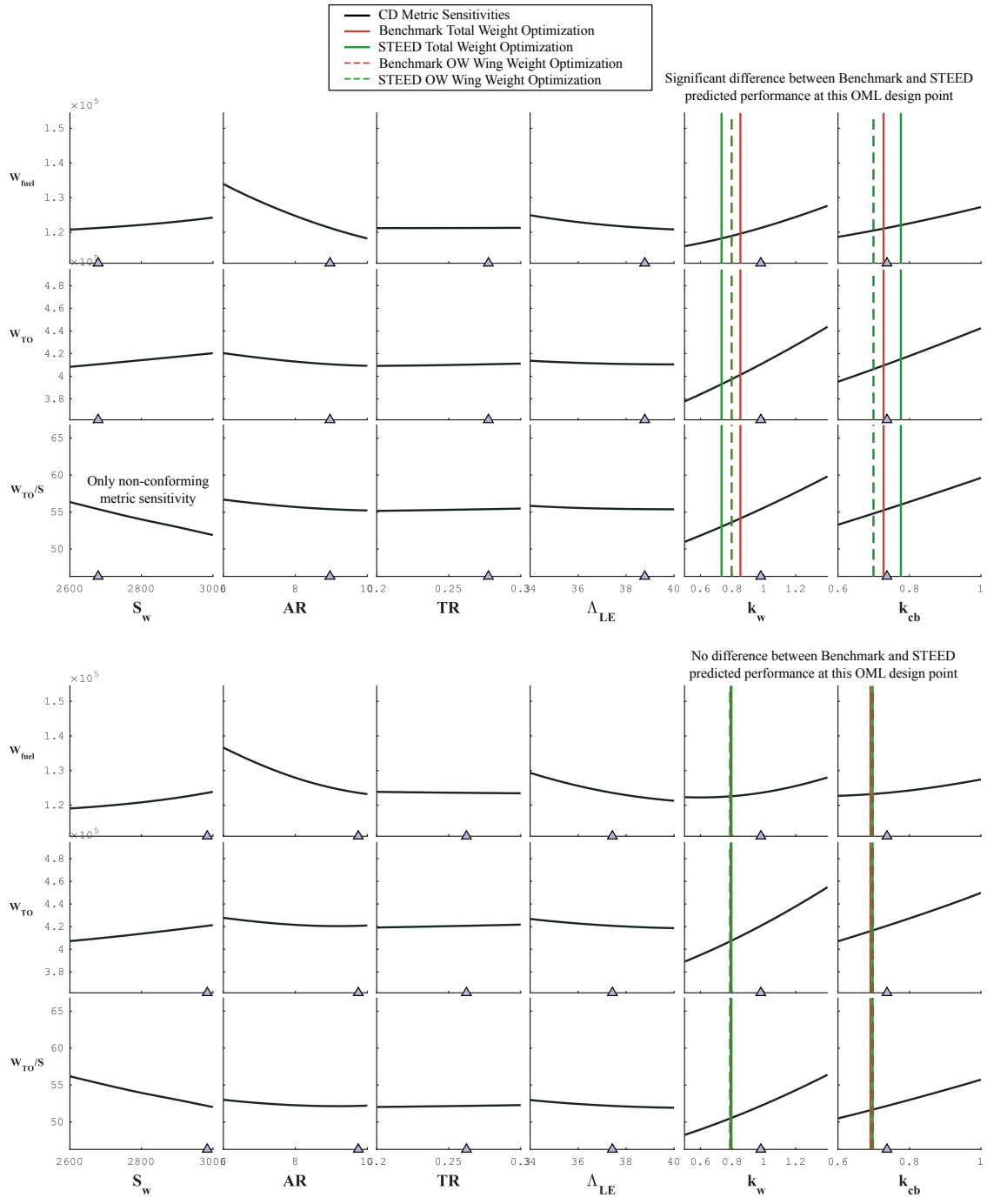

Figure 78: Sensitivities in the conceptual design space with implementation of technology performance impacts

its trend are important because this variable now presents a means in which competing realistic scenarios can be investigated.

The goal of this set of experiments is to test Hypothesis 4 of the research formulation and to validate the STEED performance characterization approach. Hypothesis 4 was stated as:

Hypothesis 4: The structural technology selection risk and implementation risk due to an incomplete characterization of weight reduction performance is greater than the standard risk due to technology immaturity.

Identifying uncertainty due to technology immaturity as a metric for method comparison means that somehow, uncertainty needs to be quantified for the technology given its TRL value. After the multi-bay box demonstration test, PRSEUS moved to the TRL 5 technology maturity echelon. However, some of the assumptions made in performance estimation for this test case were representative of PRSEUS in its ERA development stages, with a TRL value of 3 or 4.

In studies of technology portfolios, TRL uncertainty for technologies has been represented by Weibull distributions [44], which take the form of the following probability density function:

$$f\left(x;\alpha,\beta\right)=\begin{cases}\frac{\alpha}{\beta}\left(\frac{x}{\beta}\right)^{\alpha-1}\exp^{-(x/\beta)^{\alpha}} & x\geq 0,\\ 0 & x<0,\end{cases} \tag{58}$$

The suggested hyperparameter values to represnt TRL uncertainty were defined as $\beta = 2$, and $\alpha = [0.05 : 0.35]$. A limiting assumption in this TRL uncertainty representation is that the target impact value for the technology does not change as a function of TRL. Considering this assumption, a conservative estimate for α was chosen in this case study, representative of a TRL 3 technology. The corresponding

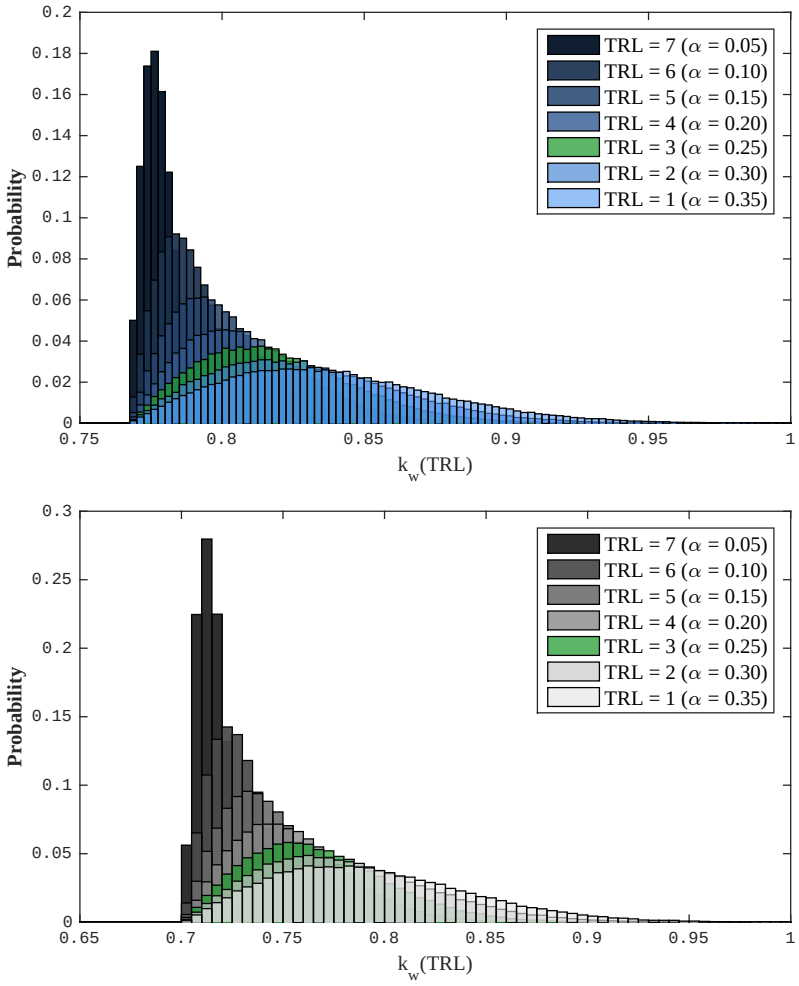

Figure 79: Assumptions for TRL uncertainty in k_w and k_cb implementation

k_w and k_{cb} distributions are highlighted in Fig. 79 in green. Target values of performance in these distributions were obtained for the fuel weight minimization objective in Scenario 1.

6.2 Experiment 4A: Scenario 1 (Technology Selection)

The first scenario, represented in Experiment 4A, follows the TIES technology selection method. The objective of this experiment is to quantify the error between selecting technologies based on the benchmark approach, which treats technology performance as a scalar, compared to the functional approach developed through STEED. For this experiment, the process was simplified to assume that the PRSEUS

structural technology was to be selected, and only the impact of this technology was considered. Furthermore, an assumption was made to focus on one conceptual metric objective per evaluation rather than multiple objectives. For example, surrogates were made for three conceptual design metrics shown in the formulation of Eqn. 57. If requirements were placed on all three metrics, it is unlikely that a single technology can enable feasibility for each requirement, or even make a significant contribution to each. Therefore, Experiment 4A for Scenario 1 was performed three times for: 1) fuel burn optimization, 2) takeoff gross weight optimization, and 3) wing loading optimization. The other metrics in each of these 3 cases were still calculated and are presented with the results.

The steps of Experiment 4A are described as follows to mimic the technology selection approach within TIES:

1. **Determine Baseline** An optimal design point, $\mathbf{x}^*_{OML}$, is found through gradient-based optimization that minimizes the respective objective metric, W_{fuel}, NO_x, or W_{TO}.

2. **Quantify Technology Impact** The technology impact factor is determined by B) the benchmark approach and S) the function developed with the STEED approach.

3. **Recalculate Baseline Performance with $\mathbf{k}_{ST}$** The impact factors $k_{ST}\left(\mathbf{x}^*_{OML}\right)$ are implemented back into the conceptual design model to recalculate the respective conceptual design metric.

4. **Resize Aircraft with $\mathbf{k}_{ST}$** A re-optimization is performed in the conceptual design space with B) k_{ST} treated as a scalar and S) $k_{ST}\left(\mathbf{X}_{OML}\right)$.

The resulting change in conceptual design metrics and conceptual design variables is noted between approach B) for the benchmark and approach S) for the STEED functional treatment of structural technology impact. Table 18 contains the results

for this process given the objective of fuel burn minimization, W_{fuel}.

For each scenario, a requirement was set based on reduction compared to a nominal configuration. The nominal configuration was:

$$\mathbf{x}_{OML,\text{nom}} = \left[S = 2,778 \text{ ft}^2, AR = 8.0, TR = 0.25, \Lambda_{LE} = 37^\circ\right] \tag{59}$$

Metric values for this configuration were a fuel burn of $W_{fuel} = 132,932$ lb, takeoff gross weight of $W_{TO} = 448,961$ lb, and a wing loading of $^{W_{TO}}/_{S} = 58.86\text{ft}^2$.

This demonstration test case assumes that a technology development program is looking to invest in technologies that push the envelope, similar to the NASA ERA program. Therefore, a fuel burn reduction requirement was set at an ambitious value of 25%, corresponding to $W_{TO} = 99,700$ lb. The first line in Table 18 reflects this reduction value. Simply by resizing the aircraft as a function of the $\mathbf{X}_{OML}$ parameters defined for this case study, fuel burn is reduced by 7.01% to 123,620 lb. Aspect ratio of this optimal design point for outboard wing is significantly increased, as expected, due to superior aerodynamic efficiency. Sweep is also increased near its upper bound because its affect on reduction of wave drag. Since optimization of the aircraft OML was not enough to achieve the requirement, then technologies must be selected. Assuming PRSEUS was one of the technologies being considered, then analysis must be performed to assess its independent contribution to help achieve feasibility.

The benchmark approach, in this scenario, performs off-line high fidelity weight reduction estimation. In a conservative assessment of the STEED approach, the benchmark performance values that were predicted considered structural layout optimization of the baseline configuration, but this structural layout design was implement on the PRSEUS configuration as well. There is a slight difference in the estimated performance impacts using the STEED and benchmark approaches for this given OML design point, but it is less than 1% for both centerbody and wing performance. Percent, in this case, is in terms of the actual k value rather than in terms of percent

Table 18: Scenario 1 results for a W_{fuel} optimization objective

Step	**Benchmark**	**STEED**	$\%\boldsymbol{\Delta}\,(\mathbf{S} \rightarrow \mathbf{B})$
Requirement (W_{fuel}), lb	– $99,700$ ($\sim 25\%$ reduction) –		
1: $(*)$ $W_{fuel}\left(\mathbf{x}^{*1}_{OML}\right)$, lb	[$123,620$]		–
1: $W_{TO}\left(\mathbf{x}^{*1}_{OML}\right)$, lb	[$439,402$]		–
1: ${}^{W_{TO}}/_{S}\left(\mathbf{x}^{*1}_{OML}\right)$, ${}^{lb}/_{ft^2}$	[60.28]		–
$S^{*1}_{w}\left(k\right), ft^2$	[$2,619$]		–
$AR^{*1}_{ow}\left(k\right)$	[9.84]		–
$TR^{*1}_{ow}\left(k\right)$	[0.242]		–
$\Lambda^{*1}_{0.25c,ow}\left(k\right)$, deg	[39.8]		–
2: $k_{w}\left(\mathbf{x}^{*1}_{OML}\right)$	0.769	0.767	-0.21
2: $k_{cb}\left(\mathbf{x}^{*1}_{OML}\right)$	0.702	0.709	0.93
3: $(*)$ $W_{fuel}\left(\mathbf{x}^{*1}_{OML}, k\right)$, lb	$114,629$	$114,712$	0.07
3: $W_{TO}\left(\mathbf{x}^{*1}_{OML}, k\right)$, lb	$387,734$	$388,317$	0.15
3: ${}^{W_{TO}}/_{S}\left(\mathbf{x}^{*1}_{OML}, k\right)$, ${}^{lb}/_{ft^2}$	53.16	53.25	0.15
4: $(*)$ $W_{fuel}\left(\mathbf{x}^{*2}_{OML}, k\right)$, lb	$114,668$	$114,715$	0.04
4: $W_{TO}\left(\mathbf{x}^{*2}_{OML}, k\right)$, lb	$387,938$	$387,555$	-0.10
4: ${}^{W_{TO}}/_{S}\left(\mathbf{x}^{*2}_{OML}, k\right)$, ${}^{lb}/_{ft^2}$	53.08	52.98	-0.20
$S^{*}_{w}\left(k\right)$	$2,627$	$2,630$	0.12
$AR_{ow}\left(k\right)$	9.88	9.84	-0.35
$TR_{ow}\left(k\right)$	0.243	0.224	-8.44
$\Lambda_{0.25c,ow}\left(k\right)$	39.7	39.7	0.17
$k_{w}\left(\mathbf{x}^{*2}_{OML}\right)$	0.769	0.757	-1.52
$k_{cb}\left(\mathbf{x}^{*2}_{OML}\right)$	0.702	0.708	0.82

weight.

The next step, (3), was applying this technology impact to the initial optimal design point, $\mathbf{x}^{*1}_{OML}$, and comparing the difference in estimates of both approaches for each metric. Fuel burn reduction with the Benchmark approach is only slightly over-predicted by about 0.07%, which is not significant enough to warrant concern between the two approaches. Additionally, in the resizing step (4), there is an even smaller difference between fuel burn estimates for the STEED functional performance estimation approach and the benchmark approach that holds performance constant, where $\Delta(\mathbf{S} \rightarrow \mathbf{B}) = 37$ lb or 0.04%. There are a few reasons this particular design scenario with this particular metric objective experiences such little change between approaches.

It can be seen in Fig. 78 that the sensitivities of fuel burn (top row) are all somewhat linear and cause the most optimal design point for minimal W_{TO} to exist at the bounds of all $\mathbf{X}_{OML}$ design parameters considered in this limited demonstration test case. Had nonlinearity existed in any of the OML design variables and a natural minimum would exist at a point within the design rather than one of the side constraints, then there may have been a larger difference between the two approaches. Additionally, if the metric objective for minimization had been different in resizing than in the initial baseline optimization without technologies, the first step (1), then a larger difference between estimates would be witnessed as well. This scenario is actually discussed in the next section. However, with a limited subset of OML design variables and only one design objective considered, this scenario shows very little difference between final estimated fuel burn performance. The optimal OML design point is only slightly different as well, mainly for taper ratio, which has the least impact on fuel burn among the $x_{OML} \in \mathbf{X}_{OML}$.

Another potential reason for little difference between approaches for this scenario is that fuel burn calculations are dependent on much more than just structural

weight. The top row of each plot shown in Fig. 78 shows a very significant sensitivity between fuel burn and AR. This trend indicates a strong connection between fuel burn and aerodynamics of the aircraft. Reduction of structural weight has a somewhat significant impact as well, as shown by the slope of the lines for $W_{fuel}\left(k_{ST,w}\right)$ and $W_{fuel}\left(k_{ST,cb}\right)$, i.e. the top row in columns 5 and 6. However, for different OML settings, i.e. between top and bottom sensitivity sets in the figure, the slope of this sensitivity changes. Weight impacts are overshadowed by aerodynamic efficiency effects for regions of this limited OML design space, meaning that drag plays a significant role in the estimation of fuel burn and muddle the effects of the structural technology. This observation is further supported by the relationship between fuel burn and Λ_{LE}, in which larger values have an indirect relationship with wave drag.

Figure 80 shows how the two approaches affect the rest of the design space rather than the bottom-line value for fuel burn. Each histogram in the top plot shows fuel burn as a function of the design space, color coordinated to assumptions. The dark grey distribution is fuel burn calculated simply as a function of the OML design parameters with ignoring structural technology impacts, i.e. $k_{ST,w} = 1$ and $k_{ST,cb} = 1$. The dark blue and light grey histograms show technology performance infused in the conceptual design space with benchmark definition and assumptions. Structural technology impacts are implemented as a scalar value for the dark blue distribution while TRL uncertainty effects are implemented on the scalar value in the light grey distribution. The yellow histogram implements technology impacts in their functional form from the STEED approach.

First, it can be seen that the spread of all distributions are relatively equal, with each progression in assumptions stretching slightly further toward the right, i.e. larger fuel burn. Technology reduction of fuel burn for any implementation is less than about half of the total range of the initial fuel burn distribution, which shows that variation

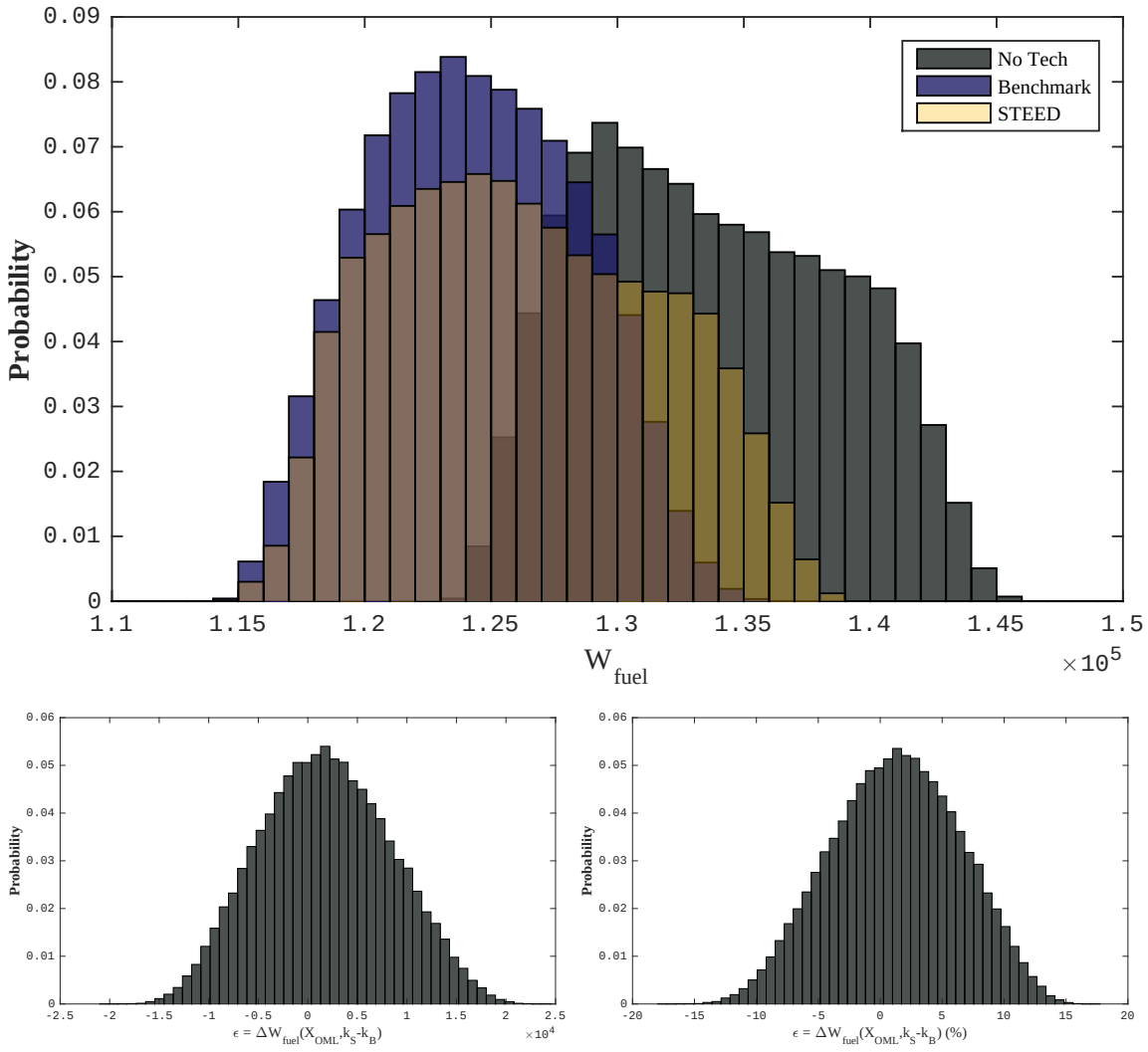

Figure 80: Variability of W_{fuel} in the $\mathbf{X}_{OML}$ design space and error in Benchmark estimates of W_{fuel} by neglecting $\Delta W_S \sim f(\mathbf{X}_{OML})$

in the OML creates a significant effect on aerodynamics and accounts for a large portion of the variability in fuel burn. While the lower bound of each technology infused histogram is near equal, representative of results in Table 18, the upper bound of the STEED distribution stretches further into adverse fuel burn values. This difference indicates that if the scalar value of performance is used from this scenario, in which the initial baseline configuration was optimized for fuel burn, for another design objective with competing trends as fuel burn, then W_{fuel} reduction performance will be over-predicted. The error of this over-prediction is shown in terms of actual magnitude and percent difference in the bottom two histograms in Fig. 80, respectively. These error distributions are calculating the difference between the yellow and dark blue histograms of the top plot, i.e.:

$$\varepsilon = W_{fuel}\left(\mathbf{X}_{OML}, k_s\right) - W_{fuel}\left(\mathbf{X}_{OML}, k_f\right) \tag{60}$$

where k_s represents the scalar benchmark value,

$$k_s = 1 - \frac{W_{S,B}\left(\mathbf{x}^*_{OML}, \mathbf{x}^*_{SL,B}\right) - W_{S,T}\left(\mathbf{x}^*_{OML}, \mathbf{x}^*_{SL,B}\right)}{W_{S,B}\left(\mathbf{x}^*_{OML}, \mathbf{x}^*_{SL,B}\right)} \tag{61}$$

and the function relationship of the STEED approach is found as:

$$k_f = 1 - \frac{W_{S,B}\left(\mathbf{x}^*_{OML}, \mathbf{x}^*_{SL,B}\right) - W_{S,T}\left(\mathbf{x}^*_{OML}, \mathbf{x}^*_{SL,T}\right)}{W_{S,B}\left(\mathbf{x}^*_{OML}, \mathbf{x}^*_{SL,B}\right)} \tag{62}$$

respectively. Although the distributions are relatively similar for each approach, this error distribution shows a total range of error of approximately 30%, a substantial difference when using the benchmark scalar performance estimate compared to the functional STEED performance.

Another conceptual design objective was investigated in this scenario – the minimization of takeoff gross weight, W_{TO}. Results from this scenario are shown in Table 19 and Fig. 80. The same requirement of 25% metric reduction was placed on this design objective as well. Sensitivities of W_{TO} to conceptual design variables mimic those witnessed for W_{fuel}, and therefore similar results were expected for this

Table 19: Scenario 1 results for a W_{TO} optimization objective

Step	**Benchmark**	**STEED**	$\%\boldsymbol{\Delta}\,(\mathbf{S} \rightarrow \mathbf{B})$
Requirement (W_{TO}), lb	– $336,700$ ($\sim 25\%$ reduction) –		
1: $W_{fuel}\left(\mathbf{x}^{*1}_{OML}\right)$, lb	[$123,588$]		–
1: $(*)$ $W_{TO}\left(\mathbf{x}^{*1}_{OML}\right)$, lb	[$438,380$]		–
1: ${}^{W_{TO}}/_{S}\left(\mathbf{x}^{*1}_{OML}\right)$, ${}^{lb}/_{ft^2}$	[60.15]		–
$S^{*1}_{w}\left(k\right), ft^2$	[$2,619$]		–
$AR^{*1}_{ow}\left(k\right)$	[9.83]		–
$TR^{*1}_{ow}\left(k\right)$	[0.214]		–
$\Lambda^{*1}_{0.25c,ow}\left(k\right)$, deg	[39.8]		–
2: $k_{w}\left(\mathbf{x}^{*1}_{OML}\right)$	0.774	0.755	-2.53
2: $k_{cb}\left(\mathbf{x}^{*1}_{OML}\right)$	0.696	0.704	1.16
3: $W_{fuel}\left(\mathbf{x}^{*1}_{OML}, k\right)$, lb	$114,623$	$114,554$	-0.06
3: $(*)$ $W_{TO}\left(\mathbf{x}^{*1}_{OML}, k\right)$, lb	$387,000$	$386,580$	-0.11
3: ${}^{W_{TO}}/_{S}\left(\mathbf{x}^{*1}_{OML}, k\right)$, ${}^{lb}/_{ft^2}$	53.06	53.00	-0.11
4: $W_{fuel}\left(\mathbf{x}^{*2}_{OML}, k\right)$, lb	$114,785$	$114,506$	-0.24
4: $(*)$ $W_{TO}\left(\mathbf{x}^{*2}_{OML}, k\right)$, lb	$387,055$	$386,913$	-0.04
4: ${}^{W_{TO}}/_{S}\left(\mathbf{x}^{*2}_{OML}, k\right)$, ${}^{lb}/_{ft^2}$	53.17	53.04	-0.25
$S^{*}_{w}\left(k\right)$	$2,612$	$2,620$	0.28
$AR_{ow}\left(k\right)$	9.82	9.87	0.58
$TR_{ow}\left(k\right)$	0.220	0.223	1.34
$\Lambda_{0.25c,ow}\left(k\right)$	39.4	39.8	0.91
$k_{w}\left(\mathbf{x}^{*2}_{OML}\right)$	0.774	0.758	-2.17
$k_{cb}\left(\mathbf{x}^{*2}_{OML}\right)$	0.696	0.705	1.23

design objective in Scenario 1. However, a significant difference exists between the two objectives. While Table 19 shows relatively the same values for differences in metrics and design variables for the takeoff gross weight minimization design objective, the aggregate performance throughout the design space, shown in Fig. 80, is substantially different.

The separation between aggregate means of W_{TO} for the nominal design space and technology-infused design spaces is much larger considering the spread of each distribution. Also, the scalar distribution (dark blue) is more heavily weighted to minimized takeoff gross weight than performance modeled as a functional relationship

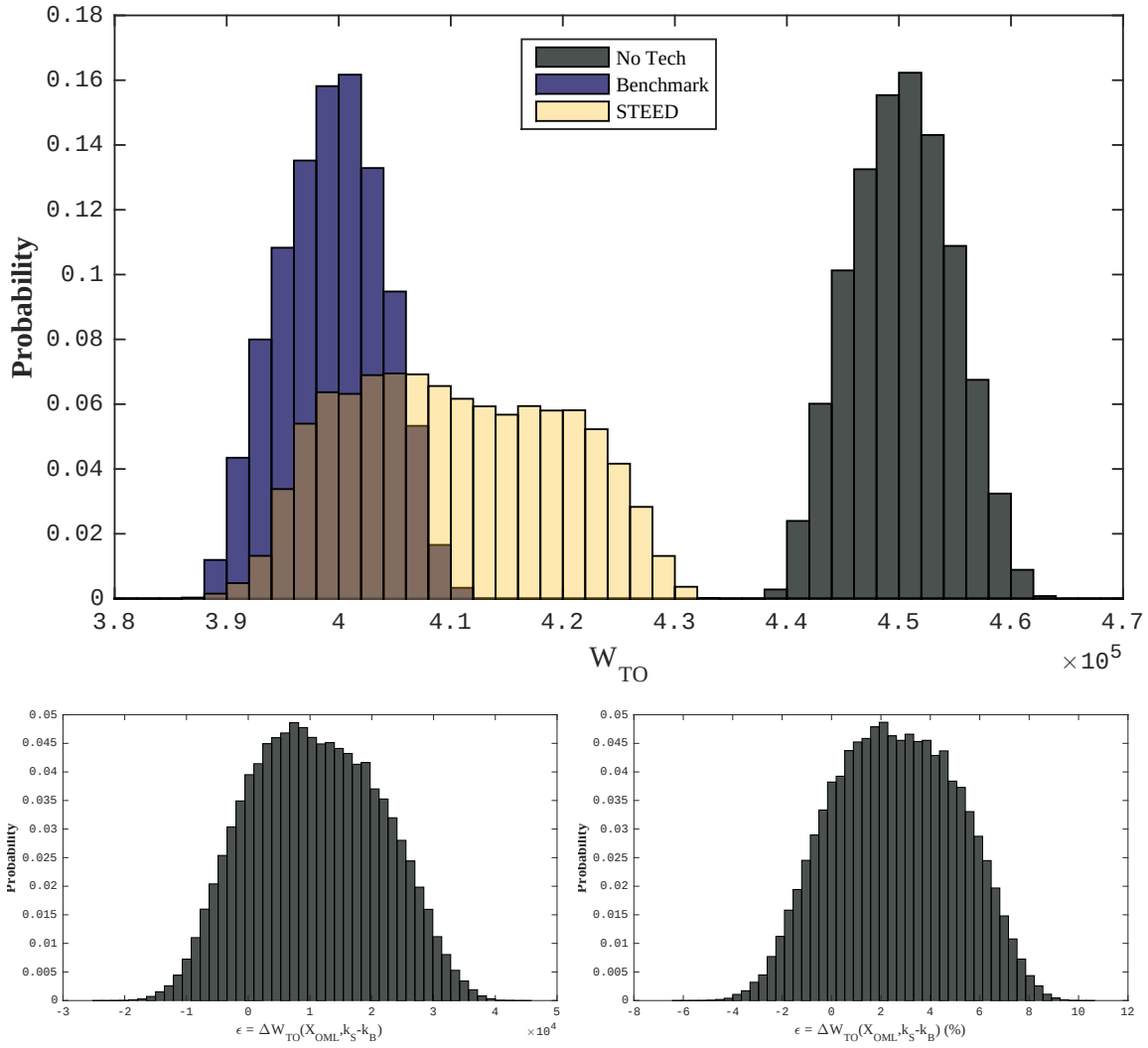

Figure 81: Variability of W_{TO} in the $\mathbf{X}_{OML}$ design space and error in Benchmark estimates of W_{TO} by neglecting $\Delta W_S \sim f\left(\mathbf{X}_{OML}\right)$

(yellow). This phenomenon shows in the aggregate error, which has a total range of approximately 60,000 lb and 15%. Although the specific scenario listed in Table 19 does not display significant separation in technology performance value, OML designs, or conceptual design performance metrics, the aggregate design space tells a much different story. The same conclusions can be drawn for takeoff gross weight as fuel burn – if more design objectives and conceptual design parameters were considered in this optimization scenario, which would drive the W_{TO} metric away from the OML design variable side constraints, then a more prevalent difference between benchmark and STEED performance estimates would occur. Estimates of conceptual design metrics, as a consequence, would also witness a larger error. Scenario 2, discussed for Experiment 4B in the next section, investigates an objective that represents a slightly similar situation even within the constraints of a number of design space parameters and conceptual design metrics.

6.3 Experiment 4B: Scenario 2 (Technology Selection)

The scenario in Experiment 4B, similar to Experiment 4A, relates to structural technology selection; however, the manner in which benchmark technology performance is estimated is the key difference between the scenarios. In Scenario 2, it is assumed that structural technology performance has been previously estimated via a different technology development program. For further development, another development program has taken interest in the technology for a different objective. In this demonstration, there is a limited number of objectives to choose from, and since a tradeoff exists for wing loading in terms of outboard wing area with W_{TO} and W_{fuel}, it was used as the demonstration metric of Scenario 2. Both minimization and maximization of this metric is investigated, presenting two objective scenarios: **Minimization** is representative of an aircraft configuration which requires versatility in the number of airports it can fly into, necessitating a reduction in approach velocity for smaller

runways, and **Maximization** is representative of an aircraft that requires improved maneuverability.

Table 20 shows results for the minimization case. Scalar performance values were taken from the first case presented in Scenario 1, an OML design point which minimized fuel burn. This performance uses the benchmark definition. The main difference between baseline optimized values in the first step (1) of this scenario compared to the one from which performance was derived is the wing area. A much larger wing area, effectively at the upper bound of the design parameter was found to be optimal. This trend matches the sensitivities presented at the beginning of the chapter. STEED performance values for this configuration, however, are not much different than those calculated in the first scenario due to a weak relationship between outboard wing area and performance. The resulting effect is again only a slight change in conceptual design metrics that were estimated with the Benchmark approach and the STEED approach.

The second case of wing loading maximization is unique and somewhat unrealistic for a commercial aircraft configuration. Not many scenarios exist in which an increased wing loading is required of this type of transport; but this objective fits the purpose of a hypothetical test case to mimic realistic conceptual design conditions in which not objective and requirement possesses the same functional relationship with conceptual design parameters. The requirement listed in this scenario is a wing loading of 70 $^{lb}/_{ft^2}$, and immediate differentiation between the previously considered scenarios is witnessed in Step (1). The baseline optimal design point is drastically different: a much higher fuel burn and takeoff gross weight as well as a smaller aspect ratio and leading edge sweep. This design point results in a substantially different value of PRSEUS performance for the wing, showing that weight is actually added by implementing PRSEUS on the aircraft. A significant risk is presented in this case when using the benchmark approach, because performance is over-predicted by

Table 20: Scenario 2 results for a $^{W_{TO}}/_{S}$ minimization objective

Step	**Benchmark (Lit)**	**STEED**	$\%\boldsymbol{\Delta}$ **(S** $\rightarrow$ **B)**
Requirement ($^{W_{TO}}/_{S}$), $^{lb}/_{ft^2}$		– 45.0 –	
1: $(*)$ $W_{fuel}\left(\mathbf{x}^{*1}_{OML}\right)$, lb	[127,000]		–
1: $W_{TO}\left(\mathbf{x}^{*1}_{OML}\right)$, lb	[448,602]		–
1: $^{W_{TO}}/_{S}\left(\mathbf{x}^{*1}_{OML}\right)$, $^{lb}/_{ft^2}$	[55.60]		–
$S^{*1}_{w}\left(k\right), ft^2$	[2,988]		–
$AR^{*1}_{ow}\left(k\right)$	[9.49]		–
$TR^{*1}_{ow}\left(k\right)$	[0.212]		–
$\Lambda^{*1}_{0.25c,ow}\left(k\right)$, deg	[39.8]		–
2: $k_w\left(\mathbf{x}^{*1}_{OML}\right)$	0.769	0.824	6.66
2: $k_{cb}\left(\mathbf{x}^{*1}_{OML}\right)$	0.702	0.707	0.73
3: $(*)$ $W_{fuel}\left(\mathbf{x}^{*1}_{OML}, k\right)$, lb	120,213	120,558	0.29
3: $W_{TO}\left(\mathbf{x}^{*1}_{OML}, k\right)$, lb	398,614	402,876	1.06
3: $^{W_{TO}}/_{S}\left(\mathbf{x}^{*1}_{OML}, k\right)$, $^{lb}/_{ft^2}$	49.43	49.96	1.06
4: $(*)$ $W_{fuel}\left(\mathbf{x}^{*2}_{OML}, k\right)$, lb	120,647	119,509	−0.95
4: $W_{TO}\left(\mathbf{x}^{*2}_{OML}, k\right)$, lb	398,738	400,422	0.42
4: $^{W_{TO}}/_{S}\left(\mathbf{x}^{*2}_{OML}, k\right)$, $^{lb}/_{ft^2}$	49.46	49.64	0.37
$S^{*}_{w}\left(k\right)$	2,987	2,986	−0.04
$AR_{ow}\left(k\right)$	9.36	9.84	4.85
$TR_{ow}\left(k\right)$	0.206	0.248	16.84
$\Lambda_{0.25c,ow}\left(k\right)$	39.5	39.8	0.66
$k_w\left(\mathbf{x}^{*2}_{OML}\right)$	0.769	0.791	2.74
$k_{cb}\left(\mathbf{x}^{*2}_{OML}\right)$	0.702	0.698	−0.62

Table 21: Scenario 2 results for a $^{W_{TO}}/_{S}$ maximization objective

Step	**Benchmark (Lit)**	**STEED**	$\%\boldsymbol{\Delta}$ **(S** $\rightarrow$ **B)**
Requirement ($^{W_{TO}}/_{S}$), $^{lb}/_{ft^2}$		– 70.0 –	
1: $(*)$ $W_{fuel}\left(\mathbf{x}^{*1}_{OML}\right)$, lb	[143,967]		–
1: $W_{TO}\left(\mathbf{x}^{*1}_{OML}\right)$, lb	[455,621]		–
1: $^{W_{TO}}/_{S}\left(\mathbf{x}^{*1}_{OML}\right)$, $^{lb}/_{ft^2}$	[62.54]		–
$S^{*1}_{w}\left(k\right), ft^2$	[2,616]		–
$AR^{*1}_{ow}\left(k\right)$	[6.13]		–
$TR^{*1}_{ow}\left(k\right)$	[0.253]		–
$\Lambda^{*1}_{0.25c,ow}\left(k\right)$, deg	[34.4]		–
2: $k_w\left(\mathbf{x}^{*1}_{OML}\right)$	0.769	1.034	25.65
2: $k_{cb}\left(\mathbf{x}^{*1}_{OML}\right)$	0.698	0.745	6.31
3: $(*)$ $W_{fuel}\left(\mathbf{x}^{*1}_{OML}, k\right)$, lb	131830	136931	3.72
3: $W_{TO}\left(\mathbf{x}^{*1}_{OML}, k\right)$, lb	402319	425276	5.40
3: $^{W_{TO}}/_{S}\left(\mathbf{x}^{*1}_{OML}, k\right)$, $^{lb}/_{ft^2}$	55.27	58.42	5.40
4: $(*)$ $W_{fuel}\left(\mathbf{x}^{*2}_{OML}, k\right)$, lb	131,751	136,945	3.79
4: $W_{TO}\left(\mathbf{x}^{*2}_{OML}, k\right)$, lb	402,510	425,224	5.34
4: $^{W_{TO}}/_{S}\left(\mathbf{x}^{*2}_{OML}, k\right)$, $^{lb}/_{ft^2}$	55.25	58.47	5.51
$S^{*}_{w}\left(k\right)$	2,619	2,613	−0.24
$AR_{ow}\left(k\right)$	6.15	6.13	−0.21
$TR_{ow}\left(k\right)$	0.285	0.256	−11.28
$\Lambda_{0.25c,ow}\left(k\right)$	34.2	34.3	0.36
$k_w\left(\mathbf{x}^{*2}_{OML}\right)$	0.769	1.035	25.66
$k_{cb}\left(\mathbf{x}^{*2}_{OML}\right)$	0.698	0.744	6.25

approximately 25%. The resultant different in conceptual design metrics is about $3-5\%$, and the same relative relationships exist after OML resizing in Step (4). In this context, this amount of avoidable error is extremely consequential for the design process. Targets are set in the conceptual design phase, especially for weight, which must be met in later design phases. For this particular case, the more accurate performance technology performance estimate adds approximately $23,000$ lb to takeoff gross weight. A significant burden is placed, then, on later phase design teams to identify areas of potential weight reduction, and risk is high that costly late-phase redesign will need to take place.

Figure 82 shows wing loading as an aggregate of the OML design space for the various formulations of technology performance estimation. The substantial difference between the effect of Benchmark and STEED performance estimation is evident in this plot. Similar to the previous scenarios, the minimum value of the metric has only a small relative difference while the rest of the design space shows a somewhat substantial error comparatively, with total range of approximately 25%. With risk being defined in the tails of these error distributions, these are trends than cannot be ignored. An additional observation is that technology performance is not the driver in any of these scenarios, it is only a fallout of the OML design parameters that have been optimized. All configurations found optimal design points at the extents of the design space rather than toward the interior.

6.4 Experiment 4C: Scenario 3 (Technology Implementation)

The first two scenarios of this chapter were focused on selection of the structural technology, while also providing comments on the aggregate OML design space. Scenario 3, however, is fully focused on assessing aggregate conceptual design metrics for technology implementation in the $\mathbf{X}_{OML}$ design space. This scenario makes no assumptions regarding conceptual design objectives. The goal of Experiment 4C is simply

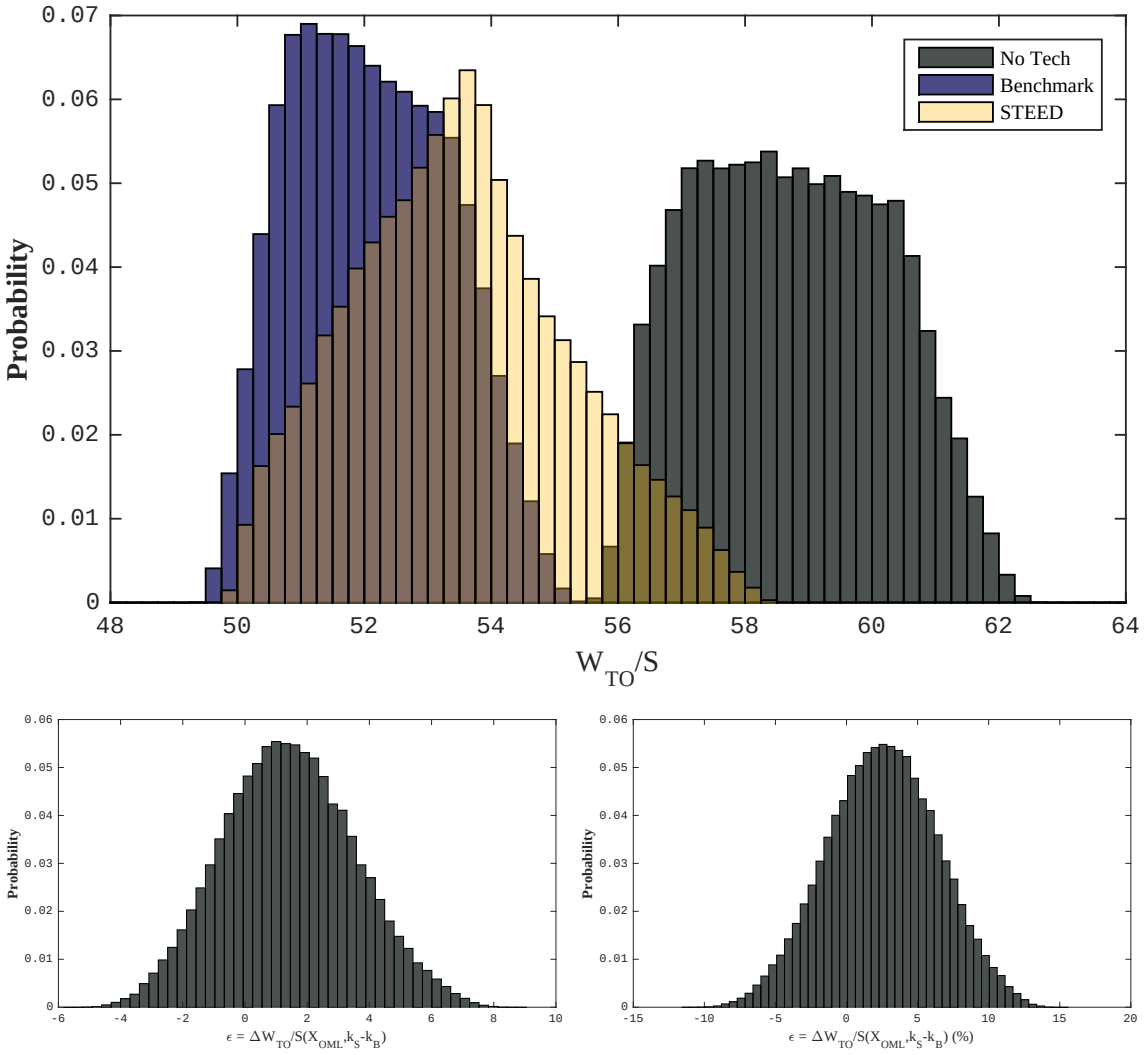

Figure 82: Variability of wing loading in the $\mathbf{X}_{OML}$ design space and error in Benchmark estimates of wing loading by neglecting $\Delta W_S \sim f\left(\mathbf{X}_{OML}\right)$

to assess the potential implementation error of a technology in the conceptual design space by neglecting the $\Delta W_S(\mathbf{X}_{OML})$ relationship. Being consistent with Hypothesis 4, error due to implementing scalar performance values and not $\Delta W_S(\mathbf{X}_{OML})$ is compared against uncertainty in performance due to technology immaturity, captured through Weibull distributions shown in Fig. 79.

Comparisons are shown for W_{fuel}, W_{TO}, $^{W_{TO}}/_{S}$ in Figs. 83–85, respectively. Each error and uncertainty distribution is displayed in terms of actual design metric values and percentages. Metric histograms were calculated by performing a Monte Carlo simulation of 100,000 cases for each conceptual design metric for each technology implementation: 1) scalar values of $k_{ST,w}$ and $k_{ST,cb}$ determined by fuel burn minimization for an OML baseline and subsequent benchmark performance estimation, 2) TRL distributions using technology performance values from (1) as the target performance, and 3) functional values of $k_{ST,w}$ and $k_{ST,cb}$ generated with the STEED approach. At each Monte Carlo OML design point, TRL uncertainty and STEED metric values were compared to scalar benchmark metric values.

Results for Scenario 3 show overwhelmingly that as an aggregate of the OML design space, the relationship between structural technology weight reduction performance and the outer mold line, $\Delta W_S(\mathbf{X}_{OML})$ shown in yellow histograms, causes significant variation in conceptual design metrics. The first observation witnessed when comparing these histograms is their placement along the x-axis. Each distribution exists almost fully in the positive error/uncertainty region, and since the following definitions were used for uncertainty:

$$\begin{aligned} \varepsilon_{\mathrm{R},unc} &= \mathrm{R}(\mathbf{X}_{OML}, k_{TRL}) - \mathrm{R}(\mathbf{X}_{OML}, k_s) \\ \varepsilon_{\mathrm{R},unc}(\%) &= 100 \cdot \left(\frac{\mathrm{R}(\mathbf{X}_{OML}, k_{TRL}) - \mathrm{R}(\mathbf{X}_{OML}, k_s)}{\mathrm{R}(\mathbf{X}_{OML}, k_{TRL})} \right) \end{aligned} \tag{63}$$

where R represents a generic conceptual design response. Error due to an incomplete

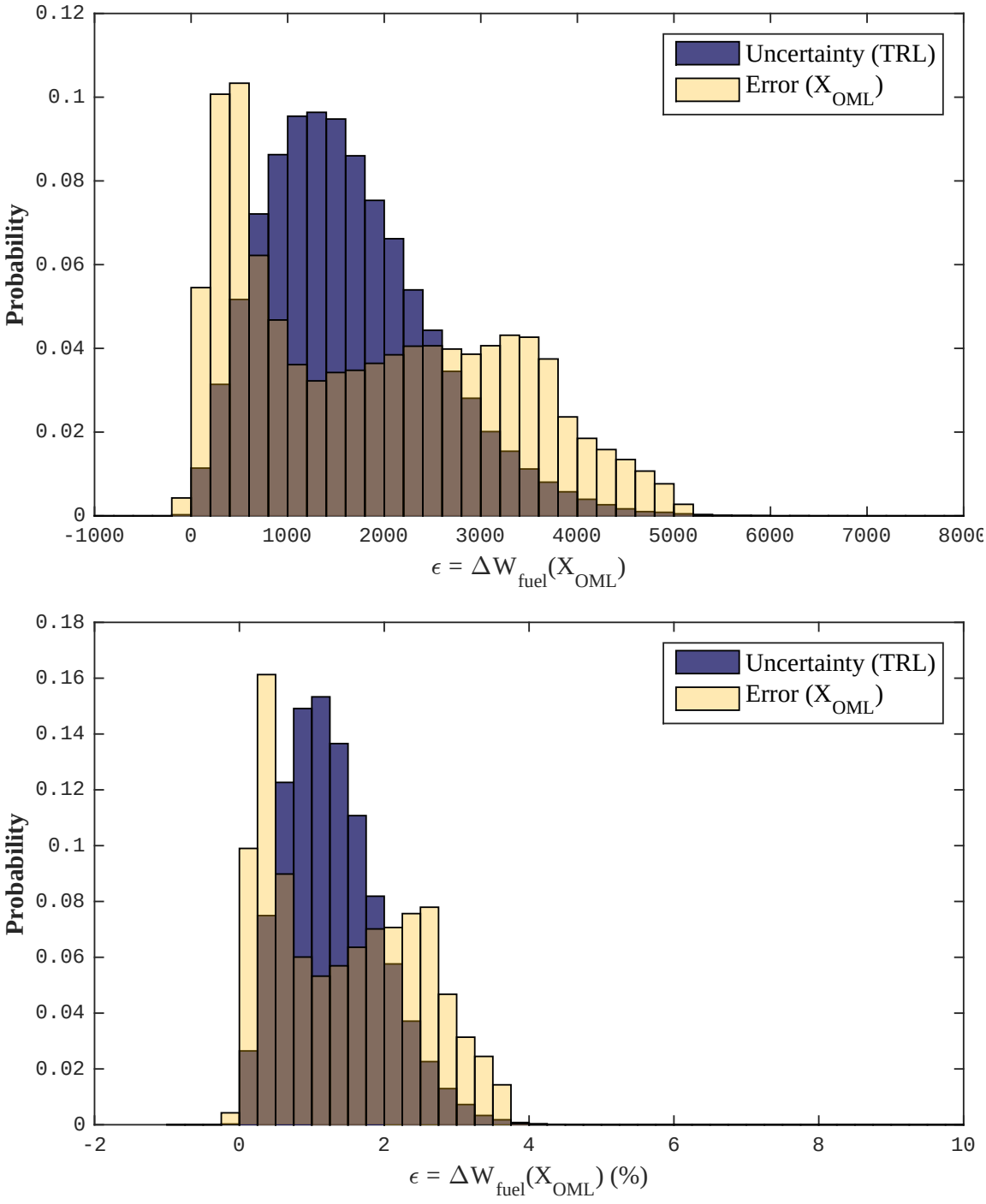

Figure 83: Error in fuel burn, W_{fuel}, for PRSEUS conceptual design implementation by neglecting $\Delta W_S \sim f\left(\mathbf{X}_{OML}\right)$

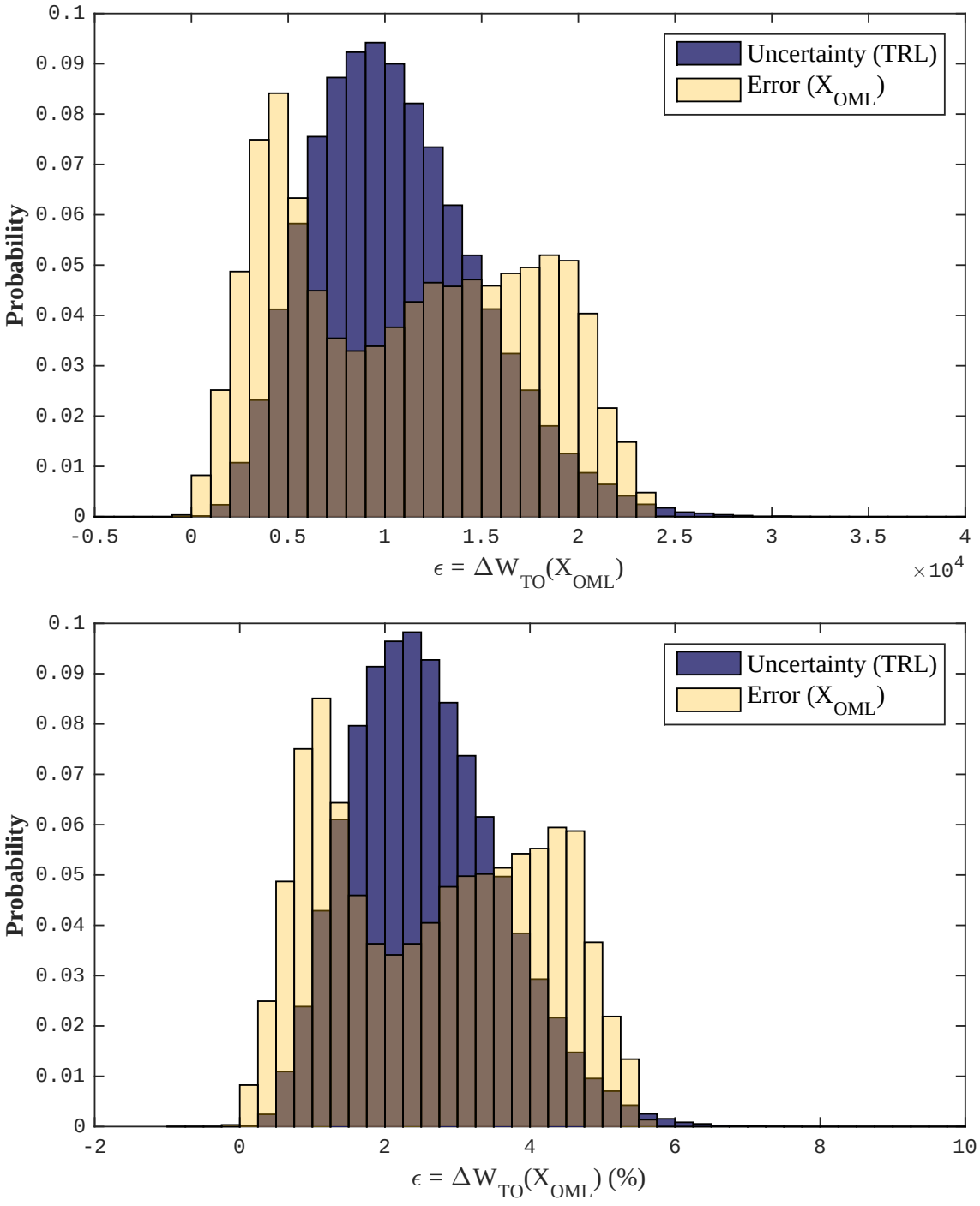

Figure 84: Error in takeoff gross weight, W_{TO}, for PRSEUS conceptual design implementation by neglecting $\Delta W_S \sim f\left(\mathbf{X}_{OML}\right)$

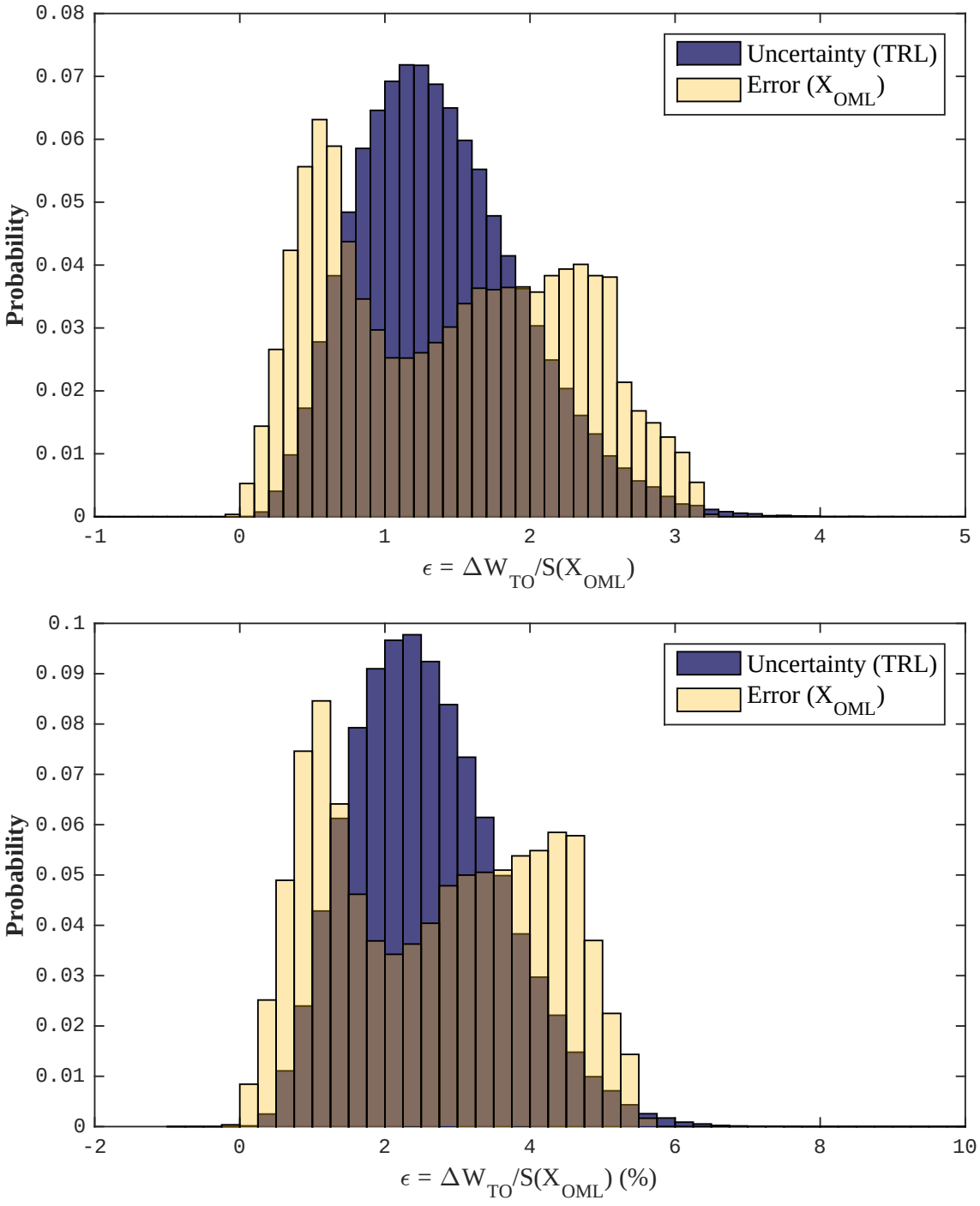

Figure 85: Error in wing loading, W_{TO}/S, for PRSEUS conceptual design implementation by neglecting $\Delta W_S \sim f\left(\mathbf{X}_{OML}\right)$

characterization of structural technology performance:

$$\varepsilon_{\mathrm{R},OML} = \mathrm{R}\left(\mathbf{X}_{OML}, k_f\right) - \mathrm{R}\left(\mathbf{X}_{OML}, k_s\right)$$
$$\varepsilon_{\mathrm{R},OML}\left(\%\right) = 100 \cdot \left(\frac{\mathrm{R}\left(\mathbf{X}_f, k_{TRL}\right) - \mathrm{R}\left(\mathbf{X}_{OML}, k_s\right)}{\mathrm{R}\left(\mathbf{X}_{OML}, k_f\right)}\right) \tag{64}$$

This phenomena indicates a systematic over-prediction of technology performance within the conceptual design space. By assumptions used in the definition of TRL uncertainty, this trend was expected. However, error due to neglect of the functional performance relationship with the aircraft OML was less expected. The source of this phenomena has been discussed in the previous section through inspection of the conceptual design space. It is shown that all but one of the twelve total metric sensitivities have slopes in the same direction, pushing optimality (defined as a minimum for each metric) to the same point in the OML design space. It can be inferred that if a realistic full-scale conceptual design exploration was being performed and baseline optimization was performed using a multi-objective formulation, then error in implementation would not be as heavily one-sided.

In addition to the x-axis location, the range, and more importantly, 95% confidence interval, for the yellow error distributions exceeds that of the distribution representing TRL uncertainty (blue). This observation is significant in the assessment of Hypothesis 4 as well as the identification of the $\Delta W_S\left(\mathbf{X}_{OML}\right)$ relationship as a significant source of epistemic, i.e. reducible, uncertainty [80]. Theoretically, the uncertainty distribution represented by TRL and indicating technology immaturity should capture effects from all significant sources of uncertainty. It stands to reason that the blue TRL distribution should be much larger than the yellow error distribution because this source of potential uncertainty is being accounted for. However, their range is on the same order, meaning uncertainty due to the $\Delta W_S\left(\mathbf{X}_{OML}\right)$ relationship was previously an "unknown unknown" in technology performance. The

STEED approach, then, was able to identify a source of uncertainty that was previously unidentified and it can now be quantified and reduced through characterization and quantification.

6.5 Summary

It was shown in the first conceptual design scenario that given a single conceptual design objective with a small subset of conceptual design variables, there is little difference between estimated performance values using the Benchmark and STEED approaches when the baseline configuration is redesigned with the technology in mind. In the case of the PRSEUS technology, this phenomenon is the result of the optimal baseline design point existing at design parameter side constraints, i.e. the extents of the $\mathbf{X}_{OML}$ design space. Little correlation existed between technology performance impact and the OML design parameters that were considered, and therefore, redesign of the OML with the implementation of PRSEUS had no effect on the estimated optimal fuel burn performance. It was shown and inferred, however, through aggregate histograms of the design space that there is a much larger risk and potential error in both technology performance estimates and conceptual design performance metrics if a larger number of design parameters and objectives are considered in the conceptual design process. These latter scenarios are more realistic than the assumptions made for demonstration purposes in this test case. Scenarios 2 and 3 supported this notion, showing that implementing performance for a specific objective that was estimated for a configuration designed with a competing objective generates larger errors for performance estimates using the Benchmark when compared with the STEED method. Consequently, these larger errors increase risk in using the benchmark approach to estimate structural technology performance.

Also discussed in the research formulation was the potential for performance to be discontinuous or nonlinear because of separate optimization of structural layout for

baseline and technology configurations. There was concern as to whether this would have an impact on assessing conceptual metrics, and if infinite loops were a possibility if optimization in conceptual design with a tool like FLOPS was driven toward a design point near a potential discontinuity. FLOPS is an optimization program that determines what the shape of the vehicle should be based on the objectives of the mission analysis. For example, if the aircraft is optimized for range, then variable settings are determined for $\mathbf{X}_{OML}$ design variables and the conceptual level metrics are determined for the optimized $\mathbf{x}_{OML}^{*1}$. However, the structural technology technically operates on one of the metric outputs for this process, i.e. structural weight.

If the structural technology k-factor is applied to structural weight and the overall gross weight is reduced, the estimates for other metrics like fuel burn are no longer valid. An iteration must occur where the aircraft is resized based on this k-factor, $k\left(\mathbf{x}_{OML}^{*1}\right)$. Since performance is dependent on the OML, then new optimized design vector, $\mathbf{x}_{OML}^{*2}$, instantiates a new value of technology performance, $k\left(\mathbf{x}_{OML}^{*2}\right)$. This iterative process continues until convergence occurs. Can convergence occur if $k\left(\mathbf{X}_{OML}\right)$ is not a smooth or continuous function? Will large discontinuities in performance values create an infinite loop if the optimized configuration is near that performance discontinuity? This is a potential avenue of future research.

In the formulation presented with the STEED approach, this potentiality was not an issue. Characterization of performance with STEED, discussed in Sec. 5.4.2 and which were a fallout of phenomena shown in Fig. 89, were still represented with a continuous mathematical form of an approximation model. The issue is then translated to large slopes and deviations that occur in the OML design space. This phenomena may have an impact if iterative optimization is taking place directly in a conceptual design tool like FLOPS or EDS; however, the surrogate formulation that was used in this chapter develops a closed-form approximation equation for the conceptual design

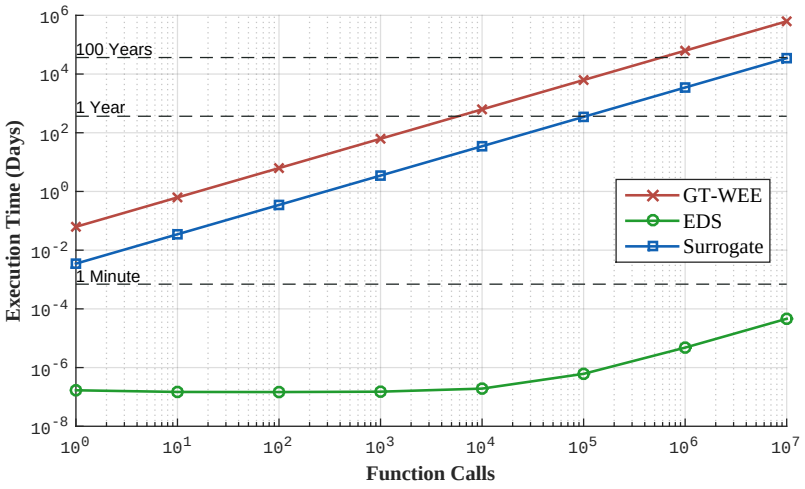

Figure 86: Comparative execution times of performance estimation and conceptual design surrogate models compared to EDS, and GT-WESt

metrics from data samples generated by these design tools as well. Therefore, if convergence is an issue, a random search approach can be used with a number of samples that is otherwise intractable if the actual design tool was used, and this concept is shown in Fig. 86 (similar to the plot presented in the last chapter).

The most significant conclusion drawn from investigation of the conceptual design implementation of the PRSEUS structural technology is effect that each design scenario has on technology performance estimation and its impact on conceptual design metrics. If a small number of non-competing design objectives is considered in the conceptual design phase, while exploring only a small number of conceptual design parameters, then error between the benchmark and STEED approaches and its corresponding risk are relatively low. The conceptual design process, however, is traditionally a study in trades with competing objectives. Therefore, the results shown as an aggregate of the OML design space hold greater weight compared to the individual case studies presented in this chapter. Hypothesis 4 is considered supported, then, by evidence presented for PRSEUS under the assumptions of this test case, shown in Figs. 83–85. As was the case with previous hypotheses, a generalized statement cannot be confirmed or refuted by the evidence presented until more

structural technologies are able to be tested using the STEED approach.

CHAPTER VII

TECHNOLOGY EXPERIMENT DESIGN

Each step in the STEED approach up to this point has been an investigation of translating inputs to outputs and quantifying the relationship between structural technology performance and a particular level of design space. In this chapter, these relationships are put to use in the technology development and demonstration process. Experiment design for a structural technology is an important mechanism in the process of building confidence in its performance. The end goal of technology development is to ensure the structural technology behaves as expected within its specified operating conditions so it can buy its way onto an aircraft.

One of the challenges mentioned regarding experiment design for structural technologies with the STEED approach is data management. If program objectives are less strictly defined and all data in the four levels of characterization are available to the technology development team, where do they start? Hypothesis 5 was stated as:

Hypothesis 5: If performance of the three design space levels, $\mathbf{X}_{OML}$, $\mathbf{X}_{SL}$, and $\mathbf{X}_{T}$, can be connected through similar aggregate parameters in the experiment characterization process, then a larger number of objectives can be considered for experiment design.

This hypothesized treatment of data and determining causality is examined in this chapter through various objective scenarios, similar to the last chapter for technology implementation in conceptual design. Two categories of scenarios are examined and discussed: 1) risk reduction and 2) uncertainty reduction. In each scenario, differences between the STEED approach and Benchmark approach are highlighted. Traceability

of the STEED approach is also assessed to determine if 1) identification of causality is enabled and 2) each element of the structural technology experiment can be defined from a particular observation at a higher level.

7.1 Objective 1: Risk Reduction

The first objective examined for technology advancement is the reduction of risk. This objective is similar to reduction of uncertainty, but there is one important differentiating characteristic: while both definitions deal with probabilistic distributions, risk is more focused on the tail ends of the distribution and the consequences associated with them. Uncertainty, on the other hand, refers to the general state of unknown surrounding a particular estimate. Identification of risk is paramount for technology advancement, and an example is examined to highlight this notion.

7.1.1 Test Case Example

In Sec. 5.4.1, aggregate trends were examined for structural technology performance using the STEED approach compared to scalar assessments using Benchmark and Uninformed treatment of the structural layout. The objective for optimization in these trade studies was the minimization of total aircraft structural weight. In the test case, however, assumptions were made for the sake of demonstration to only consider outboard wing structural layout design parameters in this optimization formulation. How would weight reduction performance be affected if the goal of topology optimization was to minimize the structural weight of a particular aircraft section, namely the outboard wing? Figure 87 shows the resulting aggregate performance distributions, total weight reduction (top) and outboard wing weight reduction (bottom), for the $\mathbf{X}_{OML}$ design space with this optimization objective.

Similar to results from the total aircraft weight minimization objective, by optimizing the structural layout with the outboard wing in mind, the tails of the performance distributions are truncated. Therefore, risk is reduced in technology

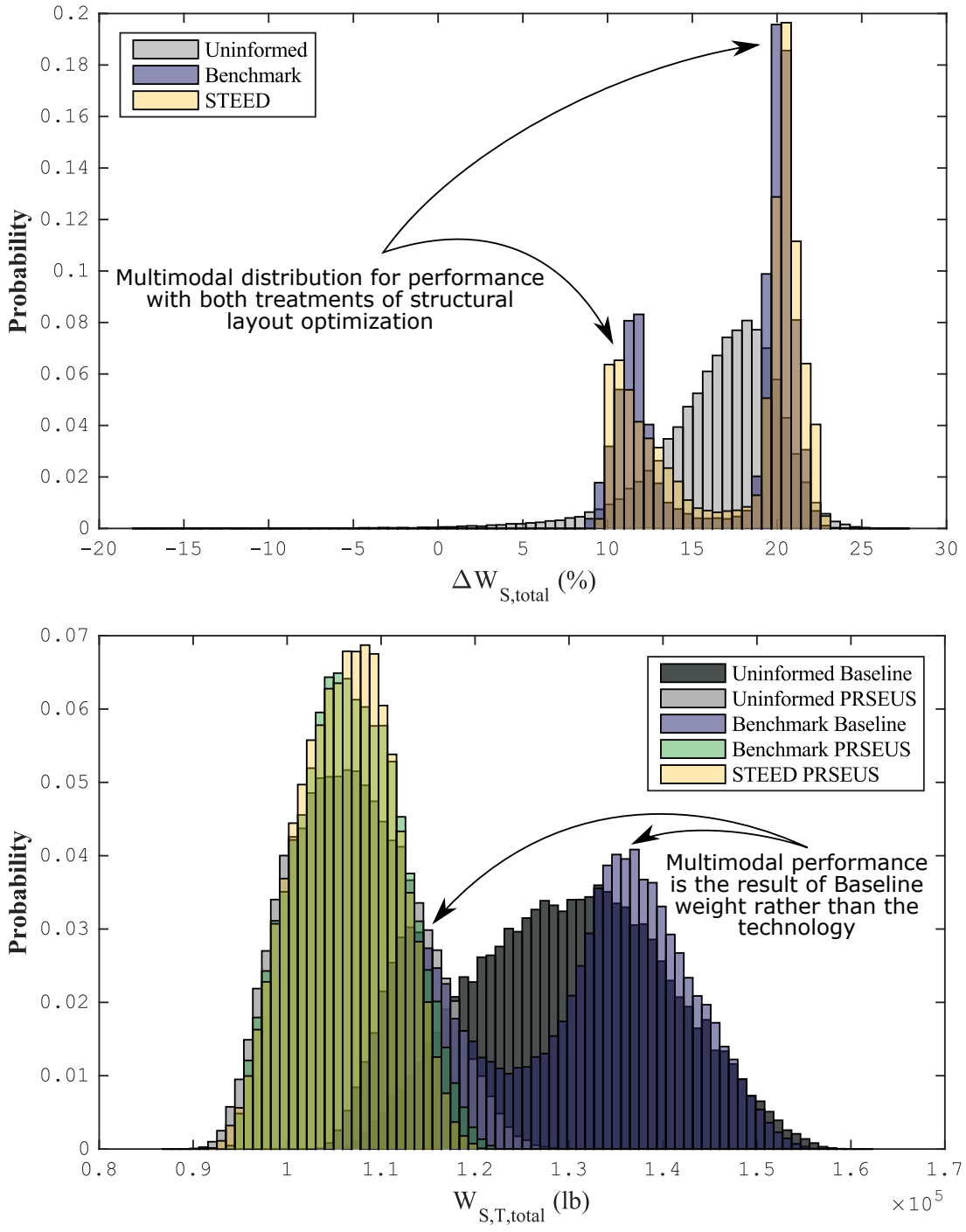

Figure 87: PRSEUS performance aggregate for the total aircraft (top) and for the underlying structural weights that comprise performance (bottom) for Uninformed (grey), Benchmark (blue), and STEED (yellow) approaches

performance estimates simply by implementing a more appropriate treatment of the structural layout compared to the Uninformed approach. Performance distributions with this particular objective, however, have a much different aggregate shape than those that were generated with a minimization objective of total structural weight, as shown in Fig. 70. The multimodality of the Benchmark and STEED distributions, blue and yellow, respectively, indicate some underlying phenomena within the design space that converges the optimization to design points that create two favored performance values for the total aircraft. There is not a significant difference between the Benchmark and STEED distributions.

This example could be an instance in which the technology development team sees the bimodal shapes of the performance distributions as an indication of error in the structural weight estimation model or of some phenomena that had not been considered. Therefore, further investigation of the trend would be initiated. The bottom plot in Fig. 87 shows total aircraft structural weights of each of configuration that affects the performance distributions in the top plot. These structural weight histograms show that the resultant shape of the performance distributions is due to the shape of the optimized baseline structural weight function. This observation is troublesome if PRSEUS performance estimates are being significantly affected by attributes outside of the development team's control. What is the root cause of this shape for the Benchmark optimized baseline configuration? Would the distribution shape remain the case if a different baseline was used?

The next step in determining causality would be to assess aggregate PRSEUS performance on the outboard wing because structural weight of this aircraft section was the objective of structural layout optimization. Figure 88 shows this information in the same manner of Fig. 87. The main difference for the outboard wing section is that only the blue histogram in this plot is multimodal, whereas the bottom line performance has been increased by optimizing each structural configuration separately,

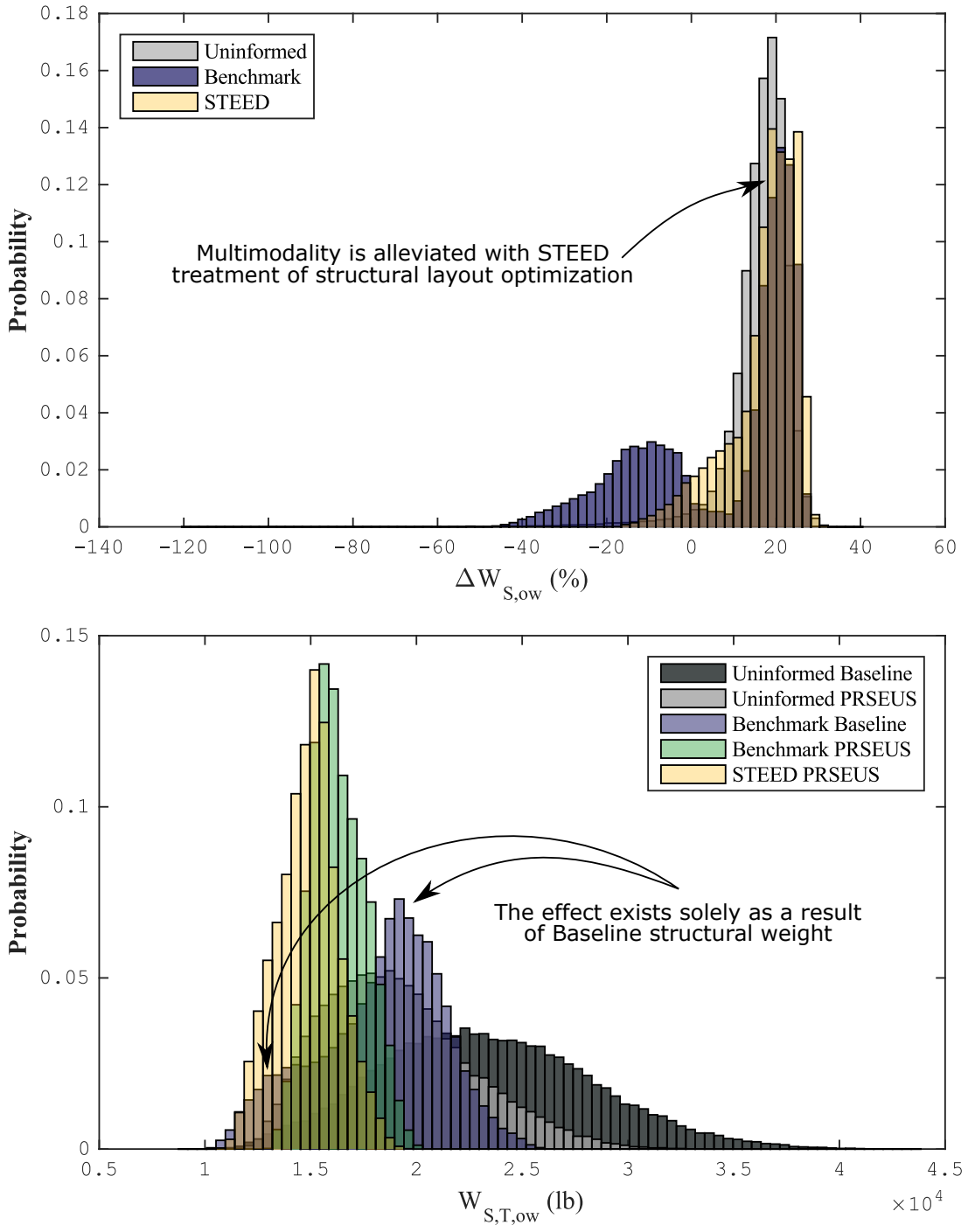

Figure 88: PRSEUS performance aggregate for the outboard wing (top) and for the underlying structural weights that comprise performance (bottom) for Uninformed (grey), Benchmark (blue), and STEED (yellow) approaches

shown with the yellow histogram. Therefore, the effects of optimal structural layout configurations in the outboard wing must proliferate through the rest of the aircraft and cause the double-peak features of the STEED (yellow) histogram for total aircraft weight in the top plot of Fig. 87. This notion is confirmed by examining the OML design space in greater detail for structural weights of the Baseline configuration, shown in Fig. 89, in the same manner as Experiment 3B.

Detailed sensitivities display a discontinuity in the design space for structural weights of aircraft sections other than the outboard wing. It was discussed in Sec. 5.4.2 that competing trends in outboard and trapezoidal structural weight for each of the structural layout design parameters can create convergence to each side constraint of these design variables. The effect is more pronounced in this test case shown in Fig. 89. This tradeoff point of the optimization process from outboard wing to trapezoidal wing nearly divides the design space in half, which accounts for the multimodality of the histograms in Fig. 87. Information garnered during this causality study is enabled by the STEED process and helps support the development team in a decision of whether to pursue further testing of whether this effect is real or artificial, assessments of other baselines, etc.

Aside from determining causality of performance distribution multimodality, how is risk quantified and managed for this example? For instance, the functional relationship of $\Delta W_S\left(\mathbf{X}_{OML}\right)$ had a bottom-line structural technology performance value for the outboard wing of -20% when the structural layout was optimized for the minimum outboard wing weight setting. This performance value meant OML design points existed in which PRSEUS was adding 20% structural weight by being implemented in the design. The opposite end of that distribution, shown in Fig. 87, is skewed toward 30% weight reduction. Risk is present in both these cases but for different consequences: a consequence of not being selected or implemented on an

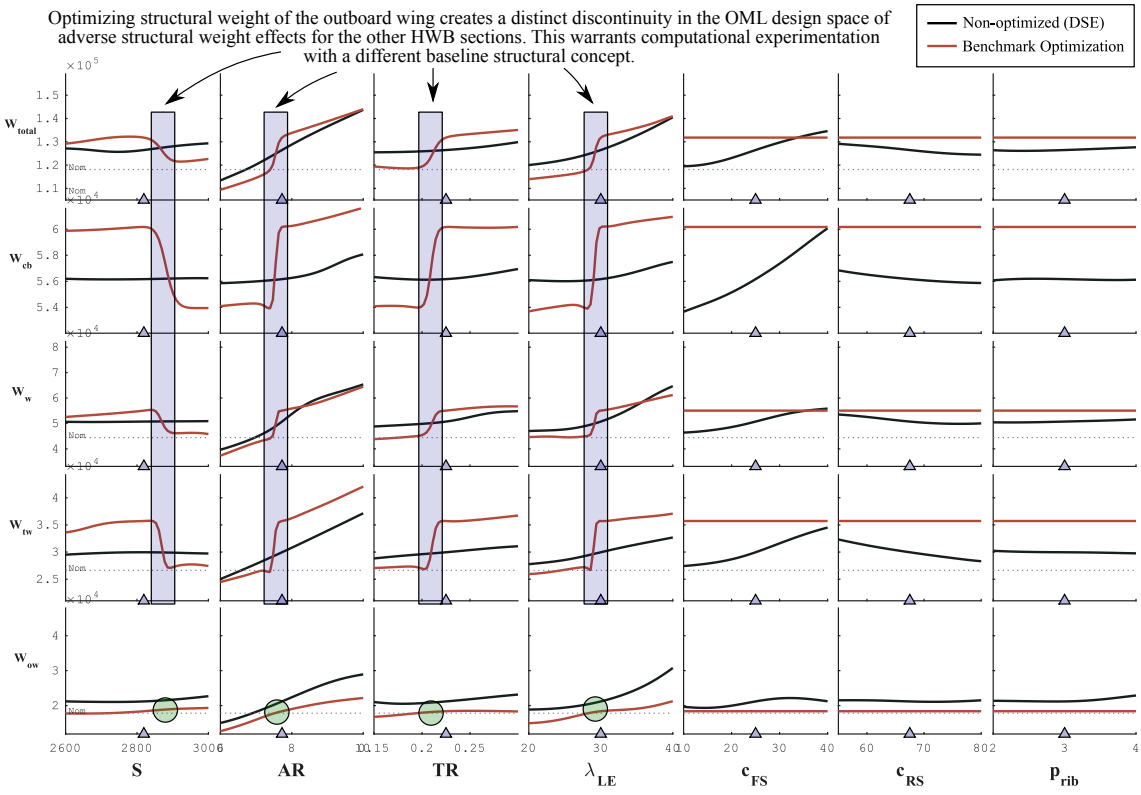

Figure 89: Structural weight discontinuities in Baseline configuration due to optimization

aircraft and a consequence of performance over-prediction with the potential for late-phase redesigns. This example shows that risk quantification is a useful approach to technology developers looking to advance their structural technology and instill confidence in decision-makers that these scenarios have been thoroughly investigated.

How, then, is risk identified, categorized, and quantified using data generated from the STEED approach and the Benchmark approach? What are some advantages and disadvantages to each? An investigation into several potential experiment objectives and the process taken for each objective to determine technology experiment elements is discussed for each process.

7.1.2 Risk Mitigation Experiment Design with STEED

A program objective of generic risk mitigation for a structural technology opens the door a number of interpretations, especially with the enormous amount of data available to the technology development team from the STEED characterization of technology performance. First, this hierarchy of data is reviewed from each level of design and metric space to understand how each level is connected:

Conceptual Design Metrics At the highest level are the trends that were investigated in Ch. 6. A desire to reduce risk at this level may come from the chain of command of decision-makers for a specific requirement, design region, etc. For example, an environmentally focused program like NASA ERA would potentially want to reduce negative consequential risk for the most promising fuel burn estimates. Then, a filtering process can be performed on the left end of the yellow distribution shown in Fig. 80 at a desired confidence level. Since a Monte Carlo simulation was performed to generate these results, trends can be examined on the following parameters that caused the best performance in fuel burn: 1) OML design points and 2) technology performance levels of each of the design points filtered from the Monte Carlo. This data can then be sent

down to the next lowest levels of the hierarchy.

Technology Performance In the desire to quantify risk, any metric from one of these levels can be chosen for assessment, and these risks can flow down from a higher level or be chosen directly by the technology developer. At the technology performance level, bottom-line performance can be chosen for any of the aircraft sections as a risk desired to be quantified. For example, objectives of PRSEUS development during NASA ERA have been discussed, and one risk that would be quantified using similar objectives would be the performance of the HWB centerbody section. However, centerbody performance is now defined as a function of the design space, and the number of contributing factors to performance has increased significantly. Figure 74 shows trends of centerbody performance to centerbody weight as a function of the OML design space. Either of these parameters can be filtered to assess which: 1) structural layout design, 2) global load case, 3) internal loads, 4) technology design parameters, 5) failure modes, and 6) OML design parameters. Distributions of values are sent further down the line for each one of these options to be further investigated.

Outer Mold Line At this level, risk is likely identified as a consequence or fallout from the conceptual design metrics. For instance, the tail end of optimal fuel burn performance was shown to contain high sweep and high aspect ratio outboard wing OML designs, based on visualization of the conceptual design space. The OML acts then as a transfer point to lower level design features that can be tested through experimentation. Which global load cases size the most structure for this region of the OML design space? What technology design parameters and internal loads account for the most sized structural weight in this region of the OML design space? These types of questions will help the technology developer in the search for appropriate experiment settings.

Structural Layout Since structural layout designs were optimized for each structural configuration in the STEED approach, trends exist for both the baseline and PRSEUS configurations. Perhaps the technology development team desires to investigate multimodality trends in baseline structural weight to increase confidence in PRSEUS performance estimates. Potential experiments, then, have a number of options between: performing higher fidelity modeling with the baseline to assess whether discontinuity in weight as a function of structural layout optimization is artificial or real, investigating other potential baseline structural concepts for comparison, etc. In this case, nothing is even done with the PRSEUS technology, but the basis by which it is compared for performance estimates is just as important. An additional option is the result of a filtering case from higher levels. A trend was identified for largest PRSEUS performance estimates and minimum structural weight of PRSEUS-enabled design points in the OML design space in terms of the optimized structural layout: rib spacing for the outboard wing was at its highest setting – $p_{rib} = 4$ft. The risk identified in this case is that not enough failure conditions were included in the weight estimation model. Rib spacing for a two spar wing configuration is typically limited by global stability and resistance to flutter. Flutter failures were not considered in GT-WESt, and a static linear elastic analysis method was used to determine the internal loads that Hypersizer used in the local sizing process. Consequence of this risk is a decreased technology performance estimate if the more efficient structural layout PRSEUS was enabling was actually infeasible. Therefore, a suggested experiment in this scenario is higher fidelity modeling for flutter analysis on the optimized structural layout configuration.

Technology This lowest level is like those above it in that objectives can trickle down from risks identified at higher levels, or risks can be identified because

of the technology level performance estimation process and available interactive environments created with STEED. This level ultimately dictates the local loading conditions, i.e. operating conditions, that the test article is placed in, and it also determines what the test article looks like.

Then, similar to a Vee diagram approach in which potential causality was broken down, it can now be synthesized from its lowest level components to aid in decision making. How much does each one of the lowest level technology design variables or local loading conditions influence structural weight? If one of these parameters was identified without considering its effect on the Perhaps these conditions exist in less than 1% of designs throughout the entire OML design spaces. A tradeoff must then be quantified to assess whether the source cause of investigation of these technology parameters is extreme enough to warrant resources being expended to witness the phenomena.

7.1.3 Benchmark Experiment Design

Since risk quantification is enabled by probabilistic methods, the benchmark approach to experiment design suffers from a lack of useful data and relies heavily on subject matter experts to determine which experiment objectives are worth pursuing Risk with this approach occupies only the lowest level of design space discussed with the STEED approach, because technology level settings, local loading conditions, and failure modes are the only data of which multiple points exist. These data points are representative of each component within the performance estimation structural model. The most extreme values of these parameters could be targeted by experimentation, and design of the experiment is completely direct once the decision is made for an objective. Test article design and loading/boundary conditions are dictated by single configuration sized structural model. Although traceability exists in terms of this design, it is lacking in decision-making for the experiment objective.

7.2 Objective 2: Uncertainty Reduction

Uncertainty reduction occurs for a technology by identifying prevalent sources of uncertainty and targeting them through experimentation. Similar to risk, reduction of uncertainty occurs at the tails of distributions but in a two-sided manner rather than one-sided like risk. Shrinking these tails is dependent on the ability to find experiment elements that correlate with sources of uncertainty. It was shown in the previous chapter that the functional relationship of performance itself was a significant source of potential structural technology uncertainty if unaccounted for. Therefore, simply by quantifying this relationship, uncertainty reduction has already occurred over the benchmark approach by using STEED to characterize performance.

More direct approaches of uncertainty propagation exist, and these approaches are traceable from the metrics at any level down to the detailed structural technology level. Sources of uncertainty in structural technologies are typically manifested through design assumptions or physical characteristics. Knockdowns on allowable strains, for example, is a source of uncertainty that is a modeling assumption based on physical characteristics, and it is mapped to that physical characteristic in its modeling implementation. Through the process of uncertainty propagation, the effect of lower level epistemic technology uncertainties can be assessed at the technology performance level. However, implementation of technology uncertainties in the weight estimation process is under the same challenges discussed earlier for performance characterization: computation and model pre-processing expense.

Implementation of sources of uncertainty at the material level cannot be performed in an automated fashion with GT-WESt, and therefore, incorporation into the STEED approach is currently intractable and a potential area of future research. However, a process for structural uncertainty propagation for performance uncertainty quantification has been implemented on a single OML and SL design point within this research, similar to the benchmark approach [15]. With expansion of the process

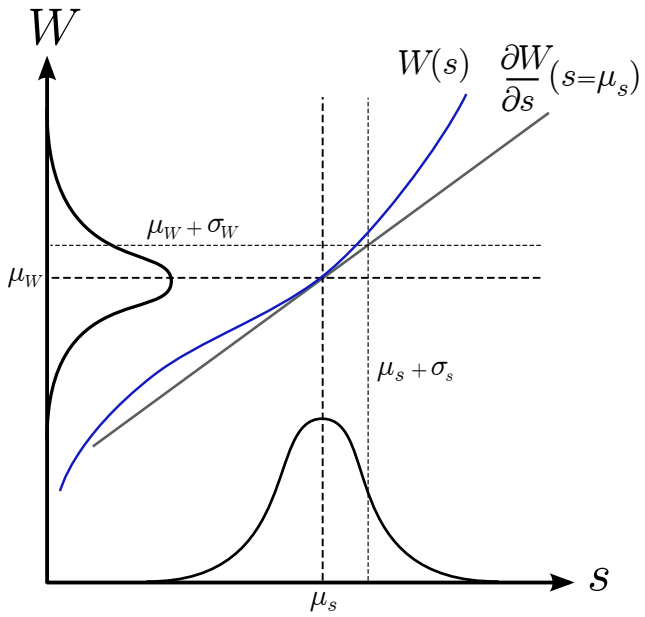

Figure 90: Linear expansion concept for uncertainty propagation in one dimension

to the STEED functional approach, performance uncertainty could also be quantified as a function of the $\mathbf{X}_{OML}$ and $\mathbf{X}_{SL}$ design spaces. In this manner, experiment design using the STEED approach would have an additional benefit over the benchmark process. The process of uncertainty propagation is described here with implications in targeting sources of uncertainty and identifying important correlations between design variables and uncertainty sources.

Because of computational expense concerns of the GT-WESt and global-local benchmark structural sizing approach, first-order linear expansion method, based on the work of Arras[6], was used to propagate structural uncertainties to vehicle level weight metrics. This approach, in terms of the case study variables, can be seen graphically in one dimension in Fig. 90, where W is a generic structural weight and s is a source of uncertainty. Assuming $W(s)$ is relatively linear in the region of the uncertain variable mean, μ_s, which is also the optimized configuration without uncertainty, then the projection of $\mu_s + \sigma_s$ on the linear weight function, with a slope of $\frac{\partial W}{\partial s}|_{s=\mu_s}$, provides a good estimate of $\mu_W + \sigma_W$.

Table 22: Sources of structural uncertainty

Description	μ_s	σ_s
Composite Laminate Density, ρ_ℓ $\left(lb/in^3\right)$	0.057	0.002 (3.5%)
Change in Stress/Strain Allowables, $\Delta\sigma_a$ & $\Delta\epsilon_a$ (%)	0.0	2.0
Change in Laminate Ply Angles, $\Delta\phi_{\text{ply}}$ (deg.)	0.0	2.0
Change in Fiber Stiffness, ΔE_f & ΔG_f (%)	0.0	2.0
Change in Calibration Factor, Δk_{scale} (%)	0.0	2.0

To expand this formulation to multiple uncertain variables, $s_i \in \mathbf{s}$, a first order Taylor series expansion can be defined as:

$$W = W\left(\mu_{s_1}, \mu_{s_2}, \ldots, \mu_{s_n}\right) + \sum_{i=1}^{n} \frac{\partial W}{\partial s}\left(\mu_{s_1}, \mu_{s_2}, \ldots, \mu_{s_n}\right)\left(s_i - \mu_{s_i}\right) \tag{65}$$

In order to obtain the distribution for weight based on multiple sources of uncertainty, the variance can be found from this expansion with:

$$\sigma_W^2 = \sum_{i=1}^{n} \left(\frac{\partial W}{\partial s}\right)^2 \sigma_{s_i}^2 \tag{66}$$

where $\frac{\partial W}{\partial s}$ is evaluated at all μ_{s_i} and $\sigma_{s_i}^2$ is the variance of each uncertainty source, s_i. By using these equations, it is assumed that each of the sources of uncertainty is normally distributed and there is no correlation between any s_i. These assumptions are important, especially for composite structures in which there are many variables that could be affected by uncertainty. As more uncertain variables are considered, the likelihood of interdependence increases, especially for manufacturing and fabrication uncertainties. For this study, a small number of uncertain variables was considered and the assumption of independence introduces little error for the variables chosen.

Technology design variables for structural optimization in Hypersizer are listed in Table 12. Five sources of uncertainty were used for this case study demonstration and are shown in Table 22. These sources represent uncertainty that should be planned for in the conceptual design process, even though some are more linked to the fabrication process. For instance, composite laminate density has a direct physical connection to

weight and varies due to the materials and processes used during fabrication. When an aircraft is built, its weight is a single deterministic value regardless of the difference between actual and predicted values of these densities, or other fabrication variations like thicknesses, laminate ply orientations, etc.

The other uncertain variables listed in Table 22 have a more indirect relationship with physical weight, but are directly related to constraints in the design process. Material properties like stress and strain allowables affect the structural geometry constrained by strength- and stability-based failure modes. For calibration factors, uncertainty can be introduced by choosing an inappropriate functional relationship of the calibration variable – for example, a scale factor on primary structural weight. It can also be introduced if the calibration point is not considered a complete "truth model." For example, the weight values to which this environment was calibrated[46] were generated with a proprietary computational model and do not represent an as-built configuration. Calibration efforts were augmented by modeling physical PRSEUS experiments, however, which reduces this source of uncertainty. Nevertheless, an inherent uncertainty exists in these values if the goal of this environment is to predict 'actual' physical weight, and that is why calibration factors are included in this case study.

Since uncertainties are applied across multiple values for the same variable, e.g. allowables for both stresses and strains, the representative uncertainties are listed as percentages in Table 22.

7.2.1 Assumptions and Limitations

The approach presented in this section has its limitations. Since normality in uncertainty distributions must be assumed, a limited number of uncertain variables was investigated. Characterization of the sources of uncertainty was outside the scope of this project, so nominal distributions were chosen to highlight the uncertainty

propagation technique. A degree of accuracy is maintained under the assumption of functional linearity for this propagation method, so long as the relationship is linear within the bounds of the uncertain variable distribution. The variation in weights shown in the next section is simply due to the sources of uncertainty considered in the study and is not an all-encompassing estimate of uncertainty in the conceptual design process. As the weight estimation environment is concerned, some weight savings opportunities for each structural configuration may be lost because of the discrete nature of the sizing process in Hypersizer. Further, including secondary structure in the finite element model would decrease the uncertainty in scale factors.

7.2.2 Structural Weights

The aggregate impact of all sources of structural uncertainties is shown in this subsection. Through propagation with the first-order method, structural weight distributions for various sections of the N2A are shown for the two structural concepts in Fig. 91. The weight distributions are shown on a reverse x-axis to highlight the subtraction of distributions of the baseline configuration (black) by the PRSEUS configuration (blue). The resulting weight reduction distribution is shown on the right side in red for each metric. Comparing these normal distributions is done by subtracting mean values and adding variances, as shown in Eq. 67 and 68, respectively:

$$\mu_{\Delta W} = \mu_{W_{S,B}} - \mu_{W_{S,T}} \tag{67}$$

$$\sigma^2_{\Delta W} = \sigma^2_{W_{S,B}} + \sigma^2_{W_{S,T}} \tag{68}$$

This trend can be seen from Fig. 91, in which the spread of the resultant weight savings distribution (red) is larger than each of the component distributions. One anomaly that can be seen in this figure is the structural weight increase in the outboard wing when PRSEUS is used as the structural concept in this region. There are two potential explanations for this. First, the discretization scheme in Hypersizer did not allow for a truly optimal configuration to be found for PRSEUS, but it may have for traditional

Table 23: Distributions of weight changes with PRSEUS for N2A

Section	$\mu_{\Delta W}$ (lb)	$\sigma_{\Delta W}$ (lb)
ΔW_{cb}	-17,688 (-29.1%)	2,952 (4.9%)
ΔW_{rcb}	-3,939 (-34.6%)	545 (4.8%)
ΔW_{ow}	-2,134 (-13.6%)	1,218 (7.8%)
ΔW_{tw}	+749 (+2.9%)	1,662 (6.5%)
ΔW_{total}	-23,009 (-20.3%)	5,615 (5.0%)

composites. Second, the upper limit for spar thickness was not large enough at the inboard section so unnecessary weight was added to the configuration by auxiliary means, e.g. bulky stiffeners. The latter is supported by larger variation of weight in the outboard wing, as seen in Table 23 This highlights the importance of setting reasonable variable bounds in the structural sizing process.

Weight savings distributions for all metrics are listed in Table 23

7.2.3 Weight Sensitivities to Sources of Uncertainty

The spread of the aggregate distributions in the previous subsection are the result of multiple variance effects as defined by Eq. 66. A mapping of the uncertainty of total structural weight due to material density can be found in Fig. 92. Uncertainty is mapped to both the baseline and PRSEUS N2A configurations, which are drawn to the same scale. It is shown in this figure, due to the larger slope of the baseline configuration, that uncertainty in density will propagate to a larger amount of uncertainty in the structural weight of the baseline than that of the PRSEUS design.

Non-graphical data for more mappings is found in Table 24. This table shows the effects of two sources of uncertainty, laminate density (ρ) and stress/strain allowables (σ_a and ϵ_a). The top two rows represent effects on the baseline, designated with the subscript b, while the bottom two rows show effects for the PRSEUS-enabled N2A, designated with the subscript p. Columns in Table 24 represent the slope or

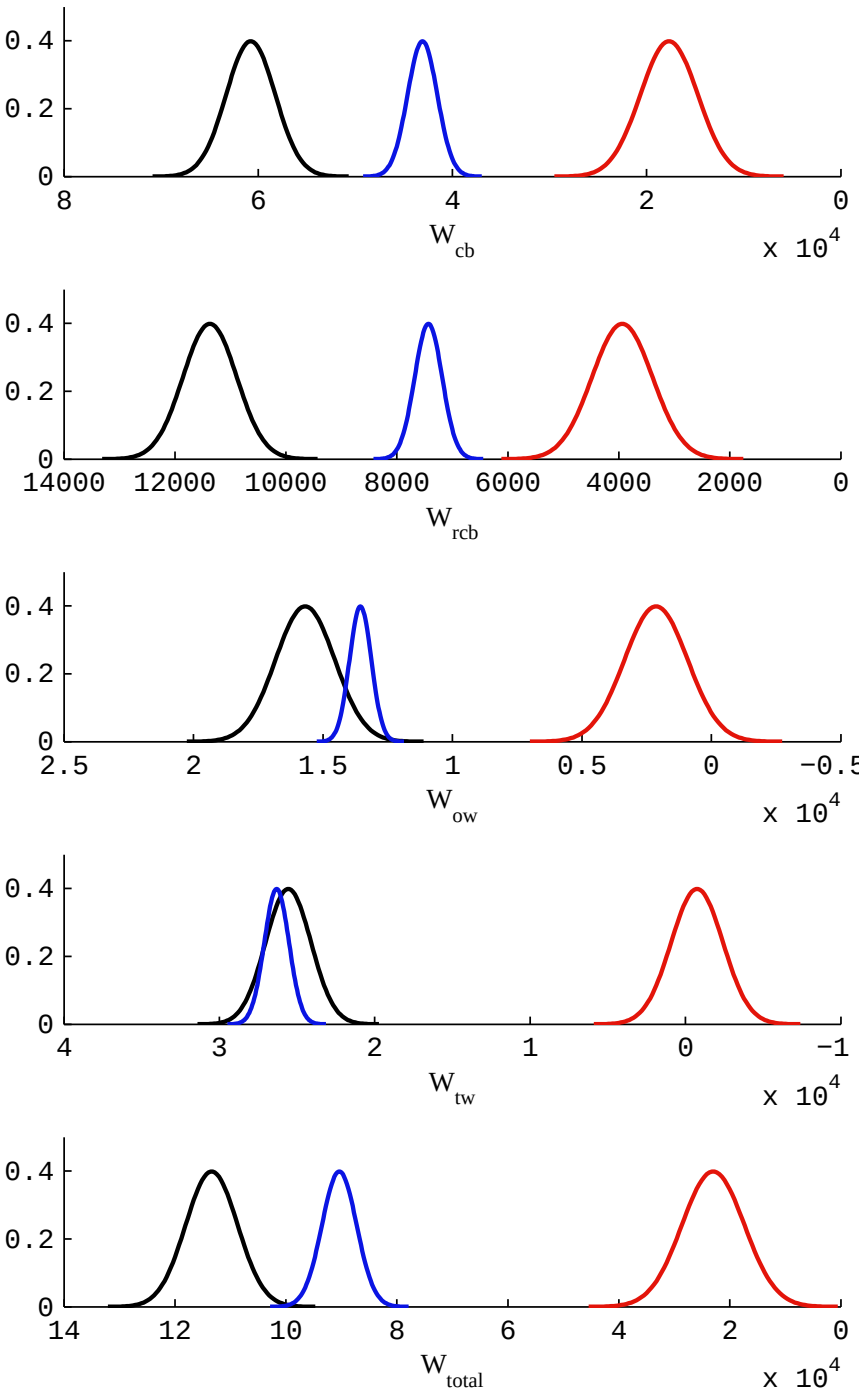

Figure 91: Uncertainty distribution of PRSEUS performance (red), baseline weight (black) and PRSEUS weight (blue)

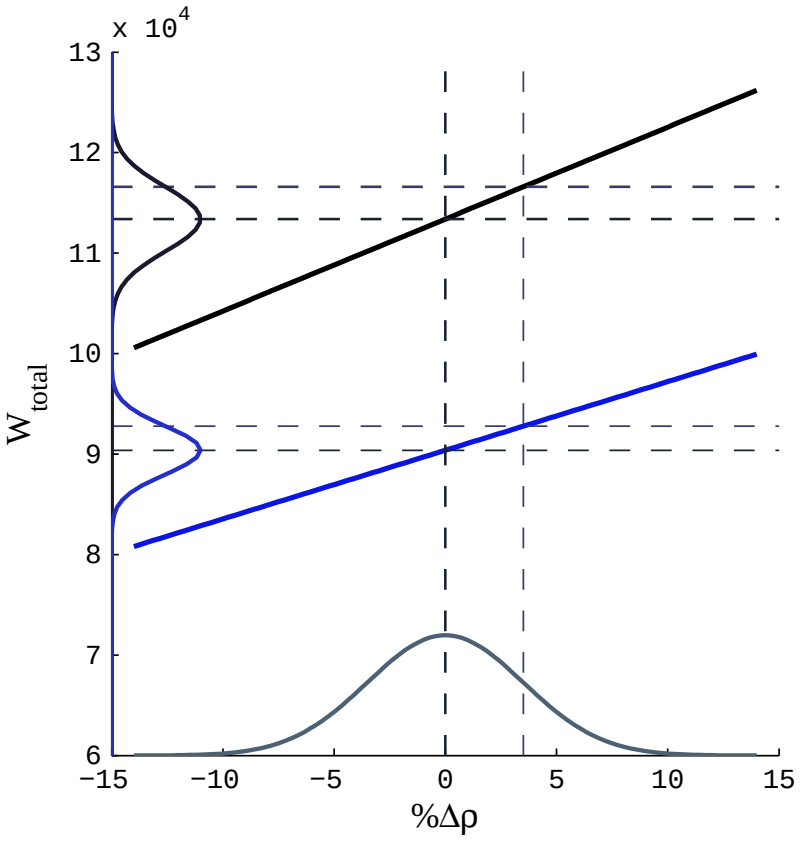

Figure 92: Mapping of percentage change in density uncertainty to total structural weight for baseline and PRSEUS configurations

sensitivity of the weight function to each source of uncertainty, $\frac{\partial W}{\partial s}$, and the variance of weight due to each source, σ_W, for the centerbody, rear centerbody, outboard wing, trap wing, and total vehicle, respectively. There are two instances of a reduction in weight when adverse values for uncertainties are applied, shown with negative slopes. This is most likely a result of course discretization on structural design variables in Hypersizer, and the brute force method uncovering weight opportunities with small changes in the uncertain variables.

It was shown in this limited demonstration case that uncertainty in material density, given the input variance, had the most significant impact on uncertainty in structural weight. This source of uncertainty stemmed from an immature fabrication process in the early phases of PRSEUS development. In this case, to target the most influential source of uncertainty, experiments in panel fabrication at different sizes and different PRSEUS design parameters would be suggested for both benchmark and STEED experiment design.

7.3 Summary

Using the full-scale performance characterization approach enables a greater degree of traceability in the technology development experiment design process, especially for decisions made regarding experiment objective. For each design space exploration added in the characterization above the benchmark process, an additional set of objectives can be examined, the and a much larger set of data is available to set the experiment design parameters. A previous example had set an expected value of degrees of freedom available to experiment designers; however, it is shown that each level of performance estimation design space can be modeled as a continuous design space. This characteristic provides infinite degrees of freedom to the technology development team and a functional mapping between levels to enable investigations in causality through experimentation.

Table 24: Sensitivities of weights to sources of uncertainty and standard deviation of weight components

s	$\frac{\partial W_{cb}}{\partial s}$	$\sigma_{W_{cb}}$	$\frac{\partial W_{rcb}}{\partial s}$	$\sigma_{W_{rcb}}$	$\frac{\partial W_{ow}}{\partial s}$	$\sigma_{W_{ow}}$	$\frac{\partial W_{tw}}{\partial s}$	$\sigma_{W_{tw}}$	$\frac{\partial W_{total}}{\partial s}$	$\sigma_{W_{total}}$
ρ_b	301	1,058	94	328	215	756	303	1,065	915	3,212
$\sigma_{a,b}$ & $\epsilon_{a,b}$	-301	602	29	58	356	712	402	803	487	975
ρ_p	304	1,069	44	156	115	403	220	771	683	2,339
$\sigma_{a,p}$ & $\epsilon_{a,p}$	314	629	-8	16	42	85	0	0	348	697

CHAPTER VIII

CONCLUDING REMARKS

The research presented in this thesis addressed a problem in structural technology performance estimation that was shown to be responsible for a significant source of performance uncertainty. Neglecting the impact of the conceptual design space on technology performance results in potential risk at multiple levels in the characterization process. A systematic approach was developed to expend as little effort as possible to draw conclusions on this relationship and determine whether further efforts would provide value. This approach followed a research formulation with a natural tollgate process, which included means of assessment of the performance function and the approach itself. Discussed in this chapter is an assessment of that research formulation, important findings, and suggestions for future research.

8.1 Assessment of Research Formulation

The formulation of research developed in Chapter 3 set up a generalized approach for research that identified metrics for each hypothesis. These metrics helped develop experiments that were performed on a test case structural technology. To make a sweeping characterization that evidence presented in the test case supports hypotheses of the research formulation for all weight reducing structural technologies is a inadvisable. Although this conclusion is not refuted by evidence, only support can be drawn for Hypotheses 1-5 of the PRSEUS technology in particular. These research statements are simply used as guidelines for other technologies within the STEED approach until sufficient observations have been made with numerous technologies that the statements can be made completely generalized. This section discusses observations and evidence for the PRSEUS test case.

Hypothesis 1: $\mathbf{X}_T$ Level Supporting evidence was provided to substantiate the notion that the $\Delta W_S(\mathbf{X}_{OML})$ function can be indicated at the lowest level of the structural technology performance estimation process. Not only did aggregate measures of performance as a function of technology design parameters and operating conditions show significant spread in performance variation, but individual trades within the design space were witnessed as well: large degrees of nonlinearity in component structural weight and performance, tradeoffs of multiple failure criteria in specific design regions, and the optimized performance function crossing the $\Delta W_{S,i} = 0$ threshold at multiple points within the design space. While these indicating factors themselves support Hypothesis 1, confirmation was obtained when variation in the actual $\Delta W_S(\mathbf{X}_{OML})$ function was observed for the PRSEUS technology.

Hypothesis 2: $\mathbf{X}_{SL}$ Level The hypothesis at the structural layout level within the tollgate framework was supported weakly by evidence garnered at this level of the design space. Two OML design points were investigated for the effect of structural layout on performance, and the main goal of this study was to determine proper treatment of the structural layout within the OML design space. **Hypothesis 2.1** was confirmed for PRSEUS when a relative range for weight reduction performance of $\sim 12\%$ of the total baseline aircraft structural weight was witnessed. This variability was significant enough to show that a default structural layout design could not be used throughout the OML design space without introducing error into performance. **Hypothesis 2.2**, however, was not supported until the full characterization of the OML design space was performed. This showed a significant deviation throughout the design space between benchmark and STEED treatments of the structural layout optimization. Variation in conceptual design metrics also helped confirm that separate optimization of the baseline structural configuration and PRSEUS technology

configuration was an appropriate treatment. Revisiting Hypothesis 2, the experiments at this level only needed to obtain just enough information to show that a full characterization at the OML design space level was warranted, and the differing shapes of structural weight functions between the N2A and HWB301 was an indicating factor that OML may have an impact on performance worth quantifying. Results of the technology level helped display the synthesis of a breadth of technology performance knowledge and helped in the decision to advance from the $\mathbf{X}_{SL}$ level to $\mathbf{X}_{OML}$.

Hypothesis 3: $\mathbf{X}_{OML}$ Level The last hypothesis in the tollgate framework of the research formulation, Hypothesis 3 was supported by some of the same observations that were made at the technology level – both aggregate and local indicating factors that the $\Delta W_S(\mathbf{X}_{OML})$ would have a significant quantifiable impact on the applications of this research, conceptual design implementation and experiment design. **Hypothesis 3.1** was also supported for PRSEUS when variability in the performance functional relationship translated to the same order of variation that was a result of technology immaturity (measured by TRL).

Overarching Performance Hypothesis The Vee representation of this hypothesis was the basis of the tollgate framework in STEED, and it provided a systematic approach that was cognizant of the allocation of resources in the characterization effort. For PRSEUS, this hypothesis was confirmed because of the evidence of variability and the risk and consequences that were attributed neglecting the performance function and treating structural technology weight reduction as a scalar.

Hypothesis 4: Conceptual Design It was shown that risk was evident in conceptual design metrics as well by neglecting this relationship. Conceptual design technology selection scenarios were provided that showed a glimpse of minuscule impact, and it was determined that this trend would continue if the conceptual

design process did not include competing objectives for design. Evidence supporting Hypothesis 4 came broad implementation of the PRSEUS technology in conceptual design. Throughout the entire design space, significant error was witnessed through neglecting the $\Delta W_S\left(\mathbf{X}_{OML}\right)$ relationship, shown in Figs. 80–82.

Hypothesis 5: Experiment Design It was shown that the experiment design process benefits from a more complete characterization of performance with infinitely more degrees of freedom available for experiment element selection, and experiment objectives could be instantiated at any design space level and be mapped to technology level variables through aggregate parameters of internal loads, technology design variables, etc. Also introduced was potential solution to enable other traceable methods of resource allocation through direct quantification of uncertainty in References [27], [9], and [38].

Thesis Statement Finally, success was achieved in terms of the research objective because a systematic method was developed with the ability to quantify structural technology performance that significantly improves capabilities over state of the art and enables more informed implementation of structural technologies in conceptual design and more traceable experiment design for technology development.

Surrogate models were an immense enabler in this approach, and the use of neural networks helped capture nonlinearities in the design space that were otherwise intractable because of the computational cost of higher fidelity structural weight estimation with GT-WESt. These approximations also helped enable the design space mapping and assessment of aggregate performance throughout each level of design space. Observations witnessed with the STEED approach presents a significant advantage in structural technology performance estimation with better informed characterization.

8.2 Potential Future Research Efforts

Throughout this document, notes have been made regarding additional gaps int he problem and assumptions taken that could be future areas of research to improve the STEED approach. First, an additional layer could be added to the Vee diagram representation of Overarching Performance Hypothesis at the top level. Estimates of conceptual design performance presented in Ch. 6 can be improved if conceptual design feasibility was implemented at the next highest level on the left side of the Vee representation. This added layer could enable design space tailoring techniques [52] and one of the challenges mentioned in this thesis would need addressed – estimation of conceptual design metrics like takeoff gross weight at the outset of the performance characterization process. Estimation of W_{TO} is required for initiation of aerodynamic load cases in the weight estimation environment and assumptions were made in this research that could be improved upon.

Next, implementation of structural performance estimation with GT-WESt was limited in the number of structural concepts that could be tested and for the weight reduction comparison. However, it is anticipated that accuracy can be increased by considering a larger number of structural concepts for the baseline configuration – which could also mitigate the multimodality effects that were witnessed in Sec. 5.4.1. Additionally, the technology-infused configuration should not necessarily include *only* technology structure. Design rules can be developed that implements multiple structural concepts for a given configuration: 1) so long as the model allows it and 2) so long as underlying assumptions are not affected. For example, one of the benefits of PRSEUS structure is unitization and the ability to cure large panels to reduce the number of joints and fasteners the structural configuration needs. If PRSEUS structure was interchangeable with another structural concept when knockdown and non-optimal factors were set with the assumption that PRSEUS spans the entire structure, error is introduced in the performance estimation process.

8.3 Contributions

This research and the STEED approach present a systematic and repeatable process to estimate structural technology weight reduction performance. Trends were observed for the PRSEUS test case that were otherwise intractable with other implementations of performance estimation. While methods were available for parametric performance estimation, each fell short of required fidelity to capture impacts of detailed technology characteristics and complex failure modes. These features were critical in the applications of the STEED performance characterization method: technology development experimental design and conceptual design implementation. Both applications were shown to be improved by a more complete performance characterization.

REFERENCES

[1] Adams, D. F., "High-performance composite material airframe weight and cost estimating relations," *Journal of Aircraft*, vol. 11, pp. 751–757, 1974.

[2] Administration, F. A., "Electronic code of federal regulations: Chapter 1, subchapter c, part 25," 2017.

[3] Airbus, "Global market forecast: Flying on demand 2014-2033," tech. rep., Airbus, 2014.

[4] Airplanes, B. C., "Current market outlook: 2014-2033," tech. rep., Boeing, 2014.

[5] Ardema, M. D., Chambers, M. C., Patron, A. P., Hahn, A. S., Miura, H., and Moore, M. D., "Analytical fuselage and wing weight estimation of transport aircraft," tech. rep., NASA Ames Research Center, 1996.

[6] Arras, K. O., "An introduction to error propagation," *Swiss Federal Institute of Technology Lausanne, Tech. Rep*, 1998.

[7] Bergan, A. C., Bakuckas, J. G. J., Lovejoy, A. E., Jegley, D. C., Awerbuch, J., and Tan, T.-M., "Assessment of damage containment features of a full-scale prseus fuselage panel through test and teardown," in *27th ASC Technical Conference*, 2012.

[8] Bindolino, G., Ghiringhelli, G., Ricci, S., and Terraneo, M., "Multilevel structural optimization for preliminary wing-box weight estimation," *Journal of Aircraft*, vol. 47, pp. 475 – 489, 2010.

[9] Bjorkman, E. A., *Test and Evaluation Resource Allocation Using Uncertainty Reduction as a Measure of Test Value*. PhD thesis, 2012.

[10] Bradley, K. R., "A sizing methodology for the conceptual design of blended-wing-body transports," tech. rep., NASA/CR-2004-213016, 2004.

[11] Collier, C., Yarrington, P., and Van West, B., "Composite, grid-stiffened panel design for post buckling using hypersizer," in *43rd AIAA/ASME/ASCE/AHS/ASC Structures, Structural Dynamics, and Materials Conference*, p. 1222, 2002.

[12] Collier, F., Thomas, R., Burley, C., Nickol, C., Lee, C.-M., and Tong, M., "Environmentally responsible aviation: Real solutions for environmental challenges facing aviation," in *27TH INTERNATIONAL CONGRESS OF THE AERONAUTICAL SCIENCES*, 2010.

[13] Combes, R. C. J., "Design for damage tolerance," *Journal of Aircraft*, vol. 7, pp. 18–20, 1969.

[14] Corman, J. and German, B., "A comparison of metamodeling techniques for engine cycle design data," in *13th AIAA/ISSMO Multidisciplinary Analysis Optimization Conference*, p. 9352, 2010.

[15] Corman, J. A. and Mavris, D., "Assessing structural technology performance for the hybrid wing body through probabilistic weight estimation," in *ICAS 2014*, 2014.

[16] DeLaGarza, A. P. I., McCulley, C. M., Johnson, J. C., Hunten, K. A., Action, J. E., Skillen, M. D., and Zink, P. S., "Recent advances in rapid airframe modeling at lockheed martin aeronautics company," in *27th NATO Applied Vehicle Technology Panel*, 2011.

[17] DeLoach, R., "Bayesian inference in the modern design of experiments," in *46th AIAA Aerospace Sciences Meeting and Exhibit*, 2008.

[18] Derringer, D. and Suich, R., "Simultaneous optimization of several response variables," *Journal of Quality Technology*, 1980.

[19] Dow, M. B. and Dexter, H. B., "Development of stitched, braided and woven composite structures in the act program and at langley research center (1985 to 1997)," tech. rep., NASA Langley Research Center, Hampton, VA, 1997.

[20] Eisenhauer, E., Therasse, P., Bogaerts, J., Schwartz, L., Sargent, D., Ford, R., Dancey, J., Arbuck, S., Gwyther, S., Mooney, M., and others, "New response evaluation criteria in solid tumours: revised recist guideline (version 1.1)," *European journal of cancer*, vol. 45, no. 2, pp. 228–247, 2009.

[21] Elham, A., "Structural design: Weight estimation," *Encycolpedia of Aerospace Engineering*, 2012.

[22] Elham, A., La Rocca, G., and van Tooren, M. J. L., "Development and implementation of an advanced, design-sensitive method for wing weight estimation," *Aerospace Science and Technology*, 2013.

[23] Elham, A. and van Tooren, M. J. L., "Winglet multi-objective shape optimization," *Aerospace Science and Technology*, 2014.

[24] Engler, W., Biltgen, P., and Mavris, D., "Concept selection using an interactive reconfigurable matrix of alternatives (irma)," in *45th AIAA aerospace sciences meeting and exhibit*, p. 1194, 2007.

[25] Fisher, R. A., "The use of multiple measurements in taxonomic problems," *Annals of eugenics*, vol. 7, no. 2, pp. 179–188, 1936.

[26] Forrester, A. I. J., Keane, A. J., and Bressloff, N. W., "Design and analysis of "noisy" computer experiments," *AIAA Journal*, vol. 44, pp. 2331 – 2339, 2006.

[27] Gatian, K. N., *A Quantitative, Model-Driven Approach to Technology Selection and Development through Epistemic Uncertainty Reduction*. PhD thesis, Georgia Institute of Technology, 2015.

[28] Gendler, T. S., "Thought experiments rethoughtand reperceived," *Philosophy of Science*, vol. 71, no. 5, pp. 1152–1163, 2004.

[29] Gern, F. H., "Finite element based hwb centerbody structural optimization and weight prediction," in *53rd AIAA/ASME/ASCE/AHS/ASC Structures, Structural Dynamics and Materials Conference*, 2012.

[30] Gern, F. H., "Conceptual design and structural analysis of an open rotor hybrid wing body aircraft," in *54th AIAA/ASME/ASCE/AHS/ASC Structures, Structural Dynamics, and Materials Conference*, 2013.

[31] Gern, F. H., Naghshineh-Pour, A. H., Sulaeman, E., Kapania, R. K., and Haftka, R. T., "Structural wing sizing for multidisciplinary design optimization of a strut-braced wing," *Journal of Aircraft*, vol. 38, pp. 154–163, 2001.

[32] Glaessgen, E., Raju, I., and C.C., J. P., "Fracture mechanics analysis of stitched stiffener-skin debonding," in *39th AIAA/ASME/ASCE/AHS/ASC Structures, Structural Dynamics, and Materials Conference and Exhibit*, 1998.

[33] Gould, K., Lovejoy, A. E., Jegley, D., Neal, A. L., Linton, K. A., Bergan, A. C., and John G., J. B., "Nonlinear analysis and post-test correlation for a curved prseus panel," in *54th AIAA/ASME/ASCE/AHS/ASC Structures, Structural Dynamics, and Materials Conference*, 2013.

[34] Horne, M. R. and Madaras, E. I., "Initial evaluation of acoustic emission shm of prseus multi-bay box tests," tech. rep., NASA Langley Research Center (NASA/TM2016-218976), 2016.

[35] Howe, D., *Aircraft Loading and Structural Layout*. AIAA Education Series, 2004.

[36] Hutchinson, Virgil L., J. and Olds, J. R., "Estimation of launch vehicle propellant tank structural weight using simplified beam approximation," in *40th AIAA/ASME/SAE/ASEE Joint Propulsion Conference and Exhibit*, 2004.

[37] Hyperworks, A., "Hypermesh 11.0 user guide," tech. rep., Altair Engineering, 2011.

[38] Jacobs, R. B., *A Framework for Designing Technology Development Activities*. PhD thesis, 2016.

[39] Jegley, D., "Failure at frame-stringer intersections in prseus panels," tech. rep., NF1676L-14189, 2012.

[40] Jegley, D. C. and Lovejoy, A. E., "The use of the stags finite element code in stitched structures development," in *55th AIAA/ASMe/ASCE/AHS/SC Structures, Structural Dynamics, and Materials Conference*, p. 0845, 2014.

[41] Jegley, D. C., Rouse, M., Przekop, A., and Lovejoy, A. E., "The behavior of a stitched composite large-scale multi-bay pressure box," tech. rep., NASA Langley Research Center (NASA/TM-2016-218972), 2016.

[42] Jegley, D. C. and Velicki, A., "Status of advanced stitched unitized composite aircraft structures," in *51st AIAA Aerospace Sciences Meeting including the New Horizons Forum and Aerospace Exposition*, 2013.

[43] Jegley, D. C. and Velicki, A., "Development of the prseus multi-bay pressure box for a hybrid wing body vehicle," in *AIAA SciTech*, 2015.

[44] Jimenez, H., Burdette, G., Schutte, J., and Mavris, D., "Probabilistic technology assessment for nasa environmentally responsible aviation (era) vehicle concepts," in *Proceedings of the 11th AIAA Aviation Technology, Integration, and Operations (ATIO) Conference*, pp. 20–22, 2011.

[45] Kaufmann, M., Zenkert, D., and Wennhage, P., "Integrated cost/weight optimization of aircraft structures," *Structural and Multidisciplinary Optimization*, 2010.

[46] Kawai, R., "Acoustic prediction methodology and test validation for an efficient low-noise hybrid wing body subsonic transport," tech. rep., NASA ARMD Subsonic Fixed Wing Project Contract NNL07AA54C, 2011.

[47] Kennedy, G. J., "A comparison of metallic, composite and nanocomposite optimal transonic transport wings," tech. rep., NASA Langley Research Center, 2014.

[48] Kennedy, G. J., "Discrete thickness optimization via piecewise constraint penalization," *Structural and Multidisciplinary Optimization*, 2014.

[49] Kirby, M., *A Methodology for Technology Identification, Evaluation, and Selection in Conceptual and Preliminary Aircraft Design*. PhD thesis, 2001.

[50] Kirby, M. R., "The environmental design space," in *International Congress of the Aeronautical Sciences (ICAS)*, 2008.

[51] Kirby, M. R. and Mavris, D. N., "A method for technology selection based on benefit, available schedule and budget resources," in *World Aviation Conference*, 2000.

[52] Kizer, J., *Aircraft Conceptual Design Enabled by a Set-Based Approach for the Exploration and Bounding of Non-Hypercubic Design Spaces*. PhD thesis, 2016.

[53] Laughlin, T. W., "A parametric and physics-based approach to structural weight estimation of the hybrid wing body aircraft," Master's thesis, Georgia Institute of Technology, 2012.

[54] Laughlin, T. W., Corman, J. A., and Mavris, D. N., "A parametric and physics-based approach to structural weight estimation of the hybrid wing body aircraft," in *51st AIAA Aerospace Sciences Meeting including the New Horizons Forum and Aerospace Exposition*, 2013.

[55] Lee, D. H., Hilton, H. H., and Velicki, A., "Optimum designer material properties and geometries for stitched prseus composites," in *52nd AIAA/ASME/ASCE/AHS/ASC Structures, Structural Dynamics and Materials Conference*, 2011.

[56] Lee, D. H., Hilton, H. H., and Velicki, A., "Optimum stress and material distributions in stitched prseus composites," in *53rd AIAA/ASME/ASCE/AHS/ASC Structures, Structural Dynamics and Materials Conference*, 2012.

[57] Li, V. and Velicki, A., "Advanced prseus structural concept design and optimization," in *12th AIAA/ISSMO Multidisciplinary Analysis and Optimization Conference*, 2008.

[58] Liebeck, R., "Design of the blended wing body subsonic transport," *Journal of Aircraft*, vol. 41, pp. 10–25, 2004.

[59] Linton, K. A., Velicki, A., Hoffman, K., Thrash, P., Pickell, R., and Turley, R., "Prseus panel fabrication final report," tech. rep., NASA Langley Research Center, 2014.

[60] Locatelli, D., Riggins, B., Schetz, J. A., Kapania, R. K., Robic, B., Leenaert, C., and Poquet, T., "Aircraft conceptual design: Tools evaluation," in *14th AIAA Aviation Technology, Integration, and Operations Conference*, p. 2030, 2014.

[61] Lovejoy, A. E., "Prseus pressure cube test data and response," tech. rep., NASA/TM2013-217795, 2013.

[62] Lovejoy, A. E. and Poplawski, S., "Preliminary design and analysis of an in-plane prseus joint," in *54th AIAA/ASME/ASCE/AHS/ASC Structures, Structural Dynamics, and Materials Conference*, 2013.

[63] Lovejoy, A. E., Rouse, M., Linton, K. A., and Li, V. P., "Pressure testing of a minimum gauge prseus panel," in *52nd AIAA/ASME/ASCE/AHS/ASC Structures, Structural Dynamics and Materials Conference*, 2011.

[64] Mankins, J., "Technology readiness levels," tech. rep., NASA Office of Space Access and Technology, 1995.

[65] Mavris, D. N., Baker, A. P., and Schrage, D. P., "Ippd through robust design simulation for an affordable short haul civil tiltrotor," 1997.

[66] Mavris, D. N., Kirby, M. R., and Qiu, S., "Technology impact forecasting for a high speed civil transport," in *World Aviation Conference*, 1998.

[67] McAllister, J. W., "The evidential significance of thought experiment in science," *Studies In History and Philosophy of Science Part A*, vol. 27, no. 2, pp. 233–250, 1996.

[68] McCullers, L., "Flight optimization system, release 6.12, user's guide." NASA, 2004.

[69] Montgomery, D. C., "Experimental design for product and process design and development," *Journal of the Royal Statistical Society: Series D (The Statistician)*, vol. 48, no. 2, pp. 159–177, 1999.

[70] MSC Software Corporation, *MSC Nastran 2012: Quick Reference Guide*, 2012.

[71] Mukhopadhyay, V., "Hybrid wing-body pressurized fuselage modeling, analysis, and design for weight reduction," in *53rd AIAA/ASME/ASCE/AHS/ASC Structures, Structural Dynamics and Materials Conference*, 2012.

[72] Mukhopadhyay, V., Sobieszczanksi-Sobieski, J., Kosaka, I., Quinn, G., and Vanderplaats, G., "Analysis, design, and optimization of noncylindrical fuselage for blended-wing-body vehicle," *Journal of Aircraft*, 2004.

[73] Nickol, C. and Mccullers, L., "Hybrid wing body configuration system studies," in *47th AIAA Aerospace Sciences Meeting including The New Horizons Forum and Aerospace Exposition*, p. 931, 2009.

[74] Nickol, C. L., "Hybrid wing body configuration scaling study," in *50th AIAA Aerospace Sciences Meeting including the New Horizons Forum and Aerospace Exposition*, 2012.

[75] Nickol, C. L., "Technologies and concepts for reducing the fuel burn of subsonic transport aircraft," tech. rep., NF1676L-15121, 2012.

[76] Nigam, N., Ayyalasomayajula, S. K., Qi, X., Chen, P. C., and Alonso, J. J., "High-fidelity weight estimation for aircraft conceptual design optimization," in *16th AIAA/ISSMO Multidisciplinary Analysis and Optimization Conference*, p. 3360, 2015.

[77] Niskode, P., Stickes, R., Allmon, B., and DeJong, R., "Faa cleen consortium open session," *Presentation CLEEN Consortium Open Session, Georgia Institute of Technology, Atlanta, GA, October*, vol. 27, 2010.

[78] Niu, C., *Airframe structural design: practical design information and data on aircraft structures*. Conmilit Press, 1988.

[79] Niu, M. C.-Y., *Composite airframe structures: practical design information and data*. Adaso Adastra Engineering Center, 1992.

[80] Oberkampf, W., DeLand, S., Rutherford, B., Diegert, K., and Alvin, K., "Error and uncertainty in modeling and simulation," *Reliability Engineering & System Safety*, vol. 75, no. 3, pp. 333–357, 2002.

[81] Pacelab, A., "Pacelab apd 3.0. 0," *PACE Aerospace Engineering and Information Technology GmbH*, 2012.

[82] Przekop, A., "Repair concepts as design constraints of a stiffened composite prseus panel," in *53rd AIAA/ASME/ASCE/AHS/ASC Structures, Structural Dynamics and Materials Conference 20th AIAA/ASME/AHS Adaptive Structures Conference 14th AIAA*, p. 1444, 2012.

[83] Przekop, A. and Jegley, D. C., "Evaluation of a metallic repair on a rod-stiffened composite panel," *Journal of Aircraft*, vol. 51, no. 3, pp. 792–804, 2014.

[84] Przekop, A., Wu, H.-Y. T., and Shaw, P., "Nonlinear finite element analysis of a composite non-cylindrical pressurized aircraft fuselage structure," in *55th AIAA/ASMe/ASCE/AHS/SC Structures, Structural Dynamics, and Materials Conference*, p. 1064, 2014.

[85] Quinlan, J. and Gern, F. H., "Conceptual design and structural optimization of nasa environmentally responsible aviation (era) hybrid wing body aircraft," in *57th AIAA/ASCE/AHS/ASC Structures, Structural Dynamics, and Materials Conference*, p. 0229, 2016.

[86] Quinlan, J. and Gern, F. H., "Optimization of an advanced hybrid wing body concept using hcdstruct version 1.2," in *16th AIAA Aviation Technology, Integration, and Operations Conference*, p. 3460, 2016.

[87] Raymer, D. P., *Aircraft Design: A Conceptual Approach*. AIAA Education Series, 2006.

[88] Research, C., *HyperSizer Rod/Bulb Stiffened Panel Family, User's Manual Edition 5.9*, 2010.

[89] Risch, T., Cosentino, G., Regan, C. D., Kisska, M., and Princen, N., "X-48b flight-test progress overview," in *47th AIAA Aerospace Sciences Meeting Including The New Horizons Forum and Aerospace Exposition*, 2009.

[90] Rocha, H., Li, W., and Hahn, A., "Principal component regression for fitting wing weight data of subsonic transports," *Journal of Aircraft*, 2006.

[91] Rouse, M., "Methodologies for combined loads tests using a multi-actuator test machine," in *2013 SEM Annual Conference & Exposition on Experimental & Applied Mechanics*, 2013.

[92] Rouse, M. and Jegley, D., "Preparation for testing a multi-bay box subjected to combined loads," *NASA Langley Research Center*, 2015.

[93] Schutte, J. and Mavris, D. N., "Evaluation of n+2 technologies and advanced vehicle concepts," in *AIAA SciTech*, 2015.

[94] Schutte, J. S. and Jimenez, H., "Technology assesment of nasa enviromentally responsible aviation advanced vehicle concepts," in *49th AIAA Aerospace Sciences Meeting*, 2011.

[95] Sensmeier, M. D. and Samareh, J. A., "A study of vehicle structural layouts in post-wwii aircraft," in *45th AIAA/ASME/ASCE/AHS/ASC Structures, Structural Dynamics and Materials Conference*, 2004.

[96] Shirley, C. M., Schetz, J. A., Kapania, R. K., and Haftka, R. T., "Tradeoffs of wing weight and lift/drag in design of medium-range transport aircraft," *Journal of Aircraft*, vol. 53, pp. xx–xx, 2014.

[97] Simodynes, E. E., "Gradient optimization of structural weight for specified flutter speed," *Journal of Aircraft*, 1974.

[98] Simpson, T. W., Toropov, V., Balabanov, V., and Viana, F. A. C., "Design and analysis of computer experiments in multidisciplinary design optimization: A review of how far we have come or not," in *12th AIAA/ISSMO Multidisciplinary Analysis and Optimization Conference*, 2008.

[99] Software, M., "Patran 2012: User guide," tech. rep., MSC Software, 2012.

[100] Sorensen, R. A., *Thought experiments*, vol. 205. JSTOR, 1992.

[101] Staton, R., *Introduction to Aircraft Weight Engineering*. Society of Allied Weight Engineers, 1996.

[102] Tong, L.-I., Wang, C.-H., and Chen, H.-C., "Optimization of multiple responses using principal component analysis and technique for order preference by similarity to ideal solution," *The International Journal of Advanced Manufacturing Technology*, vol. 27, no. 3-4, pp. 407–414, 2005.

[103] Triantaphyllou, E., "Multi-criteria decision making methods," in *Multi-criteria Decision Making Methods: A Comparative Study*, pp. 5–21, Springer, 2000.

[104] Tsai, S. W. and Wu, E. M., "A general theory of strength for anisotropic materials," tech. rep., Air Force Materials Laboratory, 1972.

[105] Velicki, A., "Damage arresting composites for shaped vehicles: Phase 1 final report," tech. rep., NASA/CR-2009-215932, 2009.

[106] Velicki, A. and Jegley, D., "Prseus development for the hybrid wing body aircraft," in *AIAA Centennial of Naval Aviation Forum "100 Years of Achievement and Progress"*, 2011.

[107] Velicki, A. and Jegley, D., "Prseus structural concept development," in *AIAA SciTech*, 2014.

[108] Velicki, A., Yovanof, N., Baraja, J., Linton, K., Li, V., Hawley, A., Thrash, P., DeCoux, S., and Pickell, R., "Damage arresting composites for shaped vehicles: Phase ii final report," tech. rep., NASA/CR2011-216880, 2011.

[109] Vos, R. and Hoogreef, M., "Semi-analytical weight estimation method for fuselages with oval cross-section," in *54th AIAA/ASME/ASCE/AHS/ASC Structures, Structural Dynamics, and Materials Conference*, 2013.

[110] Wakayama, S. and Kroo, I., "Subsonic wing planform design using multidisciplinary optimization," *Journal of Aircraft*, 1995.

[111] Weed, P. A., "Hybrid wing-body aircraft noise and performance assessment," Master's thesis, Massachusetts Institute of Technology, 2010.

[112] Wilhite, A. W., Gholston, S. E., Farrington, P. A., and Swain, J. J., "Evaluating technology projections and weight prediction method uncertainty of future launch vehicles," *Journal of Spacecraft and Rockets*, vol. 45, pp. 587–591, 2008.

[113] Yovanof, N., Lovejoy, A. E., Baraja, J., and Gould, K., "Design, analysis and testing of a prseus pressure cube to investigate assembly joints," tech. rep., NASA Langley Research Center, 2012.

[114] Yovanof, N. P. and Jegley, D. C., "Compressive behavior of frame-stiffened composite panels," in *52nd AIAA/ASME/ASCE/AHS/ASC Structures, Structural Dynamics and Materials Conference*, 2011.

[115] Zanakis, S. H., Solomon, A., Wishart, N., and Dublish, S., "Multi-attribute decision making: A simulation comparison of select methods," *European journal of operational research*, vol. 107, no. 3, pp. 507–529, 1998.

VITA

Jason A. Corman was born on March 5, 1986 in Youngstown, OH to Dave and Cathy Corman. He attended Youngstown State University as part of the University Scholars program and graduated with a B.E. in Mechanical Engineering in May 2009. While pursuing his undergraduate degree, Jason participated in research and internship opportunities in the aerospace field with GE Aviation, Texas A&M University, and NASA Glenn Research Center. After obtaining his undergraduate degree, Jason attended the Georgia Institute of Technology, where he was a fellow of the Graduate Student Researchers Program (GSRP) at NASA Langley Research Center. During this fellowship, Jason's research focus was in the field of uncertainty quantification and propagation to help plan for reconciling differences between actual and predicted entry, descent, and landing trajectories of the 2012 Mars Science Laboratory mission. Graduating with a M.S. in August 2011, Jason then joined the Aerospace Systems Design Laboratory at Georgia Tech and focused his research toward airframe structures. This continued through the GSRP fellowship, and he also participated in other structures-related projects with Airbus and NASA Langley Research Center. Jason graduated with a Ph.D. in Aerospace Engineering in May 2017.